NISTIR 8331 DRAFT SUPPLEMENT

Ongoing Face Recognition Vendor Test (FRVT)

Part 6B: Face recognition accuracy with face masks using post-COVID-19 algorithms

Mei Ngan
Patrick Grother
Kayee Hanaoka
Information Access Division
Information Technology Laboratory

This document is a draft supplement of NIST Interagency Report 8331.

Last updated: 2022/01/20

National Institute of Standards and Technology
U.S. Department of Commerce

NISTIR 8331 DRAFT SUPPLEMENT

Face Recognition Vendor Test (FRVT)

Part 6B: Face recognition accuracy with face masks using post-COVID-19 algorithms

Mei Ngan
Patrick Grother
Kayee Hanaoka
Information Access Division
Information Technology Laboratory

January 2022

U.S. Department of Commerce
Gina M. Raimondo, Secretary

National Institute of Standards and Technology
James K. Olthoff, Performing the Non-Exclusive Functions and Duties of the Under Secretary of Commerce for Standards and Technology & Director, National Institute of Standards and Technology

Status and Changelog

Prior editions of this report are maintained on the FRVT Face Mask Effects website. This evaluation remains open to new algorithm submissions indefinitely. This report will be updated as new algorithms are evaluated, as new datasets are added, and as new analyses are included. Comments and suggestions should be directed to frvt@nist.gov.

2022-01-20 changes since 2021-03-04

- This report documents results from testing 266 face recognition algorithms provided to NIST since the onset of the pandemic in mid-March 2020, and includes cumulative results for 319 algorithms evaluated to date (submitted both prior to and after mid-March 2020).

2021-03-04 changes since 2020-11-30

- This report adds 35 new algorithms submitted to FRVT 1:1 since the last report (and includes cumulative results for 198 algorithms evaluated to date).

Executive Summary

OVERVIEW This is a draft supplement to the second report on the performance of face recognition algorithms on faces occluded by protective face masks [2] commonly worn to reduce inhalation and exhalation of viruses. Inspired by the COVID-19 pandemic response, this is a continuous study being run under the Ongoing Face Recognition Vendor Test (FRVT) executed by the National Institute of Standards and Technology (NIST). In our first report [7], we tested ”pre-pandemic” algorithms that were already submitted to FRVT 1:1 prior to mid-March 2020. This report augments its predecessor with results for more recent algorithms provided to NIST after mid-March 2020. While we do not have information on whether or not a particular algorithm was designed with face coverings in mind, the results show evidence that a number of developers have adapted their algorithms to support face recognition on subjects potentially wearing face masks. The algorithms tested were one-to-one algorithms submitted to the FRVT 1:1 Verification track.

WHAT'S NEW This report includes

- ▷ Results from testing 266 face recognition algorithms provided to NIST since mid-March 2020
- ▷ Cumulative results for 319 algorithms evaluated to date (submitted both prior to and after mid-March 2020)

MOTIVATION Traditionally, face recognition systems (in cooperative settings) are presented with mostly non-occluded faces, which include primary facial features such as the eyes, nose, and mouth. However, there are a number of circumstances in which faces are occluded by masks such as in pandemics, medical settings, excessive pollution, or laboratories. Inspired by the COVID-19 pandemic response, the widespread requirement that people wear protective face masks in public places has driven a need to understand how cooperative face recognition technology deals with occluded faces, often with just the periocular area and above visible. An increasing number of research publications have surfaced on the topic of face recognition on people wearing masks along with face-masked research datasets [9]. A number of commercial providers have announced the availability of face recognition algorithms capable of handling face masks, and this report documents performance results for 266 algorithms submitted to NIST after mid-March 2020. This report includes results for all algorithms evaluated to date. At the time of this writing, we are not aware of any large-scale, independent, and publicly reported evaluation on the effects of face mask occlusion on face recognition.

WHAT WE DID The NIST Information Technology Laboratory (ITL) quantified the accuracy of face recognition algorithms on faces occluded by masks applied digitally to a large set of photos that has been used in an FRVT verification benchmark since 2018. These algorithms were submitted to FRVT 1:1 and includes 266 new algorithms provided to NIST since mid-March 2020. While we do not have information on whether or not a particular algorithm was designed with face coverings in mind, the algorithms were submitted with the expectation that NIST would execute them on masked face images. Using the original unmasked images to form a baseline for accuracy, we measured the impact of occlusion by digitally applying a mask to the face and varying mask shape, mask color, and nose coverage.

We ran these algorithms over a large set of photographs collected in U.S. governmental applications that are currently in operation: **application photographs** from a global population of applicants for immigration benefits and **border crossing photographs** of travelers entering the United States. Both datasets were collected for authorized travel or immigration processes.

WHAT WE DID (CONTINUED)

The application photos (used as reference images) have good compliance with image capture standards. The border crossing photos (used as probe images) are not in good compliance with image capture standards given possible constraints on capture equipment, duration, facilities, and environment. We evaluated the case where the application photos were left unmasked, and synthetic masks were applied to the border crossing photos. This mimics an operational scenario where a person wearing a mask attempts to authenticate against a prior visa or passport photo. We also evaluated when both the application photos and border crossing photos were masked. This mimics, for example, a seamless travel scenario through an airport where a masked face image captured at check-in is enrolled and used during subsequent authentication attempts of the passenger still wearing a face mask. Together these datasets allowed us to process a total of 6.2 million images through a cumulative total of 319 algorithms.

Our use of software to apply masks to face images has the following advantages: it allows very rapid characterization of the effect of masks on face recognition; it allows controlled exploration of factors such as mask size, shape, and color; it affords repeatability, which is key to the fair comparison of algorithms; it scales to very large datasets - in our study, some 6.2 million photographs - which allows fine-grained characterization of false positive rates in addition to false negative rates. Conversely, our use of digital masks presents a number of limitations - please see the *Limitations* section of this executive summary for a more detailed discussion on the limitations of this study.

WHAT WE FOUND

The following results represent observations on algorithms provided to NIST both before and after the COVID-19 pandemic to date. We do not have information on whether or not a particular algorithm was designed with face coverings in mind. The results documented capture a snapshot of algorithms submitted to the FRVT 1:1 in face recognition on subjects potentially wearing face masks.

▷ **False rejection performance**: All algorithms submitted after the pandemic continue to give increased false non-match rates (FNMR) when the probes are masked. A number of developers have submitted algorithms after the pandemic showing significantly improved accuracy and are now among the most accurate in our test. Using border crossing images, without masks, the most accurate algorithms will fail to authenticate about 0.2% of persons while falsely accepting no more than 1 in 100000 impostors (i.e. FNMR= 0.002 at FMR= 0.00001). With a typical medium coverage wide mask and the most accurate algorithms, this failure rate rises to about 1 to 2% (FNMR = 0.01 to 0.02). This is noteworthy given that around 70% of the face area is occluded by the mask. However, many algorithms submitted since mid-March 2020 remain much less tolerant: some algorithms that are quite competitive with unmasked faces (FNMR < 0.01) still fail to authenticate between 10% to 40% of masked images (FNMR $\rightarrow 0.4$).

See Figures 14, 15 and Table 8

For the case where both the enrollment and verification images are masked, interestingly, many algorithms show a reduction in false non-match rates compared to when only the verification image is masked, at a fixed threshold. While the reduction in FNMR is favorable, we observe much larger false match rates when both images are masked. These findings are discussed in subsequent sections of this executive summary. *See Figure 73*

In cooperative access control applications, false rejections can traditionally be remedied by users making second attempts. This is effective when users correct pose, expression, or illumination aspects of their presentation. With masked faces, however, a second attempt may not be effective if the failure is a systematic property of the algorithm.

FNMR(T) "False non-match rate"
FMR(T) "False match rate"

WHAT WE FOUND (CONTINUED)

▷ **Evolution of algorithms on face masks**: We observe that a number of algorithms submitted since mid-March 2020 show notable reductions in error rates with face masks over their pre-pandemic predecessors. When comparing error rates for unmasked versus masked faces, the median FNMR across algorithms submitted since mid-March 2020 has been reduced by around 35% from the median pre-pandemic results. The figure below presents examples of developer evolution on both masked and unmasked datasets. For some developers, false rejection rates in their algorithms submitted since mid-March 2020 decreased by as much as a factor of 10 over their pre-pandemic algorithms, which is evidence that some providers are adapting their algorithms to handle face masks. However, in the best cases, when comparing results for unmasked images to masked images, false rejection rates have increased from 0.2%-0.4% (unmasked) to 1%-3% (masked). The current performance of face recognition with face masks is comparable to the state-of-the-art on unmasked images in mid-2018 [**?**].

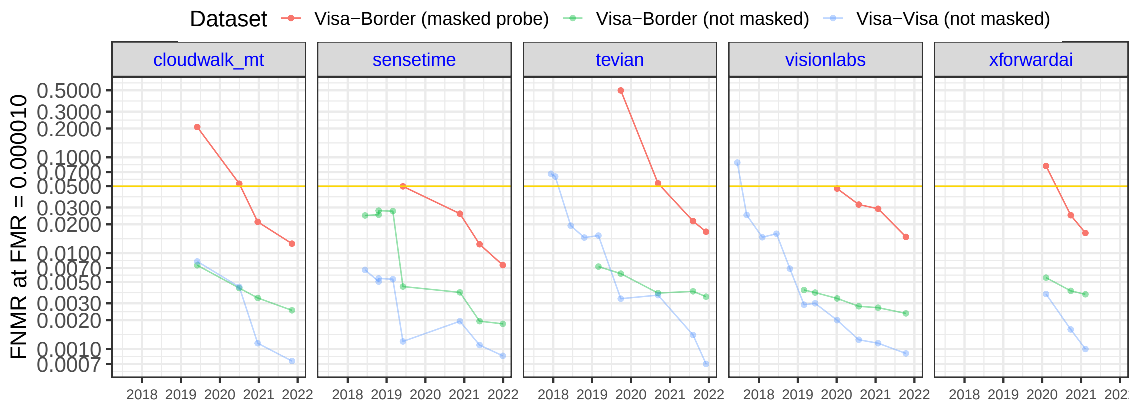

Figure 1: Examples of developer evolution of accuracy on masked and unmasked datasets.

See Figures 14, 5, and 15

▷ **False acceptance performance**: As most systems are configured with a fixed threshold, it is necessary to report both false negative and false positive rates for each group at that threshold. When comparing a masked probe to an unmasked enrollment photo, in most cases, false match rates (FMR) are reduced by masks. The effect is generally modest with reductions in FMR usually being smaller than a factor of two. This property is valuable in that masked probes do not impart adverse false match security consequences for verification.

However, when both the enrollment and verification images are masked, most algorithms give elevated false match rates, with FMR ranging from 10 to 100 times higher than when only the probe is masked or both images are unmasked, at the same threshold. This behavior applies to most algorithms tested, with the exception of particular algorithms from a small number of developers (e.g., idemia-006, pensees-001, neurotechnology-011, glory-003, geo-003). *See Figure 73*

▷ **Mask-agnostic face recognition**: All 1:1 verification algorithms submitted to the FRVT test since the start of the pandemic are evaluated on both masked and unmasked datasets. The test is designed this way to mimic operational reality: some images will have masks, some will not (especially enrollment samples from a database or ID card). And to the extent that the use of protective masks will exist for some time, our test will continue to evaluate algorithmic capability on verifying all combinations of masked and unmasked faces.

WHAT WE FOUND (CONTINUED)

Several developers have developed algorithms that work with any combination of masked and unmasked images, generating approximately constant FMR across any masked/unmasked combination, and similarly, yield approximately constant FNMR across masked-probe and masked-enrollment-and-probe combinations.

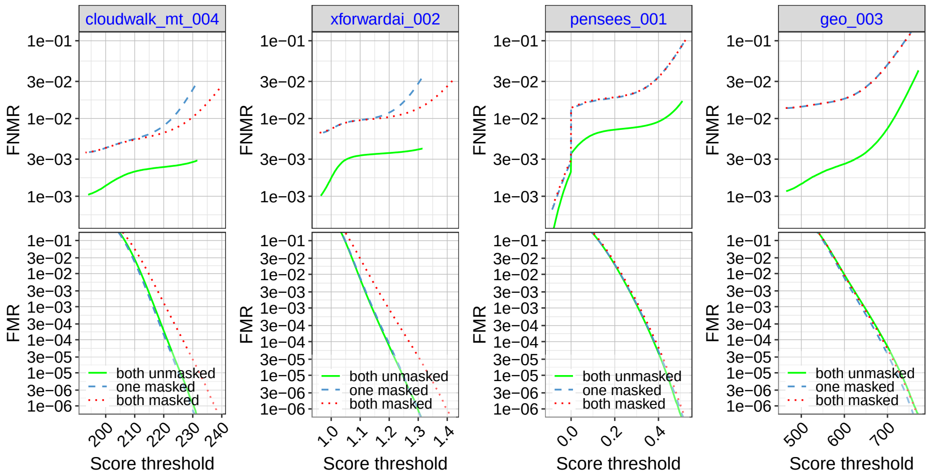

Figure 2: FNMR and FMR calibration curves on masked/unmasked combinations.

An example of an integrated approach might be: 1) inclusion of a mask detector 2) on an unmasked image, extract features from both the full face and the periocular region 3) on a detected masked image, extract features from the periocular region 4) at match time, compare full-face templates when both images are unmasked, and periocular templates otherwise.

▷ **Coverage of the masks**: Masks that occlude more of the face give larger false non-match rates. We surveyed over the extent to which the mask covers the nose, from not at all ("low") to typical ("medium") to near the eyes ("high"). We baselined those with unmasked faces with the result that FNMR increases as the amount of mask coverage increases. However, algorithms vary considerably in the their tolerance of coverage, so readers should consult tabulated values for specific algorithms.

See Table 8 and Figures 17, 19

We included the "low" option not because it is a common position for a mask but as an option for authentication applications where it would be tenable to ask the user to pull the mask down to just below the nose for the duration of the authentication attempt.

▷ **Color of the masks**: We considered white, light-blue, red, and black masks. Some algorithms have higher error rates in black and red masks than light-blue and white masks. The reason for observed accuracy differences between mask color is unknown but is a point for consideration by impacted developers. Mask color also affects the rate at which some algorithms fail to produce a template from an image. *See Figure 46 and Table 16*

▷ **Shape of the masks**: The shape of the masks matters. Full-face-width masks generally cover more of the face than rounder N95 type masks. Post-pandemic algorithm results show that wide-width masks generally give false negative rates about a factor of 1.6 higher than do rounder type masks. *See Figure 16*

▷ **Failure to detect and template:** The false negative rates in this report include the effects of both face detection and localization errors, and low-similarity matching errors. We separately include tables detailing how often an algorithm does not make a template from an input image. While many algorithms give low failure-to-template rates, some give high values ranging close to 100%. Conversely, the successful creation of a template does not guarantee proper facial localization. Such localization failures will not be captured as a failure to detect and template event but will impact accuracy rates nonetheless. *See Table 16 and Figure 18*

LIMITATIONS As a simulation, this study likely doesn't fully capture the effects of masks on face recognition. Particularly the following points should be weighed by readers in the near term. Some of these will be addressed in subsequent work at NIST.

- **Train algorithms:** As with all NIST evaluations, we regard the software as a black box whose parameters (models) remain fixed for the entirety of its use without learning from the test data. We do not train or fine-tune algorithms.
- **Evaluate one-to-many algorithms:** We have only run one-to-one verification algorithms with masks. This elicits data on the effect of masks on the underlying feature extraction and discrimination of algorithms and can therefore be be expected to give first-order indications of the effect on one-to-many identification algorithms.
- **Consider the effect of eye occlusion:** We did not address the effect of eye-glasses or eye-protection. While our dataset includes examples of people wearing glasses, we didn't collect such data nor simulate it with digital addition.
- **Test with images of real masks:** Given time and resource constraints, we didn't collect photos of subjects wearing masks. The possible downsides of this are several. First, our digital masks are tailored to faces; while a few don't fit realistically, mass-produced real masks may not fit all actual persons correctly either. We were not able to pursue an exhaustive simulation of the endless variations in color, design, shape, texture, bands, and ways masks can be worn. Second, because many cameras run with exposure-control, it is possible that a dark mask will cause less light to be reflecting and the camera to increase gain on the sensor causing overexposure of the periocular region. Likewise a white mask could lead to underexposure problems. Third, it is possible that some cameras that include a face detector, may fail to focus or acquire a masked face correctly.
- **Use textured masks:** All masks synthesized by NIST in this study have a uniform color. The consequences of this are that we do not capture the impact of mask texture or pattern on face recognition. The possibility exists for patterned masks to induce higher facial localization errors, which is not captured in our current study. We received a suggestion that such information may serve as a soft biometric, in that a subject that always wears the same textured mask will be more identifiable. We don't intend to encourage algorithm development along this line, because as mass-produced high-efficacy masks become more common, mask diversity may actually drop.
- **Study demographic effects on masked images:** This report estimates overall performance of existing algorithms on recognition of faces occluded by masks. We deferred tabulating accuracy for different demographic groups until more capable mask-enabled algorithms have been submitted to FRVT.
- **Evaluate algorithms on non-cooperative, unconstrained imagery:** This report documents results for matching masked webcam images to unmasked portrait-style photos. While the properties of the two sets of images differ, subjects are operating in cooperative mode and are for the most part, looking at the camera.
- **Consider effects of human examination:** This report does not consider the various ways humans are involved in face recognition systems. For example, analysts can correct face detection or localization errors induced by masks, prior to automated recognition. Likewise, humans are often tasked with adjudication of images following a rejection or other exception from an automated system. Analysis of human capability and role is pertinent to those operations, but is beyond the scope of this study.

IMPLICATIONS AND FUTURE WORK

Know Your Algorithm: Operational implementations usually employ a single face recognition algorithm. Given algorithm-specific sensitivities to masks and other image or subject properties, it is incumbent upon the system owner to know their algorithm. While publicly available test data from NIST and elsewhere can inform owners, it will usually be informative to specifically measure accuracy of the operational algorithm on the operational image data collected with actual masks.

NIST plans on releasing a series of reports, iteratively assessing different aspects and use cases of face masking on recognition performance.

ACKNOWLEDGMENTS

This work was conducted in collaboration with the Department of Homeland Security's Science & Technology Directorate (S&T), Office of Biometric Identity Management (OBIM), and Customs and Border Protection (CBP). Additionally, the authors are grateful to staff in the NIST Biometrics Research Laboratory for infrastructure supporting rapid evaluation of algorithms.

DISCLAIMER

INSTITUTIONAL REVIEW BOARD

The National Institute of Standards and Technology's Research Protections Office reviewed the protocol for this project and determined it is not human subjects research as defined in Department of Commerce Regulations, 15 CFR 27, also known as the Common Rule for the Protection of Human Subjects (45 CFR 46, Subpart A).

Contents

List of Tables

List of Figures

1 Face Mask Effects

1.1 Status

NIST has conducted a series of tests aimed at quantifying face recognition accuracy for people wearing masks. Our initial approach has been to apply masks to faces digitally (i.e., using software to apply a synthetic mask). This allowed us to leverage large datasets that we already have. This report documents results for 1:1 verification algorithms. In our first report [7], we tested ”pre-pandemic” algorithms that were already submitted to FRVT 1:1 prior to mid-March 2020. This report augments its predecessor with results for more recent algorithms provided to NIST **after the COVID-19 pandemic**. While we do not have information on whether or not a particular algorithm was designed with face coverings in mind, the algorithms were submitted with the expectation that NIST would execute them on masked face images. In addition to reporting results for when only the verification image is masked, we also document the effects for the case when both enrollment and verification images are masked. This report quantifies the effect of masks on both false negative and false positives match rates and tracks developer evolution of face recognition accuracy with face masks.

The FRVT evaluation is an ongoing test that remains open to new participation. Comments and suggestions should be directed to frvt@nist.gov.

1.2 Introduction

The majority of face recognition systems have been deployed in applications where subjects make cooperative presentations to a camera, for example as part of an application for a benefit or ID credential, or as during access control. With very few exceptions such images would not include face masks or other occlusions. However, with the COVID-19 pandemic, we can anticipate a demand to authenticate persons wearing masks, for example in immigration settings, without the need to the subjects to remove those masks. This presents a problem for face recognition, because regions of the face occluded by masks - the mouth and nose - include information useful for both recognition and, potentially, the detection stage that precedes it.

Previous work on face recognition of occluded faces has been directed at situations such as crime scenes where subjects were actively un-cooperative i.e. acting to evade face detection and recognition. Those applications are often characterized by image properties (low resolution, video compression, uncontrolled head orientation) that are known [4] to degrade recognition accuracy.

2 Image Datasets

2.1 Application Images

The images are collected in an attended interview setting using dedicated capture equipment and lighting. The images are of size 300x300 pixels. The images are all high-quality frontal portraits collected in immigration offices and with a white background. As such, potential quality related drivers of high false match rates (such as blur) can be expected to be absent. The images are encoded as ISO/IEC 10918 i.e. JPEG. Over a random sample of 1000 images, the images have compressed file sizes (mean: 42KB, median: 58KB, 25-th percentile: 15KB, and 75-th percentile: 66KB). The implied bit-rates are mostly benign and superior to many e-Passports. When these images are provided as input into the algorithm, they are labeled with the type ”ISO”.

Figure 3: Examples of images with properties similar to the enrollment application photos used in this study. The subjects in the photos are all NIST employees.

2.2 Webcam Images

These images are taken with a camera oriented by an attendant toward a cooperating subject. This is done under time constraints, so there are roll, pitch, and yaw angle variations. Also, background illumination is sometimes bright, so the face is under exposed. Sometimes, there is perspective distortion due to close range images. The images are generally in poor conformance with the ISO/IEC 19794-5 Full Frontal image type. The images have mean interocular distance of 38 pixels. The images are all live capture. When these images are provided as input into the algorithm, they are labeled with the type ”WILD”. Examples of such images are included in Figure 4 and Figure 4 in NIST Interagency Report 8271. Results for verification of these images (unmasked) appear in FRVT Part 1 - Verification both compared against images of the same type, and with those described in section 2.1.

Description	#
Total images	6 244 865
Application (enrollment) images	1 019 232
Subjects in application images	1 019 232
Webcam (verification) images	5 225 633
Subjects in webcam (verification) images	2 535 329
Mated comparisons	3 225 633
Impostor comparisons	200 000 000
Subjects in mated comparisons	535 329
Subjects in impostor comparisons	3 019 232

Table 1: Summary quantities of the dataset used in this evaluation.

2.3 Synthetically Masked Images

In this test, synthetically-generated masks were overlaid on top of 1) just the probe image (webcam images described in Section 2.2) or 2) both the enrollment (application photos described in Section 2.1) and probe images. The Dlib [6] C++ toolkit version 19.19 was used to detect and establish key facial points on the face, and with the facial points, solid masks of different shape, height, and color were drawn on the face. The exact Dlib facial points and details used to generate the masks are documented in Appendix A. In the event that Dlib was unable to detect a face in the image, eye coordinates were used to generate a mask leveraging standardized token frontal geometry [1].

Examples of synthetically-masked probe images are presented in Figures 4.

FNMR(T) "False non-match rate"
FMR(T) "False match rate"

Figure 4: Examples of synthetically-generated face masks used in this study. The original images are from the NIST MEDS-II Dataset [3]. They were collected in operational settings using the same camera and procedure as is used for the border images that form the mainstay of the experiments in this report.

3 Metrics

3.1 Matching accuracy

Given a vector of N genuine scores, u, the false non-match rate (FNMR) is computed as the proportion below some threshold, T:

$$\text{FNMR}(T) = 1 - \frac{1}{N} \sum_{i=1}^{N} H(u_i - T) \tag{1}$$

where $H(x)$ is the unit step function, and $H(0)$ taken to be 1.

Similarly, given a vector of N impostor scores, v, the false match rate (FMR) is computed as the proportion above T:

$$\text{FMR}(T) = \frac{1}{N} \sum_{i=1}^{N} H(v_i - T) \tag{2}$$

The threshold, T, can take on any value. We typically generate a set of thresholds from quantiles of the observed impostor scores, v, as follows. Given some interesting false match rate range, $[\text{FMR}_L, \text{FMR}_U]$, we form a vector of K thresholds corresponding to FMR measurements evenly spaced on a logarithmic scale

$$T_k = Q(1 - \text{FMR}_k) \tag{3}$$

where Q is the quantile function, and FMR_k comes from

$$\log_{10} \text{FMR}_k = \log_{10} \text{FMR}_L + \frac{k}{K} \left[\log_{10} \text{FMR}_U - \log_{10} \text{FMR}_L\right] \tag{4}$$

Detection error tradeoff (DET) characteristics are plots of FNMR(T) vs. FMR(T). These are plotted with $\text{FMR}_U \rightarrow 1$ and FMR_L as low as is sustained by the number of impostor comparisons, N. This is somewhat higher than the "rule of three" limit $3/N$ [5] because samples are not independent, due to re-use of images.

3.2 Failure to Enroll

Failure to enroll (FTE) is the proportion of failed template generation attempts. Failures can occur because the software throws an exception, or because the software electively refuses to process the input image. This would typically occur if a face is not detected. FTE is measured as the number of function calls that give EITHER a non-zero error code OR that give a "small" template. This is defined as one whose size is less than 60 bytes. This second rule is needed because some algorithms incorrectly fail to return a non-zero error code when template generation fails yet do return a valid default data structure.

The effects of FTE are included in the accuracy results of this report by regarding any template comparison involving a failed template to produce a low similarity score. Thus higher FTE results in higher FNMR and lower FMR.

4 Algorithms

The FRVT activity is open to participation worldwide, and the test will evaluate submissions on an ongoing basis. There is no charge to participate. The process and format of algorithm submissions to NIST are described in the FRVT 1:1 Verification Application Programming Interface (API) [8] document. Participants provide their submissions in the form of libraries compiled on a specific Linux kernel, which are linked against NIST's test harness to produce executables. NIST provides a validation package to participants to ensure that NIST's execution of submitted libraries produces the expected output on NIST's test machines.

This report documents the results of algorithms submitted to FRVT 1:1 for testing both before (prior to mid-March 2020) and after the COVID-19 pandemic. Table 7 lists the algorithms that were tested. Note that algorithms that are expired or retired are not included in this report.

	Developer	Algorithm	Submission Date
1	20Face	20face-000	2021-04-12
2	20Face	20face-001	2021-09-29
3	3Divi	3divi-006	2021-04-14
4	3Divi	3divi-007	2021-09-27
5	ACI Software	acisw-003	2020-08-03
6	ACI Software	acisw-007	2021-11-15
7	ADVANCE.AI	advance-002	2019-12-19
8	ADVANCE.AI	advance-003	2021-08-05
9	ASUSTek Computer Inc	asusaics-000	2019-10-24
10	AYF Technology	ayftech-001	2020-07-06
11	Ability Enterprise - Andro Video	androvideo-000	2021-01-25
12	Acer Incorporated	acer-001	2020-06-30
13	Acer Incorporated	acer-002	2021-11-10
14	Adera Global PTE	adera-002	2021-02-16
15	Adera Global PTE	adera-003	2021-07-12
16	Ai First	aifirst-001	2019-11-21
17	AiUnion Technology	aiunionface-000	2019-10-22
18	Aigen	aigen-001	2020-10-06
19	Aigen	aigen-002	2021-03-15
20	Ajou University	ajou-001	2021-03-08
21	Akurat Satu Indonesia	ptakuratsatu-000	2020-09-11
22	Alchera Inc	alchera-002	2021-03-05
23	Alchera Inc	alchera-003	2021-07-13
24	Alfabeta	alfabeta-001	2021-12-02
25	Alice Biometrics	alice-000	2021-06-15
26	AlphaSSTG	alphaface-002	2020-02-20
27	Anke Investments	anke-005	2019-11-21
28	Antheus Technologia	antheus-000	2019-12-05
29	Antheus Technologia	antheus-001	2020-06-25
30	AnyVision	anyvision-005	2021-02-03
31	Armatura LLC	armatura-001	2022-01-04
32	AuthenMetric	authenmetric-003	2021-08-09
33	AuthenMetric	authenmetric-004	2022-01-03
34	Aware	aware-005	2020-02-27
35	Aware	aware-006	2021-07-03
36	Awidit Systems	awiros-001	2019-09-23
37	Awidit Systems	awiros-002	2020-10-28
38	BOE Technology Group	boetech-002	2021-12-21
39	Bee the Data	beethedata-000	2021-07-26
40	Beihang University-ERCACAT	ercacat-001	2020-07-06
41	Beijing Alleyes Technology	alleyes-000	2020-03-09
42	Beijing DeepSense Technologies	deepsense-000	2021-03-19
43	Beijing Hisign Technology	hisign-001	2021-09-24
44	Beijing Mendaxia Technology	mendaxiatech-000	2021-09-15
45	Beyne.AI	beyneai-000	2022-01-03
46	BioID Technologies SA	bioidtechswiss-001	2020-08-28
47	BioID Technologies SA	bioidtechswiss-002	2021-02-17
48	Biocube Matrics	biocube-001	2021-09-08
49	BitCenter UK	farfaces-001	2021-04-09
50	Bresee Technology	bresee-001	2020-12-30
51	CSA IntelliCloud Technology	intellicloudai-001	2019-08-13
52	CSA IntelliCloud Technology	intellicloudai-002	2020-12-17
53	CTBC Bank	ctbcbank-000	2019-06-28
54	CUDO Communication	cudocommunication-001	2021-10-20
55	Camvi Technologies	camvi-004	2019-07-12
56	Canon Inc	canon-002	2020-12-29
57	Canon Inc	canon-003	2021-09-15

Table 2: List of algorithms included in this report. Algorithms in black were submitted prior to mid-March 2020, and algorithms in blue were submitted thereafter.

	Developer	Algorithm	Submission Date
58	China Electronics Import-Export Corp	ceiec-003	2020-01-06
59	China Electronics Import-Export Corp	ceiec-004	2021-01-18
60	China University of Petroleum	upc-001	2019-06-05
61	Chinese University of Hong Kong	cuhkee-001	2020-03-18
62	Chosun University	chosun-001	2020-07-01
63	Chosun University	chosun-002	2020-11-25
64	Chunghwa Telecom	chtface-003	2020-06-24
65	Chunghwa Telecom	chtface-004	2021-10-08
66	Clearview AI Inc	clearviewai-000	2021-09-22
67	Closeli Inc	closeli-001	2021-07-15
68	CloudSmart Consulting LLC	csc-002	2021-03-24
69	CloudSmart Consulting LLC	csc-003	2021-08-26
70	Cloudmatrix	cloudmatrix-000	2021-10-22
71	Cloudwalk - Hengrui AI Technology	cloudwalk-hr-003	2020-09-25
72	Cloudwalk - Hengrui AI Technology	cloudwalk-hr-004	2021-02-10
73	Cloudwalk - Hengrui AI Technology	cloudwalk-mt	2021-11-09
74	Cloudwalk - Moontime Smart Technology	cloudwalk-mt-003	2020-12-22
75	Code Everest Pvt	facex-001	2021-03-08
76	Code Everest Pvt	facex-002	2021-08-24
77	Cognitec Systems GmbH	cognitec-002	2021-02-24
78	Cognitec Systems GmbH	cognitec-003	2021-07-30
79	Coretech Knowledge Inc	coretech-000	2021-07-12
80	Corsight	corsight-001	2021-03-11
81	Corsight	corsight-002	2021-09-01
82	Cortica	cor-001	2020-09-24
83	Cubox	cubox-001	2020-12-07
84	Cubox	cubox-002	2021-08-24
85	Cybercore	cybercore-000	2020-08-26
86	Cyberlink Corp	cyberlink-007	2021-07-16
87	Cyberlink Corp	cyberlink-008	2022-01-07
88	DSK	dsk-000	2019-06-28
89	Dahua Technology	dahua-006	2020-12-30
90	Dahua Technology	dahua-007	2021-12-20
91	Daon	daon-000	2021-11-03
92	Decatur Industries Inc	decatur-000	2020-08-18
93	Decatur Industries Inc	decatur-001	2021-09-27
94	Deepglint	deepglint-003	2021-03-03
95	Deepglint	deepglint-004	2021-09-17
96	Deepsense	dps-000	2021-07-16
97	Dermalog	dermalog-008	2021-03-25
98	Dermalog	dermalog-009	2021-10-06
99	DiDi ChuXing Technology	didiglobalface-001	2019-10-23
100	Ekin Smart City Technologies	ekin-002	2021-05-04
101	Enface	enface-000	2021-04-09
102	Enface	enface-001	2021-12-17
103	Euronovate SA	euronovate-001	2021-11-15
104	Expasoft LLC	expasoft-001	2020-09-03
105	Expasoft LLC	expasoft-002	2021-07-26
106	FaceOnLive Inc	faceonlive-001	2021-11-23
107	FaceSoft	facesoft-000	2019-07-10
108	FaceTag Co	facetag-000	2021-03-22
109	FaceTag Co	facetag-002	2022-01-06
110	Fiberhome Telecommunication Technologies	fiberhome-nanjing-003	2021-03-12
111	Fiberhome Telecommunication Technologies	fiberhome-nanjing-004	2021-09-14
112	Fincore Ltd	fincore-000	2021-06-07
113	Fujitsu Research and Development Center	fujitsulab-002	2021-02-24
114	Fujitsu Research and Development Center	fujitsulab-003	2021-07-12

Table 3: List of algorithms included in this report. Algorithms in black were submitted prior to mid-March 2020, and algorithms in blue were submitted thereafter.

	Developer	Algorithm	Submission Date
115	Gemalto Cogent	cogent-005	2020-12-29
116	Gemalto Cogent	cogent-006	2021-07-28
117	GeoVision Inc	geo-002	2021-04-01
118	GeoVision Inc	geo-003	2021-09-15
119	Glory	glory-002	2019-11-12
120	Glory	glory-003	2021-01-15
121	Gorilla Technology	gorilla-007	2021-06-28
122	Gorilla Technology	gorilla-008	2021-11-08
123	Griaule	griaule-000	2021-08-20
124	Guangzhou Pixel Solutions	pixelall-006	2021-06-17
125	Guangzhou Pixel Solutions	pixelall-007	2021-12-01
126	Herta Security	hertasecurity-000	2021-01-05
127	HyperVerge Inc	hv-001	2020-12-13
128	HyperVerge Inc	hyperverge-002	2021-05-27
129	ICM Airport Technics	icm-002	2020-11-13
130	ICM Airport Technics	icm-003	2021-09-06
131	ID3 Technology	id3-006	2020-12-17
132	ID3 Technology	id3-008	2021-11-10
133	ITMO University	itmo-007	2020-01-06
134	ITMO University	itmo-008	2021-11-19
135	IVA Cognitive	ivacognitive-001	2021-01-29
136	Idemia	idemia-007	2020-12-04
137	Idemia	idemia-008	2021-07-07
138	Imageware Systems	iws-000	2020-08-12
139	Imagus Technology Pty	imagus-002	2020-12-31
140	Imagus Technology Pty	imagus-004	2021-09-20
141	Imperial College London	imperial-002	2019-08-28
142	Incode Technologies Inc	incode-009	2021-06-22
143	Incode Technologies Inc	incode-010	2021-10-22
144	Innef Labs	innefulabs-000	2020-09-04
145	Innovative Technology	innovativetechnologyltd-002	2020-02-26
146	Innovatrics	innovatrics-007	2020-08-19
147	Innovatrics	innovatrics-008	2021-12-15
148	InsightFace AI	insightface-000	2021-03-17
149	InsightFace AI	insightface-001	2021-09-27
150	Institute of Computing Technology	icthtc-000	2020-11-29
151	Institute of Information Technologies	iit-002	2019-12-04
152	Institute of Information Technologies	iit-003	2020-12-01
153	Intel Research Group	intelresearch-003	2021-01-18
154	Intel Research Group	intelresearch-004	2021-08-24
155	Intellivision	intellivision-002	2019-08-23
156	IrexAI	irex-000	2020-12-17
157	Kakao Enterprise	kakao-005	2021-03-09
158	Kakao Pay Corp	kakaopay-001	2021-07-06
159	Kedacom International Pte	kedacom-000	2019-06-03
160	Kneron Inc	kneron-005	2020-02-21
161	Kookmin University	kookmin-002	2021-03-05
162	KuKe3D Technology	kuke3d-001	2021-10-28
163	Lema Labs	lemalabs-001	2021-04-13
164	Line Corporation	line-000	2021-03-31
165	Line Corporation	line-001	2021-09-26
166	Lomonosov Moscow State University	intsysmsu-002	2020-03-12
167	Lookman Electroplast Industries	lookman-004	2019-06-03
168	Luxand Inc	luxand-000	2019-11-07
169	MVision	mvision-001	2019-11-12
170	Mantra Softech India	mantra-000	2021-10-28
171	Maxvision Technology	maxvision-000	2021-10-27

Table 4: List of algorithms included in this report. Algorithms in black were submitted prior to mid-March 2020, and algorithms in blue were submitted thereafter.

	Developer	Algorithm	Submission Date
172	Megvii/Face++	megvii-003	2021-03-08
173	Megvii/Face++	megvii-004	2021-11-19
174	Minivision	minivision-000	2020-10-28
175	Mobbeel Solutions	mobbl-001	2021-06-16
176	Mobbeel Solutions	mobbl-002	2021-12-16
177	Mobipin Technology	mobipintech-000	2021-11-23
178	Momentum Digital	sertis-000	2019-10-07
179	Momentum Digital	sertis-002	2021-05-13
180	MoreDian Technology	moredian-000	2021-02-24
181	Multi-Modality Intelligence	multimodality-000	2021-10-19
182	N-Tech Lab	ntechlab-010	2021-04-30
183	N-Tech Lab	ntechlab-011	2021-09-13
184	NEO Systems	neosystems-002	2021-07-03
185	NEO Systems	neosystems-003	2021-11-11
186	NHN Corp	nhn-001	2021-03-15
187	NHN Corp	nhn-002	2021-07-15
188	NSENSE Corp	nsensecorp-002	2021-05-06
189	NSENSE Corp	nsensecorp-003	2021-10-29
190	Nanjing Kiwi Network Technology	kiwitech-000	2021-03-19
191	Naver Corp	clova-000	2020-10-21
192	Neosecu Co	openface-001	2021-06-15
193	Netbridge Technology Incoporation	netbridgetech-001	2020-01-08
194	Netbridge Technology Incoporation	netbridgetech-002	2020-08-11
195	Neurotechnology	neurotechnology-012	2021-07-26
196	Neurotechnology	neurotechnology-013	2022-01-07
197	Nodeflux	nodeflux-002	2019-08-13
198	NotionTag Technologies Private Limited	notiontag-001	2021-03-04
199	NotionTag Technologies Private Limited	notiontag-002	2021-09-17
200	Omnigarde Ltd	omnigarde-000	2021-04-05
201	Omnigarde Ltd	omnigarde-001	2021-08-23
202	Oz Forensics LLC	oz-003	2021-08-09
203	Oz Forensics LLC	oz-004	2021-12-13
204	PXL Vision AG	pxl-001	2020-06-30
205	Panasonic R+D Center Singapore	psl-008	2021-07-21
206	Panasonic R+D Center Singapore	psl-009	2021-12-08
207	Papilon Savunma	papsav1923-001	2021-03-10
208	Paravision (EverAI)	paravision-004	2019-12-11
209	Paravision (EverAI)	paravision-008	2021-06-30
210	Pensees Pte	pensees-001	2020-08-17
211	Qnap Security	qnap-000	2021-08-09
212	Qnap Security	qnap-001	2021-12-09
213	Quantasoft	quantasoft-003	2021-04-19
214	Rank One Computing	rankone-011	2021-08-27
215	Rank One Computing	rankone-012	2021-12-27
216	Realnetworks Inc	realnetworks-004	2021-04-15
217	Realnetworks Inc	realnetworks-005	2021-09-27
218	Regula Forensics	regula-000	2021-04-13
219	Regula Forensics	regula-001	2021-12-14
220	Remark Holdings	remarkai-003	2021-06-22
221	Rendip	rendip-000	2021-04-19
222	Reveal Media Ltd	revealmedia-005	2021-09-24
223	Rokid Corporation	rokid-000	2019-08-01
224	SK Telecom	sktelecom-000	2021-07-09
225	SQIsoft	sqisoft-001	2021-07-27
226	SQIsoft	sqisoft-002	2021-11-03
227	Samsung S1 Corp	s1-003	2021-08-24
228	Samsung S1 Corp	s1-004	2022-01-04

Table 5: List of algorithms included in this report. Algorithms in black were submitted prior to mid-March 2020, and algorithms in blue were submitted thereafter.

	Developer	Algorithm	Submission Date
229	Samsung-SDS	samsungsds-000	2021-10-28
230	Satellite Innovation/Eocortex	eocortex-000	2020-08-26
231	Scanovate	scanovate-002	2020-06-26
232	Scanovate	scanovate-003	2021-11-15
233	Securif AI	securifai-003	2021-08-03
234	Securif AI	securifai-004	2021-12-21
235	Sensetime Group	sensetime-005	2021-05-24
236	Sensetime Group	sensetime-006	2021-12-28
237	Seventh Sense Artificial Intelligence	seventhsense-000	2021-06-29
238	Shanghai Jiao Tong University	sjtu-003	2020-11-02
239	Shanghai Jiao Tong University	sjtu-004	2021-05-13
240	Shanghai Ulucu Electronics Technology	uluface-002	2019-07-10
241	Shanghai University - Shanghai Film Academy	shu-002	2019-12-10
242	Shanghai University - Shanghai Film Academy	shu-003	2020-06-24
243	Shenzhen AiMall Tech	aimall-002	2020-03-12
244	Shenzhen AiMall Tech	aimall-003	2020-08-12
245	Shenzhen Intellifusion Technologies	intellifusion-002	2020-03-18
246	Shenzhen University-Macau University of Science and Technology	sztu-000	2020-12-17
247	Shenzhen University-Macau University of Science and Technology	sztu-001	2021-07-13
248	Smart Engines	smartengines-000	2021-08-25
249	Sodec App Inc	sodec-000	2021-06-02
250	Staqu Technologies	staqu-000	2020-07-15
251	Star Hybrid Limited	starhybrid-001	2019-06-19
252	Su Zhou NaZhiTianDi intelligent technology	nazhiai-000	2020-06-25
253	Suprema	suprema-000	2021-03-31
254	Suprema ID Inc	suprema-001	2021-09-23
255	Suprema ID Inc	supremaid-001	2021-05-04
256	Synology Inc	synology-000	2019-10-23
257	Synology Inc	synology-002	2020-08-20
258	TUPU Technology	tuputech-000	2019-10-11
259	Taiwan AI Labs	ailabs-001	2019-12-18
260	Taiwan-Certificate Authority Incorporation	twface-000	2021-05-14
261	Taiwan-Certificate Authority Incorporation	twface-001	2021-09-14
262	Tech5 SA	tech5-004	2020-03-09
263	Tech5 SA	tech5-005	2020-07-24
264	Techsign	techsign-000	2021-08-25
265	Tencent Deepsea Lab	deepsea-001	2019-06-03
266	Tevian	tevian-007	2021-08-06
267	Tevian	tevian-008	2021-12-06
268	TigerIT Americas LLC	tiger-005	2021-07-29
269	TigerIT Americas LLC	tiger-006	2021-12-13
270	Tinkoff Bank	tinkoff-001	2021-05-13
271	Toppan ID Gate	toppanidgate-000	2021-09-28
272	Toshiba	toshiba-004	2021-09-27
273	Tripleize	aize-001	2021-04-23
274	Tripleize	aize-002	2021-10-08
275	Trueface.ai	trueface-002	2021-03-29
276	Trueface.ai	trueface-003	2021-09-30
277	Unissey	unissey-001	2021-11-29
278	Universidade de Coimbra	visteam-001	2021-03-16
279	Universidade de Coimbra	visteam-002	2021-08-20
280	Veridas Digital Authentication Solutions S.L.	veridas-006	2021-04-15
281	Veridas Digital Authentication Solutions S.L.	veridas-007	2021-09-02
282	Verigram	verigram-000	2021-09-06
283	Verihubs	verihubs-inteligensia-000	2021-07-27
284	Via Technologies Inc	via-001	2020-01-08
285	Videmo Intelligente Videoanalyse	videmo-000	2019-12-19

Table 6: List of algorithms included in this report. Algorithms in black were submitted prior to mid-March 2020, and algorithms in blue were submitted thereafter.

	Developer	Algorithm	Submission Date
286	Videmo Intelligente Videoanalyse	videmo-001	2021-12-22
287	Videonetics Technology Pvt	videonetics-002	2019-11-21
288	Vietnam Posts and Telecommunications Group	vnpt-002	2021-06-08
289	Vietnam Posts and Telecommunications Group	vnpt-003	2021-12-01
290	Viettel Group	vts-000	2020-11-04
291	Viettel High Technology	viettelhightech-000	2021-08-04
292	Vigilant Solutions	vigilantsolutions-010	2021-04-07
293	Vigilant Solutions	vigilantsolutions-011	2021-08-07
294	VinAI Research VietNam	vinai-000	2020-09-24
295	VinBigData	vinbigdata-001	2022-01-06
296	Visage Technologies	visage-000	2020-12-09
297	Visidon	vd-002	2021-04-12
298	Visidon	vd-003	2021-10-12
299	Vision Intelligence Center of Meituan	meituan-000	2021-05-14
300	Vision-Box	visionbox-002	2021-04-29
301	VisionLabs	visionlabs-010	2021-01-25
302	VisionLabs	visionlabs-011	2021-10-13
303	Vocord	vocord-008	2020-01-31
304	Vocord	vocord-009	2020-12-28
305	Winsense	winsense-001	2019-10-16
306	Winsense	winsense-002	2020-11-20
307	Wuhan Tianyu Information Industry	wuhantianyu-001	2021-08-05
308	X-Laboratory	x-laboratory-001	2020-01-21
309	Xforward AI Technology	xforwardai-001	2020-09-25
310	Xforward AI Technology	xforwardai-002	2021-02-10
311	Xiamen University	xm-000	2020-10-19
312	YooniK	yoonik-002	2021-09-06
313	YooniK	yoonik-003	2022-01-06
314	Yuan High-Tech Development	yuan-002	2021-05-17
315	Yuan High-Tech Development	yuan-003	2021-09-17
316	Yuntu Data and Technology	ytu-000	2021-06-16
317	iQIYI Inc	iqface-000	2019-06-04
318	iQIYI Inc	iqface-003	2021-02-23
319	iSAP Solution Corporation	isap-002	2020-09-01
320	ioNetworks Inc	ionetworks-000	2021-07-20

Table 7: List of algorithms included in this report. Algorithms in black were submitted prior to mid-March 2020, and algorithms in blue were submitted thereafter.

5 Results

This section includes accuracy results for the 152 one-to-one verification algorithms listed in Section 4, of which 266 were submitted to FRVT after mid-March 2020 and are labeled in blue in figures and tables throughout this report. We do not include speed and computational resource requirements - they are given in Table 1 in the FRVT 1:1 report. Missing entries generally mean the algorithm was not run on that particular mask variation due to time and resource constraints. The results, which span many pages, are comprised of:

- ▷ **Evolution of algorithm performance with face masks**: This section of figures shows the evolution of performance with face masks for developers that have submitted algorithms since mid-March 2020.
- ▷ **FNMR - summary**: Figure 14 gives a summary of false non-matches rates between pre and post-COVID algorithms with a common type of mask. FNMR values are stated at a fixed threshold calibrated to give FMR = 0.00001 on unmasked images.
- ▷ **FNMR - detailed**: Table 8 tabulates false non-match rates by color, shape, and nose coverage. It includes also FNMR without any mask. FNMR values are stated at a fixed threshold calibrated to give FMR = 0.00001 on unmasked images.
- ▷ **Mask vs. no mask**: The scatter plot in Figure 15 shows variation across all algorithms of FNMR without masks against FNMR with a common type of mask, broken out by pre and post-COVID algorithms.
- ▷ **Mask shape**: The scatter plot in Figure 16 shows for all algorithms the increase in false negative results for wide masks vs. narrower round masks, broken out by pre and post-COVID algorithms.
- ▷ **Mask nose coverage**: The scatter plot in Figure 17 shows for all algorithms the increase in false negative rates for masks that substantially cover the nose and those pulled beneath the nose, broken out by pre and post-COVID algorithms.
- ▷ **FTE**: Table 16 gives empirical failure-to-template results by color, shape, and nose coverage. The table was produced using 10 000 images of each kind of mask.
- ▷ **FTE as contributor to FNMR**: The FNMR results include failure-to-template rates (FTE). Figure 18 shows the proportion of template generation failures, broken out by pre and post-COVID algorithms.
- ▷ **DET - impact of mask nose coverage and shape**: This section of figures shows detection error tradeoff characteristics for each algorithm, across different mask nose coverages and shapes.
- ▷ **DET - impact of mask color**: This section of figures shows detection error tradeoff characteristics for each algorithm, across mask colors.
- ▷ **FNMR and FMR vs. threshold**: This section of figures shows the explicit dependence of false non-match rate and false match rate on threshold.

The following plots show evolution of accuracy with face masks for developers that have submitted algorithms since mid-March 2020.

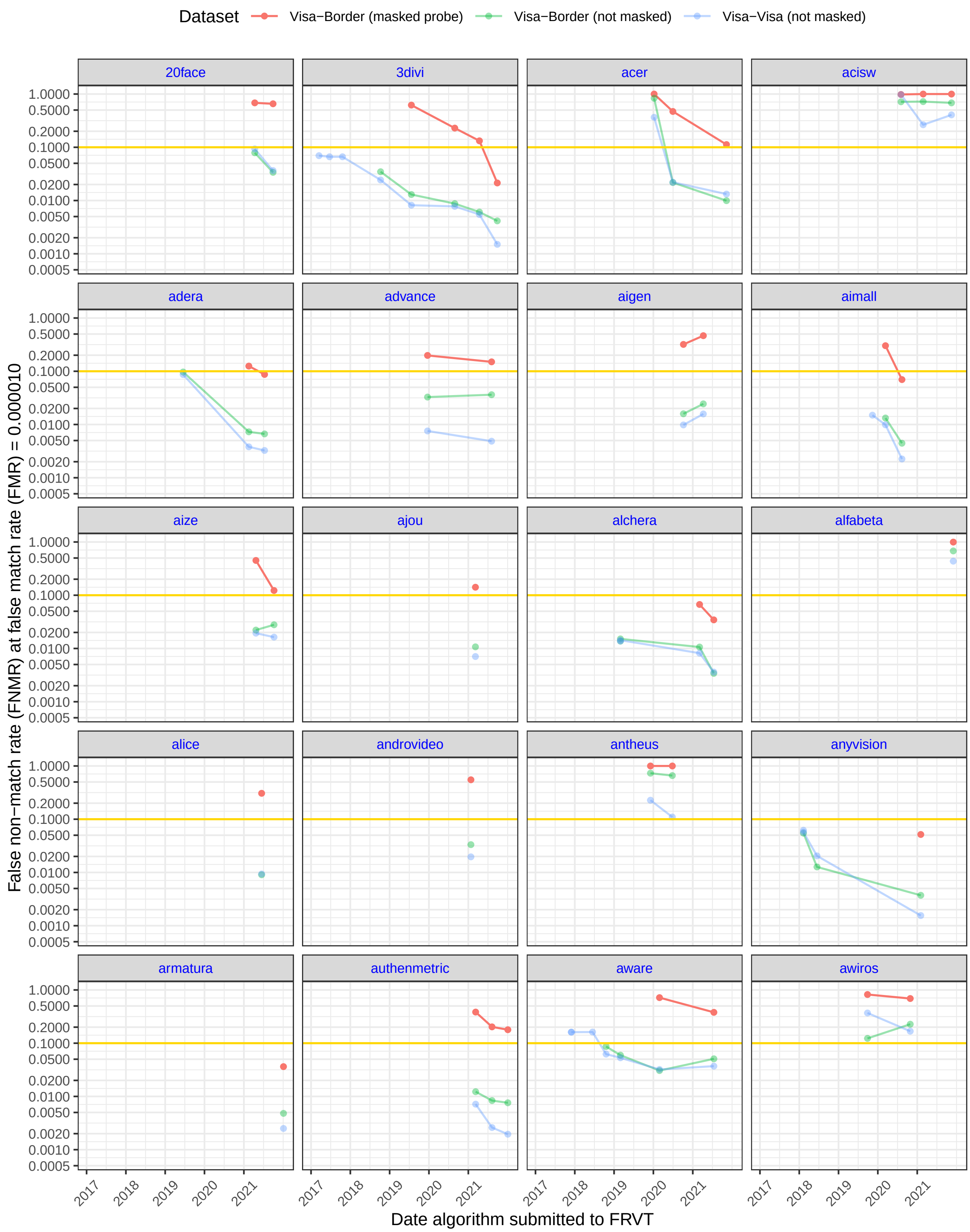

Figure 5: Evolution of accuracy with face masks for developers that have submitted algorithms since mid-March 2020. The red line represents results on a masked dataset (masked probe), and for reference, the blue and green lines are results for unmasked datasets. FNMR on masked dataset is for medium, wide, lightblue masks. The horizontal gold line shows where FNMR=10%.

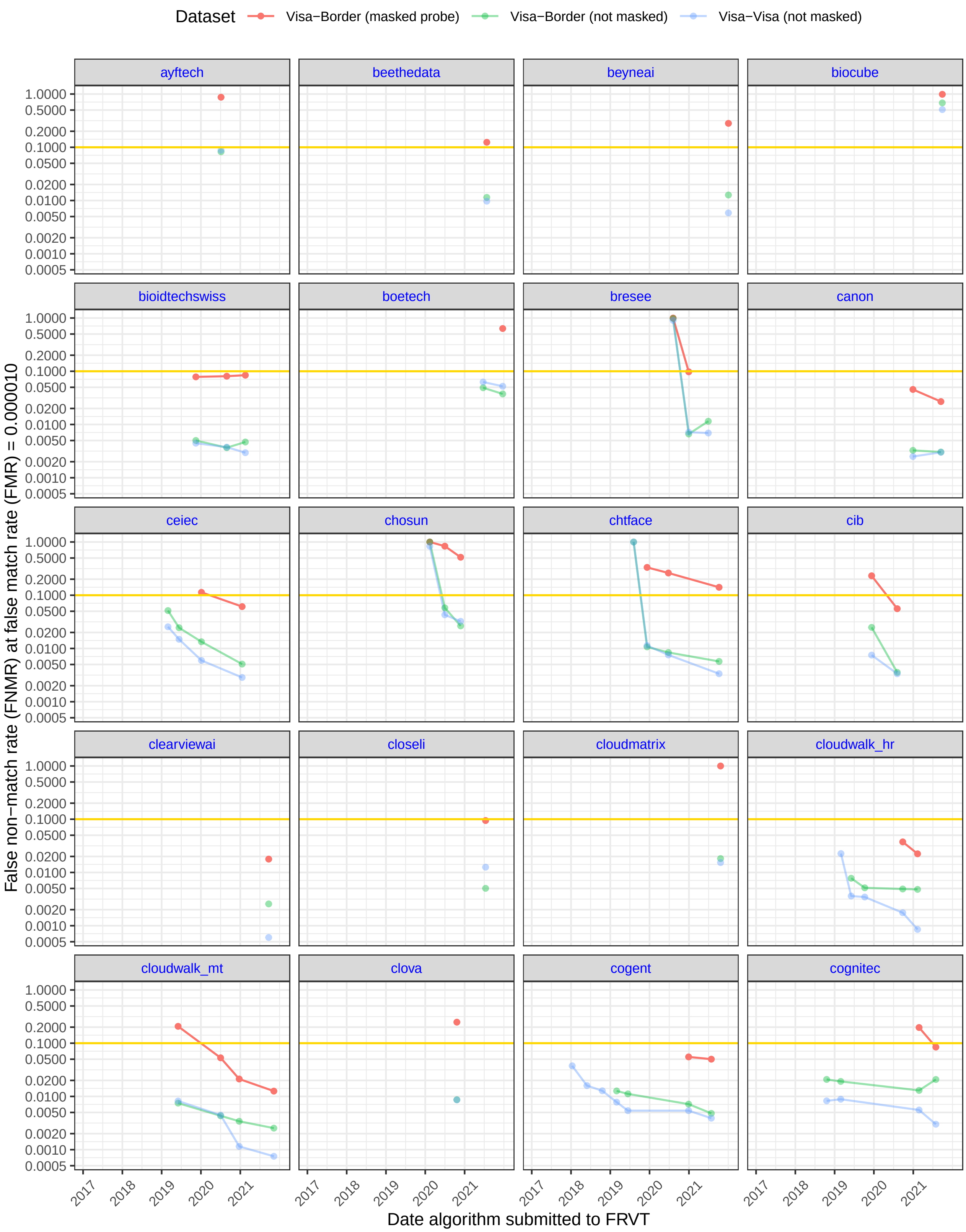

Figure 6: Evolution of accuracy with face masks for developers that have submitted algorithms since mid-March 2020. The red line represents results on a masked dataset (masked probe), and for reference, the blue and green lines are results for unmasked datasets. FNMR on masked dataset is for medium, wide, lightblue masks. The horizontal gold line shows where FNMR=10%.

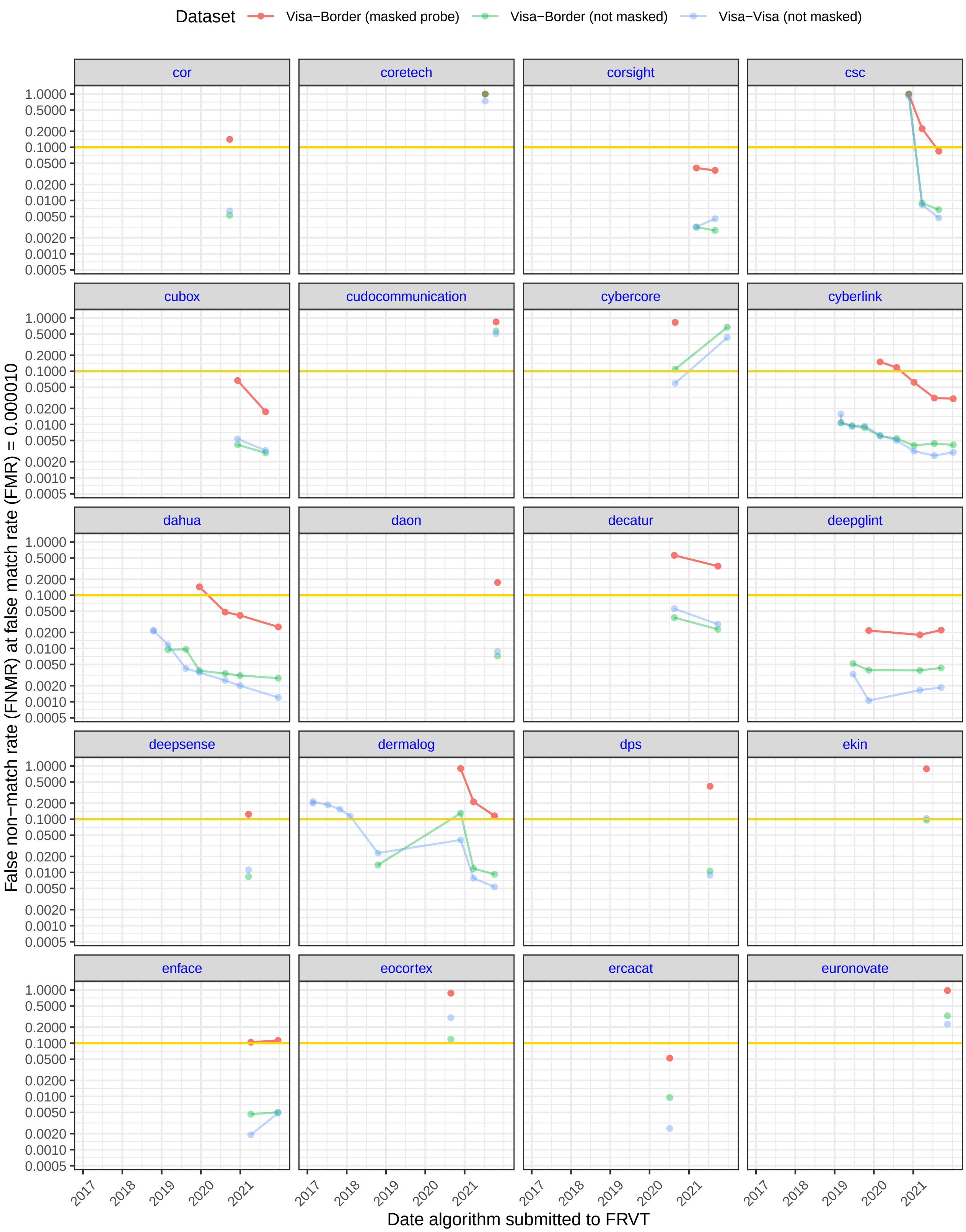

Figure 7: Evolution of accuracy with face masks for developers that have submitted algorithms since mid-March 2020. The red line represents results on a masked dataset (masked probe), and for reference, the blue and green lines are results for unmasked datasets. FNMR on masked dataset is for medium, wide, lightblue masks. The horizontal gold line shows where FNMR=10%.

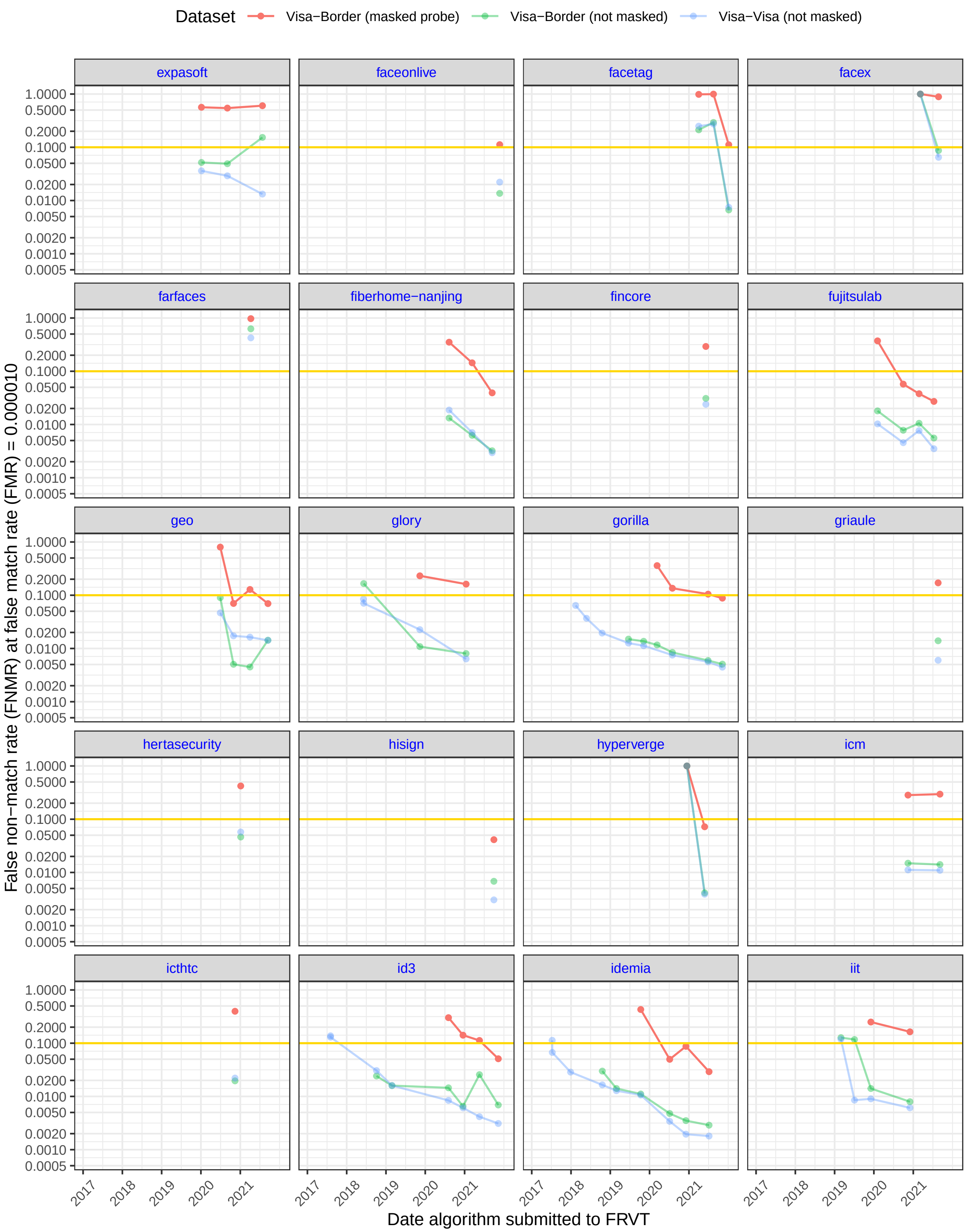

Figure 8: Evolution of accuracy with face masks for developers that have submitted algorithms since mid-March 2020. The red line represents results on a masked dataset (masked probe), and for reference, the blue and green lines are results for unmasked datasets. FNMR on masked dataset is for medium, wide, lightblue masks. The horizontal gold line shows where FNMR=10%.

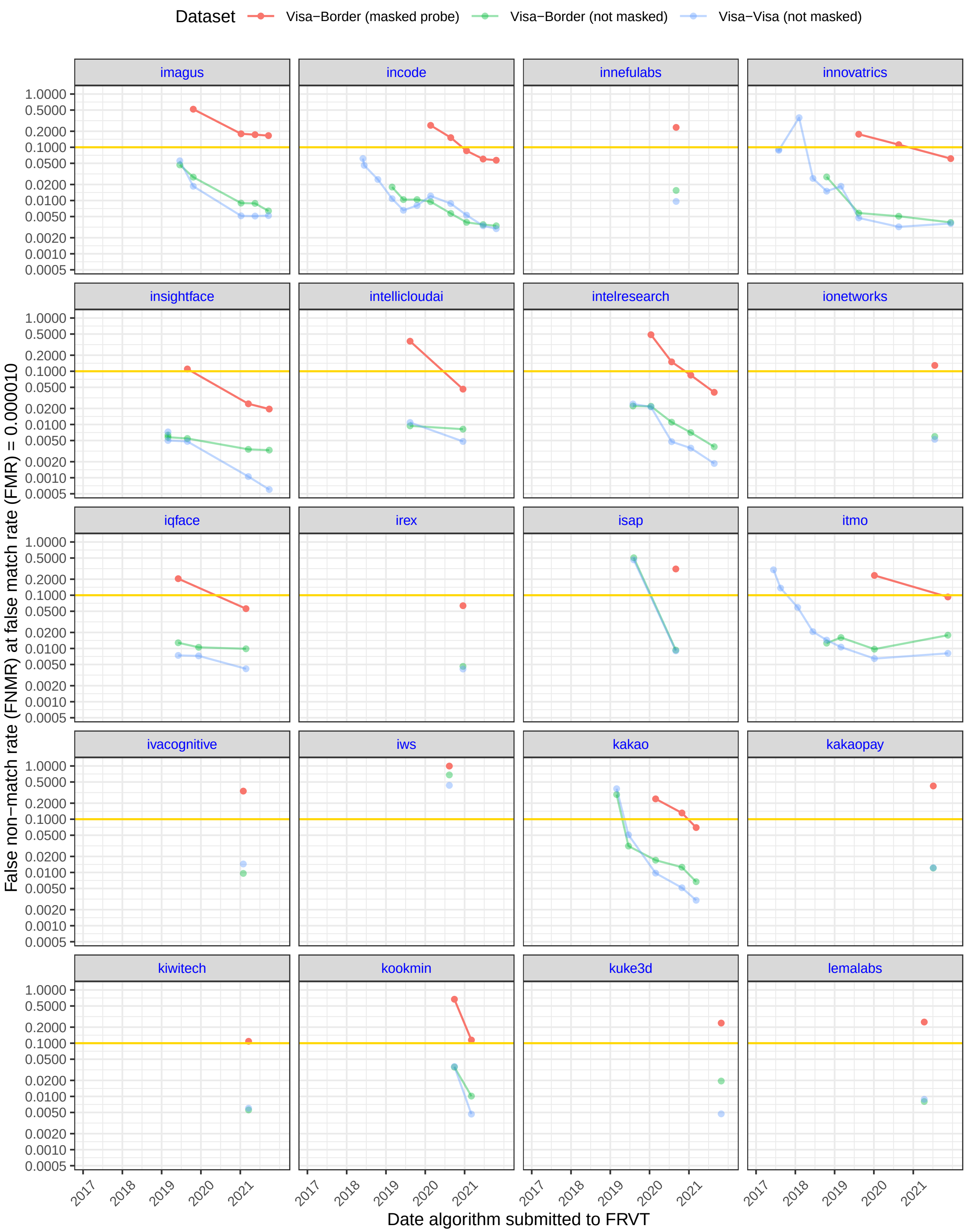

Figure 9: Evolution of accuracy with face masks for developers that have submitted algorithms since mid-March 2020. The red line represents results on a masked dataset (masked probe), and for reference, the blue and green lines are results for unmasked datasets. FNMR on masked dataset is for medium, wide, lightblue masks. The horizontal gold line shows where FNMR=10%.

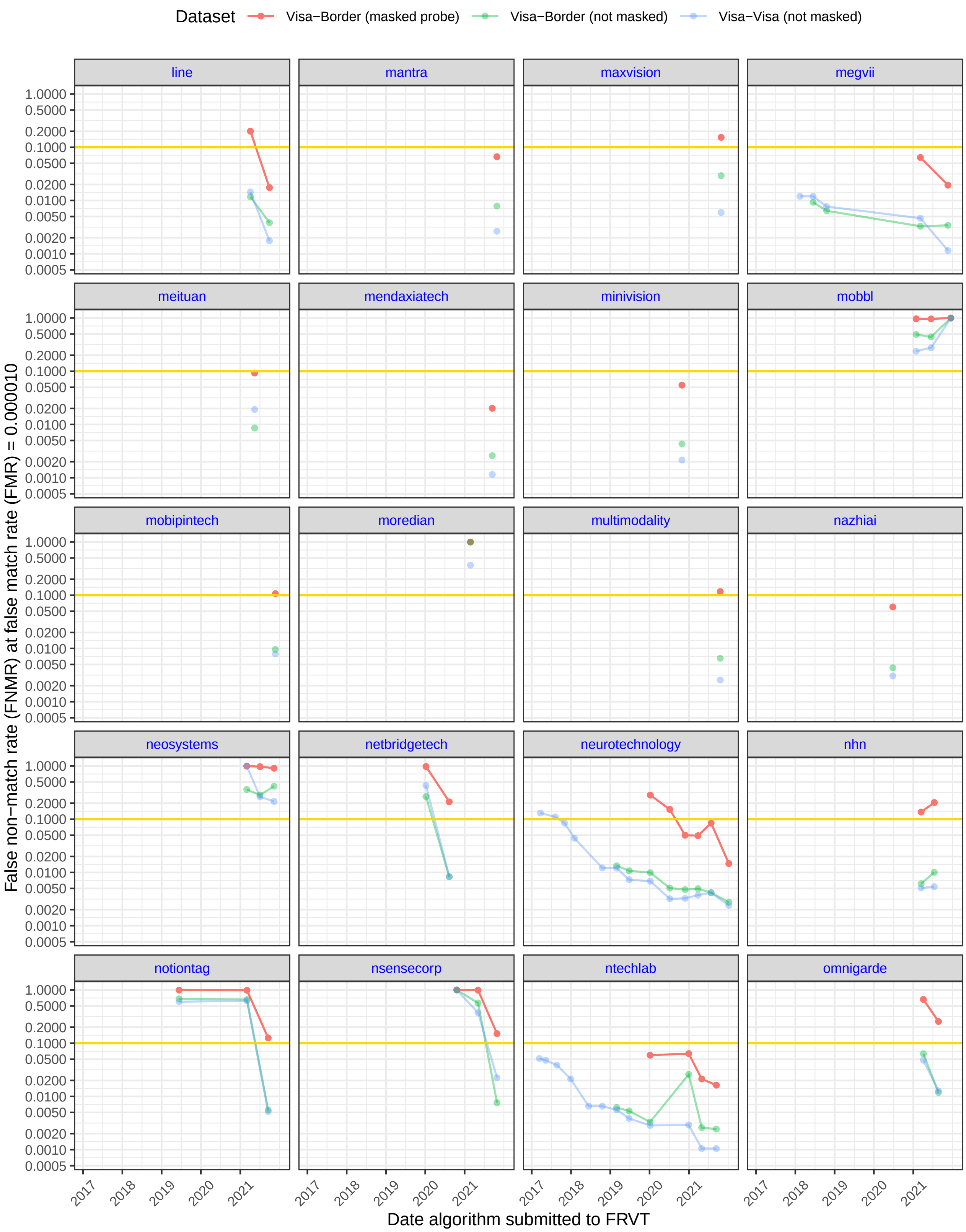

Figure 10: Evolution of accuracy with face masks for developers that have submitted algorithms since mid-March 2020. The red line represents results on a masked dataset (masked probe), and for reference, the blue and green lines are results for unmasked datasets. FNMR on masked dataset is for medium, wide, lightblue masks. The horizontal gold line shows where FNMR=10%.

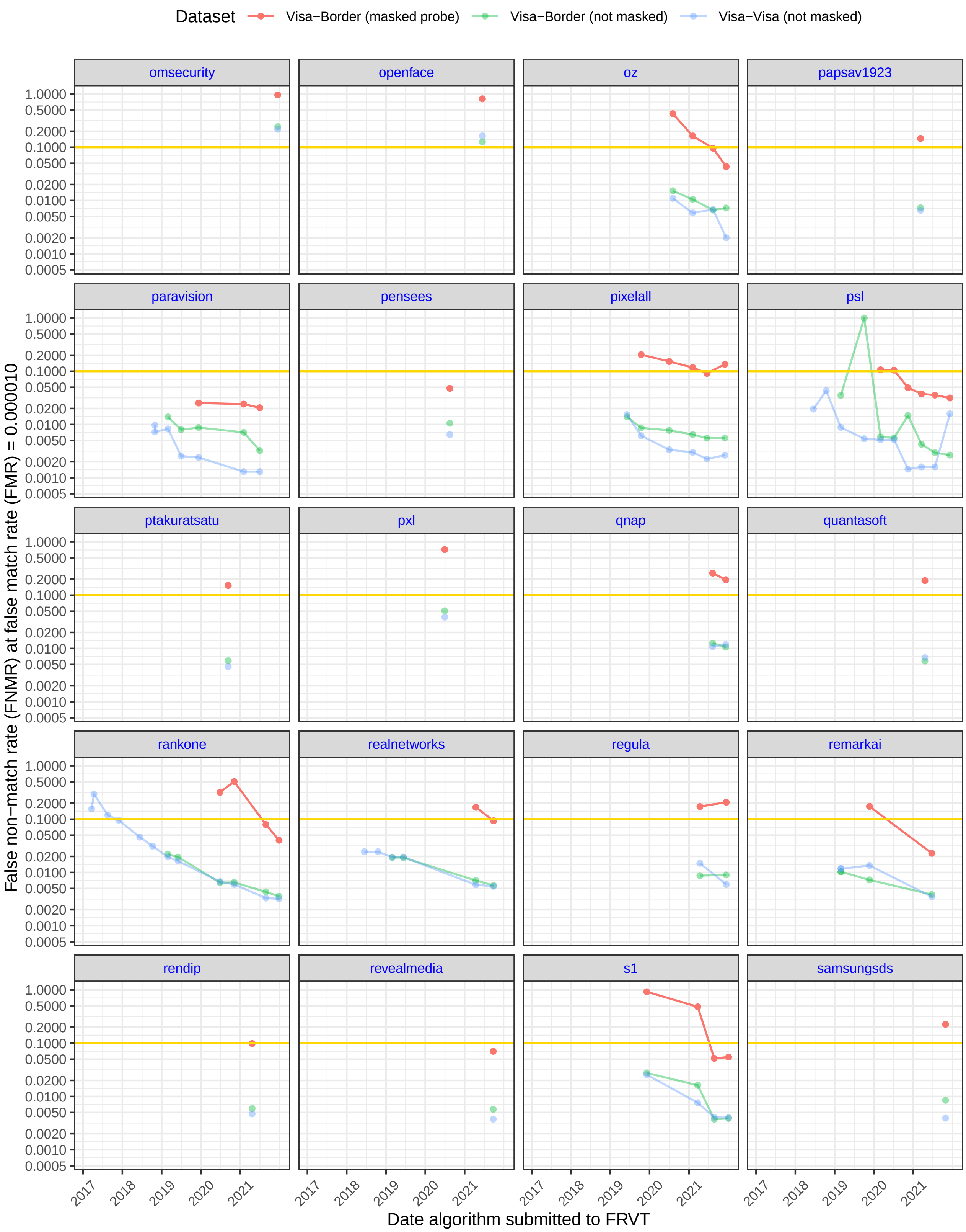

Figure 11: Evolution of accuracy with face masks for developers that have submitted algorithms since mid-March 2020. The red line represents results on a masked dataset (masked probe), and for reference, the blue and green lines are results for unmasked datasets. FNMR on masked dataset is for medium, wide, lightblue masks. The horizontal gold line shows where FNMR=10%.

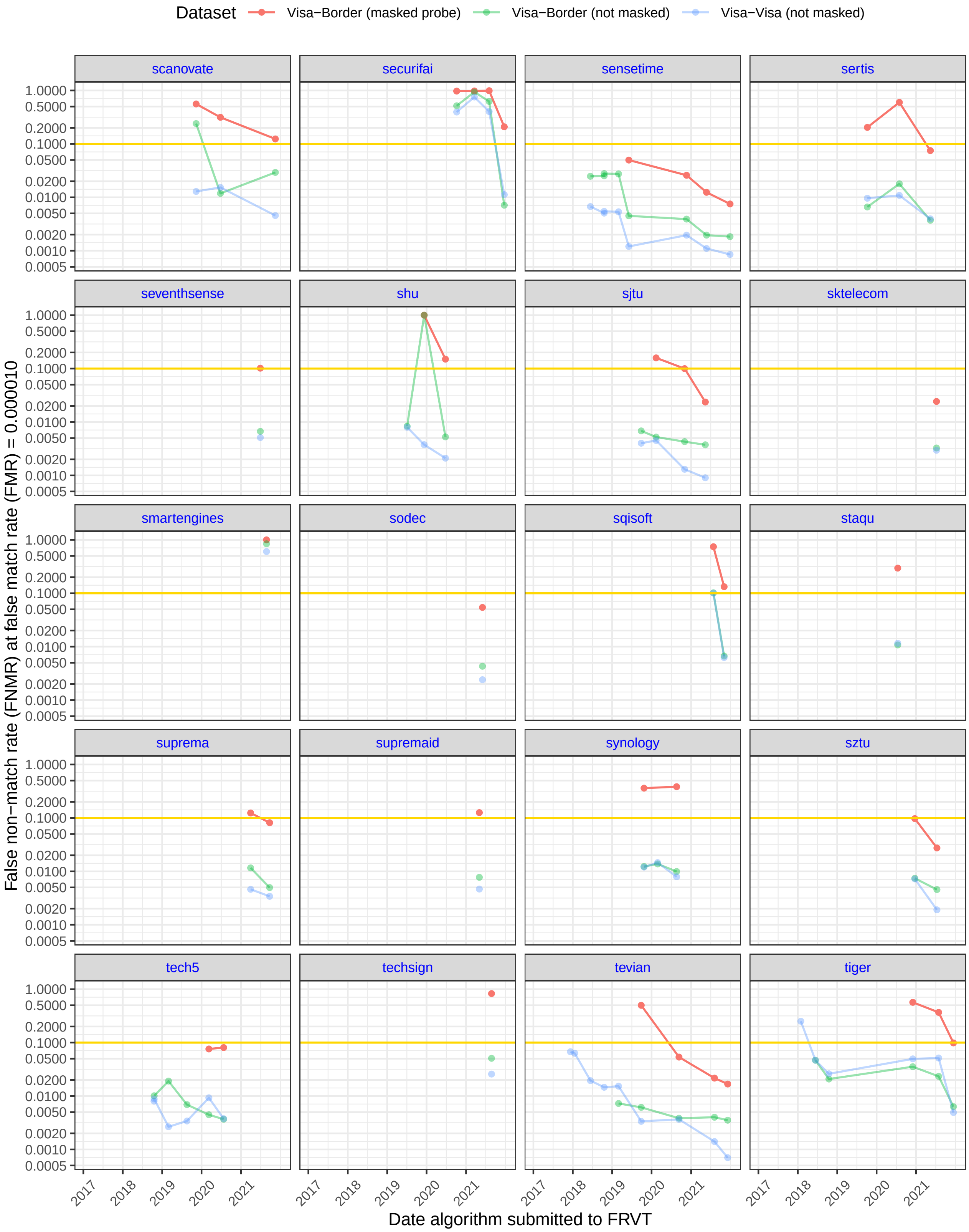

Figure 12: Evolution of accuracy with face masks for developers that have submitted algorithms since mid-March 2020. The red line represents results on a masked dataset (masked probe), and for reference, the blue and green lines are results for unmasked datasets. FNMR on masked dataset is for medium, wide, lightblue masks. The horizontal gold line shows where FNMR=10%.

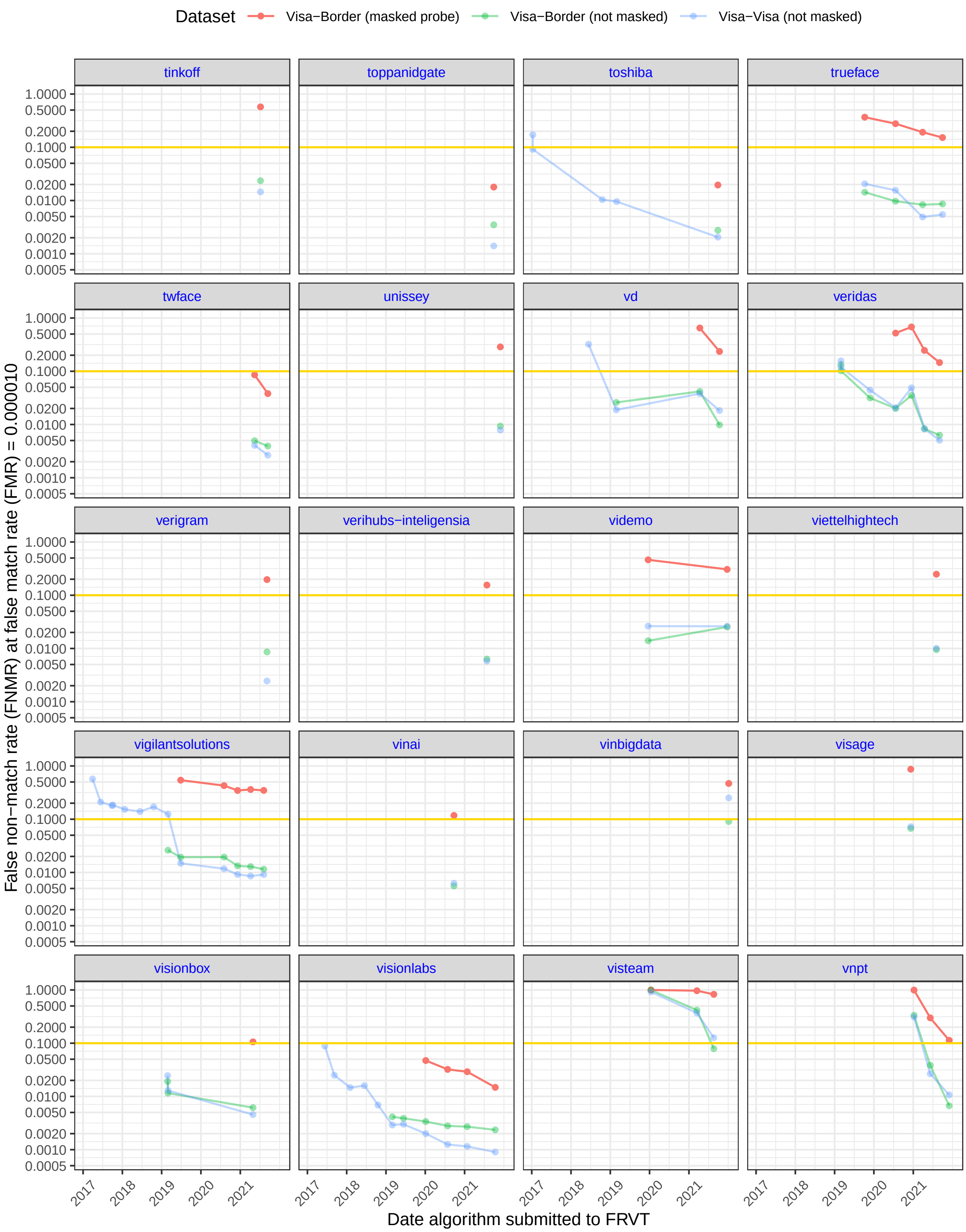

Figure 13: Evolution of accuracy with face masks for developers that have submitted algorithms since mid-March 2020. The red line represents results on a masked dataset (masked probe), and for reference, the blue and green lines are results for unmasked datasets. FNMR on masked dataset is for medium, wide, lightblue masks. The horizontal gold line shows where FNMR=10%.

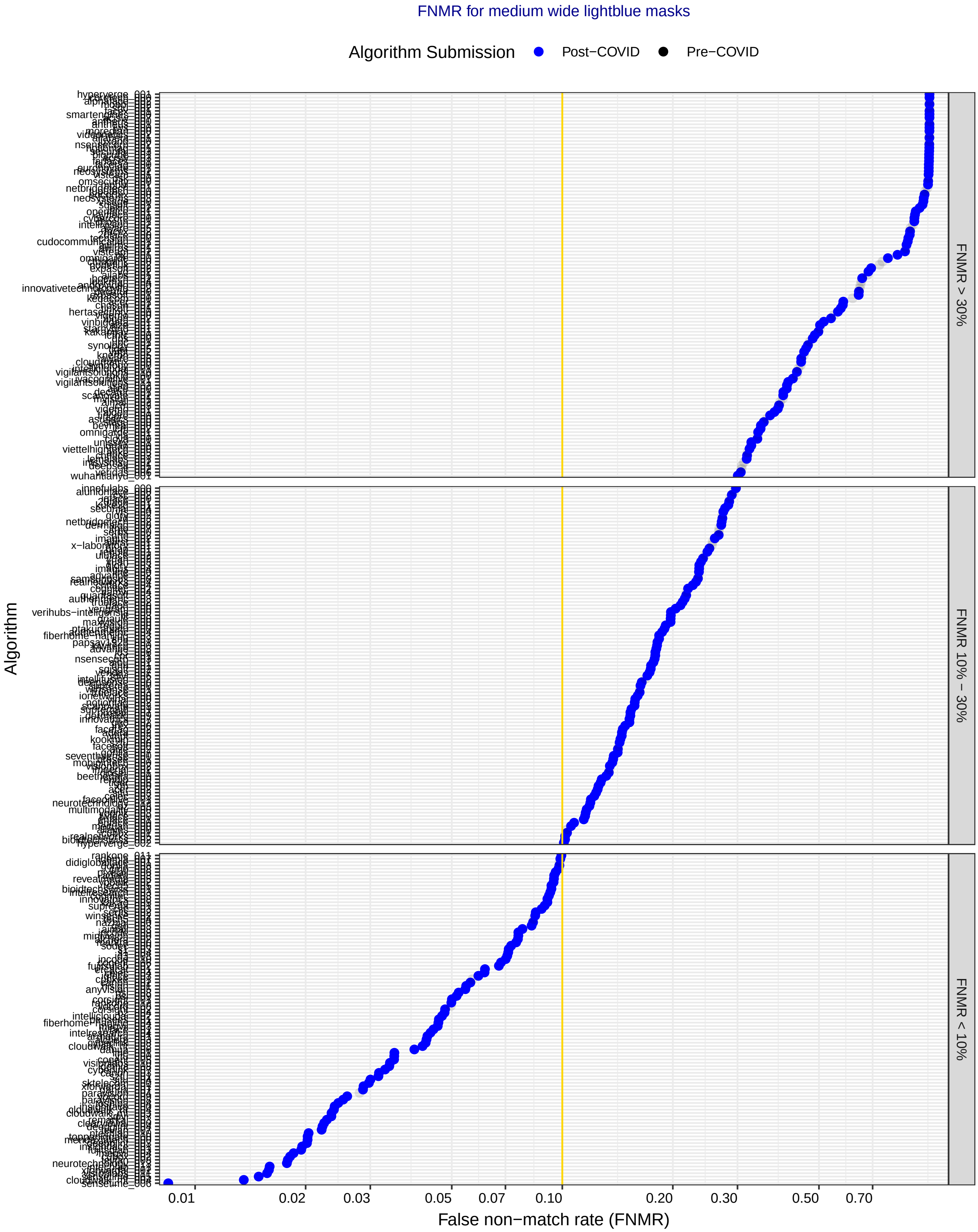

Figure 14: For each algorithm, each dot shows FNMR @ FMR=0.00001, where the threshold is set for FMR on unmasked probe images. The results are for when the probe is masked, and the enrollment image is unmasked. Gray dots represent results for algorithms submitted prior to mid-March 2020 (pre-COVID), and blue dots represent algorithms submitted thereafter (post-COVID).

	Algorithm Name	NOT MASKED	MASK COLOR = LIGHTBLUE, SHAPE = WIDE			MASK COLOR = LIGHTBLUE, SHAPE = ROUND			COLOR = BLACK, SHAPE = WIDE			COLOR = RED, SHAPE = WIDE	COLOR = WHITE, SHAPE = WIDE
	COVERAGE		LO	MED	HI	LO	MED	HI	LO	MED	HI	MED	MED
1	20face-000	0.0795^{276}	0.6110^{88}	0.8836^{278}	0.9006^{100}	-	-	-	-	-	-	-	-
2	20face-001	0.0340^{256}	-	0.2848^{201}	-	-	-	-	-	-	-	-	-
3	3divi-006	0.0061^{111}	0.0408^{45}	0.1710^{149}	0.2226^{61}	-	-	-	-	-	-	-	-
4	3divi-007	0.0042^{57}	-	0.0236^{20}	-	-	-	-	-	-	-	-	-
5	acer-001	0.0219^{238}	0.2587^{79}	0.5835^{258}	0.6719^{94}	0.1536^{32}	0.4325^{48}	0.6831^{27}	0.3132^{36}	0.6304^{49}	0.7143^{34}	-	-
6	acer-002	0.0100^{189}	-	0.1253^{115}	-	-	-	-	-	-	-	-	-
7	acisw-003	0.7160^{311}	0.9810^{96}	0.9970^{301}	0.9970^{105}	-	-	-	0.9883^{41}	0.9997^{54}	-	-	-
8	acisw-007	0.6830^{310}	-	0.9999^{313}	-	-	-	-	-	-	-	-	-
9	adera-002	0.0073^{143}	0.0475^{50}	0.1461^{132}	0.1944^{52}	-	-	-	-	-	-	-	-
10	adera-003	0.0067^{128}	-	0.0953^{91}	-	-	-	-	-	-	-	-	-
11	advance-002	0.0328^{254}	-	0.2351^{179}	-	-	-	-	-	-	-	0.2333^{42}	-
12	advance-003	0.0363^{257}	-	0.1803^{157}	-	-	-	-	-	-	-	-	-
13	aifirst-001	0.0079^{151}	0.0778^{59}	0.2567^{188}	-	-	-	-	-	-	-	0.2624^{44}	-
14	aigen-001	0.0159^{229}	0.1268^{73}	0.3790^{225}	0.4432^{86}	-	0.2880^{47}	-	0.1956^{35}	0.4761^{48}	0.6329^{33}	0.3189^{45}	0.3754^{44}
15	aigen-002	0.0245^{244}	0.2127^{78}	0.5392^{253}	0.6070^{92}	-	-	-	-	-	-	-	-
16	ailabs-001	0.0243^{243}	-	0.6792^{266}	-	-	-	-	-	-	-	-	-
17	aimall-002	0.0133^{218}	-	0.3919^{228}	-	-	-	-	-	-	-	-	-
18	aimall-003	0.0045^{70}	0.0188^{29}	0.0781^{76}	0.1325^{40}	0.0175^{12}	0.0524^{31}	0.1021^{15}	0.0223^{14}	0.0913^{27}	0.1577^{18}	0.0738^{22}	0.0800^{28}
19	aiunionface-000	0.0094^{178}	0.0917^{67}	0.2935^{204}	-	-	-	-	-	-	-	-	-
20	aize-001	0.0223^{239}	-	0.5052^{251}	-	-	-	-	-	-	-	-	-
21	aize-002	0.0280^{248}	-	0.1422^{126}	-	-	-	-	-	-	-	-	-
22	ajou-001	0.0108^{199}	0.0761^{58}	0.1776^{153}	0.2245^{63}	-	-	-	-	-	-	-	-
23	alchera-002	0.0107^{197}	0.0459^{47}	0.0764^{74}	0.1144^{35}	-	-	-	-	-	-	-	-
24	alchera-003	0.0034^{29}	-	0.0431^{43}	-	-	-	-	-	-	-	-	-
25	alfabeta-001	0.6804^{308}	-	0.9994^{307}	-	-	-	-	-	-	-	-	-
26	alice-000	0.0091^{174}	-	0.4092^{233}	-	-	-	-	-	-	-	-	-
27	alleyes-000	0.0044^{67}	-	0.1038^{103}	-	0.0181^{16}	0.0542^{33}	0.1050^{16}	0.0262^{19}	0.1287^{33}	0.1991^{21}	0.1066^{28}	0.1098^{33}
28	alphaface-002	1.0000^{317}	1.0000^{101}	1.0000^{318}	-	-	-	-	-	-	-	-	-
29	androvideo-000	0.0333^{255}	0.3168^{81}	0.6488^{263}	0.7517^{97}	-	-	-	-	-	-	-	-
30	anke-005	0.0062^{114}	0.0671^{55}	0.3207^{213}	-	-	-	-	-	-	-	-	-
31	antheus-000	0.7319^{312}	0.9994^{100}	0.9999^{312}	-	-	-	-	-	-	-	-	-
32	antheus-001	0.6608^{305}	0.9988^{99}	0.9998^{311}	0.9998^{111}	0.9993^{37}	0.9998^{55}	0.9998^{31}	0.9993^{42}	0.9998^{55}	0.9998^{39}	-	-
33	anyvision-005	0.0037^{40}	0.0119^{20}	0.0548^{58}	0.0828^{27}	-	0.0345^{19}	-	-	-	-	-	0.0506^{21}
34	armatura-001	0.0048^{79}	-	0.0431^{44}	-	-	-	-	-	-	-	-	-
35	asusaics-000	0.0090^{172}	-	0.3616^{223}	-	-	-	-	-	-	-	-	-
36	authenmetric-003	0.0084^{159}	-	0.2155^{172}	-	-	-	-	-	-	-	-	-
37	authenmetric-004	0.0076^{147}	-	0.1870^{162}	-	-	-	-	-	-	-	-	-
38	aware-005	0.0308^{252}	0.4962^{85}	0.8876^{280}	-	-	-	-	-	-	-	-	-
39	aware-006	0.0514^{270}	-	0.4474^{241}	-	-	-	-	-	-	-	-	-
40	awiros-001	0.1233^{285}	0.6823^{91}	0.8635^{274}	-	-	-	-	-	-	-	-	-
41	awiros-002	0.2283^{292}	0.6356^{89}	0.8671^{275}	0.9221^{101}	-	0.7932^{52}	-	0.7703^{40}	0.9068^{53}	0.9379^{36}	0.8628^{48}	0.8508^{45}
42	ayftech-001	0.0828^{278}	0.6740^{90}	0.9132^{284}	0.9333^{103}	0.5865^{36}	0.8519^{53}	0.9538^{30}	0.7540^{39}	0.9048^{52}	0.9705^{38}	-	-
43	beethedata-000	0.0115^{202}	-	0.1318^{119}	-	-	-	-	-	-	-	-	-
44	beyneai-000	0.0127^{213}	-	0.3474^{220}	-	-	-	-	-	-	-	-	-
45	biocube-001	0.6827^{309}	-	0.9972^{302}	-	-	-	-	-	-	-	-	-

Table 8: This table summarizes False Non-Match Rate (FNMR) on unmasked and masked probe images. FNMR is the proportion of mated comparisons below a threshold set to achieve FMR=1e-05 on unmasked probe images. False Match Rate (FMR) is the proportion of impostor comparisons at or above that threshold. The red superscripts give rank over all algorithms in that column. Missing entries generally mean the algorithm was not run on that particular mask variation due to time and resource constraints. Algorithms with FTE=1.00 were not run at all. Algorithms in black were submitted prior to mid-March 2020, and algorithms in blue were submitted thereafter.

FNMR(T) "False non-match rate"
FMR(T) "False match rate"

	Algorithm Name	NOT MASKED	MASK COLOR = LIGHTBLUE SHAPE = WIDE			SHAPE = ROUND			COLOR = BLACK SHAPE = WIDE			COLOR = RED SHAPE = WIDE	COLOR = WHITE SHAPE = WIDE
	COVERAGE		LO	MED	HI	LO	MED	HI	LO	MED	HI	MED	MED
46	bioidtechswiss-001	0.0037^{37}	0.0225^{33}	0.0945^{89}	0.1519^{46}	0.0180^{15}	0.0524^{32}	0.1070^{18}	0.0254^{17}	0.0986^{29}	0.1571^{17}	0.0979^{25}	0.0945^{32}
47	bioidtechswiss-002	0.0047^{77}	-	0.1021^{101}	0.1643^{48}	-	-	-	-	-	-	-	-
48	boetech-002	0.0375^{258}	-	0.6558^{265}	-	-	-	-	-	-	-	-	-
49	bresee-001	0.0067^{127}	-	0.1382^{124}	0.1885^{51}	-	-	-	-	-	-	-	-
50	camvi-004	0.0063^{115}	0.0697^{56}	0.2179^{173}	-	-	-	-	-	-	-	0.3337^{46}	-
51	canon-002	0.0033^{25}	0.0125^{22}	0.0565^{60}	0.0888^{29}	-	-	-	0.0138^{9}	0.0629^{22}	-	0.0729^{21}	0.0602^{22}
52	canon-003	0.0030^{18}	-	0.0320^{33}	-	-	-	-	-	-	-	-	-
53	ceiec-003	0.0134^{219}	-	0.1230^{113}	-	-	-	-	-	-	-	-	-
54	ceiec-004	0.0051^{88}	-	0.0618^{64}	0.0984^{33}	-	0.0310^{17}	-	-	-	-	-	0.0625^{23}
55	chosun-001	0.0582^{271}	0.5759^{86}	0.9091^{282}	0.9263^{102}	0.5021^{35}	0.8531^{54}	0.9278^{29}	0.5158^{37}	0.9031^{51}	0.9409^{37}	-	-
56	chosun-002	0.0266^{247}	-	0.5807^{257}	0.6969^{96}	-	0.4707^{49}	-	-	-	-	-	-
57	chtface-003	0.0084^{161}	0.1008^{68}	0.3201^{212}	-	0.0774^{29}	0.2393^{45}	0.4387^{24}	0.1232^{34}	0.3309^{46}	0.5044^{31}	-	-
58	chtface-004	0.0057^{101}	-	0.2274^{176}	-	-	-	-	-	-	-	-	-
59	clearviewai-000	0.0026^{6}	0.0058^{8}	0.0225^{18}	0.0386^{10}	-	0.0109^{4}	-	-	-	-	-	-
60	closeli-001	0.0050^{84}	-	0.1338^{120}	-	-	-	-	-	-	-	-	-
61	cloudmatrix-000	0.0183^{232}	-	0.4471^{240}	-	-	-	-	-	-	-	-	-
62	cloudwalk-hr-003	0.0049^{81}	0.0133^{23}	0.0419^{41}	0.0613^{21}	0.0122^{6}	0.0247^{16}	0.0475^{7}	0.0142^{10}	0.0527^{20}	0.0914^{8}	0.0542^{17}	0.0476^{19}
63	cloudwalk-hr-004	0.0048^{78}	0.0086^{17}	0.0240^{22}	0.0373^{9}	-	0.0135^{8}	-	-	0.0313^{12}	-	0.0302^{9}	0.0282^{12}
64	cloudwalk-mt-003	0.0034^{31}	0.0076^{13}	0.0237^{21}	0.0447^{15}	0.0078^{3}	0.0156^{11}	0.0324^{5}	0.0082^{3}	0.0254^{8}	0.0482^{3}	0.0235^{6}	0.0268^{8}
65	cloudwalk-mt-004	0.0025^{5}	0.0049^{4}	0.0137^{2}	0.0285^{3}	-	0.0100^{3}	-	-	-	-	-	-
66	clova-000	0.0087^{166}	0.0881^{65}	0.3411^{218}	0.5017^{88}	-	0.1752^{42}	-	0.0950^{32}	0.3051^{44}	0.4211^{29}	-	-
67	cogent-005	0.0072^{140}	0.0260^{38}	0.0351^{38}	0.0631^{22}	-	-	-	0.0252^{16}	0.0349^{15}	-	0.0335^{12}	0.0363^{15}
68	cogent-006	0.0048^{80}	-	0.0693^{66}	-	-	-	-	-	-	-	-	-
69	cognitec-002	0.0130^{216}	-	0.2201^{175}	0.2820^{73}	-	-	-	-	-	-	-	-
70	cognitec-003	0.0208^{237}	-	0.0920^{86}	-	-	-	-	-	-	-	-	-
71	cor-001	0.0053^{91}	0.0504^{51}	0.1802^{156}	0.2470^{67}	0.0300^{21}	0.0864^{36}	-	0.0364^{25}	0.1328^{34}	0.1828^{19}	0.1527^{33}	-
72	coretech-000	1.0000^{320}	-	1.0000^{320}	-	-	-	-	-	-	-	-	-
73	corsight-001	0.0032^{20}	-	0.0504^{55}	-	-	-	-	-	-	-	-	-
74	corsight-002	0.0027^{11}	-	0.0479^{52}	-	-	-	-	-	-	-	-	-
75	csc-002	0.0089^{170}	-	0.2895^{203}	0.3163^{77}	-	-	-	-	-	-	-	-
76	csc-003	0.0068^{134}	-	0.0878^{82}	-	-	-	-	-	-	-	-	-
77	ctbcbank-000	0.0133^{217}	0.1594^{76}	0.7448^{270}	-	-	-	-	-	-	-	-	-
78	cubox-001	0.0042^{58}	0.0233^{35}	0.1037^{102}	0.1818^{50}	-	0.0477^{28}	-	-	-	-	-	0.1274^{34}
79	cubox-002	0.0029^{16}	0.0055^{7}	0.0181^{9}	0.0415^{12}	-	-	-	-	0.0191^{4}	-	0.0187^{4}	0.0189^{3}
80	cudocommunication-001	0.5718^{301}	-	0.8730^{276}	-	-	-	-	-	-	-	-	-
81	cuhkee-001	0.0041^{54}	0.0143^{25}	0.0572^{61}	0.0963^{32}	0.0143^{8}	0.0333^{18}	0.0715^{8}	0.0164^{11}	0.0652^{23}	0.1193^{10}	-	-
82	cybercore-000	0.1096^{283}	-	0.9097^{283}	-	-	-	-	-	-	-	-	-
83	cyberlink-007	0.0044^{68}	-	0.0331^{34}	-	-	-	-	-	-	-	-	-
84	cyberlink-008	0.0041^{55}	-	0.0425^{42}	-	-	-	-	-	-	-	-	-
85	dahua-006	0.0031^{19}	0.0100^{19}	0.0399^{40}	0.0701^{24}	-	-	-	0.0098^{6}	0.0370^{16}	-	0.0350^{14}	0.0393^{16}
86	dahua-007	0.0028^{13}	-	0.0289^{28}	-	-	-	-	-	-	-	-	-
87	daon-000	0.0072^{141}	-	0.2107^{170}	-	-	-	-	-	-	-	-	-
88	decatur-000	0.0384^{259}	-	0.6440^{261}	-	-	-	-	-	-	-	-	-
89	decatur-001	0.0231^{240}	-	0.4027^{231}	-	-	-	-	-	-	-	-	-
90	deepglint-003	0.0039^{48}	0.0068^{12}	0.0202^{12}	0.0388^{11}	0.0070^{2}	0.0121^{7}	0.0239^{1}	0.0078^{2}	0.0238^{7}	0.0465^{2}	-	0.0215^{6}

Table 9: This table summarizes False Non-Match Rate (FNMR) on unmasked and masked probe images. FNMR is the proportion of mated comparisons below a threshold set to achieve FMR=1e-05 on unmasked probe images. False Match Rate (FMR) is the proportion of impostor comparisons at or above that threshold. The red superscripts give rank over all algorithms in that column. Missing entries generally mean the algorithm was not run on that particular mask variation due to time and resource constraints. Algorithms with FTE=1.00 were not run at all. Algorithms in black were submitted prior to mid-March 2020, and algorithms in blue were submitted thereafter.

	Algorithm Name	NOT MASKED	MASK COLOR = LIGHTBLUE, SHAPE = WIDE			MASK COLOR = LIGHTBLUE, SHAPE = ROUND			COLOR = BLACK, SHAPE = WIDE			COLOR = RED, SHAPE = WIDE	COLOR = WHITE, SHAPE = WIDE
	COVERAGE		LO	MED	HI	LO	MED	HI	LO	MED	HI	MED	MED
91	deepglint-004	0.0043[63]	-	0.0224[17]	-	-	-	-	-	-	-	-	-
92	deepsea-001	0.0110[201]	0.1218[70]	0.3094[209]	0.3778[83]	0.0922[31]	0.2217[44]	0.4469[26]	-	-	-	-	-
93	deepsense-000	0.0084[160]	-	0.1645[147]	-	-	-	-	-	-	-	-	-
94	dermalog-008	0.0119[207]	-	0.2723[194]	-	-	-	-	-	-	-	-	-
95	dermalog-009	0.0093[175]	-	0.1542[138]	-	-	-	-	-	-	-	-	-
96	didiglobalface-001	0.0050[85]	-	0.0986[95]	0.1517[44]	0.0255[17]	0.0515[29]	0.0979[14]	0.0291[21]	0.1033[31]	0.1558[15]	0.1241[29]	0.1655[39]
97	dps-000	0.0106[195]	-	0.4809[247]	-	-	-	-	-	-	-	-	-
98	dsk-000	0.1961[288]	0.9108[94]	0.9929[295]	-	-	-	-	-	-	-	-	-
99	ekin-002	0.0966[281]	-	0.9399[286]	-	-	-	-	-	-	-	-	-
100	enface-000	0.0046[76]	-	0.1079[105]	0.1381[41]	-	-	-	-	-	-	-	-
101	enface-001	0.0051[86]	-	0.1148[106]	-	-	-	-	-	-	-	-	-
102	eocortex-000	0.1187[284]	-	0.9694[290]	-	-	-	-	-	-	-	-	-
103	ercacat-001	0.0096[182]	0.0187[28]	0.0616[63]	0.0994[34]	0.0173[11]	0.0357[20]	0.0728[9]	0.0200[13]	0.0663[24]	0.1114[9]	0.0679[20]	0.0648[26]
104	euronovate-001	0.3291[296]	-	0.9956[298]	-	-	-	-	-	-	-	-	-
105	expasoft-001	0.0492[267]	-	0.6414[260]	-	-	-	-	-	-	-	-	-
106	expasoft-002	0.1532[287]	-	0.6950[267]	-	-	-	-	-	-	-	-	-
107	faceonlive-001	0.0137[220]	-	0.1199[111]	-	-	-	-	-	-	-	-	-
108	facesoft-000	0.0057[102]	0.0397[44]	0.1428[128]	-	-	-	-	-	0.1573[38]	-	0.1446[32]	0.1428[37]
109	facetag-000	0.2130[290]	-	0.9957[299]	0.9980[108]	-	-	-	-	-	-	-	-
110	facetag-002	0.0067[129]	-	0.1466[133]	-	-	-	-	-	-	-	-	-
111	facex-001	1.0000[318]	-	1.0000[315]	1.0000[112]	-	-	-	-	-	-	-	-
112	facex-002	0.0872[279]	-	0.8851[279]	-	-	-	-	-	-	-	-	-
113	farfaces-001	0.6274[304]	-	0.9970[300]	0.9976[107]	-	-	-	-	-	-	-	-
114	fiberhome-nanjing-003	0.0063[116]	-	0.1840[161]	0.2437[66]	-	-	-	-	-	-	-	-
115	fiberhome-nanjing-004	0.0032[21]	-	0.0460[48]	-	-	-	-	-	-	-	-	-
116	fincore-000	0.0311[253]	-	0.3696[224]	-	-	-	-	-	-	-	-	-
117	fujitsulab-002	0.0106[194]	0.0433[46]	0.0677[65]	0.0954[31]	0.0433[26]	0.0472[27]	-	-	-	-	-	0.0635[25]
118	fujitsulab-003	0.0056[95]	-	0.0195[10]	-	-	-	-	-	0.0221[6]	-	0.0348[13]	0.0207[4]
119	geo-002	0.0045[73]	-	0.1531[135]	0.2215[60]	-	-	-	-	-	-	-	-
120	geo-003	0.0144[226]	-	0.0831[77]	-	-	-	-	-	-	-	-	-
121	glory-002	0.0109[200]	-	0.2729[196]	-	-	-	-	-	-	-	-	-
122	glory-003	0.0081[154]	-	0.2370[182]	0.2673[72]	-	-	-	-	-	-	-	-
123	gorilla-007	0.0060[110]	-	0.1425[127]	-	-	-	-	-	-	-	-	-
124	gorilla-008	0.0051[89]	-	0.0991[97]	-	-	-	-	-	-	-	-	-
125	griaule-000	0.0140[222]	-	0.1972[165]	-	-	-	-	-	-	-	-	-
126	hertasecurity-000	0.0464[266]	-	0.5644[255]	0.6583[93]	-	-	-	-	-	-	-	-
127	hisign-001	0.0068[135]	-	0.0549[59]	-	-	-	-	-	-	-	-	-
128	hyperverge-001	1.0000[319]	-	1.0000[319]	1.0000[162]	-	-	-	-	-	-	-	-
129	hyperverge-002	0.0041[56]	-	0.1016[99]	-	-	-	-	-	-	-	-	-
130	icm-002	0.0150[227]	-	0.3484[221]	-	-	-	-	-	-	-	-	-
131	icm-003	0.0141[225]	-	0.3908[227]	-	-	-	-	-	-	-	-	-
132	icthtc-000	0.0197[234]	-	0.4887[248]	0.5438[91]	-	-	-	-	-	-	-	-
133	id3-006	0.0066[123]	-	0.1800[155]	0.2529[70]	-	-	-	-	-	-	-	-
134	id3-008	0.0069[136]	-	0.0712[68]	-	-	-	-	-	-	-	-	-
135	idemia-007	0.0035[33]	-	0.0988[96]	-	-	-	-	-	-	-	-	-

Table 10: This table summarizes False Non-Match Rate (FNMR) on unmasked and masked probe images. FNMR is the proportion of mated comparisons below a threshold set to achieve FMR=1e-05 on unmasked probe images. False Match Rate (FMR) is the proportion of impostor comparisons at or above that threshold. The red superscripts give rank over all algorithms in that column. Missing entries generally mean the algorithm was not run on that particular mask variation due to time and resource constraints. Algorithms with FTE=1.00 were not run at all. Algorithms in black were submitted prior to mid-March 2020, and algorithms in blue were submitted thereafter.

FNMR(T) "False non-match rate"
FMR(T) "False match rate"

	Algorithm Name	NOT MASKED	MASK COLOR = LIGHTBLUE						COLOR = BLACK			COLOR = RED	COLOR = WHITE
			SHAPE = WIDE			SHAPE = ROUND			SHAPE = WIDE			SHAPE = WIDE	SHAPE = WIDE
	COVERAGE		LO	MED	HI	LO	MED	HI	LO	MED	HI	MED	MED
136	idemia-008	0.0029[15]	-	0.0338[35]	-	-	-	-	-	-	-	-	-
137	iit-002	0.0141[224]	-	0.3078[208]	-	-	-	-	-	-	-	-	-
138	iit-003	0.0080[152]	-	0.1975[166]	0.2866[74]	-	-	-	-	-	-	-	-
139	imagus-002	0.0090[171]	-	0.2608[190]	-	-	-	-	-	-	-	-	-
140	imagus-004	0.0064[120]	-	0.2363[181]	-	-	-	-	-	-	-	-	-
141	imperial-002	0.0055[92]	0.0320[40]	0.1350[121]	0.1972[55]	0.0258[18]	0.0775[35]	0.1556[19]	0.0359[24]	0.1510[37]	0.2302[25]	0.1533[34]	0.1432[38]
142	incode-009	0.0035[35]	-	0.0765[75]	-	-	-	-	-	-	-	-	-
143	incode-010	0.0034[28]	-	0.0705[67]	-	-	-	-	-	-	-	-	-
144	innefulabs-000	0.0155[228]	-	0.2971[205]	-	-	-	-	-	-	-	-	-
145	innovativetechnologyltd-002	0.0251[245]	0.2701[80]	0.6454[262]	-	-	-	-	-	-	-	-	-
146	innovatrics-007	0.0051[87]	-	0.1537[137]	-	-	-	-	-	-	-	-	-
147	innovatrics-008	0.0039[49]	-	0.0915[85]	-	-	-	-	-	-	-	-	-
148	insightface-000	0.0034[30]	-	0.0240[23]	0.0496[17]	-	0.0184[15]	-	-	0.0210[5]	-	0.0222[5]	0.0242[7]
149	insightface-001	0.0033[27]	0.0066[10]	0.0196[11]	0.0426[13]	-	0.0158[12]	-	-	-	-	-	-
150	intellicloudai-001	0.0095[179]	0.1044[69]	0.4394[238]	-	-	-	-	-	-	-	-	-
151	intellicloudai-002	0.0082[155]	0.0226[34]	0.0470[50]	0.0792[26]	-	-	-	-	0.0450[18]	-	0.0535[16]	-
152	intellifusion-002	0.0056[99]	0.0539[53]	0.1690[148]	-	-	-	-	-	0.1822[41]	-	0.2556[43]	0.2119[42]
153	intellivision-002	0.0463[265]	0.5999[87]	0.9028[281]	-	-	-	-	-	-	-	-	-
154	intelresearch-003	0.0071[137]	0.0247[36]	0.0930[87]	0.1459[43]	-	-	-	-	-	-	-	-
155	intelresearch-004	0.0038[45]	-	0.0439[45]	-	-	-	-	-	-	-	-	-
156	intsysmsu-002	0.0089[169]	0.0827[62]	0.3138[210]	-	-	-	-	-	-	-	-	-
157	ionetworks-000	0.0060[109]	-	0.1613[143]	-	-	-	-	-	-	-	-	-
158	iqface-000	0.0128[214]	0.0885[66]	0.2867[202]	-	-	-	-	-	-	-	-	-
159	iqface-003	0.0099[187]	0.0254[37]	0.0592[62]	0.0871[28]	-	0.0420[23]	-	-	-	-	-	0.0628[24]
160	irex-000	0.0046[75]	-	0.1491[134]	0.1951[53]	-	-	-	-	-	-	-	-
161	isap-002	0.0094[176]	-	0.4090[232]	-	-	-	-	-	-	-	-	-
162	itmo-007	0.0098[185]	0.0840[63]	0.2685[193]	-	-	-	-	-	-	-	-	-
163	itmo-008	0.0178[231]	-	0.0976[94]	-	-	-	-	-	-	-	-	-
164	ivacognitive-001	0.0096[183]	-	0.4245[235]	0.4902[87]	-	-	-	-	-	-	-	-
165	iws-000	0.6797[307]	0.9960[98]	0.9997[310]	-	-	-	-	-	-	-	-	-
166	kakao-005	0.0067[133]	-	0.0914[84]	0.1180[36]	-	-	-	-	-	-	-	-
167	kakaopay-001	0.0121[210]	-	0.4990[249]	-	-	-	-	-	-	-	-	-
168	kedacom-000	0.0391[261]	0.3444[82]	0.6188[259]	0.6848[95]	0.2663[33]	0.5975[50]	-	-	-	-	-	-
169	kiwitech-000	0.0056[97]	-	0.1817[158]	0.3079[76]	-	-	-	-	-	-	-	-
170	kneron-005	0.0296[251]	-	0.4567[243]	-	-	-	-	-	-	-	-	-
171	kookmin-002	0.0102[191]	-	0.1440[130]	0.1994[57]	-	-	-	-	-	-	-	-
172	kuke3d-001	0.0195[233]	-	0.2845[200]	-	-	-	-	-	-	-	-	-
173	lemalabs-001	0.0081[153]	-	0.3186[211]	-	-	-	-	-	-	-	-	-
174	line-000	0.0118[206]	-	0.2359[180]	0.3288[78]	-	-	-	-	-	-	-	-
175	line-001	0.0038[46]	-	0.0350[37]	-	-	-	-	-	-	-	-	-
176	lookman-004	0.0398[262]	-	0.6520[264]	-	-	-	-	-	-	-	-	-
177	luxand-000	0.2167[291]	0.9732[95]	0.9988[306]	-	-	-	-	-	-	-	-	-
178	mantra-000	0.0079[150]	-	0.0751[72]	-	-	-	-	-	-	-	-	-
179	maxvision-000	0.0293[250]	-	0.1978[167]	-	-	-	-	-	-	-	-	-
180	megvii-003	0.0033[26]	-	0.0460[47]	0.0691[23]	-	-	-	-	0.0419[17]	-	0.0642[19]	0.0471[18]

Table 11: This table summarizes False Non-Match Rate (FNMR) on unmasked and masked probe images. FNMR is the proportion of mated comparisons below a threshold set to achieve FMR=1e-05 on unmasked probe images. False Match Rate (FMR) is the proportion of impostor comparisons at or above that threshold. The red superscripts give rank over all algorithms in that column. Missing entries generally mean the algorithm was not run on that particular mask variation due to time and resource constraints. Algorithms with FTE=1.00 were not run at all. Algorithms in black were submitted prior to mid-March 2020, and algorithms in blue were submitted thereafter.

FNMR(T) "False non-match rate"
FMR(T) "False match rate"

	Algorithm Name	NOT MASKED	MASK COLOR = LIGHTBLUE						COLOR = BLACK			COLOR = RED	COLOR = WHITE
			SHAPE = WIDE			SHAPE = ROUND			SHAPE = WIDE			SHAPE = WIDE	SHAPE = WIDE
	COVERAGE		LO	MED	HI	LO	MED	HI	LO	MED	HI	MED	MED
181	meituan-000	0.0086^{163}	-	0.1059^{104}	-	-	-	-	-	-	-	-	-
182	mendaxiatech-000	0.0026^{8}	-	0.0203^{13}	-	-	-	-	-	-	-	-	-
183	minivision-000	0.0043^{62}	0.0165^{26}	0.0763^{73}	0.1278^{38}	-	0.0432^{24}	-	-	-	-	-	0.0759^{27}
184	mobbl-001	0.4413^{299}	-	0.9908^{293}	-	-	-	-	-	-	-	-	-
185	mobbl-002	1.0000^{316}	-	1.0000^{317}	-	-	-	-	-	-	-	-	-
186	mobipintech-000	0.0096^{181}	-	0.1375^{123}	-	-	-	-	-	-	-	-	-
187	moredian-000	0.9949^{314}	-	0.9996^{309}	0.9997^{110}	-	-	-	-	-	-	-	-
188	multimodality-000	0.0066^{124}	-	0.1165^{109}	-	-	-	-	-	-	-	-	-
189	mvision-001	0.0137^{221}	-	0.3987^{229}	-	-	-	-	-	-	-	-	-
190	nazhiai-000	0.0043^{65}	0.0184^{27}	0.0835^{78}	0.1318^{39}	0.0156^{9}	0.0463^{25}	0.0947^{13}	0.0177^{12}	0.0764^{25}	0.1271^{12}	0.0792^{23}	0.0854^{30}
191	neosystems-002	0.2847^{295}	-	0.9954^{297}	-	-	-	-	-	-	-	-	-
192	neosystems-003	0.4185^{297}	-	0.9645^{289}	-	-	-	-	-	-	-	-	-
193	netbridgetech-001	0.2673^{294}	0.8940^{93}	0.9878^{292}	-	-	-	-	-	-	-	-	-
194	netbridgetech-002	0.0083^{156}	0.0781^{60}	0.2723^{195}	0.3522^{81}	0.0528^{27}	0.1551^{41}	-	0.0875^{31}	0.2863^{43}	0.4151^{28}	-	-
195	neurotechnology-012	0.0042^{59}	-	0.1208^{112}	-	-	-	-	-	-	-	-	-
196	neurotechnology-013	0.0028^{14}	-	0.0180^{7}	-	-	-	-	-	-	-	-	-
197	nhn-001	0.0062^{112}	-	0.1753^{152}	0.2363^{65}	-	-	-	-	-	-	-	-
198	nhn-002	0.0101^{190}	-	0.2669^{191}	-	-	-	-	-	-	-	-	-
199	nodeflux-002	0.0424^{263}	0.4177^{83}	0.7307^{269}	-	-	-	-	-	-	-	-	-
200	notiontag-001	0.6637^{306}	-	0.9986^{304}	0.9990^{109}	-	-	-	-	-	-	-	-
201	notiontag-002	0.0056^{94}	-	0.1583^{140}	-	-	-	-	-	-	-	-	-
202	nsensecorp-002	0.5705^{300}	-	0.9986^{305}	-	-	-	-	-	-	-	-	-
203	nsensecorp-003	0.0076^{148}	-	0.1784^{154}	-	-	-	-	-	-	-	-	-
204	ntechlab-010	0.0026^{7}	0.0054^{6}	0.0205^{15}	0.0304^{6}	-	-	-	-	0.0178^{3}	-	0.0176^{3}	0.0211^{5}
205	ntechlab-011	0.0024^{4}	0.0047^{3}	0.0160^{6}	0.0248^{2}	-	0.0098^{2}	-	-	-	-	-	-
206	omnigarde-000	0.0636^{273}	-	0.7711^{271}	-	-	-	-	-	-	-	-	-
207	omnigarde-001	0.0119^{208}	-	0.3414^{219}	-	-	-	-	-	-	-	-	-
208	omsecurity-000	0.2451^{293}	-	0.9918^{294}	-	-	-	-	-	-	-	-	-
209	openface-001	0.1268^{286}	-	0.9175^{285}	-	-	-	-	-	-	-	-	-
210	oz-003	0.0066^{126}	-	0.1185^{110}	-	-	-	-	-	-	-	-	-
211	oz-004	0.0072^{142}	-	0.0479^{51}	-	-	-	-	-	-	-	-	-
212	papsav1923-001	0.0073^{145}	-	0.1827^{159}	0.2521^{69}	-	-	-	-	-	-	-	-
213	paravision-004	0.0088^{168}	0.0124^{21}	0.0281^{27}	0.0476^{16}	0.0125^{7}	0.0181^{14}	0.0313^{4}	0.0135^{7}	0.0327^{14}	0.0581^{6}	0.0332^{11}	0.0313^{14}
214	paravision-008	0.0032^{23}	0.0076^{15}	0.0254^{25}	0.0499^{18}	-	0.0141^{9}	-	-	-	-	-	-
215	pensees-001	0.0106^{193}	0.0309^{39}	0.0461^{49}	0.0921^{30}	0.0326^{23}	0.0413^{22}	0.0893^{11}	0.0333^{23}	0.0579^{21}	0.1217^{11}	0.1338^{31}	0.0462^{17}
216	pixelall-006	0.0056^{93}	-	0.0961^{93}	-	-	-	-	-	-	-	-	-
217	pixelall-007	0.0056^{98}	-	0.1536^{136}	-	-	-	-	-	-	-	-	-
218	psl-008	0.0030^{17}	-	0.0522^{57}	-	-	-	-	-	-	-	-	-
219	psl-009	0.0027^{9}	-	0.0517^{56}	-	-	-	-	-	-	-	-	-
220	ptakuratsatu-000	0.0059^{107}	0.0542^{54}	0.1897^{163}	0.2485^{68}	0.0380^{25}	0.1047^{39}	-	0.0502^{29}	0.1652^{39}	0.2360^{26}	0.2003^{39}	-
221	pxl-001	0.0511^{269}	0.4879^{84}	0.8183^{272}	0.8754^{99}	0.3675^{34}	0.7276^{51}	0.9182^{28}	0.5416^{38}	0.8047^{50}	0.8718^{35}	-	-
222	qnap-000	0.0126^{212}	-	0.3284^{216}	-	-	-	-	-	-	-	-	-
223	qnap-001	0.0107^{196}	-	0.2524^{187}	-	-	-	-	-	-	-	-	-
224	quantasoft-003	0.0058^{106}	-	0.2184^{174}	0.3424^{80}	-	-	-	-	-	-	-	-
225	rankone-011	0.0043^{64}	-	0.1001^{98}	-	-	-	-	-	-	-	-	-

Table 12: This table summarizes False Non-Match Rate (FNMR) on unmasked and masked probe images. FNMR is the proportion of mated comparisons below a threshold set to achieve FMR=1e-05 on unmasked probe images. False Match Rate (FMR) is the proportion of impostor comparisons at or above that threshold. The red superscripts give rank over all algorithms in that column. Missing entries generally mean the algorithm was not run on that particular mask variation due to time and resource constraints. Algorithms with FTE=1.00 were not run at all. Algorithms in black were submitted prior to mid-March 2020, and algorithms in blue were submitted thereafter.

FNMR(T) "False non-match rate"
FMR(T) "False match rate"

	Algorithm Name	NOT MASKED	MASK COLOR = LIGHTBLUE						COLOR = BLACK			COLOR = RED	COLOR = WHITE
			SHAPE = WIDE			SHAPE = ROUND			SHAPE = WIDE			SHAPE = WIDE	SHAPE = WIDE
	COVERAGE		LO	MED	HI	LO	MED	HI	LO	MED	HI	MED	MED
226	rankone-012	0.0036^{36}	-	0.0503^{54}	-	-	-	-	-	-	-	-	-
227	realnetworks-004	0.0071^{138}	-	0.2319^{177}	0.2906^{75}	-	-	-	-	-	-	-	-
228	realnetworks-005	0.0057^{100}	-	0.1018^{100}	-	-	-	-	-	-	-	-	-
229	regula-000	0.0087^{167}	-	0.1923^{164}	0.3319^{79}	-	-	-	-	-	-	-	-
230	regula-001	0.0090^{173}	-	0.2499^{186}	-	-	-	-	-	-	-	-	-
231	remarkai-003	0.0039^{47}	-	0.0229^{19}	-	-	-	-	-	-	-	-	-
232	rendip-000	0.0060^{108}	-	0.1288^{118}	0.1994^{56}	-	-	-	-	-	-	-	-
233	revealmedia-005	0.0058^{104}	-	0.0954^{92}	-	-	-	-	-	-	-	-	-
234	rokid-000	0.0117^{205}	0.1448^{75}	0.4346^{236}	-	-	-	-	-	-	-	-	-
235	s1-003	0.0037^{42}	-	0.0715^{70}	-	-	-	-	-	-	-	-	-
236	s1-004	0.0039^{50}	-	0.0712^{69}	-	-	-	-	-	-	-	-	-
237	samsungsds-000	0.0085^{162}	-	0.2341^{178}	-	-	-	-	-	-	-	-	-
238	scanovate-002	0.0119^{209}	0.1304^{74}	0.4006^{230}	0.5142^{89}	0.0757^{28}	0.2206^{43}	0.3622^{23}	0.1215^{33}	0.3172^{45}	0.4633^{30}	-	-
239	scanovate-003	0.0292^{249}	-	0.1584^{141}	-	-	-	-	-	-	-	-	-
240	securifai-003	0.6245^{303}	-	0.9981^{303}	-	-	-	-	-	-	-	-	-
241	securifai-004	0.0071^{139}	-	0.2775^{199}	-	-	-	-	-	-	-	-	-
242	sensetime-005	0.0020^{2}	0.0039^{2}	0.0149^{3}	0.0290^{5}	-	-	-	-	0.0160^{2}	-	0.0161^{2}	0.0158^{1}
243	sensetime-006	0.0018^{1}	0.0031^{1}	0.0085^{1}	0.0177^{1}	-	-	-	-	-	-	-	-
244	sertis-000	0.0066^{125}	0.0751^{57}	0.2685^{192}	-	-	-	-	-	-	-	-	-
245	sertis-002	0.0037^{39}	-	0.0850^{81}	-	-	-	-	-	-	-	-	-
246	seventhsense-000	0.0067^{131}	-	0.1394^{125}	-	-	-	-	-	-	-	-	-
247	shu-002	1.0000^{315}	-	1.0000^{316}	-	-	-	-	-	-	-	-	-
248	shu-003	0.0053^{90}	0.0465^{48}	0.1839^{160}	0.2148^{59}	0.0379^{24}	0.1148^{40}	0.2196^{22}	0.0422^{28}	0.1702^{40}	0.2210^{23}	0.1901^{38}	-
249	sjtu-003	0.0043^{60}	0.0340^{42}	0.1239^{114}	0.1609^{47}	-	-	-	0.0276^{20}	0.1008^{30}	0.1539^{14}	0.1333^{30}	0.1323^{35}
250	sjtu-004	0.0037^{43}	-	0.0301^{31}	-	-	-	-	-	-	-	-	-
251	sktelecom-000	0.0033^{24}	-	0.0299^{30}	-	-	-	-	-	-	-	-	-
252	smartengines-000	0.8481^{313}	-	0.9999^{314}	-	-	-	-	-	-	-	-	-
253	sodec-000	0.0043^{61}	-	0.0728^{71}	-	-	-	-	-	-	-	-	-
254	sqisoft-001	0.1023^{282}	-	0.9573^{287}	-	-	-	-	-	-	-	-	-
255	sqisoft-002	0.0067^{132}	-	0.1749^{151}	-	-	-	-	-	-	-	-	-
256	staqu-000	0.0108^{198}	0.1251^{72}	0.3537^{222}	0.4429^{85}	0.0913^{30}	0.2434^{46}	0.4447^{25}	-	0.3862^{47}	0.6319^{32}	-	-
257	starhybrid-001	0.0104^{192}	0.1923^{77}	0.5033^{250}	-	-	-	-	-	-	-	-	-
258	suprema-000	0.0116^{204}	-	0.1641^{146}	0.2342^{64}	-	-	-	-	-	-	-	-
259	suprema-001	0.0050^{83}	-	0.0899^{83}	-	-	-	-	-	-	-	-	-
260	supremaid-001	0.0077^{149}	-	0.1550^{139}	-	-	-	-	-	-	-	-	-
261	synology-000	0.0123^{211}	-	0.4459^{239}	-	-	-	-	-	-	-	-	-
262	synology-002	0.0100^{188}	-	0.4666^{245}	-	-	-	-	-	-	-	-	-
263	sztu-000	0.0074^{146}	-	0.1432^{129}	0.1962^{54}	-	-	-	-	-	-	-	-
264	sztu-001	0.0046^{74}	-	0.0316^{32}	-	-	-	-	-	-	-	-	-
265	tech5-004	0.0045^{71}	0.0218^{31}	0.0839^{79}	0.1389^{42}	0.0172^{10}	0.0464^{26}	0.0905^{12}	0.0228^{15}	0.0818^{26}	0.1288^{13}	0.0826^{24}	0.0830^{29}
266	tech5-005	0.0037^{38}	0.0224^{32}	0.0941^{88}	0.1518^{45}	0.0180^{14}	0.0524^{30}	0.1066^{17}	0.0254^{18}	0.0986^{28}	0.1571^{16}	0.0979^{26}	0.0945^{31}
267	techsign-000	0.0509^{268}	-	0.8759^{277}	-	-	-	-	-	-	-	-	-
268	tevian-007	0.0040^{52}	-	0.0222^{16}	-	-	-	-	-	0.0276^{9}	-	0.0473^{15}	0.0268^{9}
269	tevian-008	0.0035^{34}	0.0067^{11}	0.0180^{8}	0.0325^{7}	-	0.0114^{5}	-	-	-	-	-	-
270	tiger-005	0.0234^{241}	-	0.4627^{244}	-	-	-	-	-	-	-	-	-

Table 13: This table summarizes False Non-Match Rate (FNMR) on unmasked and masked probe images. FNMR is the proportion of mated comparisons below a threshold set to achieve FMR=1e-05 on unmasked probe images. False Match Rate (FMR) is the proportion of impostor comparisons at or above that threshold. The red superscripts give rank over all algorithms in that column. Missing entries generally mean the algorithm was not run on that particular mask variation due to time and resource constraints. Algorithms with FTE=1.00 were not run at all. Algorithms in black were submitted prior to mid-March 2020, and algorithms in blue were submitted thereafter.

FNMR(T) "False non-match rate"
FMR(T) "False match rate"

	Algorithm Name	NOT MASKED	MASK COLOR = LIGHTBLUE						COLOR = BLACK			COLOR = RED	COLOR = WHITE
			SHAPE = WIDE			SHAPE = ROUND			SHAPE = WIDE			SHAPE = WIDE	SHAPE = WIDE
	COVERAGE		LO	MED	HI	LO	MED	HI	LO	MED	HI	MED	MED
271	tiger-006	0.0063^{118}	-	0.1278^{117}	-	-	-	-	-	-	-	-	-
272	tinkoff-001	0.0236^{242}	-	0.5734^{256}	-	-	-	-	-	-	-	-	-
273	toppanidgate-000	0.0035^{32}	-	0.0204^{14}	-	-	-	-	-	-	-	-	-
274	toshiba-004	0.0028^{12}	-	0.0247^{24}	-	-	-	-	-	-	-	-	-
275	trueface-002	0.0084^{158}	-	0.2130^{171}	0.2602^{71}	-	-	-	-	-	-	-	-
276	trueface-003	0.0086^{165}	-	0.1630^{145}	-	-	-	-	-	-	-	-	-
277	tuputech-000	0.2014^{289}	0.8743^{92}	0.9731^{291}	-	-	-	-	-	-	-	-	-
278	twface-000	0.0050^{82}	-	0.1153^{107}	-	-	-	-	-	-	-	-	-
279	twface-001	0.0039^{51}	-	0.0448^{46}	-	-	-	-	-	-	-	-	-
280	uluface-002	0.0073^{144}	0.0796^{61}	0.2450^{185}	-	-	-	-	-	-	-	0.3939^{47}	-
281	unissey-001	0.0094^{177}	-	0.3281^{215}	-	-	-	-	-	-	-	-	-
282	upc-001	0.0167^{230}	-	0.4723^{246}	-	-	-	-	-	-	-	-	-
283	vd-002	0.0462^{264}	-	0.7133^{268}	0.7875^{98}	-	-	-	-	-	-	-	-
284	vd-003	0.0098^{186}	-	0.2740^{197}	-	-	-	-	-	-	-	-	-
285	veridas-006	0.0083^{157}	-	0.3073^{207}	0.3936^{84}	-	-	-	-	-	-	-	-
286	veridas-007	0.0063^{117}	-	0.1733^{150}	-	-	-	-	-	-	-	-	-
287	verigram-000	0.0086^{164}	-	0.2037^{169}	-	-	-	-	-	-	-	-	-
288	verihubs-inteligensia-000	0.0064^{119}	-	0.1988^{168}	-	-	-	-	-	-	-	-	-
289	via-001	0.0097^{184}	0.1234^{71}	0.3406^{217}	-	-	-	-	-	-	-	-	-
290	videmo-000	0.0140^{223}	-	0.5509^{254}	-	-	-	-	-	-	-	-	-
291	videmo-001	0.0254^{246}	-	0.3872^{226}	-	-	-	-	-	-	-	-	-
292	videonetics-002	0.6032^{302}	0.9941^{97}	0.9996^{308}	-	-	-	-	-	-	-	-	-
293	viettelhightech-000	0.0095^{180}	-	0.3242^{214}	-	-	-	-	-	-	-	-	-
294	vigilantsolutions-010	0.0129^{215}	-	0.4364^{237}	0.5363^{90}	-	-	-	-	-	-	-	-
295	vigilantsolutions-011	0.0116^{203}	-	0.4130^{234}	-	-	-	-	-	-	-	-	-
296	vinai-000	0.0056^{96}	0.0388^{43}	0.1587^{142}	0.2130^{58}	0.0286^{20}	0.0965^{38}	-	0.0364^{26}	0.1487^{36}	0.2024^{22}	0.1691^{36}	0.1710^{40}
297	vinbigdata-001	0.0906^{280}	-	0.5155^{252}	-	-	-	-	-	-	-	-	-
298	visage-000	0.0674^{274}	-	0.9626^{288}	0.9742^{104}	-	-	-	-	-	-	-	-
299	visionbox-002	0.0062^{113}	-	0.1351^{122}	-	-	-	-	-	-	-	-	-
300	visionlabs-010	0.0027^{10}	0.0076^{14}	0.0342^{36}	0.0513^{19}	-	-	-	-	0.0313^{13}	-	0.0244^{7}	0.0269^{10}
301	visionlabs-011	0.0024^{3}	0.0049^{5}	0.0157^{4}	0.0289^{4}	-	0.0086^{1}	-	-	-	-	-	-
302	visteam-001	0.4187^{298}	-	0.9943^{296}	0.9976^{106}	-	-	-	-	-	-	-	-
303	visteam-002	0.0793^{275}	-	0.8577^{273}	-	-	-	-	-	-	-	-	-
304	vnpt-002	0.0384^{260}	-	0.4555^{242}	-	-	-	-	-	-	-	-	-
305	vnpt-003	0.0067^{130}	-	0.1458^{131}	-	-	-	-	-	-	-	-	-
306	vocord-008	0.0038^{44}	0.0140^{24}	0.0500^{53}	0.0762^{25}	0.0176^{13}	0.0393^{21}	0.0892^{10}	0.0135^{8}	0.0459^{19}	0.0771^{7}	0.0607^{18}	0.0482^{20}
307	vocord-009	0.0045^{72}	0.0086^{16}	0.0261^{26}	0.0438^{14}	0.0086^{4}	0.0151^{10}	0.0271^{3}	0.0093^{5}	0.0289^{10}	0.0506^{4}	0.0275^{8}	0.0271^{11}
308	vts-000	0.0199^{235}	0.0870^{64}	0.2755^{198}	0.3566^{82}	-	-	-	0.0858^{30}	0.2584^{42}	0.3898^{27}	0.2249^{40}	0.2976^{43}
309	winsense-001	0.0058^{103}	0.0473^{49}	0.1626^{144}	0.2244^{62}	0.0325^{22}	0.0946^{37}	0.1853^{21}	0.0406^{27}	0.1471^{35}	0.2231^{24}	0.1622^{35}	0.1843^{41}
310	winsense-002	0.0044^{69}	0.0213^{30}	0.0846^{80}	0.1235^{37}	-	-	-	-	-	-	0.1014^{27}	-
311	wuhantianyu-001	0.0202^{236}	-	0.3006^{206}	-	-	-	-	-	-	-	-	-
312	x-laboratory-001	0.0058^{105}	0.0517^{52}	0.2569^{189}	-	-	-	-	-	-	-	0.2333^{41}	-
313	xforwardai-001	0.0041^{53}	0.0087^{18}	0.0289^{29}	0.0536^{20}	0.0087^{5}	0.0180^{13}	0.0377^{6}	0.0090^{4}	0.0303^{11}	0.0544^{5}	0.0313^{10}	0.0294^{13}
314	xforwardai-002	0.0037^{41}	0.0062^{9}	0.0159^{5}	0.0338^{8}	0.0068^{1}	0.0119^{6}	0.0249^{2}	0.0062^{1}	0.0153^{1}	0.0310^{1}	0.0156^{1}	0.0162^{2}
315	xm-000	0.0044^{66}	0.0334^{41}	0.1255^{116}	0.1682^{49}	0.0275^{19}	0.0774^{34}	0.1648^{20}	0.0324^{22}	0.1274^{32}	0.1839^{20}	0.1706^{37}	0.1381^{36}

Table 14: This table summarizes False Non-Match Rate (FNMR) on unmasked and masked probe images. FNMR is the proportion of mated comparisons below a threshold set to achieve FMR=1e-05 on unmasked probe images. False Match Rate (FMR) is the proportion of impostor comparisons at or above that threshold. The red superscripts give rank over all algorithms in that column. Missing entries generally mean the algorithm was not run on that particular mask variation due to time and resource constraints. Algorithms with FTE=1.00 were not run at all. Algorithms in black were submitted prior to mid-March 2020, and algorithms in blue were submitted thereafter.

FNMR(T) "False non-match rate"
FMR(T) "False match rate"

	Algorithm Name	NOT MASKED	MASK COLOR = LIGHTBLUE SHAPE = WIDE			SHAPE = ROUND			COLOR = BLACK SHAPE = WIDE			COLOR = RED SHAPE = WIDE	COLOR = WHITE SHAPE = WIDE
	COVERAGE		LO	MED	HI	LO	MED	HI	LO	MED	HI	MED	MED
316	yoonik-002	0.0608^{272}	-	0.0948^{90}	-	-	-	-	-	-	-	-	-
317	yoonik-003	0.0809^{277}	-	0.1161^{108}	-	-	-	-	-	-	-	-	-
318	ytu-000	0.0032^{22}	-	0.0351^{39}	-	-	-	-	-	-	-	-	-
319	yuan-002	0.0066^{122}	-	0.2417^{184}	-	-	-	-	-	-	-	-	-
320	yuan-003	0.0065^{121}	-	0.2386^{183}	-	-	-	-	-	-	-	-	-

Table 15: This table summarizes False Non-Match Rate (FNMR) on unmasked and masked probe images. FNMR is the proportion of mated comparisons below a threshold set to achieve FMR=1e-05 on unmasked probe images. False Match Rate (FMR) is the proportion of impostor comparisons at or above that threshold. The red superscripts give rank over all algorithms in that column. Missing entries generally mean the algorithm was not run on that particular mask variation due to time and resource constraints. Algorithms with FTE=1.00 were not run at all. Algorithms in black were submitted prior to mid-March 2020, and algorithms in blue were submitted thereafter.

FNMR(T) "False non-match rate"
FMR(T) "False match rate"

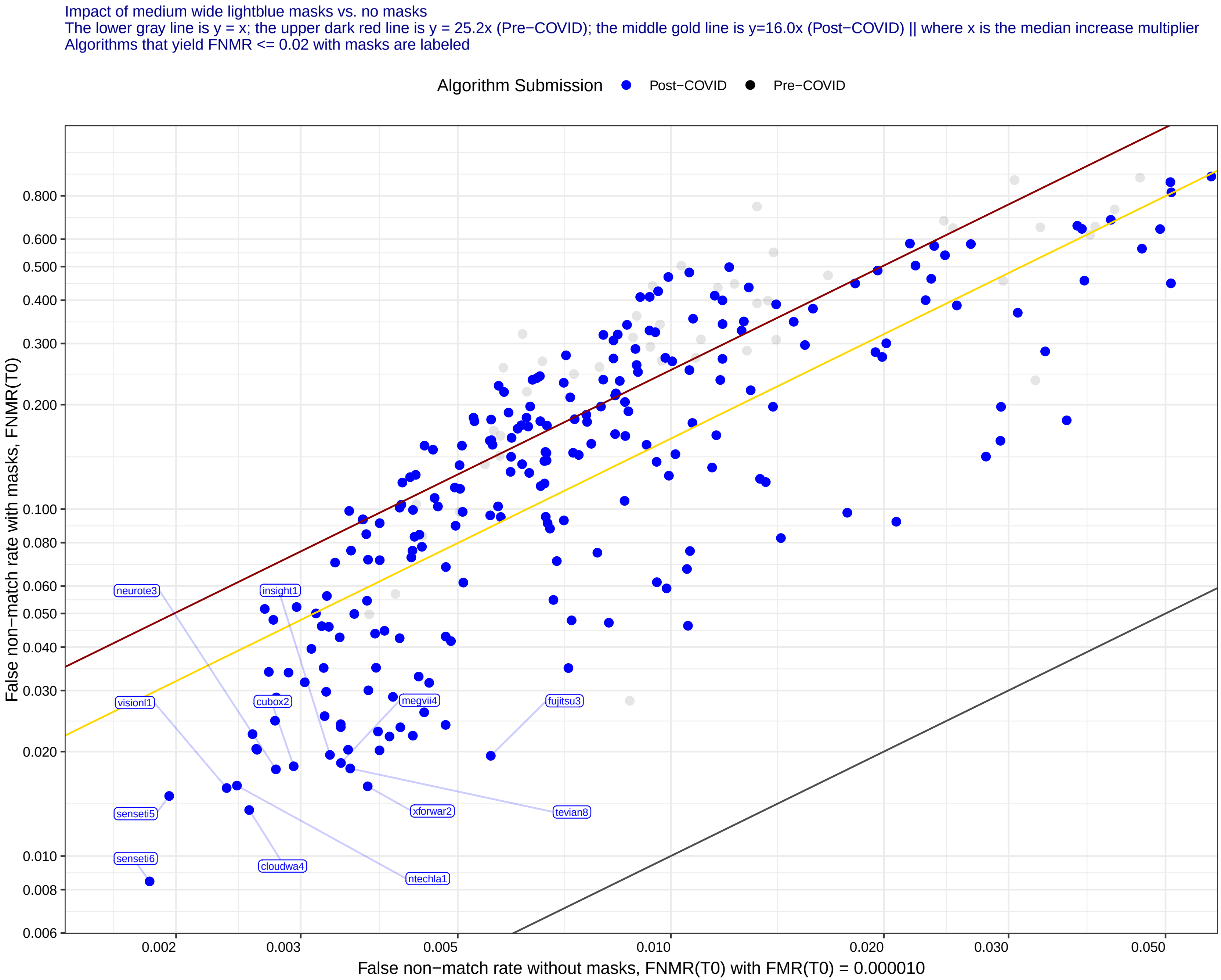

Figure 15: At a fixed threshold, a plot of FNMR with and without masks. The displacement of the dark red line relative to the black "parity" line shows a large increase in FNMR with masks for pre-COVID algorithms. The reduction in distance (relative to the black line) observed in the gold line indicates a reduction in median FNMR with masks for post-COVID algorithms. The value in the title is the median increase multiplier.

FNMR(T) "False non-match rate"
FMR(T) "False match rate"

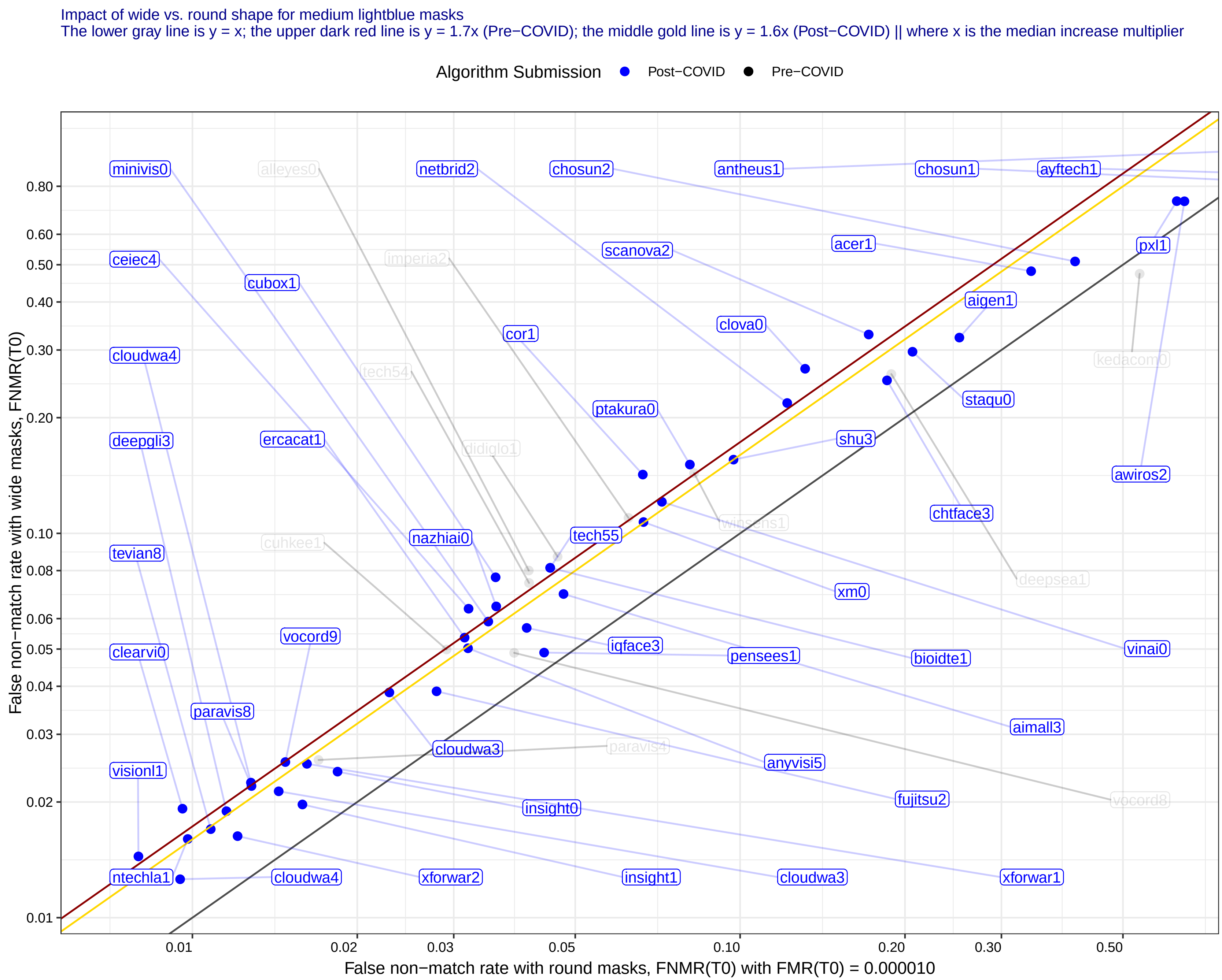

Figure 16: At a fixed threshold, a plot of FNMR with round versus wide masks. The displacement of the dark red (pre-COVID algorithms) and gold (post-COVID algorithms) lines relative to the black "parity" line shows a modest increase in FNMR with wide masks, with median post-COVID results showing nominal FNMR reductions. The value in the title is the median increase multiplier.

FNMR(T) "False non-match rate"
FMR(T) "False match rate"

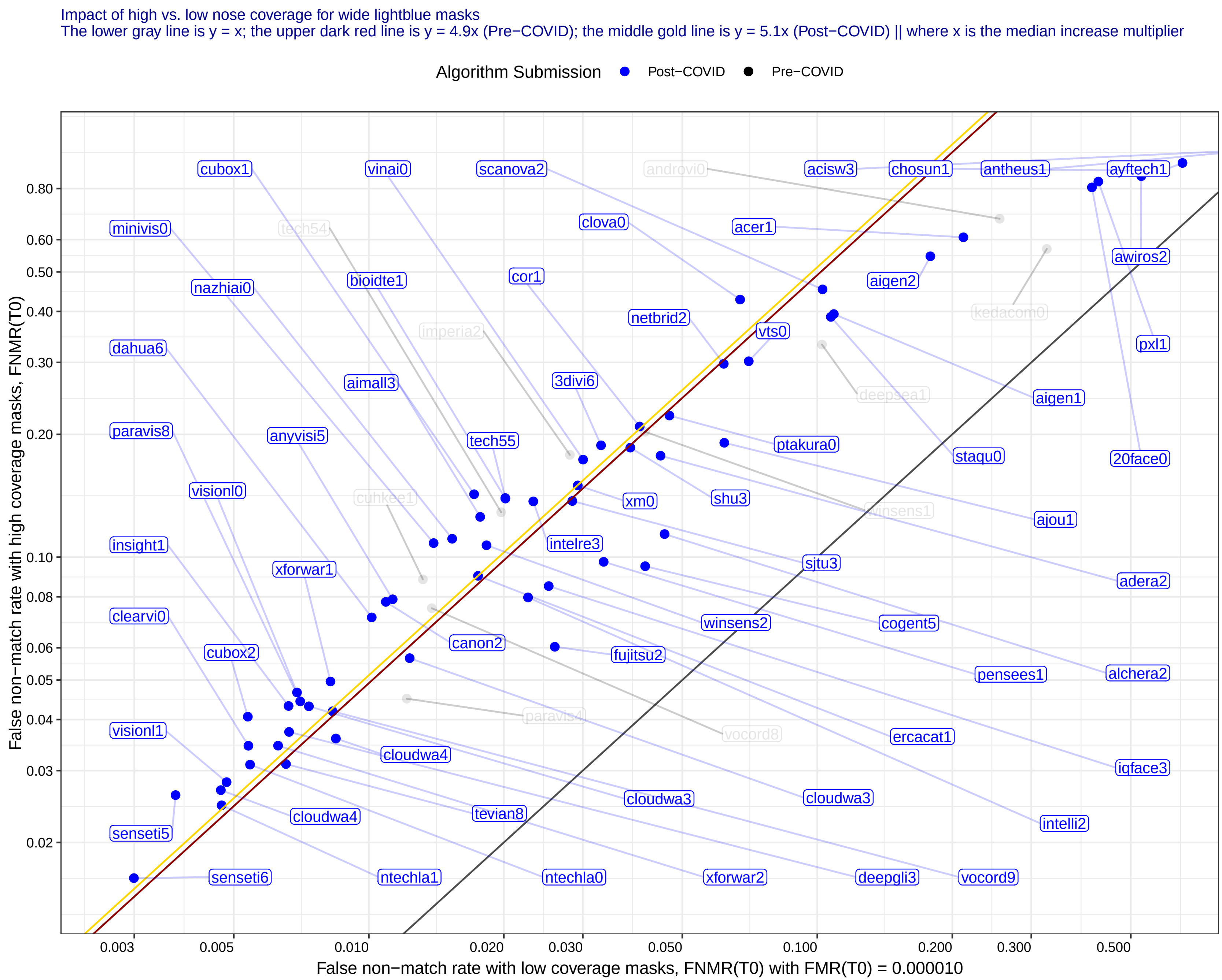

Figure 17: At a fixed threshold, a plot of FNMR with low versus high masks. The displacement of the dark red (pre-COVID algorithms) and gold (post-COVID algorithms) lines relative to the black "parity" lines shows a considerable increase in FNMR with high vs. low nose coverage masks, with median post-COVID results showing modest FNMR reductions. The value in the title is the median increase multiplier.

	Algorithm Name	COLOR = WHITE SHAPE = WIDE			COLOR = LIGHTBLUE SHAPE = WIDE			COLOR = LIGHTBLUE SHAPE = ROUND			COLOR = RED SHAPE = WIDE			COLOR = BLACK SHAPE = WIDE		
	COVERAGE	LO	MED	HI	LO	MED	HI	LO	MED	HI	LO	MED	HI	LO	MED	HI
1	20face-000	0.004	0.016	0.040	0.004	0.014	0.036	0.005	0.009	0.020	0.005	0.018	0.044	0.006	0.023	0.055
2	20face-001	0.000	0.000	0.000	0.000	0.000	0.000	0.000	0.000	0.000	0.000	0.000	0.000	0.000	0.000	0.000
3	3divi-006	0.003	0.011	0.028	0.002	0.012	0.028	0.007	0.008	0.021	0.005	0.035	0.071	0.002	0.007	0.012
4	3divi-007	0.003	0.011	0.028	0.002	0.012	0.028	0.007	0.008	0.021	0.005	0.035	0.071	0.002	0.007	0.012
5	acer-001	0.020	0.048	0.091	0.019	0.051	0.096	0.025	0.034	0.060	0.025	0.080	0.147	0.026	0.088	0.157
6	acer-002	0.005	0.020	0.043	0.006	0.021	0.047	0.005	0.010	0.024	0.006	0.022	0.050	0.007	0.034	0.080
7	acisw-003	0.000	0.000	0.000	0.000	0.000	0.000	0.000	0.000	0.000	0.000	0.000	0.000	0.000	0.000	0.000
8	acisw-007	0.000	0.000	0.000	0.000	0.000	0.000	0.000	0.000	0.000	0.000	0.000	0.000	0.000	0.000	0.000
9	adera-002	0.103	0.167	0.205	0.094	0.141	0.193	0.098	0.116	0.180	0.267	0.457	0.551	0.214	0.333	0.397
10	adera-003	0.103	0.167	0.205	0.094	0.141	0.193	0.098	0.116	0.180	0.267	0.457	0.551	0.214	0.333	0.397
11	advance-002	0.019	0.046	0.096	0.020	0.045	0.096	0.026	0.037	0.085	0.028	0.088	0.174	0.034	0.104	0.200
12	advance-003	0.014	0.034	0.083	0.014	0.034	0.083	0.019	0.027	0.066	0.018	0.055	0.143	0.018	0.067	0.169
13	aifirst-001	0.000	0.000	0.000	0.000	0.000	0.000	0.000	0.000	0.000	0.000	0.000	0.000	0.000	0.000	0.000
14	aigen-001	0.000	0.000	0.000	0.000	0.000	0.000	0.000	0.000	0.000	0.000	0.000	0.000	0.000	0.000	0.000
15	aigen-002	0.000	0.000	0.000	0.000	0.000	0.000	0.000	0.000	0.000	0.000	0.000	0.000	0.000	0.000	0.000
16	ailabs-001	0.071	0.208	0.248	0.061	0.194	0.233	0.102	0.177	0.314	0.096	0.319	0.389	0.116	0.310	0.465
17	aimall-002	0.073	0.129	0.225	0.095	0.152	0.260	0.107	0.159	0.236	0.086	0.122	0.230	0.049	0.071	0.154
18	aimall-003	0.011	0.038	0.097	0.014	0.047	0.113	0.020	0.041	0.085	0.013	0.039	0.103	0.012	0.033	0.081
19	aiunionface-000	0.000	0.000	0.000	0.000	0.000	0.000	0.000	0.000	0.000	0.000	0.000	0.000	0.000	0.000	0.000
20	aize-001	0.092	0.208	0.288	0.079	0.170	0.237	0.085	0.145	0.220	0.236	0.496	0.694	0.097	0.274	0.512
21	aize-002	0.022	0.053	0.104	0.020	0.053	0.105	0.029	0.043	0.083	0.070	0.197	0.287	0.046	0.130	0.207
22	ajou-001	0.047	0.105	0.160	0.041	0.101	0.156	0.064	0.095	0.188	0.079	0.214	0.303	0.057	0.174	0.275
23	alchera-002	0.003	0.007	0.017	0.003	0.007	0.015	0.003	0.003	0.007	0.004	0.012	0.034	0.003	0.013	0.037
24	alchera-003	0.005	0.012	0.027	0.006	0.012	0.028	0.008	0.009	0.016	0.006	0.015	0.041	0.006	0.014	0.036
25	alfabeta-001	0.489	0.829	0.795	0.476	0.827	0.804	0.627	0.800	0.937	0.387	0.873	0.895	0.512	0.961	0.984
26	alice-000	0.000	0.000	0.000	0.000	0.000	0.000	0.000	0.000	0.000	0.000	0.000	0.000	0.000	0.000	0.000
27	alleyes-000	0.006	0.023	0.062	0.006	0.020	0.056	0.007	0.012	0.028	0.007	0.035	0.088	0.010	0.043	0.104
28	alphaface-002	0.025	0.056	0.099	0.024	0.054	0.095	0.033	0.044	0.072	0.041	0.104	0.174	0.027	0.071	0.132
29	androvideo-000	0.000	0.000	0.000	0.000	0.000	0.000	0.000	0.000	0.000	0.000	0.000	0.000	0.000	0.000	0.000
30	anke-005	0.009	0.028	0.066	0.011	0.030	0.069	0.012	0.018	0.041	0.013	0.036	0.079	0.009	0.056	0.091
31	antheus-000	0.000	0.000	0.000	0.000	0.000	0.000	0.000	0.000	0.000	0.000	0.000	0.000	0.000	0.000	0.000
32	antheus-001	0.000	0.000	0.000	0.000	0.000	0.000	0.000	0.000	0.000	0.000	0.000	0.000	0.000	0.000	0.000
33	anyvision-005	0.003	0.012	0.029	0.003	0.032	0.069	0.008	0.018	0.045	0.007	0.045	0.123	0.004	0.046	0.137
34	armatura-001	0.007	0.019	0.037	0.008	0.018	0.040	0.012	0.015	0.029	0.009	0.020	0.041	0.009	0.022	0.051
35	asusaics-000	0.000	0.000	0.000	0.000	0.000	0.000	0.000	0.000	0.000	0.000	0.000	0.000	0.000	0.000	0.000
36	authenmetric-003	0.000	0.000	0.000	0.000	0.000	0.000	0.000	0.000	0.000	0.000	0.000	0.000	0.000	0.000	0.000
37	authenmetric-004	0.000	0.000	0.000	0.000	0.000	0.000	0.000	0.000	0.000	0.000	0.000	0.000	0.000	0.000	0.000
38	aware-005	0.053	0.151	0.218	0.039	0.129	0.211	0.046	0.089	0.244	0.095	0.380	0.516	0.091	0.236	0.449
39	aware-006	0.005	0.014	0.035	0.005	0.015	0.035	0.005	0.009	0.018	0.005	0.017	0.045	0.006	0.022	0.049
40	awiros-001	0.195	0.370	0.450	0.162	0.298	0.379	0.161	0.258	0.355	0.388	0.650	0.772	0.198	0.415	0.642
41	awiros-002	0.101	0.212	0.215	0.103	0.202	0.220	0.187	0.261	0.356	0.071	0.272	0.296	0.232	0.405	0.455
42	ayftech-001	0.237	0.610	0.587	0.251	0.615	0.609	0.301	0.553	0.728	0.105	0.405	0.626	0.193	0.596	0.758
43	beethedata-000	0.005	0.012	0.024	0.004	0.008	0.019	0.005	0.007	0.011	0.006	0.023	0.058	0.006	0.018	0.046
44	beyneai-000	0.000	0.000	0.000	0.000	0.000	0.000	0.000	0.000	0.000	0.000	0.000	0.000	0.000	0.000	0.000
45	biocube-001	0.130	0.220	0.271	0.126	0.197	0.246	0.122	0.174	0.233	0.232	0.459	0.613	0.134	0.268	0.435

Table 16: This table summarizes Failure to Enroll (FTE) rates surveyed over 10 000 images of each mask variant. FTE is the proportion of failed template generation attempts. Failures can occur because the software throws an exception, or because the software electively refuses to process the input image as would occur if the algorithms does not detect a face or determines that the face has insufficient information. FTE is measured as the number of function calls that give EITHER a non-zero error code OR that give a "small" template containing fewer than 60 bytes. This second rule is needed because some algorithms incorrectly fail to return a non-zero error code when template generation fails but do produce a skeletal template. The effects of FTE are included in the accuracy results of this report by regarding any template comparison involving a failed template to produce a low similarity score. Thus higher FTE results in higher FNMR and lower FMR. Algorithms in black were submitted prior to mid-March 2020, and algorithms in blue were submitted thereafter.

FNMR(T) "False non-match rate"
FMR(T) "False match rate"

	Algorithm Name	COLOR = WHITE			COLOR = LIGHTBLUE						COLOR = RED			COLOR = BLACK		
		SHAPE = WIDE			SHAPE = WIDE			SHAPE = ROUND			SHAPE = WIDE			SHAPE = WIDE		
	COVERAGE	LO	MED	HI	LO	MED	HI	LO	MED	HI	LO	MED	HI	LO	MED	HI
46	bioidtechswiss-001	0.004	0.014	0.044	0.004	0.017	0.046	0.006	0.011	0.026	0.005	0.020	0.051	0.007	0.022	0.056
47	bioidtechswiss-002	0.004	0.013	0.041	0.003	0.017	0.045	0.006	0.011	0.026	0.004	0.018	0.049	0.004	0.017	0.047
48	boetech-001	0.419	0.554	0.537	0.355	0.536	0.499	0.243	0.454	0.535	0.151	0.189	0.187	0.411	0.527	0.523
49	boetech-002	0.419	0.554	0.537	0.355	0.536	0.499	0.243	0.454	0.535	0.151	0.189	0.187	0.411	0.527	0.523
50	bresee-001	0.005	0.022	0.049	0.005	0.020	0.049	0.009	0.014	0.034	0.010	0.051	0.108	0.008	0.041	0.097
51	bresee-002	0.004	0.011	0.021	0.005	0.011	0.019	0.005	0.006	0.013	0.005	0.014	0.025	0.005	0.014	0.026
52	camvi-004	0.000	0.000	0.000	0.000	0.000	0.000	0.000	0.000	0.000	0.000	0.000	0.000	0.000	0.000	0.000
53	canon-002	0.000	0.000	0.000	0.000	0.000	0.000	0.000	0.000	0.000	0.000	0.000	0.000	0.000	0.000	0.000
54	canon-003	0.005	0.017	0.045	0.006	0.017	0.043	0.005	0.010	0.024	0.009	0.031	0.083	0.011	0.035	0.091
55	ceiec-003	0.023	0.056	0.103	0.021	0.054	0.096	0.029	0.042	0.100	0.048	0.143	0.218	0.044	0.128	0.222
56	ceiec-004	0.008	0.021	0.047	0.008	0.021	0.045	0.010	0.015	0.033	0.012	0.042	0.094	0.015	0.051	0.099
57	chosun-001	0.000	0.000	0.000	0.000	0.000	0.000	0.000	0.000	0.000	0.000	0.000	0.000	0.000	0.000	0.000
58	chosun-002	0.000	0.000	0.000	0.000	0.000	0.000	0.000	0.000	0.000	0.000	0.000	0.000	0.000	0.000	0.000
59	chtface-003	0.022	0.075	0.125	0.018	0.059	0.099	0.023	0.039	0.077	0.080	0.259	0.418	0.030	0.108	0.224
60	chtface-004	0.040	0.128	0.213	0.040	0.129	0.218	0.058	0.097	0.242	0.029	0.074	0.138	0.043	0.129	0.216
61	clearviewai-000	0.000	0.000	0.000	0.000	0.000	0.000	0.000	0.000	0.000	0.000	0.000	0.000	0.000	0.000	0.000
62	closeli-001	0.000	0.000	0.000	0.000	0.000	0.000	0.000	0.000	0.000	0.000	0.000	0.000	0.000	0.000	0.000
63	cloudmatrix-000	0.011	0.025	0.049	0.011	0.023	0.046	0.017	0.021	0.038	0.019	0.046	0.096	0.022	0.045	0.093
64	cloudwalk-hr-003	0.003	0.008	0.013	0.003	0.009	0.012	0.006	0.008	0.014	0.005	0.011	0.022	0.005	0.009	0.017
65	cloudwalk-hr-004	0.004	0.010	0.015	0.005	0.009	0.013	0.004	0.005	0.007	0.005	0.013	0.018	0.005	0.011	0.019
66	cloudwalk-mt-003	0.003	0.015	0.046	0.004	0.017	0.049	0.007	0.013	0.031	0.005	0.018	0.045	0.006	0.017	0.044
67	cloudwalk-mt-004	0.006	0.017	0.048	0.007	0.019	0.050	0.010	0.016	0.034	0.008	0.019	0.046	0.010	0.019	0.046
68	clova-000	0.035	0.089	0.149	0.033	0.081	0.136	0.039	0.059	0.128	0.071	0.245	0.361	0.049	0.146	0.252
69	cogent-005	0.000	0.000	0.000	0.000	0.000	0.000	0.000	0.000	0.000	0.000	0.000	0.000	0.000	0.000	0.000
70	cogent-006	0.000	0.000	0.000	0.000	0.000	0.000	0.000	0.000	0.000	0.000	0.000	0.000	0.000	0.000	0.000
71	cognitec-002	0.136	0.142	0.196	0.160	0.247	0.298	0.221	0.326	0.390	0.115	0.299	0.518	0.144	0.446	0.721
72	cognitec-003	0.171	0.138	0.202	0.162	0.142	0.200	0.225	0.222	0.289	0.143	0.213	0.369	0.171	0.237	0.469
73	cor-001	0.002	0.010	0.031	0.003	0.013	0.035	0.004	0.008	0.020	0.004	0.013	0.032	0.004	0.011	0.031
74	coretech-000	0.000	0.000	0.000	0.000	0.000	0.000	0.000	0.000	0.000	0.000	0.000	0.000	0.000	0.000	0.000
75	corsight-001	0.004	0.026	0.070	0.005	0.035	0.085	-	-	-	-	-	-	0.005	0.025	0.062
76	csc-002	0.034	0.082	0.154	0.038	0.089	0.171	0.057	0.093	0.268	0.040	0.103	0.204	0.045	0.136	0.285
77	csc-003	0.034	0.082	0.154	0.038	0.089	0.171	0.057	0.093	0.268	0.040	0.103	0.204	0.045	0.136	0.285
78	ctbcbank-000	0.179	0.794	0.803	0.171	0.786	0.865	0.205	0.620	0.915	0.433	0.857	0.913	0.189	0.806	0.895
79	cubox-001	0.000	0.000	0.000	0.000	0.000	0.000	0.000	0.000	0.000	0.000	0.000	0.000	0.000	0.000	0.000
80	cubox-002	0.004	0.016	0.046	0.004	0.018	0.048	0.007	0.013	0.029	0.005	0.018	0.046	0.005	0.017	0.044
81	cudocommunication-001	0.000	0.000	0.000	0.000	0.000	0.000	0.000	0.000	0.000	0.000	0.000	0.000	0.000	0.000	0.000
82	cuhkee-001	0.009	0.029	0.069	0.009	0.031	0.074	0.014	0.025	0.057	0.012	0.048	0.115	0.013	0.048	0.140
83	cybercore-000	0.194	0.376	0.371	0.222	0.447	0.453	0.267	0.461	0.751	0.191	0.432	0.554	0.367	0.678	0.805
84	cyberlink-007	0.000	0.001	0.001	0.000	0.000	0.001	0.000	0.000	0.000	0.000	0.001	0.002	0.000	0.000	0.002
85	cyberlink-008	0.001	0.003	0.003	0.001	0.001	0.002	0.001	0.001	0.001	0.001	0.002	0.003	0.001	0.002	0.003
86	dahua-006	0.000	0.000	0.000	0.000	0.000	0.000	0.000	0.000	0.000	0.000	0.000	0.000	0.000	0.000	0.000
87	dahua-007	0.000	0.000	0.000	0.000	0.000	0.000	0.000	0.000	0.000	0.000	0.000	0.000	0.000	0.000	0.000
88	daon-000	0.059	0.154	0.224	0.044	0.113	0.173	0.050	0.093	0.151	0.176	0.423	0.599	0.057	0.189	0.396
89	decatur-000	0.014	0.036	0.074	0.014	0.033	0.069	0.018	0.028	0.058	0.032	0.065	0.135	0.033	0.069	0.135
90	decatur-001	0.012	0.030	0.064	0.012	0.028	0.059	0.014	0.022	0.047	0.028	0.055	0.115	0.028	0.057	0.118

Table 17: This table summarizes Failure to Enroll (FTE) rates surveyed over 10 000 images of each mask variant. FTE is the proportion of failed template generation attempts. Failures can occur because the software throws an exception, or because the software electively refuses to process the input image as would occur if the algorithms does not detect a face or determines that the face has insufficient information. FTE is measured as the number of function calls that give EITHER a non-zero error code OR that give a "small" template containing fewer than 60 bytes. This second rule is needed because some algorithms incorrectly fail to return a non-zero error code when template generation fails but do produce a skeletal template. The effects of FTE are included in the accuracy results of this report by regarding any template comparison involving a failed template to produce a low similarity score. Thus higher FTE results in higher FNMR and lower FMR. Algorithms in black were submitted prior to mid-March 2020, and algorithms in blue were submitted thereafter.

	Algorithm Name	COLOR = WHITE SHAPE = WIDE			COLOR = LIGHTBLUE SHAPE = WIDE			COLOR = LIGHTBLUE SHAPE = ROUND			COLOR = RED SHAPE = WIDE			COLOR = BLACK SHAPE = WIDE		
	COVERAGE	LO	MED	HI	LO	MED	HI	LO	MED	HI	LO	MED	HI	LO	MED	HI
91	deepglint-003	0.002	0.009	0.026	0.002	0.011	0.030	0.003	0.006	0.016	0.003	0.012	0.033	0.003	0.009	0.022
92	deepglint-004	0.002	0.011	0.030	0.003	0.014	0.036	0.004	0.007	0.020	0.003	0.015	0.040	0.003	0.010	0.027
93	deepsea-001	0.000	0.000	0.000	0.000	0.000	0.000	0.000	0.000	0.000	0.000	0.000	0.000	0.000	0.000	0.000
94	deepsense-000	0.002	0.009	0.022	0.002	0.009	0.021	0.002	0.003	0.009	0.003	0.013	0.031	0.003	0.011	0.024
95	dermalog-008	0.003	0.006	0.008	0.003	0.005	0.008	0.004	0.004	0.004	0.004	0.007	0.010	0.004	0.006	0.008
96	dermalog-009	0.003	0.006	0.008	0.003	0.005	0.008	0.004	0.004	0.004	0.004	0.007	0.010	0.004	0.006	0.008
97	didiglobalface-001	0.025	0.056	0.099	0.024	0.054	0.095	0.033	0.044	0.072	0.041	0.104	0.174	0.027	0.071	0.132
98	dps-000	1.000	1.000	1.000	1.000	1.000	1.000	1.000	1.000	1.000	1.000	1.000	1.000	1.000	1.000	1.000
99	dsk-000	0.000	0.000	0.000	0.000	0.000	0.000	0.000	0.000	0.000	0.000	0.000	0.000	0.000	0.000	0.000
100	ekin-002	0.000	0.000	0.000	0.000	0.000	0.000	0.000	0.000	0.000	0.000	0.000	0.000	0.000	0.000	0.000
101	enface-000	0.012	0.075	0.115	0.011	0.065	0.121	0.019	0.053	0.143	0.024	0.056	0.068	0.024	0.103	0.138
102	enface-001	0.009	0.029	0.096	0.009	0.037	0.109	0.016	0.035	0.111	0.008	0.024	0.061	0.012	0.056	0.137
103	eocortex-000	0.692	0.862	0.861	0.653	0.841	0.860	0.647	0.887	0.904	0.800	0.960	0.990	0.814	0.950	0.990
104	ercacat-001	0.002	0.007	0.014	0.002	0.006	0.013	0.002	0.002	0.006	0.002	0.008	0.016	0.003	0.009	0.017
105	euronovate-001	0.025	0.036	0.055	0.026	0.038	0.056	0.031	0.034	0.043	0.026	0.040	0.053	0.025	0.038	0.064
106	expasoft-001	0.000	0.000	0.000	0.000	0.000	0.000	0.000	0.000	0.000	0.000	0.000	0.000	0.000	0.000	0.000
107	expasoft-002	0.000	0.000	0.000	0.000	0.000	0.000	0.000	0.000	0.000	0.000	0.000	0.000	0.000	0.000	0.000
108	f8-001	1.000	1.000	1.000	1.000	1.000	1.000	1.000	1.000	1.000	1.000	1.000	1.000	1.000	1.000	1.000
109	faceonlive-001	0.028	0.031	0.072	0.029	0.033	0.073	0.026	0.025	0.045	0.034	0.068	0.164	0.031	0.038	0.096
110	facesoft-000	0.000	0.000	0.000	0.000	0.000	0.000	0.000	0.000	0.000	0.000	0.000	0.000	0.000	0.000	0.000
111	facetag-000	0.000	0.000	0.000	0.000	0.000	0.000	0.000	0.000	0.000	0.000	0.000	0.000	0.000	0.000	0.000
112	facetag-002	0.000	0.000	0.000	0.000	0.000	0.000	0.000	0.000	0.000	0.000	0.000	0.000	0.000	0.000	0.000
113	facex-001	0.064	0.171	0.220	0.067	0.173	0.226	0.080	0.123	0.261	0.084	0.308	0.406	0.081	0.294	0.478
114	facex-002	0.064	0.171	0.220	0.067	0.173	0.226	0.080	0.123	0.261	0.084	0.308	0.406	0.081	0.294	0.478
115	farfaces-001	0.004	0.014	0.029	0.004	0.013	0.026	0.005	0.007	0.012	0.004	0.016	0.033	0.004	0.018	0.036
116	fincore-000	0.006	0.020	0.047	0.006	0.019	0.045	0.009	0.013	0.032	0.010	0.033	0.086	0.010	0.039	0.095
117	fujitsulab-002	0.005	0.011	0.026	0.004	0.009	0.017	0.004	0.004	0.007	0.012	0.035	0.095	0.009	0.022	0.058
118	fujitsulab-003	0.004	0.011	0.025	0.003	0.008	0.016	0.004	0.004	0.007	0.010	0.032	0.086	0.007	0.021	0.053
119	geo-002	0.038	0.091	0.174	0.051	0.126	0.224	0.075	0.134	0.246	0.026	0.079	0.170	0.038	0.095	0.187
120	geo-003	0.015	0.043	0.109	0.019	0.055	0.129	0.036	0.068	0.130	0.014	0.043	0.107	0.019	0.056	0.131
121	glory-002	0.059	0.106	0.128	0.056	0.101	0.124	0.053	0.074	0.126	0.062	0.148	0.239	0.054	0.154	0.279
122	glory-003	0.042	0.115	0.157	0.039	0.097	0.143	0.051	0.068	0.107	0.061	0.168	0.234	0.048	0.196	0.272
123	gorilla-007	0.004	0.013	0.028	0.004	0.012	0.025	0.003	0.005	0.008	0.004	0.017	0.050	0.004	0.016	0.042
124	gorilla-008	0.004	0.013	0.029	0.004	0.012	0.025	0.003	0.004	0.008	0.004	0.017	0.048	0.004	0.016	0.042
125	griaule-000	0.053	0.137	0.198	0.044	0.107	0.160	0.048	0.085	0.145	0.183	0.424	0.608	0.065	0.204	0.377
126	hertasecurity-000	0.022	0.083	0.188	0.022	0.083	0.192	0.029	0.046	0.161	0.023	0.095	0.212	0.028	0.144	0.277
127	hisign-001	0.000	0.000	0.000	0.000	0.000	0.000	0.000	0.000	0.000	0.000	0.000	0.000	0.000	0.000	0.000
128	hyperverge-001	0.082	0.202	0.290	0.069	0.155	0.227	0.073	0.124	0.207	0.227	0.477	0.662	0.084	0.239	0.484
129	icm-002	0.000	0.000	0.000	0.000	0.000	0.000	0.000	0.000	0.000	0.000	0.000	0.000	0.000	0.000	0.000
130	icthtc-000	0.114	0.272	0.362	0.095	0.208	0.286	0.101	0.176	0.292	0.293	0.586	0.758	0.118	0.320	0.581
131	id3-006	0.015	0.051	0.123	0.024	0.068	0.150	0.040	0.081	0.157	0.015	0.050	0.124	0.019	0.059	0.134
132	id3-008	0.002	0.006	0.015	0.002	0.007	0.016	0.002	0.004	0.009	0.002	0.007	0.015	0.002	0.009	0.021
133	idemia-007	0.002	0.008	0.027	0.002	0.006	0.023	0.002	0.003	0.014	0.002	0.013	0.035	0.002	0.009	0.028
134	idemia-008	0.002	0.008	0.027	0.002	0.006	0.023	0.002	0.003	0.014	0.002	0.013	0.035	0.002	0.009	0.028
135	iit-002	0.012	0.036	0.074	0.013	0.043	0.091	0.015	0.027	0.072	0.016	0.060	0.137	0.015	0.087	0.185

Table 18: This table summarizes Failure to Enroll (FTE) rates surveyed over 10 000 images of each mask variant. FTE is the proportion of failed template generation attempts. Failures can occur because the software throws an exception, or because the software electively refuses to process the input image as would occur if the algorithms does not detect a face or determines that the face has insufficient information. FTE is measured as the number of function calls that give EITHER a non-zero error code OR that give a "small" template containing fewer than 60 bytes. This second rule is needed because some algorithms incorrectly fail to return a non-zero error code when template generation fails but do produce a skeletal template. The effects of FTE are included in the accuracy results of this report by regarding any template comparison involving a failed template to produce a low similarity score. Thus higher FTE results in higher FNMR and lower FMR. Algorithms in black were submitted prior to mid-March 2020, and algorithms in blue were submitted thereafter.

	Algorithm Name	COLOR = WHITE			COLOR = LIGHTBLUE						COLOR = RED			COLOR = BLACK		
		SHAPE = WIDE			SHAPE = WIDE			SHAPE = ROUND			SHAPE = WIDE			SHAPE = WIDE		
	COVERAGE	LO	MED	HI	LO	MED	HI	LO	MED	HI	LO	MED	HI	LO	MED	HI
136	iit-003	0.004	0.018	0.050	0.005	0.021	0.055	0.006	0.013	0.039	0.005	0.020	0.052	0.005	0.022	0.053
137	imagus-002	0.004	0.013	0.034	0.004	0.012	0.030	0.005	0.007	0.016	0.006	0.019	0.052	0.006	0.021	0.056
138	imagus-004	0.000	0.000	0.000	0.000	0.000	0.000	0.000	0.000	0.000	0.000	0.000	0.000	0.000	0.000	0.000
139	imperial-002	0.000	0.000	0.000	0.000	0.000	0.000	0.000	0.000	0.000	0.000	0.000	0.000	0.000	0.000	0.000
140	incode-009	0.003	0.013	0.034	0.003	0.013	0.031	0.003	0.006	0.014	0.004	0.016	0.045	0.004	0.020	0.060
141	incode-010	0.003	0.013	0.034	0.003	0.013	0.031	0.003	0.006	0.014	0.004	0.016	0.045	0.004	0.020	0.060
142	innefulabs-000	0.007	0.024	0.064	0.009	0.028	0.069	0.014	0.027	0.053	0.008	0.025	0.060	0.009	0.025	0.064
143	innovativetechnologyltd-002	0.082	0.176	0.232	0.074	0.172	0.233	0.091	0.131	0.265	0.132	0.269	0.391	0.149	0.362	0.516
144	innovatrics-007	0.001	0.005	0.015	0.002	0.005	0.017	0.003	0.003	0.007	0.003	0.012	0.038	0.002	0.009	0.026
145	innovatrics-008	0.002	0.009	0.032	0.002	0.011	0.036	0.003	0.005	0.017	0.005	0.028	0.076	0.005	0.026	0.069
146	insightface-000	0.000	0.000	0.000	0.000	0.000	0.000	0.000	0.000	0.000	0.000	0.000	0.000	0.000	0.000	0.000
147	insightface-001	0.000	0.000	0.000	0.000	0.000	0.000	0.000	0.000	0.000	0.000	0.000	0.000	0.000	0.000	0.000
148	intellicloudai-001	0.000	0.000	0.000	0.000	0.000	0.000	0.000	0.000	0.000	0.000	0.000	0.000	0.000	0.000	0.000
149	intellicloudai-002	0.007	0.015	0.028	0.005	0.013	0.025	0.007	0.009	0.015	0.012	0.041	0.087	0.013	0.031	0.056
150	intellifusion-002	0.000	0.001	0.004	0.000	0.000	0.001	0.000	0.000	0.002	0.001	0.035	0.112	0.000	0.001	0.004
151	intellivision-002	0.073	0.213	0.267	0.068	0.210	0.261	0.143	0.204	0.340	0.308	0.517	0.618	0.137	0.396	0.469
152	intelresearch-003	0.002	0.008	0.020	0.002	0.007	0.018	0.003	0.004	0.009	0.003	0.010	0.031	0.003	0.009	0.021
153	intelresearch-004	0.003	0.010	0.028	0.002	0.009	0.027	0.003	0.006	0.015	0.003	0.013	0.037	0.003	0.014	0.036
154	intsysmsu-002	0.008	0.055	0.117	0.007	0.047	0.110	0.015	0.033	0.100	0.010	0.078	0.191	0.036	0.105	0.231
155	ionetworks-000	0.034	0.088	0.133	0.034	0.091	0.140	0.041	0.065	0.125	0.055	0.129	0.200	0.048	0.105	0.176
156	iqface-000	0.000	0.000	0.000	0.000	0.000	0.000	0.000	0.000	0.000	0.000	0.000	0.000	0.000	0.000	0.000
157	iqface-003	0.049	0.079	0.124	0.047	0.080	0.127	0.049	0.067	0.114	0.058	0.155	0.227	0.053	0.148	0.219
158	irex-000	0.003	0.011	0.027	0.003	0.012	0.026	0.004	0.006	0.012	0.003	0.020	0.054	0.006	0.032	0.066
159	isap-001	1.000	1.000	1.000	1.000	1.000	1.000	1.000	1.000	1.000	1.000	1.000	1.000	1.000	1.000	1.000
160	isap-002	0.000	0.000	0.000	0.000	0.000	0.000	0.000	0.000	0.000	0.000	0.000	0.000	0.000	0.000	0.000
161	itmo-007	0.008	0.034	0.086	0.009	0.046	0.106	0.017	0.034	0.071	0.009	0.039	0.102	0.011	0.034	0.082
162	itmo-008	0.036	0.079	0.158	0.038	0.085	0.162	0.049	0.073	0.131	0.048	0.093	0.190	0.043	0.094	0.195
163	ivacognitive-001	0.011	0.027	0.072	0.011	0.027	0.070	0.015	0.021	0.051	0.015	0.040	0.123	0.016	0.049	0.146
164	iws-000	0.489	0.829	0.795	0.476	0.827	0.804	0.627	0.800	0.937	0.387	0.873	0.895	0.512	0.961	0.984
165	kakao-005	0.000	0.000	0.000	0.000	0.000	0.000	0.000	0.000	0.000	0.000	0.000	0.000	0.000	0.000	0.000
166	kakaopay-001	0.029	0.075	0.142	0.031	0.076	0.147	0.036	0.073	0.133	0.068	0.127	0.228	0.034	0.080	0.160
167	kedacom-000	0.000	0.000	0.000	0.000	0.000	0.000	0.000	0.000	0.000	0.000	0.000	0.000	0.000	0.000	0.000
168	kiwitech-000	0.008	0.031	0.085	0.011	0.037	0.091	0.018	0.037	0.069	0.009	0.030	0.078	0.010	0.030	0.079
169	kneron-005	0.063	0.184	0.206	0.058	0.166	0.212	0.094	0.146	0.276	0.080	0.292	0.309	0.101	0.440	0.505
170	kookmin-002	0.000	0.000	0.000	0.000	0.000	0.000	0.000	0.000	0.000	0.000	0.000	0.000	0.000	0.000	0.000
171	kuke3d-001	0.000	0.000	0.000	0.000	0.000	0.000	0.000	0.000	0.000	0.000	0.000	0.000	0.000	0.000	0.000
172	lemalabs-001	1.000	1.000	1.000	1.000	1.000	1.000	1.000	1.000	1.000	1.000	1.000	1.000	1.000	1.000	1.000
173	line-000	0.000	0.000	0.000	0.000	0.000	0.000	0.000	0.000	0.000	0.000	0.000	0.000	0.000	0.000	0.000
174	line-001	0.000	0.000	0.000	0.000	0.000	0.000	0.000	0.000	0.000	0.000	0.000	0.000	0.000	0.000	0.000
175	lookman-004	0.000	0.000	0.000	0.000	0.000	0.000	0.000	0.000	0.000	0.000	0.000	0.000	0.000	0.000	0.000
176	luxand-000	0.000	0.000	0.000	0.000	0.000	0.000	0.000	0.000	0.000	0.000	0.000	0.000	0.000	0.000	0.000
177	mantra-000	0.082	0.053	0.120	0.073	0.052	0.115	0.121	0.135	0.154	0.040	0.075	0.230	0.050	0.103	0.361
178	maxvision-000	0.000	0.000	0.000	0.000	0.000	0.000	0.000	0.000	0.000	0.000	0.000	0.000	0.000	0.000	0.000
179	megvii-003	0.018	0.036	0.068	0.017	0.035	0.067	0.018	0.022	0.042	0.031	0.105	0.187	0.029	0.070	0.134
180	meituan-000	0.000	0.000	0.001	0.000	0.000	0.001	0.000	0.000	0.000	0.000	0.001	0.002	0.000	0.000	0.001

Table 19: This table summarizes Failure to Enroll (FTE) rates surveyed over 10 000 images of each mask variant. FTE is the proportion of failed template generation attempts. Failures can occur because the software throws an exception, or because the software electively refuses to process the input image as would occur if the algorithms does not detect a face or determines that the face has insufficient information. FTE is measured as the number of function calls that give EITHER a non-zero error code OR that give a "small" template containing fewer than 60 bytes. This second rule is needed because some algorithms incorrectly fail to return a non-zero error code when template generation fails but do produce a skeletal template. The effects of FTE are included in the accuracy results of this report by regarding any template comparison involving a failed template to produce a low similarity score. Thus higher FTE results in higher FNMR and lower FMR. Algorithms in black were submitted prior to mid-March 2020, and algorithms in blue were submitted thereafter.

	Algorithm Name	COLOR = WHITE			COLOR = LIGHTBLUE						COLOR = RED			COLOR = BLACK		
		SHAPE = WIDE			SHAPE = WIDE			SHAPE = ROUND			SHAPE = WIDE			SHAPE = WIDE		
	COVERAGE	LO	MED	HI	LO	MED	HI	LO	MED	HI	LO	MED	HI	LO	MED	HI
181	mendaxiatech-000	0.018	0.036	0.068	0.016	0.035	0.067	0.018	0.022	0.042	0.030	0.104	0.186	0.029	0.069	0.133
182	minivision-000	0.000	0.000	0.000	0.000	0.000	0.000	0.000	0.000	0.000	0.000	0.000	0.000	0.000	0.000	0.000
183	mobbl-001	0.132	0.233	0.251	0.133	0.200	0.232	0.139	0.190	0.282	0.309	0.565	0.691	0.166	0.318	0.452
184	mobbl-002	0.051	0.160	0.222	0.042	0.122	0.183	0.047	0.089	0.176	0.164	0.427	0.610	0.065	0.196	0.365
185	mobipintech-000	0.000	0.000	0.000	0.000	0.000	0.000	0.000	0.000	0.000	0.000	0.000	0.000	0.000	0.000	0.000
186	moredian-000	0.008	0.031	0.085	0.011	0.037	0.091	0.018	0.037	0.069	0.009	0.030	0.078	0.010	0.030	0.079
187	multimodality-000	0.000	0.000	0.000	0.000	0.000	0.000	0.000	0.000	0.000	0.000	0.000	0.000	0.000	0.000	0.000
188	mvision-001	0.000	0.000	0.000	0.000	0.000	0.000	0.000	0.000	0.000	0.000	0.000	0.000	0.000	0.000	0.000
189	nazhiai-000	0.000	0.000	0.000	0.000	0.000	0.000	0.000	0.000	0.000	0.000	0.000	0.000	0.000	0.000	0.000
190	neosystems-002	0.000	0.000	0.000	0.000	0.000	0.000	0.000	0.000	0.000	0.000	0.000	0.000	0.000	0.000	0.000
191	neosystems-003	0.000	0.000	0.000	0.000	0.000	0.000	0.000	0.000	0.000	0.000	0.000	0.000	0.000	0.000	0.000
192	netbridgetech-001	0.000	0.000	0.000	0.000	0.000	0.000	0.000	0.000	0.000	0.000	0.000	0.000	0.000	0.000	0.000
193	netbridgetech-002	0.000	0.000	0.000	0.000	0.000	0.000	0.000	0.000	0.000	0.000	0.000	0.000	0.000	0.000	0.000
194	neurotechnology-012	1.000	1.000	1.000	1.000	1.000	1.000	1.000	1.000	1.000	1.000	1.000	1.000	1.000	1.000	1.000
195	neurotechnology-013	0.003	0.007	0.012	0.002	0.006	0.012	0.002	0.003	0.005	0.004	0.012	0.026	0.004	0.009	0.018
196	nhn-001	0.040	0.095	0.150	0.035	0.089	0.150	0.058	0.084	0.165	0.068	0.191	0.282	0.054	0.162	0.252
197	nhn-002	0.002	0.007	0.017	0.002	0.006	0.015	0.002	0.004	0.009	0.003	0.016	0.038	0.003	0.011	0.023
198	nodeflux-002	0.402	0.598	0.538	0.440	0.671	0.628	0.482	0.681	0.877	0.393	0.672	0.772	0.602	0.835	0.915
199	notiontag-001	0.000	0.000	0.000	0.000	0.000	0.000	0.000	0.000	0.000	0.000	0.000	0.000	0.000	0.000	0.000
200	notiontag-002	0.000	0.000	0.000	0.000	0.000	0.000	0.000	0.000	0.000	0.000	0.000	0.000	0.000	0.000	0.000
201	nsensecorp-002	0.005	0.014	0.031	0.004	0.011	0.023	0.004	0.007	0.014	0.016	0.049	0.087	0.006	0.019	0.035
202	nsensecorp-003	0.000	0.000	0.000	0.000	0.000	0.001	0.000	0.000	0.000	0.000	0.000	0.000	0.000	0.000	0.000
203	ntechlab-010	0.008	0.020	0.047	0.008	0.019	0.048	0.009	0.014	0.030	0.009	0.025	0.057	0.009	0.025	0.059
204	ntechlab-011	0.002	0.008	0.018	0.002	0.008	0.018	0.002	0.005	0.012	0.003	0.011	0.023	0.003	0.008	0.020
205	omnigarde-000	0.005	0.015	0.050	0.005	0.015	0.046	0.006	0.011	0.027	0.007	0.025	0.072	0.008	0.028	0.072
206	omnigarde-001	0.005	0.015	0.050	0.005	0.015	0.046	0.006	0.011	0.027	0.007	0.025	0.072	0.008	0.028	0.072
207	omsecurity-000	0.000	0.000	0.000	0.000	0.000	0.000	0.000	0.000	0.000	0.000	0.000	0.000	0.000	0.000	0.000
208	openface-001	0.217	0.351	0.327	0.171	0.294	0.305	0.227	0.278	0.365	0.271	0.432	0.573	0.387	0.580	0.702
209	oz-003	0.001	0.001	0.003	0.001	0.001	0.003	0.000	0.001	0.001	0.000	0.001	0.005	0.001	0.002	0.004
210	oz-004	0.001	0.001	0.002	0.001	0.001	0.002	0.001	0.001	0.001	0.001	0.001	0.003	0.001	0.001	0.003
211	papsav1923-001	0.003	0.011	0.028	0.002	0.012	0.028	0.008	0.010	0.023	0.005	0.035	0.071	0.002	0.008	0.012
212	paravision-004	0.002	0.011	0.027	0.002	0.010	0.024	0.003	0.004	0.009	0.003	0.019	0.056	0.003	0.016	0.043
213	paravision-008	0.010	0.027	0.070	0.009	0.025	0.066	0.010	0.016	0.041	0.013	0.033	0.084	0.019	0.056	0.123
214	pensees-001	0.000	0.000	0.000	0.000	0.000	0.000	0.000	0.000	0.000	0.000	0.000	0.000	0.000	0.000	0.000
215	pixelall-006	0.000	0.000	0.000	0.000	0.000	0.000	0.000	0.000	0.000	0.000	0.000	0.000	0.000	0.000	0.000
216	pixelall-007	0.000	0.000	0.000	0.000	0.000	0.000	0.000	0.000	0.000	0.000	0.000	0.000	0.000	0.000	0.000
217	psl-008	0.001	0.002	0.006	0.001	0.002	0.005	0.001	0.001	0.003	0.001	0.004	0.009	0.001	0.003	0.007
218	psl-009	0.002	0.008	0.021	0.001	0.008	0.020	0.002	0.004	0.013	0.003	0.011	0.027	0.004	0.010	0.022
219	ptakuratsatu-000	0.001	0.005	0.015	0.002	0.005	0.017	0.003	0.003	0.007	0.003	0.012	0.038	0.002	0.009	0.026
220	pxl-001	0.096	0.268	0.329	0.082	0.208	0.273	0.090	0.161	0.294	0.272	0.579	0.712	0.116	0.302	0.500
221	qnap-000	0.001	0.002	0.006	0.001	0.001	0.005	0.001	0.001	0.001	0.001	0.002	0.006	0.002	0.005	0.013
222	qnap-001	0.000	0.000	0.000	0.000	0.000	0.000	0.000	0.000	0.000	0.000	0.000	0.000	0.000	0.000	0.000
223	quantasoft-003	0.048	0.125	0.237	0.081	0.173	0.304	0.136	0.261	0.371	0.044	0.107	0.211	0.050	0.129	0.262
224	rankone-011	0.000	0.000	0.000	0.000	0.000	0.000	0.000	0.000	0.000	0.000	0.000	0.000	0.000	0.000	0.000
225	rankone-012	0.000	0.000	0.000	0.000	0.000	0.000	0.000	0.000	0.000	0.000	0.000	0.000	0.000	0.000	0.000

Table 20: This table summarizes Failure to Enroll (FTE) rates surveyed over 10 000 images of each mask variant. FTE is the proportion of failed template generation attempts. Failures can occur because the software throws an exception, or because the software electively refuses to process the input image as would occur if the algorithms does not detect a face or determines that the face has insufficient information. FTE is measured as the number of function calls that give EITHER a non-zero error code OR that give a "small" template containing fewer than 60 bytes. This second rule is needed because some algorithms incorrectly fail to return a non-zero error code when template generation fails but do produce a skeletal template. The effects of FTE are included in the accuracy results of this report by regarding any template comparison involving a failed template to produce a low similarity score. Thus higher FTE results in higher FNMR and lower FMR. Algorithms in black were submitted prior to mid-March 2020, and algorithms in blue were submitted thereafter.

FNMR(T) "False non-match rate"
FMR(T) "False match rate"

	Algorithm Name	COLOR = WHITE SHAPE = WIDE			COLOR = LIGHTBLUE SHAPE = WIDE			COLOR = LIGHTBLUE SHAPE = ROUND			COLOR = RED SHAPE = WIDE			COLOR = BLACK SHAPE = WIDE		
	COVERAGE	LO	MED	HI	LO	MED	HI	LO	MED	HI	LO	MED	HI	LO	MED	HI
226	realnetworks-004	0.000	0.003	0.005	0.000	0.002	0.004	0.001	0.001	0.003	0.004	0.022	0.049	0.001	0.005	0.016
227	realnetworks-005	0.000	0.003	0.005	0.000	0.002	0.004	0.001	0.001	0.003	0.004	0.022	0.047	0.001	0.005	0.015
228	regula-000	0.000	0.000	0.000	0.000	0.000	0.000	0.000	0.000	0.000	0.000	0.000	0.000	0.000	0.000	0.000
229	regula-001	0.000	0.000	0.000	0.000	0.000	0.000	0.000	0.000	0.000	0.000	0.000	0.000	0.000	0.000	0.000
230	remarkai-003	0.003	0.010	0.019	0.003	0.010	0.018	0.005	0.006	0.011	0.007	0.029	0.066	0.007	0.022	0.049
231	rendip-000	0.022	0.049	0.131	0.021	0.045	0.138	0.029	0.041	0.117	0.032	0.063	0.204	0.029	0.065	0.231
232	revealmedia-005	0.004	0.015	0.034	0.004	0.016	0.037	0.007	0.013	0.027	0.006	0.022	0.049	0.008	0.028	0.061
233	rokid-000	0.194	0.372	0.370	0.220	0.444	0.450	0.265	0.457	0.749	0.191	0.431	0.553	0.367	0.677	0.806
234	s1-003	0.001	0.002	0.005	0.001	0.003	0.006	0.001	0.001	0.003	0.001	0.004	0.010	0.001	0.003	0.006
235	s1-004	0.000	0.000	0.000	0.000	0.000	0.000	0.000	0.000	0.000	0.000	0.000	0.000	0.000	0.000	0.000
236	samsungsds-000	0.136	0.242	0.268	0.158	0.329	0.393	0.191	0.301	0.438	0.110	0.204	0.266	0.142	0.354	0.563
237	scanovate-002	0.008	0.019	0.046	0.008	0.018	0.045	0.008	0.012	0.027	0.010	0.025	0.079	0.012	0.036	0.101
238	scanovate-003	0.029	0.035	0.050	0.028	0.035	0.052	0.029	0.031	0.041	0.030	0.040	0.065	0.031	0.038	0.057
239	securifai-003	0.000	0.000	0.000	0.000	0.000	0.000	0.000	0.000	0.000	0.000	0.000	0.000	0.000	0.000	0.000
240	securifai-004	0.000	0.000	0.000	0.000	0.000	0.000	0.000	0.000	0.000	0.000	0.000	0.000	0.000	0.000	0.000
241	sensetime-005	0.001	0.004	0.008	0.001	0.004	0.009	0.001	0.002	0.003	0.001	0.004	0.008	0.001	0.004	0.008
242	sensetime-006	0.001	0.004	0.008	0.001	0.004	0.009	0.001	0.002	0.003	0.001	0.004	0.008	0.001	0.004	0.008
243	sertis-000	0.002	0.012	0.034	0.002	0.012	0.032	0.003	0.005	0.013	0.003	0.016	0.047	0.005	0.020	0.052
244	sertis-002	0.002	0.009	0.029	0.002	0.010	0.026	0.002	0.004	0.010	0.003	0.012	0.040	0.004	0.016	0.044
245	seventhsense-000	0.002	0.011	0.028	0.003	0.011	0.028	0.003	0.007	0.014	0.003	0.011	0.023	0.004	0.015	0.036
246	shu-002	0.011	0.031	0.080	0.009	0.026	0.083	0.023	0.037	0.103	0.026	0.126	0.227	0.016	0.056	0.167
247	shu-003	0.003	0.006	0.013	0.002	0.004	0.008	0.003	0.005	0.009	0.008	0.031	0.070	0.004	0.014	0.040
248	sjtu-003	0.002	0.004	0.009	0.002	0.003	0.006	0.002	0.003	0.006	0.005	0.022	0.049	0.003	0.009	0.028
249	sjtu-004	0.000	0.000	0.000	0.000	0.000	0.000	0.000	0.000	0.000	0.000	0.000	0.000	0.000	0.000	0.000
250	sktelecom-000	0.005	0.013	0.032	0.004	0.012	0.028	0.007	0.010	0.022	0.008	0.027	0.070	0.006	0.017	0.044
251	smartengines-000	0.858	0.912	0.911	0.795	0.910	0.911	0.807	0.908	0.910	0.681	0.893	0.913	0.882	0.913	0.913
252	sodec-000	0.000	0.000	0.000	0.000	0.000	0.000	0.000	0.000	0.000	0.000	0.000	0.000	0.000	0.000	0.000
253	sqisoft-001	0.001	0.002	0.006	0.001	0.002	0.006	0.001	0.001	0.003	0.001	0.005	0.012	0.001	0.003	0.007
254	sqisoft-002	0.001	0.003	0.006	0.001	0.002	0.005	0.001	0.002	0.003	0.001	0.004	0.013	0.001	0.003	0.008
255	staqu-000	0.000	0.000	0.000	0.000	0.000	0.000	0.000	0.000	0.000	0.000	0.000	0.000	0.000	0.000	0.000
256	starhybrid-001	0.192	0.468	0.461	0.149	0.406	0.483	0.137	0.321	0.487	0.478	0.761	0.781	0.133	0.372	0.565
257	suprema-000	0.024	0.082	0.146	0.022	0.071	0.134	0.042	0.061	0.122	0.049	0.169	0.268	0.038	0.140	0.255
258	suprema-001	0.051	0.134	0.208	0.044	0.123	0.203	0.074	0.110	0.217	0.100	0.282	0.399	0.077	0.248	0.400
259	supremaid-001	0.047	0.105	0.160	0.041	0.101	0.156	0.064	0.095	0.188	0.079	0.214	0.303	0.057	0.174	0.275
260	synesis-006	0.001	0.003	0.007	0.001	0.003	0.007	0.001	0.001	0.003	0.001	0.005	0.011	0.001	0.004	0.008
261	synesis-007	0.007	0.021	0.047	0.008	0.028	0.056	0.013	0.025	0.056	0.007	0.046	0.114	0.018	0.124	0.134
262	synology-000	0.000	0.000	0.000	0.000	0.000	0.000	0.000	0.000	0.000	0.000	0.000	0.000	0.000	0.000	0.000
263	synology-002	0.000	0.000	0.000	0.000	0.000	0.000	0.000	0.000	0.000	0.000	0.000	0.000	0.000	0.000	0.000
264	sztu-000	0.000	0.000	0.000	0.000	0.000	0.000	0.000	0.000	0.000	0.000	0.000	0.000	0.000	0.000	0.000
265	sztu-001	0.000	0.000	0.000	0.000	0.000	0.000	0.000	0.000	0.000	0.000	0.000	0.000	0.000	0.000	0.000
266	tech5-004	0.005	0.022	0.061	0.006	0.028	0.070	0.010	0.021	0.046	0.006	0.025	0.068	0.006	0.021	0.058
267	tech5-005	0.004	0.015	0.044	0.004	0.017	0.046	0.006	0.012	0.026	0.005	0.020	0.051	0.007	0.022	0.057
268	techsign-000	0.383	0.776	0.751	0.364	0.775	0.751	0.560	0.723	0.891	0.253	0.835	0.849	0.356	0.939	0.971
269	tevian-007	0.004	0.030	0.074	0.004	0.020	0.054	0.005	0.011	0.042	0.011	0.071	0.174	0.006	0.031	0.080
270	tevian-008	0.002	0.007	0.014	0.002	0.005	0.011	0.001	0.002	0.004	0.002	0.009	0.021	0.002	0.011	0.024

Table 21: This table summarizes Failure to Enroll (FTE) rates surveyed over 10 000 images of each mask variant. FTE is the proportion of failed template generation attempts. Failures can occur because the software throws an exception, or because the software electively refuses to process the input image as would occur if the algorithms does not detect a face or determines that the face has insufficient information. FTE is measured as the number of function calls that give EITHER a non-zero error code OR that give a "small" template containing fewer than 60 bytes. This second rule is needed because some algorithms incorrectly fail to return a non-zero error code when template generation fails but do produce a skeletal template. The effects of FTE are included in the accuracy results of this report by regarding any template comparison involving a failed template to produce a low similarity score. Thus higher FTE results in higher FNMR and lower FMR. Algorithms in black were submitted prior to mid-March 2020, and algorithms in blue were submitted thereafter.

	Algorithm Name	COLOR = WHITE SHAPE = WIDE			COLOR = LIGHTBLUE SHAPE = WIDE			COLOR = LIGHTBLUE SHAPE = ROUND			COLOR = RED SHAPE = WIDE			COLOR = BLACK SHAPE = WIDE		
	COVERAGE	LO	MED	HI	LO	MED	HI	LO	MED	HI	LO	MED	HI	LO	MED	HI
271	tiger-005	0.012	0.030	0.064	0.012	0.028	0.059	0.014	0.022	0.047	0.028	0.055	0.115	0.028	0.057	0.118
272	tiger-006	0.004	0.011	0.026	0.004	0.013	0.031	0.003	0.005	0.011	0.004	0.014	0.038	0.007	0.020	0.046
273	tinkoff-001	0.003	0.013	0.038	0.003	0.013	0.037	0.004	0.010	0.026	0.004	0.018	0.055	0.005	0.020	0.062
274	toppanidgate-000	0.004	0.013	0.028	0.004	0.013	0.030	0.005	0.009	0.019	0.005	0.016	0.037	0.005	0.016	0.035
275	toshiba-004	0.000	0.000	0.000	0.000	0.000	0.000	0.000	0.000	0.000	0.000	0.000	0.000	0.000	0.000	0.000
276	trueface-002	0.109	0.216	0.258	0.096	0.201	0.262	0.095	0.148	0.308	0.288	0.519	0.643	0.192	0.386	0.574
277	trueface-003	0.109	0.216	0.258	0.096	0.201	0.262	0.095	0.148	0.308	0.288	0.519	0.643	0.192	0.386	0.574
278	tuputech-000	0.517	0.679	0.684	0.626	0.758	0.765	0.502	0.619	0.714	0.652	0.893	0.926	0.661	0.904	0.933
279	twface-000	0.000	0.000	0.000	0.000	0.000	0.000	0.000	0.000	0.000	0.000	0.000	0.000	0.000	0.000	0.000
280	twface-001	0.000	0.000	0.000	0.000	0.000	0.000	0.000	0.000	0.000	0.000	0.000	0.000	0.000	0.000	0.000
281	uluface-002	0.000	0.000	0.000	0.000	0.000	0.000	0.000	0.000	0.000	0.000	0.000	0.000	0.000	0.000	0.000
282	unissey-001	0.000	0.000	0.000	0.000	0.000	0.000	0.000	0.000	0.000	0.000	0.000	0.000	0.000	0.000	0.000
283	upc-001	0.002	0.005	0.012	0.002	0.005	0.012	0.002	0.002	0.005	0.002	0.010	0.027	0.003	0.007	0.018
284	vd-002	0.000	0.000	0.000	0.000	0.000	0.000	0.000	0.000	0.000	0.000	0.000	0.000	0.000	0.000	0.000
285	vd-003	0.097	0.262	0.337	0.086	0.210	0.279	0.094	0.175	0.265	0.246	0.532	0.681	0.099	0.286	0.510
286	veridas-006	0.047	0.136	0.200	0.041	0.110	0.161	0.046	0.083	0.152	0.106	0.401	0.568	0.053	0.208	0.382
287	veridas-007	0.047	0.136	0.200	0.041	0.110	0.161	0.046	0.083	0.152	0.106	0.401	0.568	0.053	0.208	0.382
288	verigram-000	0.175	0.306	0.317	0.173	0.333	0.372	0.188	0.268	0.423	0.364	0.605	0.707	0.222	0.410	0.564
289	via-001	0.000	0.000	0.000	0.000	0.000	0.000	0.000	0.000	0.000	0.000	0.000	0.000	0.000	0.000	0.000
290	videmo-000	0.019	0.067	0.125	0.018	0.051	0.106	0.023	0.040	0.089	0.122	0.352	0.368	0.027	0.100	0.296
291	videmo-001	0.048	0.066	0.072	0.042	0.065	0.068	0.039	0.048	0.067	0.040	0.064	0.068	0.041	0.065	0.070
292	videonetics-002	0.338	0.581	0.557	0.330	0.569	0.542	0.378	0.559	0.785	0.344	0.693	0.735	0.396	0.702	0.848
293	viettelhightech-000	0.020	0.068	0.132	0.022	0.088	0.169	0.031	0.069	0.293	0.021	0.119	0.218	0.021	0.112	0.212
294	vigilantsolutions-010	0.062	0.168	0.218	0.051	0.136	0.189	0.068	0.124	0.202	0.096	0.407	0.633	0.072	0.268	0.492
295	vigilantsolutions-011	0.062	0.168	0.218	0.051	0.136	0.189	0.068	0.124	0.202	0.096	0.407	0.633	0.072	0.268	0.492
296	vinai-000	0.000	0.000	0.000	0.000	0.000	0.000	0.000	0.000	0.000	0.000	0.000	0.000	0.000	0.000	0.000
297	vinbigdata-001	0.000	0.000	0.000	0.000	0.000	0.000	0.000	0.000	0.000	0.000	0.000	0.000	0.000	0.000	0.000
298	visage-000	0.165	0.548	0.544	0.152	0.508	0.505	0.173	0.379	0.729	0.171	0.667	0.672	0.245	0.776	0.807
299	visionbox-002	0.031	0.071	0.126	0.028	0.068	0.122	0.036	0.056	0.137	0.057	0.162	0.247	0.053	0.152	0.263
300	visionlabs-010	0.002	0.004	0.007	0.001	0.003	0.004	0.001	0.001	0.001	0.001	0.002	0.003	0.001	0.003	0.004
301	visionlabs-011	0.001	0.003	0.004	0.001	0.002	0.002	0.001	0.001	0.001	0.001	0.001	0.001	0.001	0.002	0.002
302	visteam-001	0.015	0.039	0.086	0.013	0.037	0.078	0.018	0.025	0.055	0.028	0.080	0.147	0.021	0.059	0.135
303	visteam-002	0.015	0.039	0.086	0.013	0.037	0.078	0.018	0.025	0.055	0.028	0.080	0.147	0.021	0.059	0.135
304	vnpt-002	0.000	0.002	0.004	0.001	0.002	0.004	0.001	0.001	0.002	0.001	0.002	0.005	0.001	0.002	0.004
305	vnpt-003	0.002	0.009	0.023	0.003	0.009	0.022	0.004	0.007	0.016	0.003	0.009	0.022	0.004	0.011	0.029
306	vocord-008	0.013	0.046	0.087	0.011	0.052	0.089	0.031	0.059	0.111	0.013	0.079	0.127	0.009	0.050	0.093
307	vocord-009	0.002	0.008	0.018	0.002	0.006	0.013	0.002	0.003	0.006	0.002	0.009	0.020	0.002	0.010	0.026
308	vts-000	0.011	0.029	0.072	0.012	0.028	0.074	0.015	0.020	0.048	0.014	0.043	0.129	0.016	0.051	0.149
309	winsense-001	0.000	0.000	0.000	0.000	0.000	0.000	0.000	0.000	0.000	0.000	0.000	0.000	0.000	0.000	0.000
310	winsense-002	0.000	0.000	0.000	0.000	0.000	0.000	0.000	0.000	0.000	0.000	0.000	0.000	0.000	0.000	0.000
311	wuhantianyu-001	0.004	0.015	0.033	0.004	0.014	0.031	0.005	0.009	0.016	0.007	0.025	0.063	0.008	0.030	0.069
312	xforwardai-001	0.006	0.025	0.069	0.007	0.031	0.079	0.011	0.021	0.052	0.007	0.030	0.079	0.007	0.022	0.060
313	xforwardai-002	0.006	0.025	0.069	0.007	0.031	0.079	0.011	0.021	0.052	0.007	0.030	0.079	0.007	0.022	0.060
314	xm-000	0.003	0.006	0.013	0.002	0.004	0.008	0.003	0.004	0.009	0.008	0.031	0.070	0.005	0.013	0.038
315	yoonik-002	0.005	0.023	0.065	0.007	0.026	0.069	0.014	0.026	0.051	0.007	0.025	0.062	0.009	0.024	0.065

Table 22: This table summarizes Failure to Enroll (FTE) rates surveyed over 10 000 images of each mask variant. FTE is the proportion of failed template generation attempts. Failures can occur because the software throws an exception, or because the software electively refuses to process the input image as would occur if the algorithms does not detect a face or determines that the face has insufficient information. FTE is measured as the number of function calls that give EITHER a non-zero error code OR that give a "small" template containing fewer than 60 bytes. This second rule is needed because some algorithms incorrectly fail to return a non-zero error code when template generation fails but do produce a skeletal template. The effects of FTE are included in the accuracy results of this report by regarding any template comparison involving a failed template to produce a low similarity score. Thus higher FTE results in higher FNMR and lower FMR. Algorithms in black were submitted prior to mid-March 2020, and algorithms in blue were submitted thereafter.

	Algorithm Name	COLOR = WHITE			COLOR = LIGHTBLUE						COLOR = RED			COLOR = BLACK		
		SHAPE = WIDE			SHAPE = WIDE			SHAPE = ROUND			SHAPE = WIDE			SHAPE = WIDE		
	COVERAGE	LO	MED	HI	LO	MED	HI	LO	MED	HI	LO	MED	HI	LO	MED	HI
316	ytu-000	0.018	0.036	0.068	0.017	0.035	0.067	0.018	0.022	0.042	0.031	0.105	0.187	0.029	0.070	0.134
317	yuan-002	0.016	0.050	0.115	0.019	0.061	0.138	0.029	0.057	0.110	0.017	0.053	0.130	0.015	0.042	0.104
318	yuan-003	0.016	0.050	0.115	0.019	0.061	0.138	0.029	0.057	0.110	0.017	0.053	0.130	0.015	0.042	0.104

Table 23: This table summarizes Failure to Enroll (FTE) rates surveyed over 10 000 images of each mask variant. FTE is the proportion of failed template generation attempts. Failures can occur because the software throws an exception, or because the software electively refuses to process the input image as would occur if the algorithms does not detect a face or determines that the face has insufficient information. FTE is measured as the number of function calls that give EITHER a non-zero error code OR that give a "small" template containing fewer than 60 bytes. This second rule is needed because some algorithms incorrectly fail to return a non-zero error code when template generation fails but do produce a skeletal template. The effects of FTE are included in the accuracy results of this report by regarding any template comparison involving a failed template to produce a low similarity score. Thus higher FTE results in higher FNMR and lower FMR. Algorithms in black were submitted prior to mid-March 2020, and algorithms in blue were submitted thereafter.

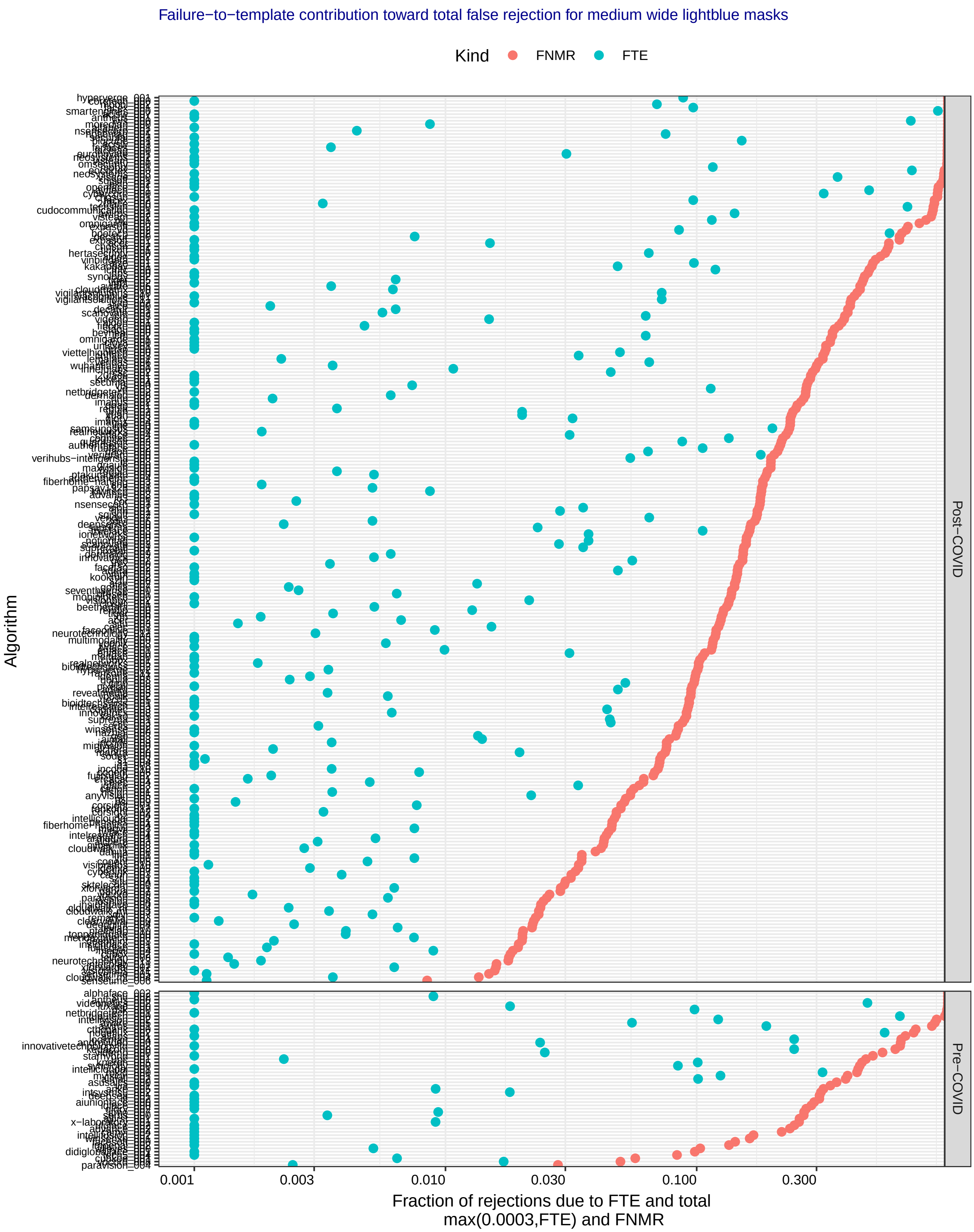

Figure 18: For each algorithm the rightmost dot shows FNMR @ FMR=0.00001 (as reported throughout this report). The left most dot shows the failure-to-template (FTE) rate over the masked verification set of 5.2M images. The gap between the two dots is attributable to low similarity score. Some FTE rates are zero - rates below 0.001 are shown as 0.001.

The following plots are detection error tradeoff (DET) characteristics for each algorithm, across different mask nose coverages and shapes.

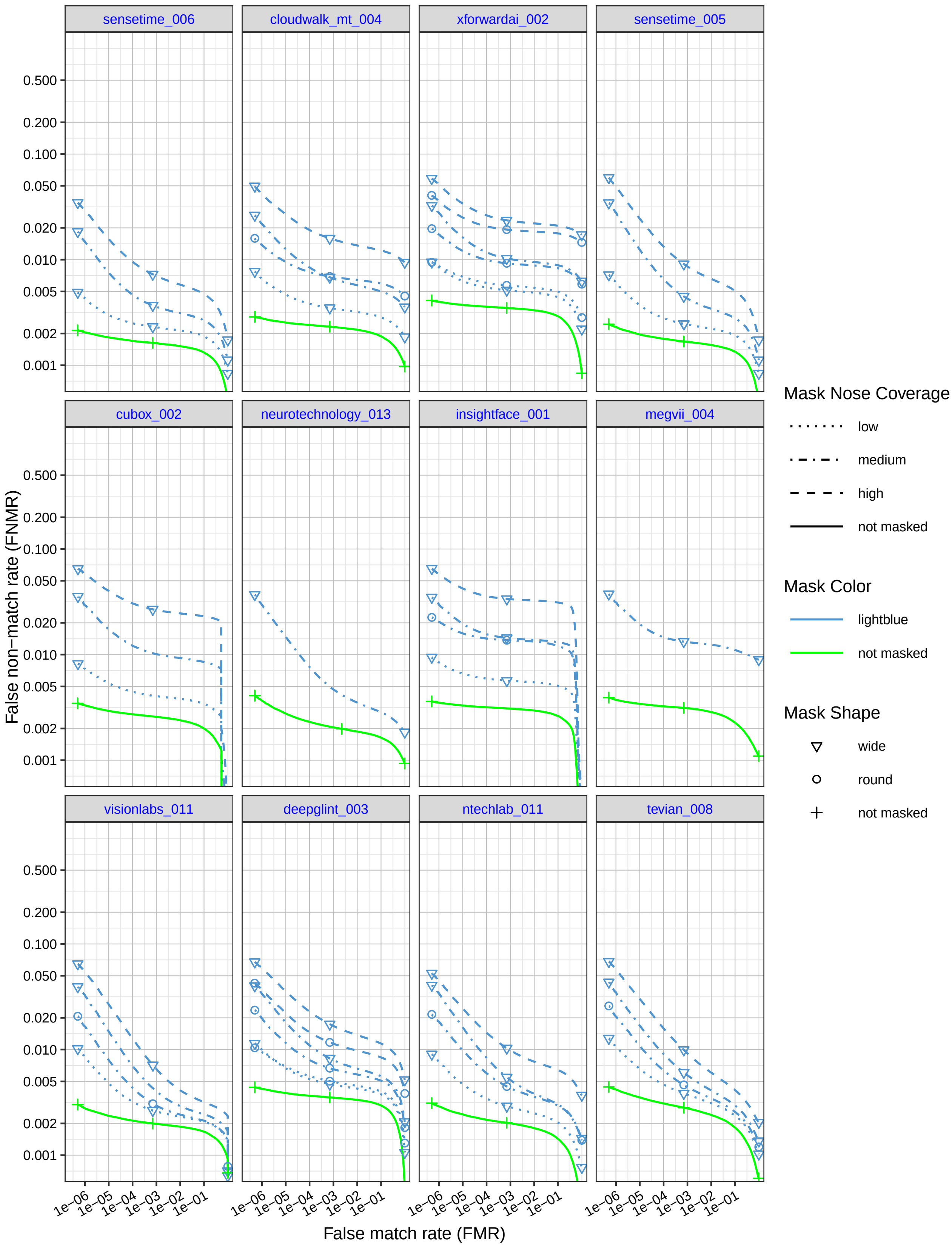

Figure 19: DET curves showing error rates on unmasked and masked probe images, broken out by mask shape and nose coverage. Algorithms in black were submitted prior to mid-March 2020, and algorithms in blue were submitted thereafter.

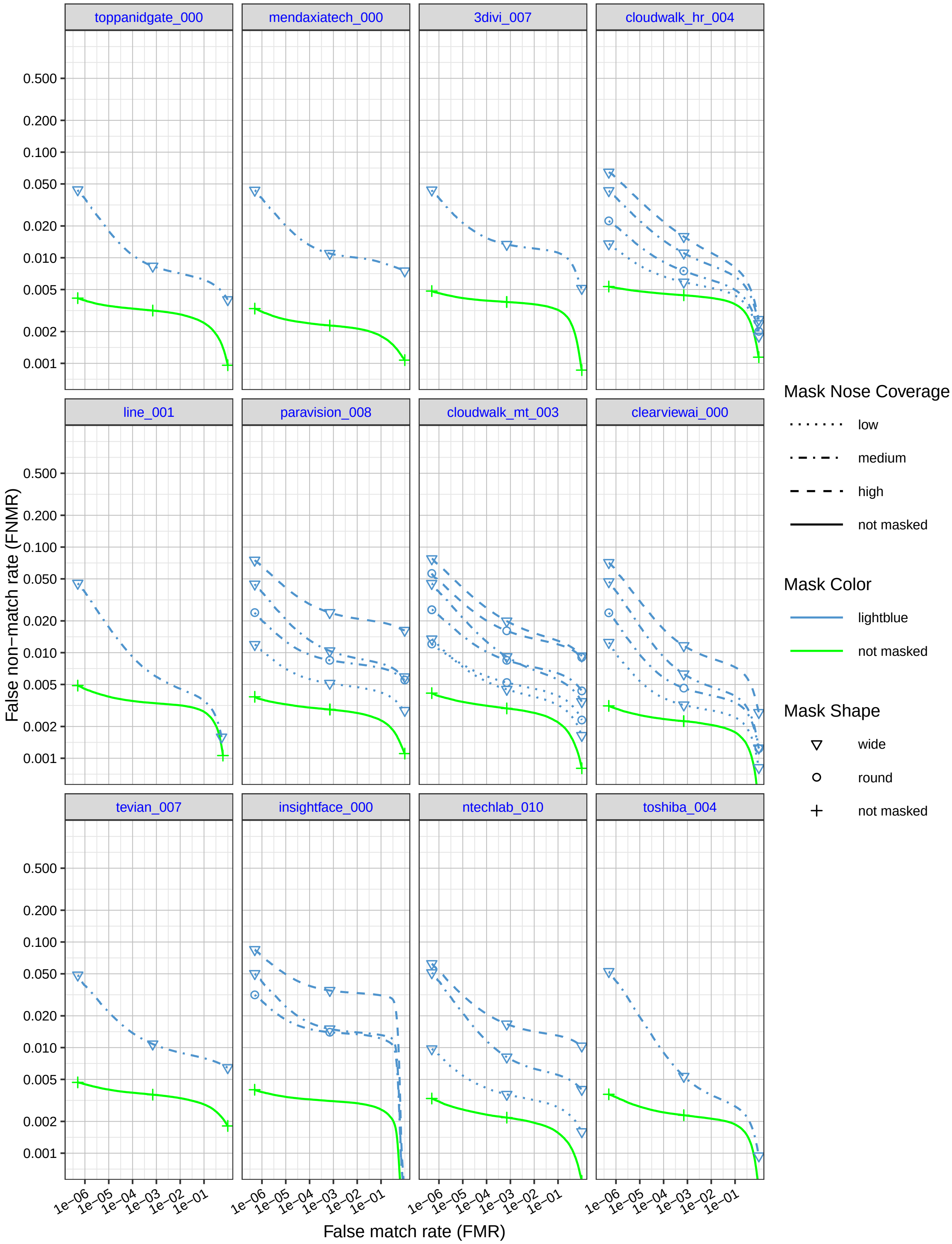

Figure 20: DET curves showing error rates on unmasked and masked probe images, broken out by mask shape and nose coverage. Algorithms in black were submitted prior to mid-March 2020, and algorithms in blue were submitted thereafter.

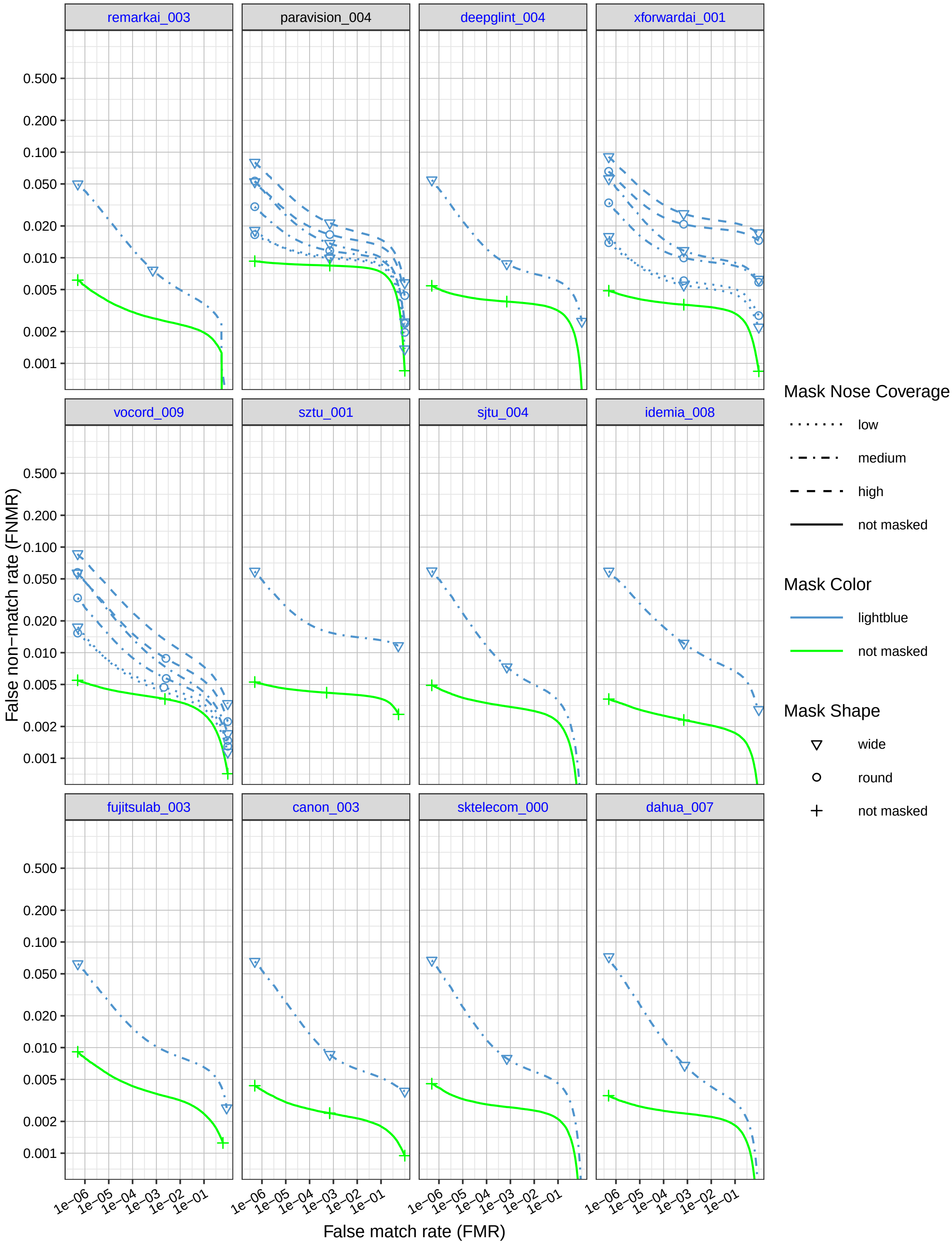

Figure 21: DET curves showing error rates on unmasked and masked probe images, broken out by mask shape and nose coverage. Algorithms in black were submitted prior to mid-March 2020, and algorithms in blue were submitted thereafter.

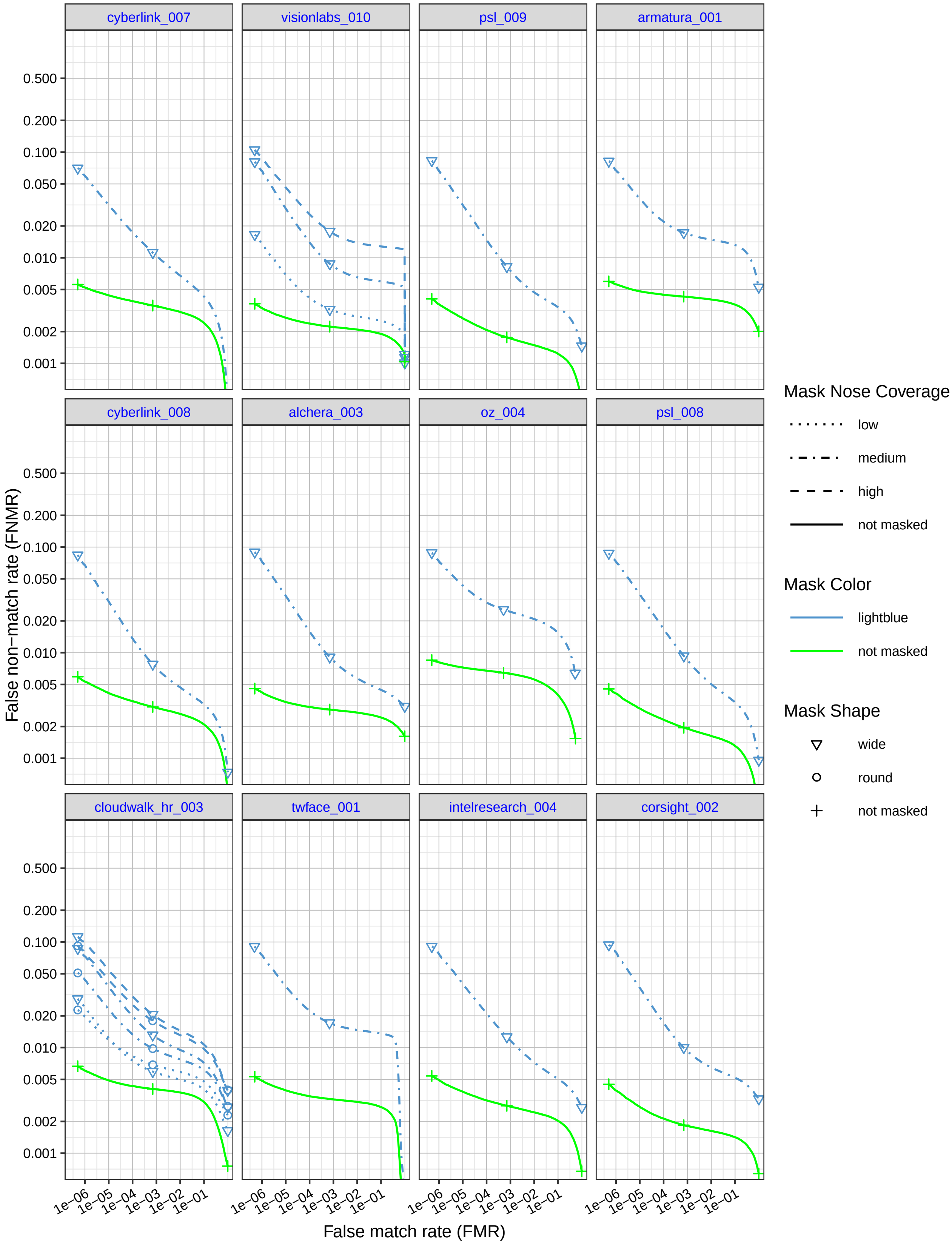

Figure 22: DET curves showing error rates on unmasked and masked probe images, broken out by mask shape and nose coverage. Algorithms in black were submitted prior to mid-March 2020, and algorithms in blue were submitted thereafter.

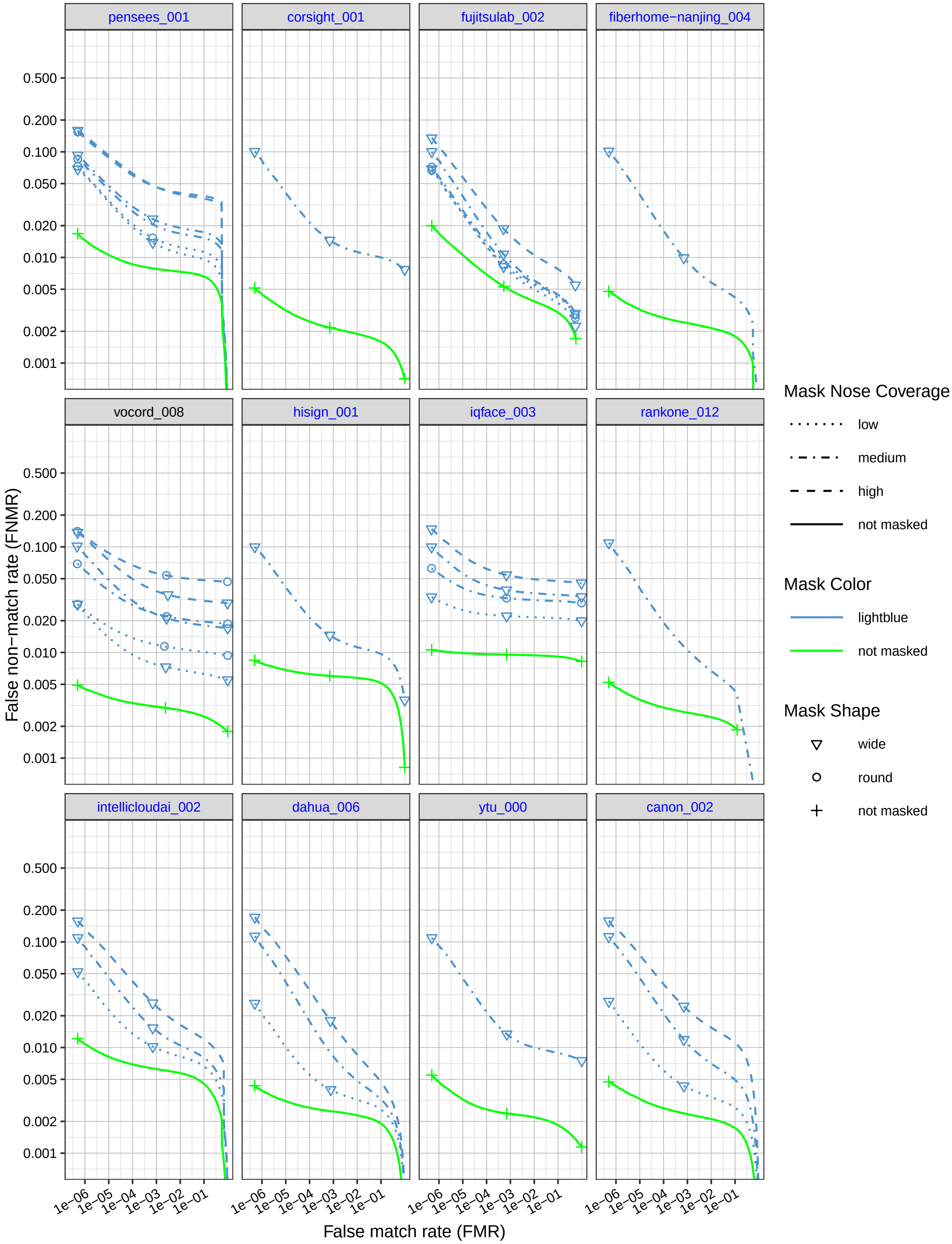

Figure 23: DET curves showing error rates on unmasked and masked probe images, broken out by mask shape and nose coverage. Algorithms in black were submitted prior to mid-March 2020, and algorithms in blue were submitted thereafter.

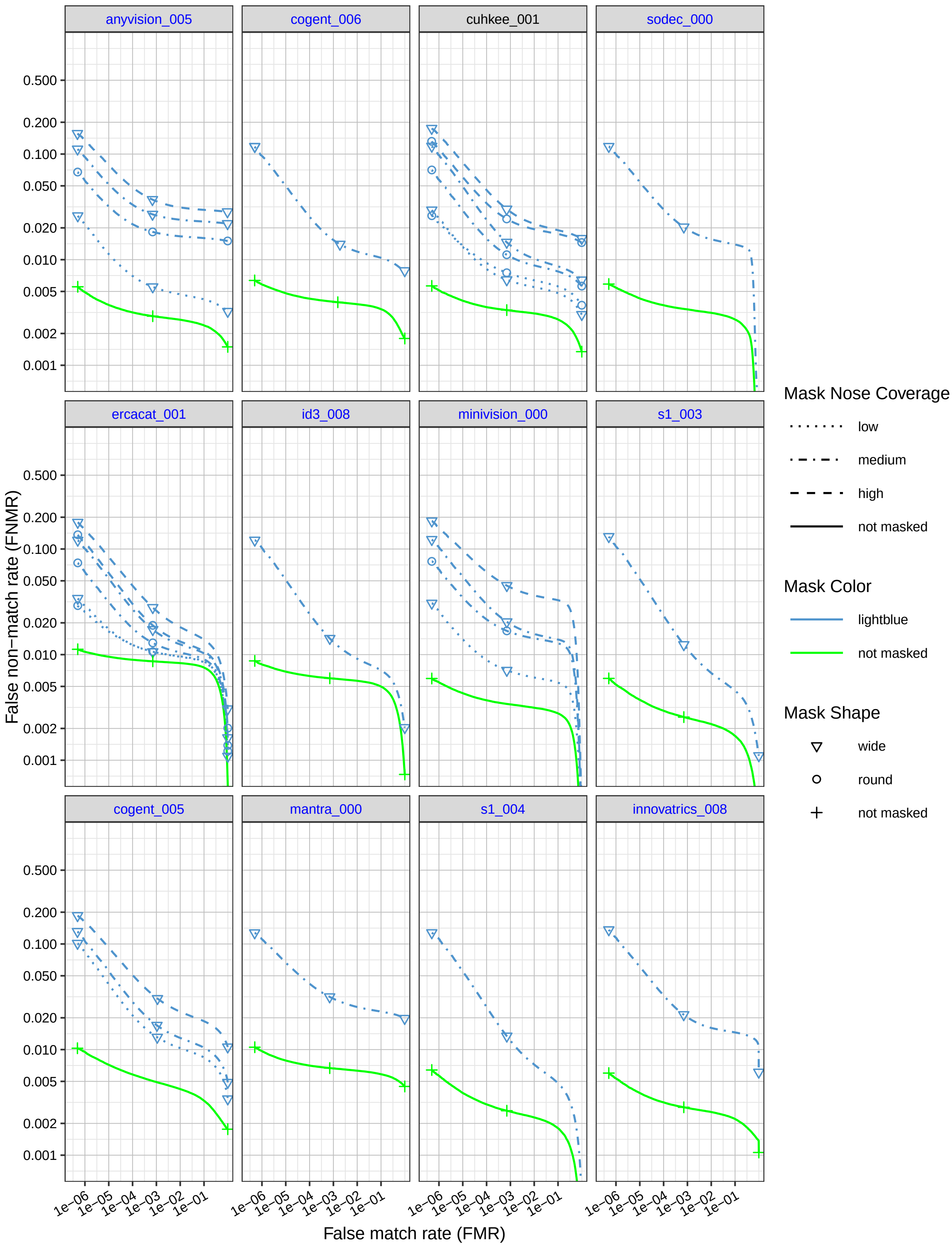

Figure 24: DET curves showing error rates on unmasked and masked probe images, broken out by mask shape and nose coverage. Algorithms in black were submitted prior to mid-March 2020, and algorithms in blue were submitted thereafter.

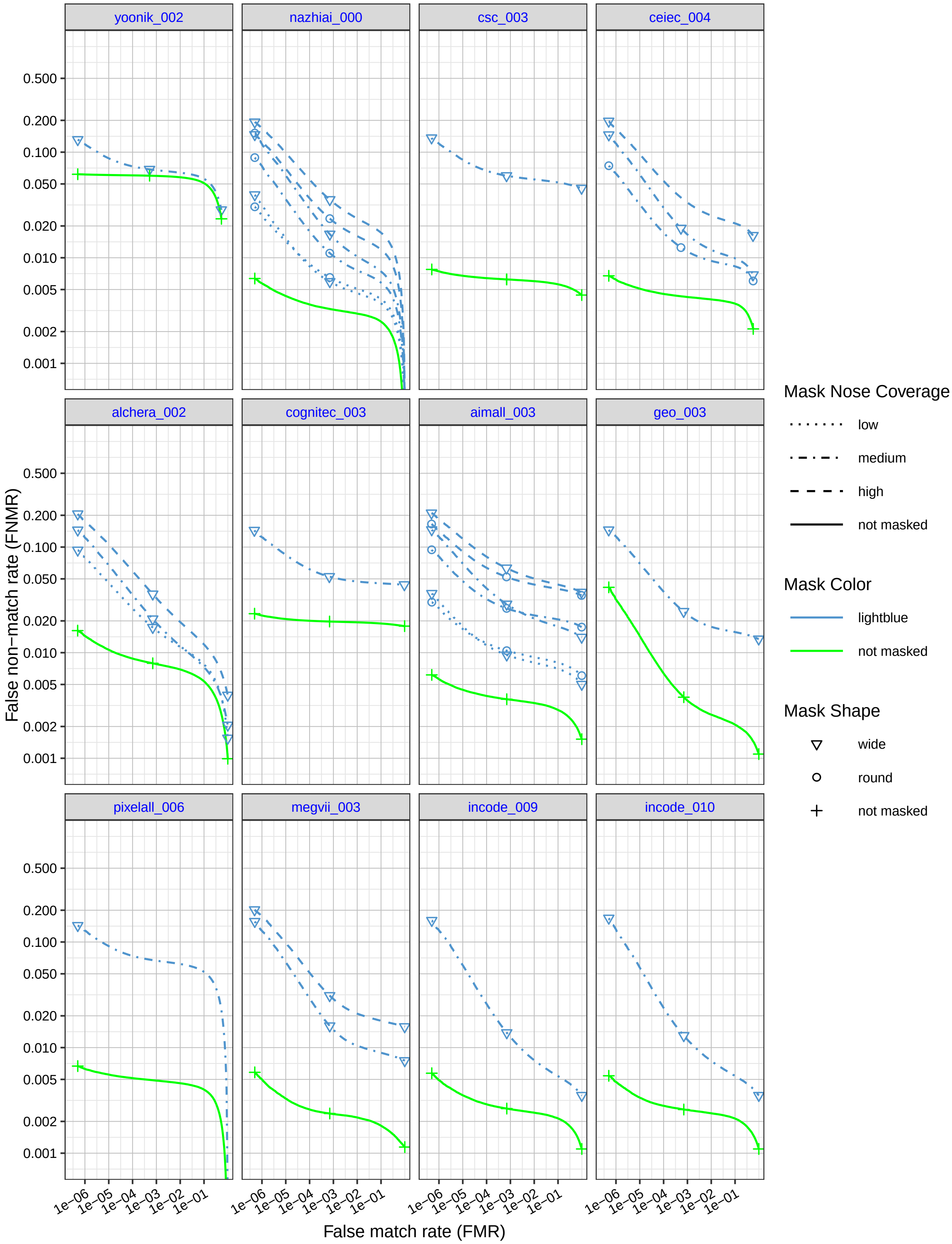

Figure 25: DET curves showing error rates on unmasked and masked probe images, broken out by mask shape and nose coverage. Algorithms in black were submitted prior to mid-March 2020, and algorithms in blue were submitted thereafter.

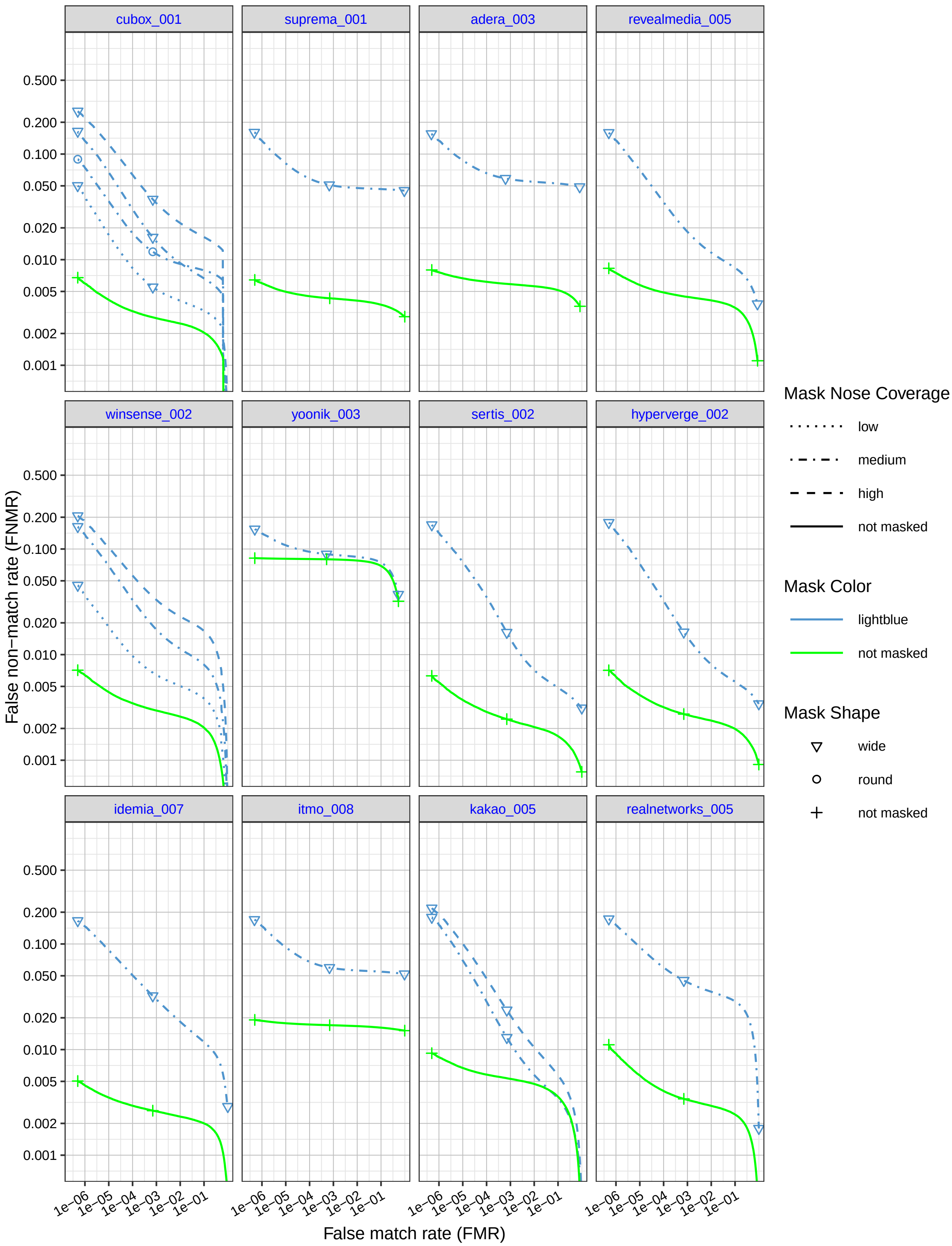

Figure 26: DET curves showing error rates on unmasked and masked probe images, broken out by mask shape and nose coverage. Algorithms in black were submitted prior to mid-March 2020, and algorithms in blue were submitted thereafter.

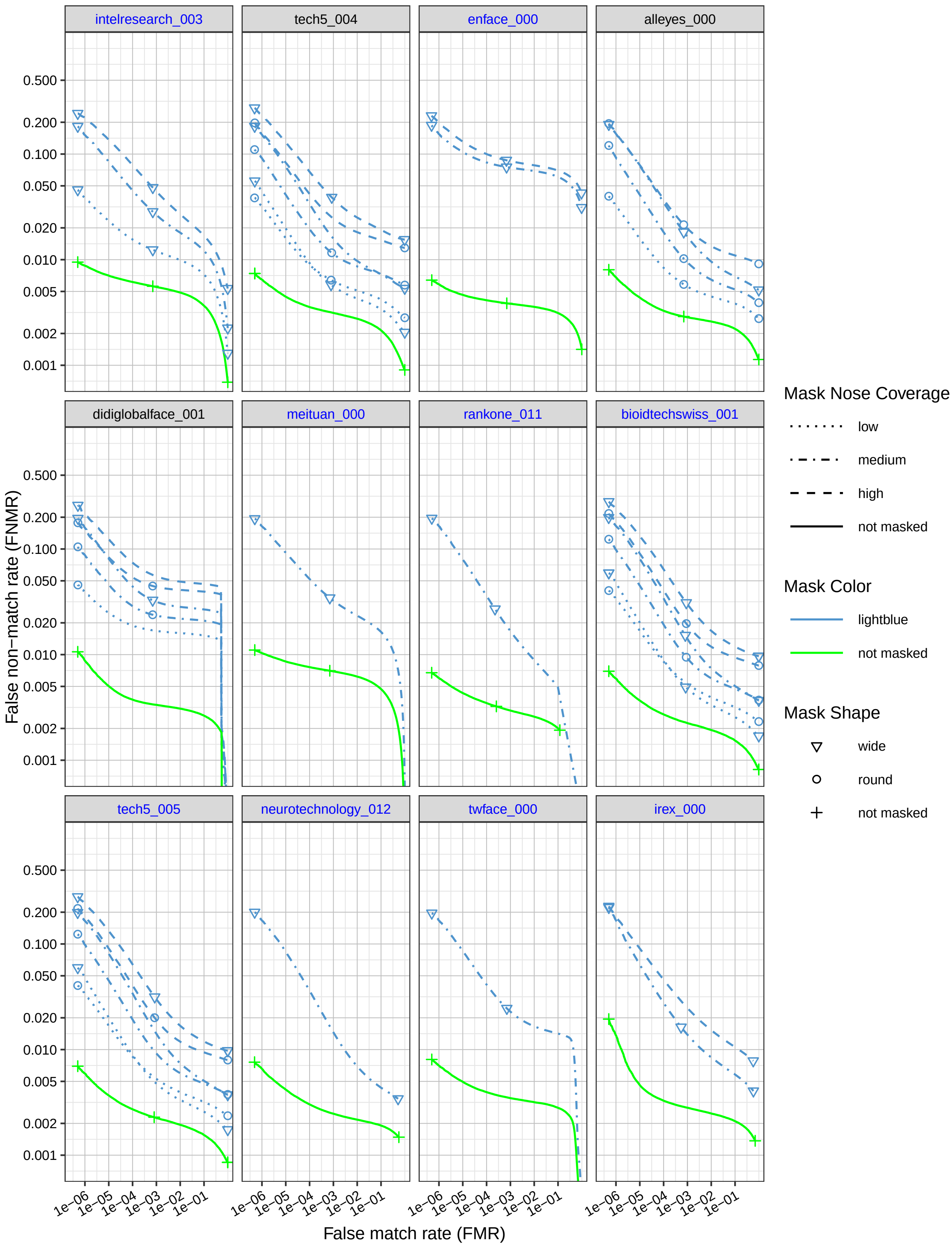

Figure 27: DET curves showing error rates on unmasked and masked probe images, broken out by mask shape and nose coverage. Algorithms in black were submitted prior to mid-March 2020, and algorithms in blue were submitted thereafter.

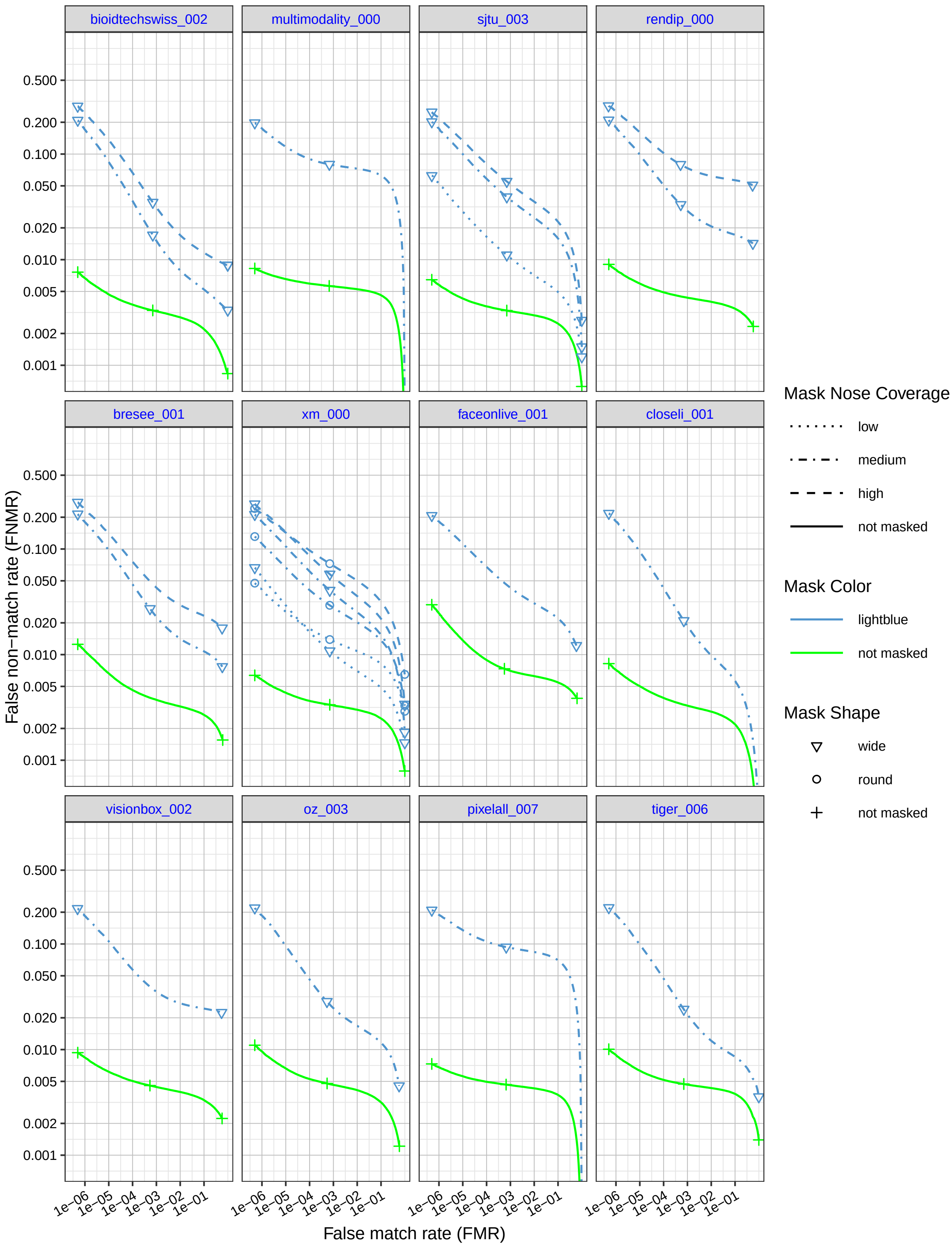

Figure 28: DET curves showing error rates on unmasked and masked probe images, broken out by mask shape and nose coverage. Algorithms in black were submitted prior to mid-March 2020, and algorithms in blue were submitted thereafter.

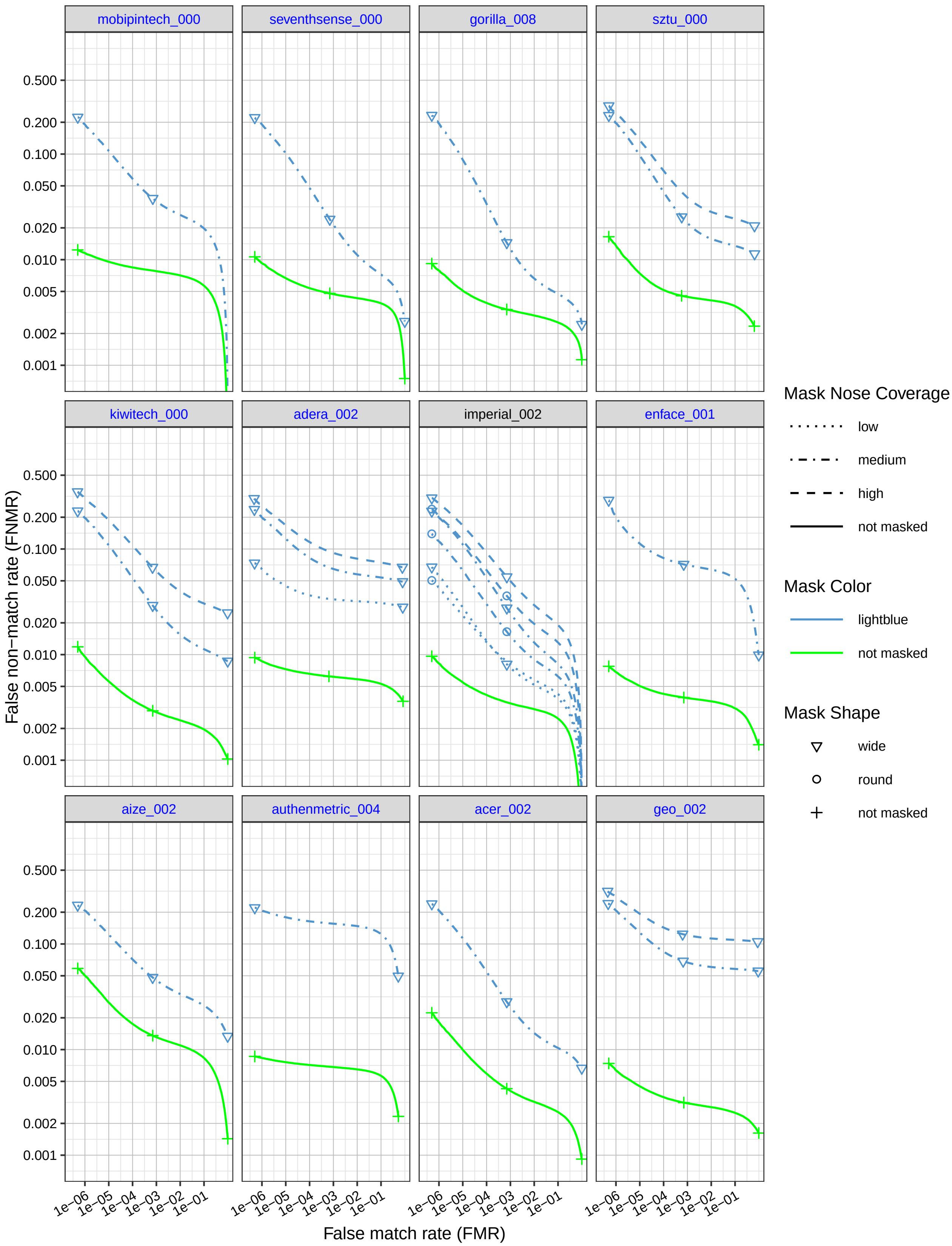

Figure 29: DET curves showing error rates on unmasked and masked probe images, broken out by mask shape and nose coverage. Algorithms in black were submitted prior to mid-March 2020, and algorithms in blue were submitted thereafter.

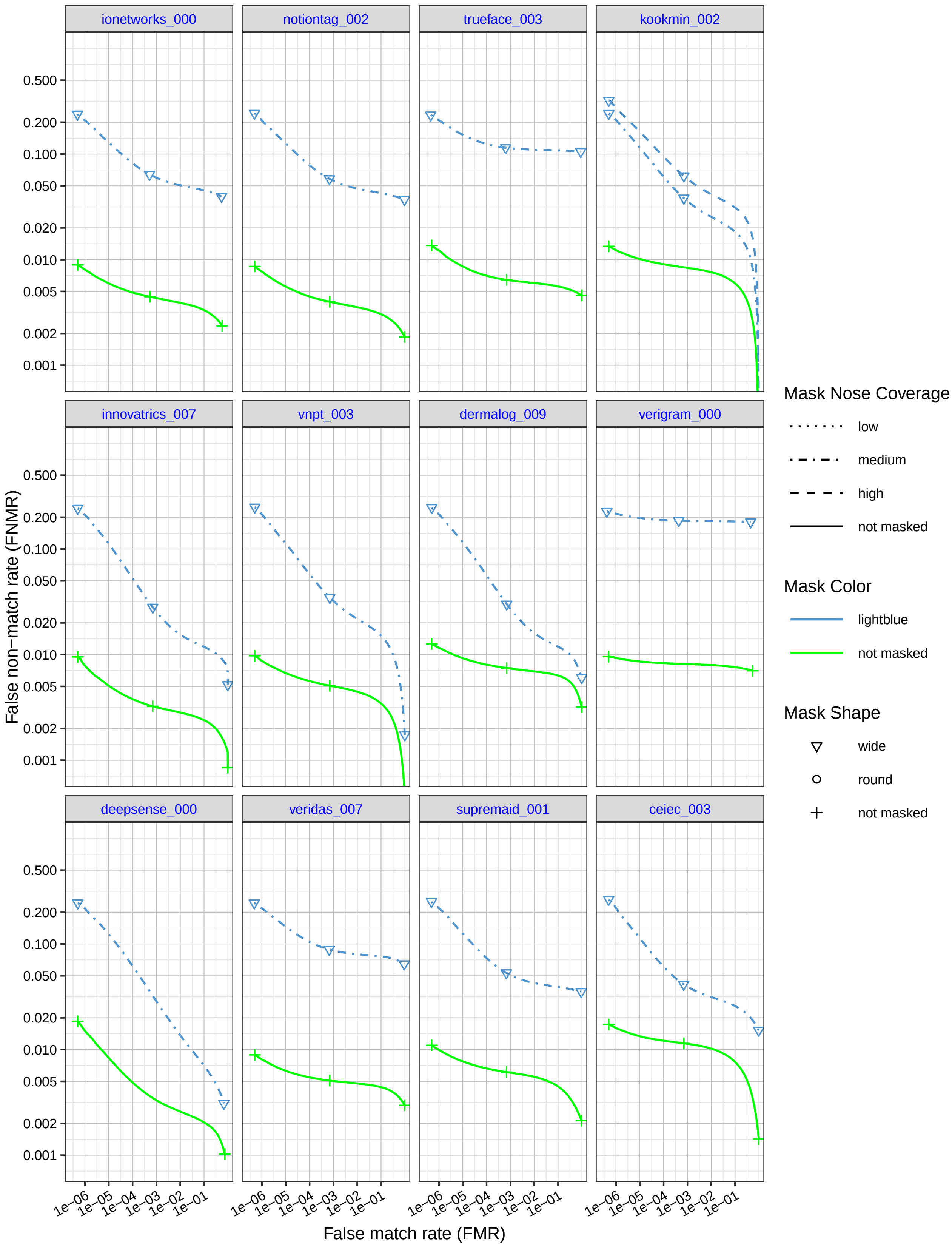

Figure 30: DET curves showing error rates on unmasked and masked probe images, broken out by mask shape and nose coverage. Algorithms in black were submitted prior to mid-March 2020, and algorithms in blue were submitted thereafter.

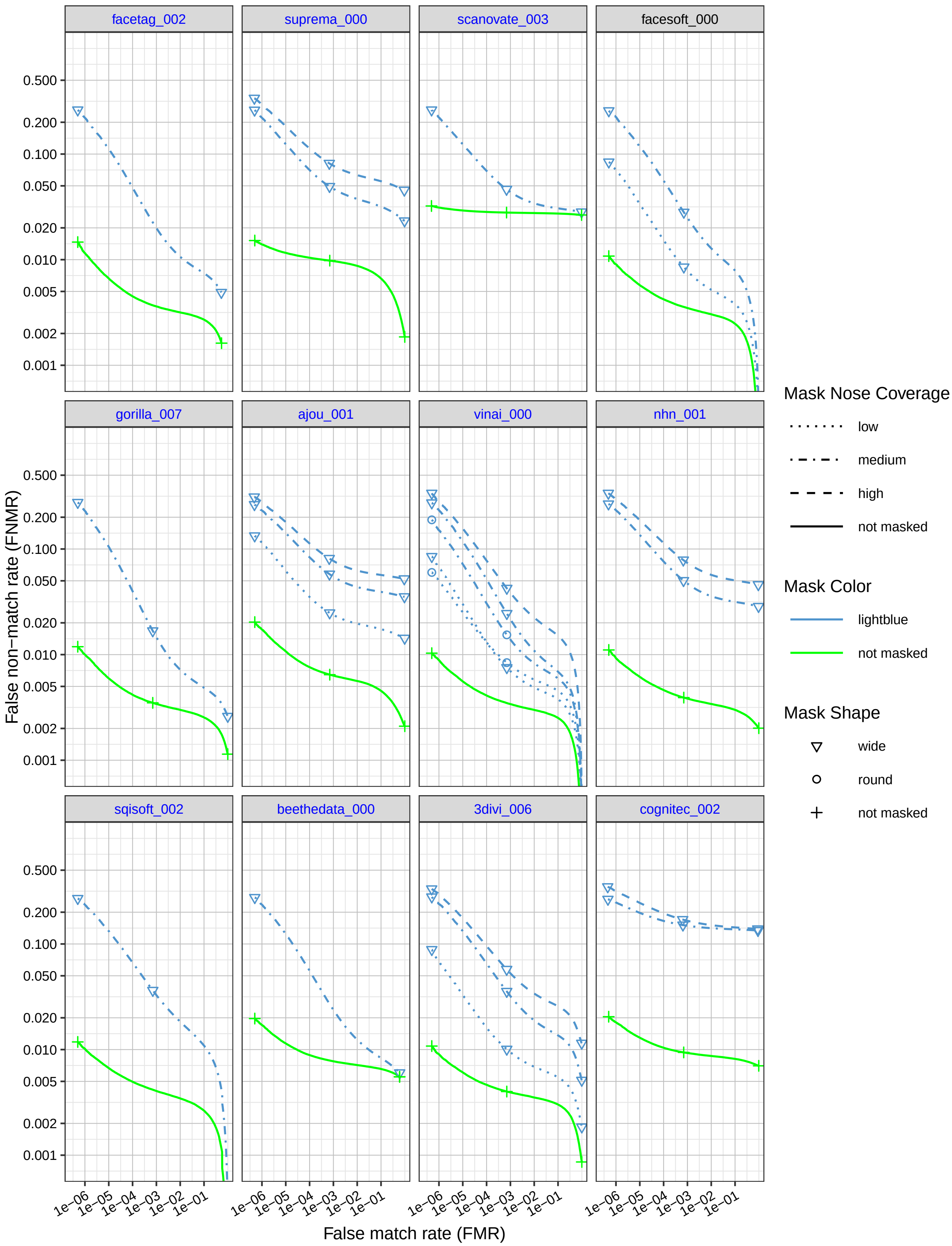

Figure 31: DET curves showing error rates on unmasked and masked probe images, broken out by mask shape and nose coverage. Algorithms in black were submitted prior to mid-March 2020, and algorithms in blue were submitted thereafter.

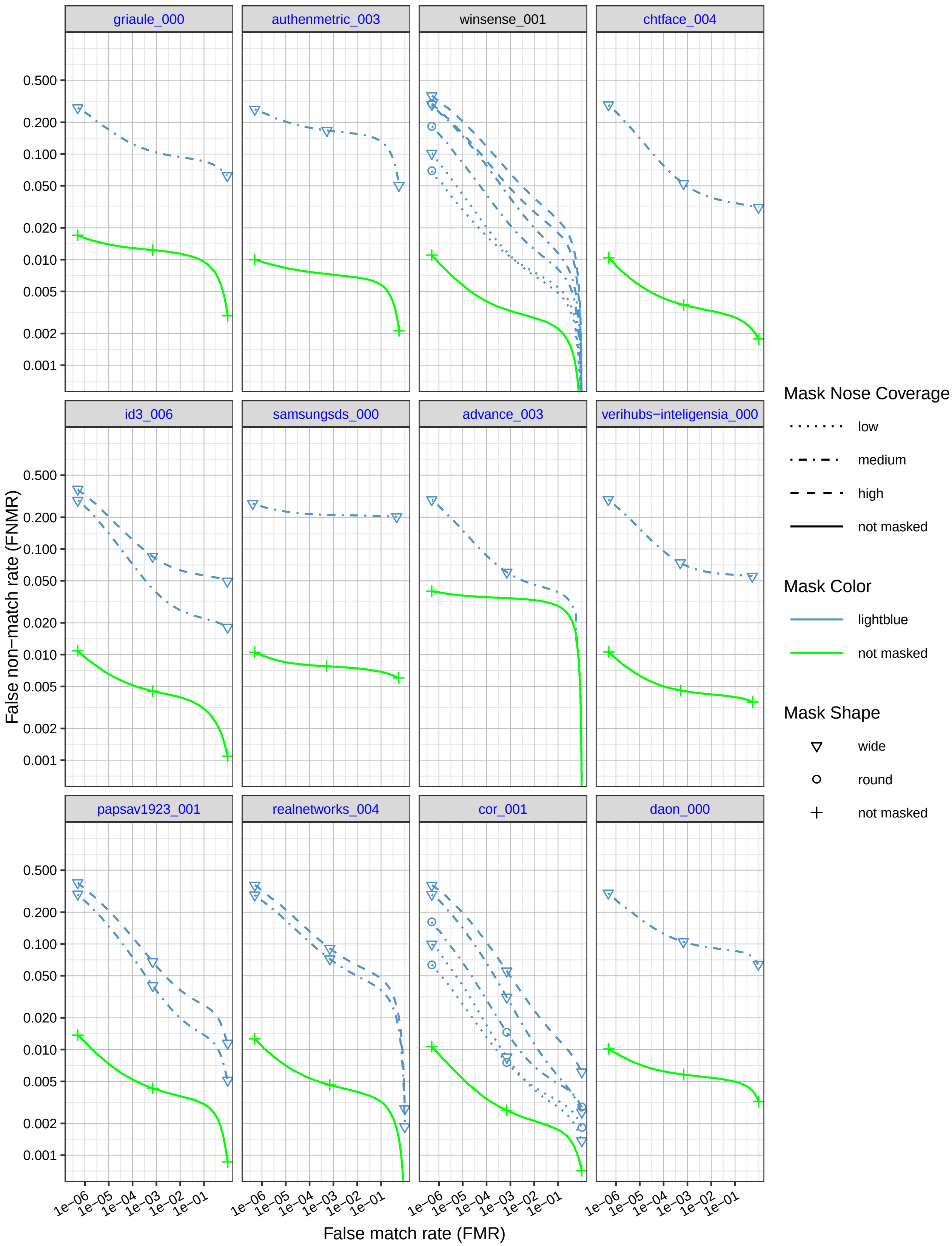

Figure 32: DET curves showing error rates on unmasked and masked probe images, broken out by mask shape and nose coverage. Algorithms in black were submitted prior to mid-March 2020, and algorithms in blue were submitted thereafter.

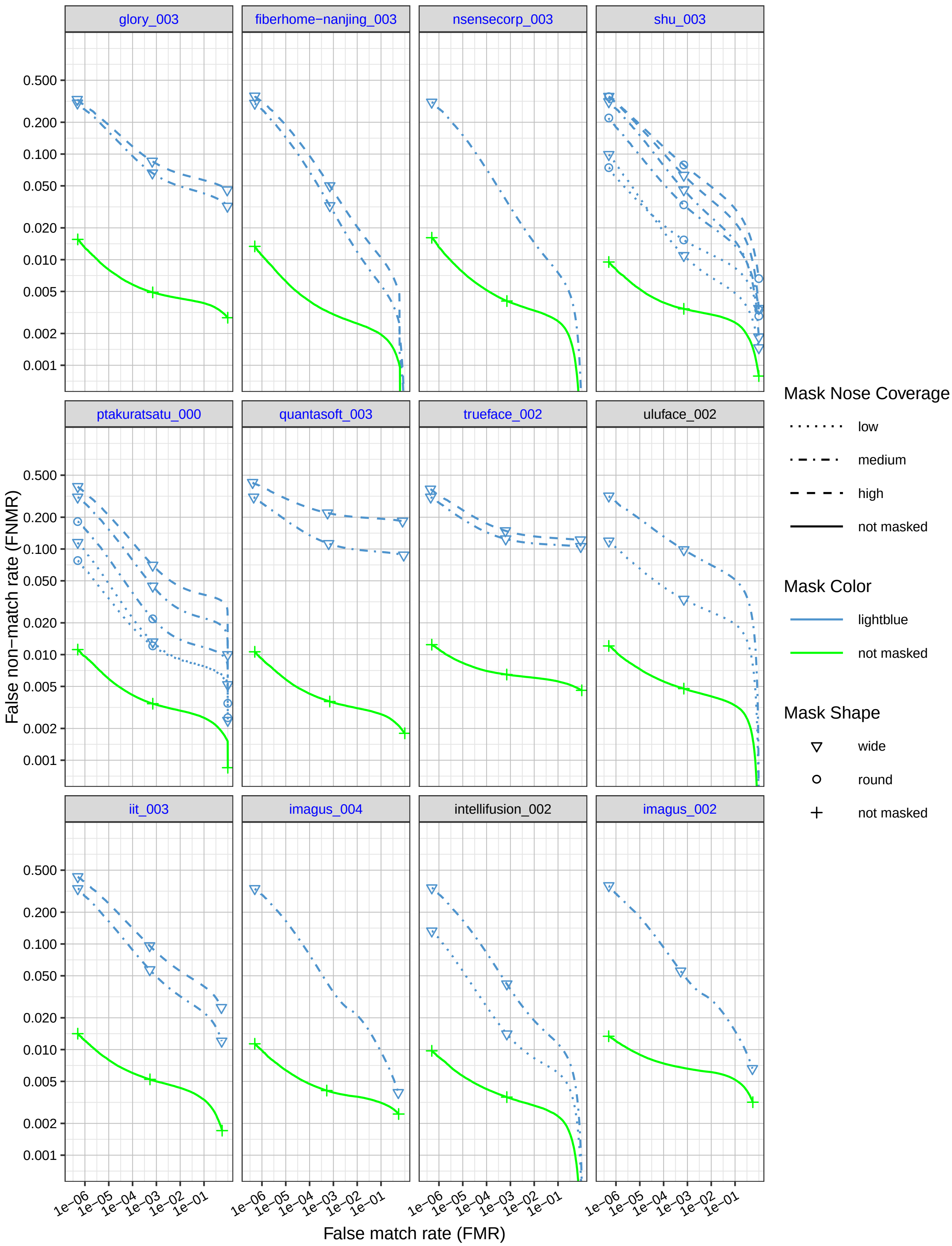

Figure 33: DET curves showing error rates on unmasked and masked probe images, broken out by mask shape and nose coverage. Algorithms in black were submitted prior to mid-March 2020, and algorithms in blue were submitted thereafter.

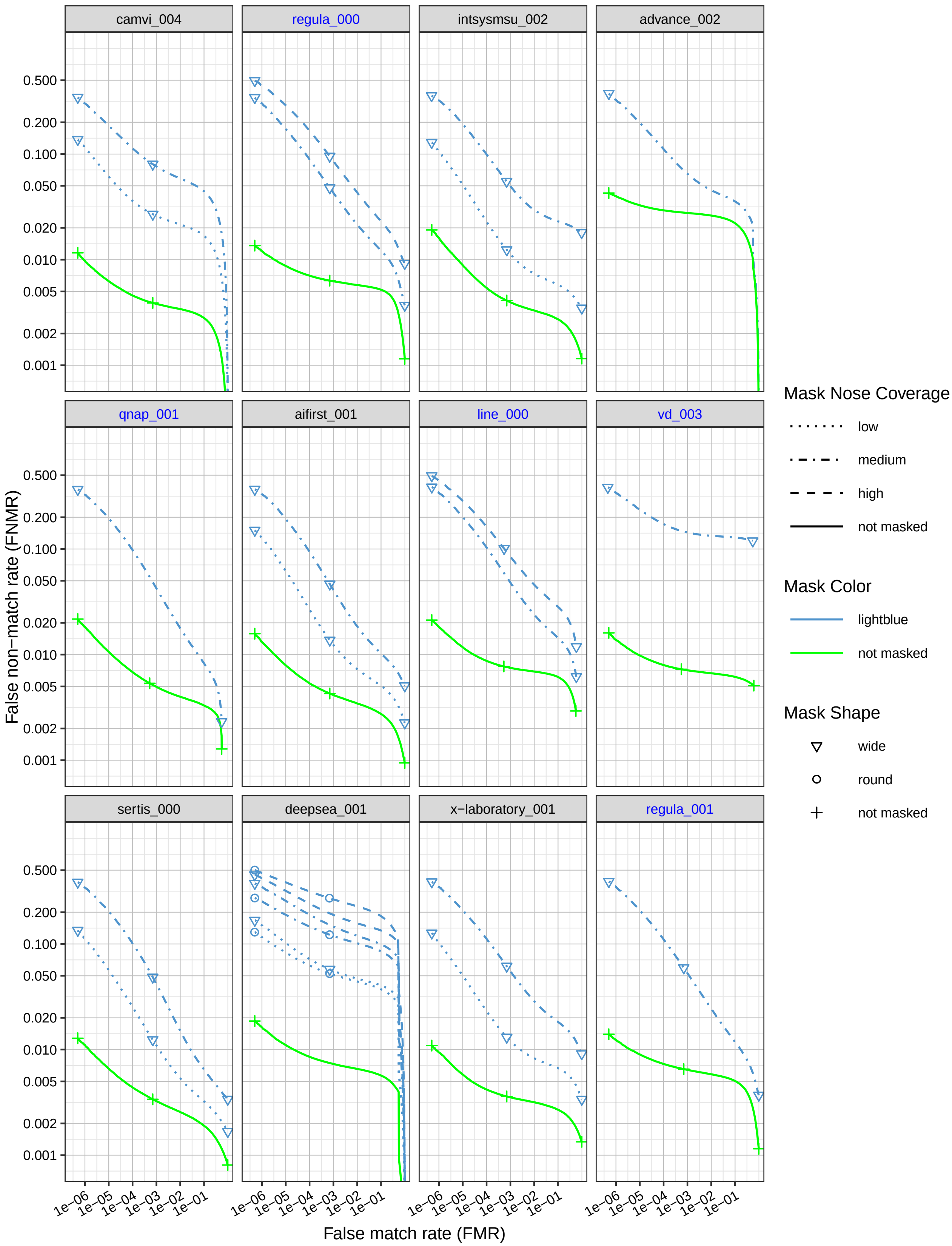

Figure 34: DET curves showing error rates on unmasked and masked probe images, broken out by mask shape and nose coverage. Algorithms in black were submitted prior to mid-March 2020, and algorithms in blue were submitted thereafter.

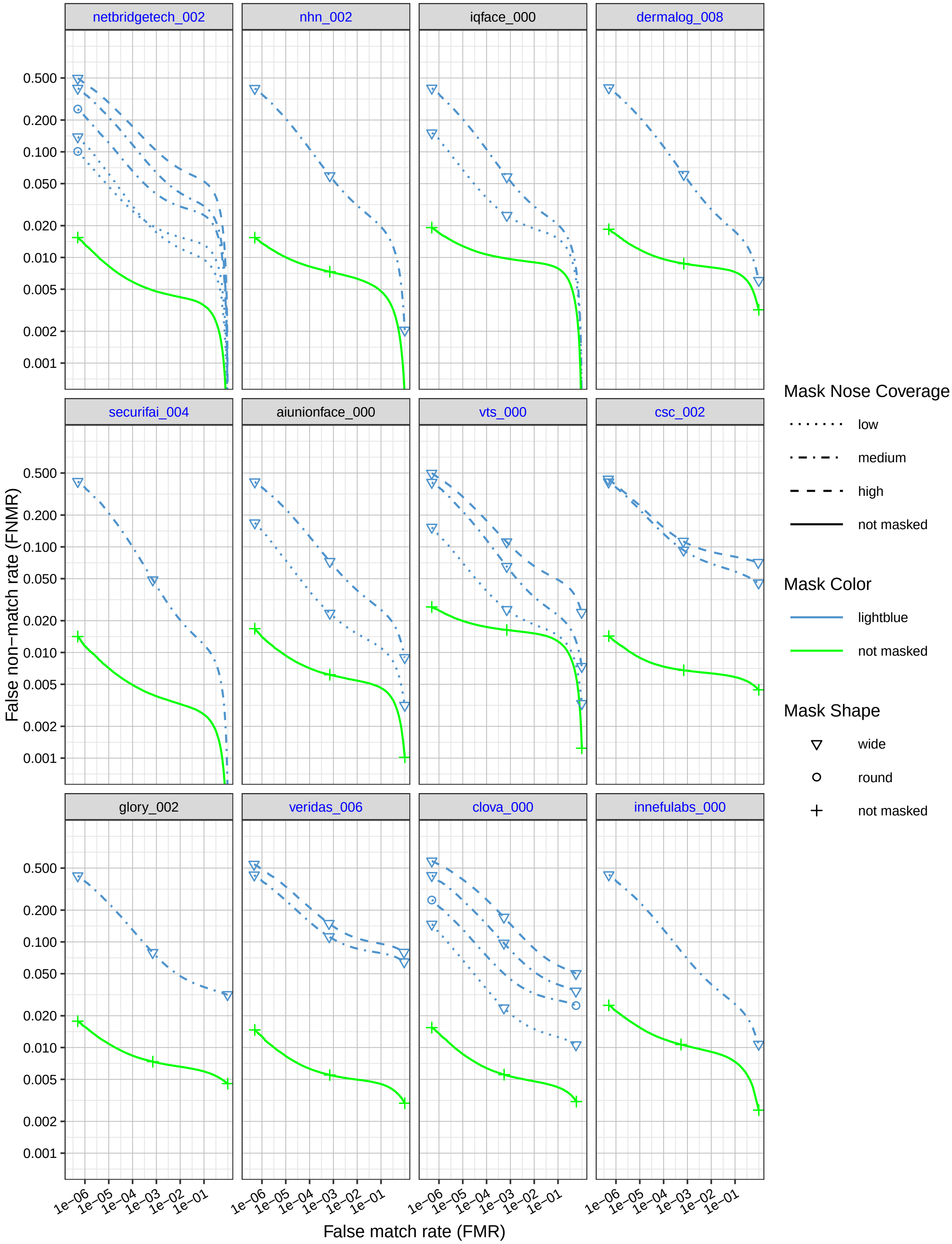

Figure 35: DET curves showing error rates on unmasked and masked probe images, broken out by mask shape and nose coverage. Algorithms in black were submitted prior to mid-March 2020, and algorithms in blue were submitted thereafter.

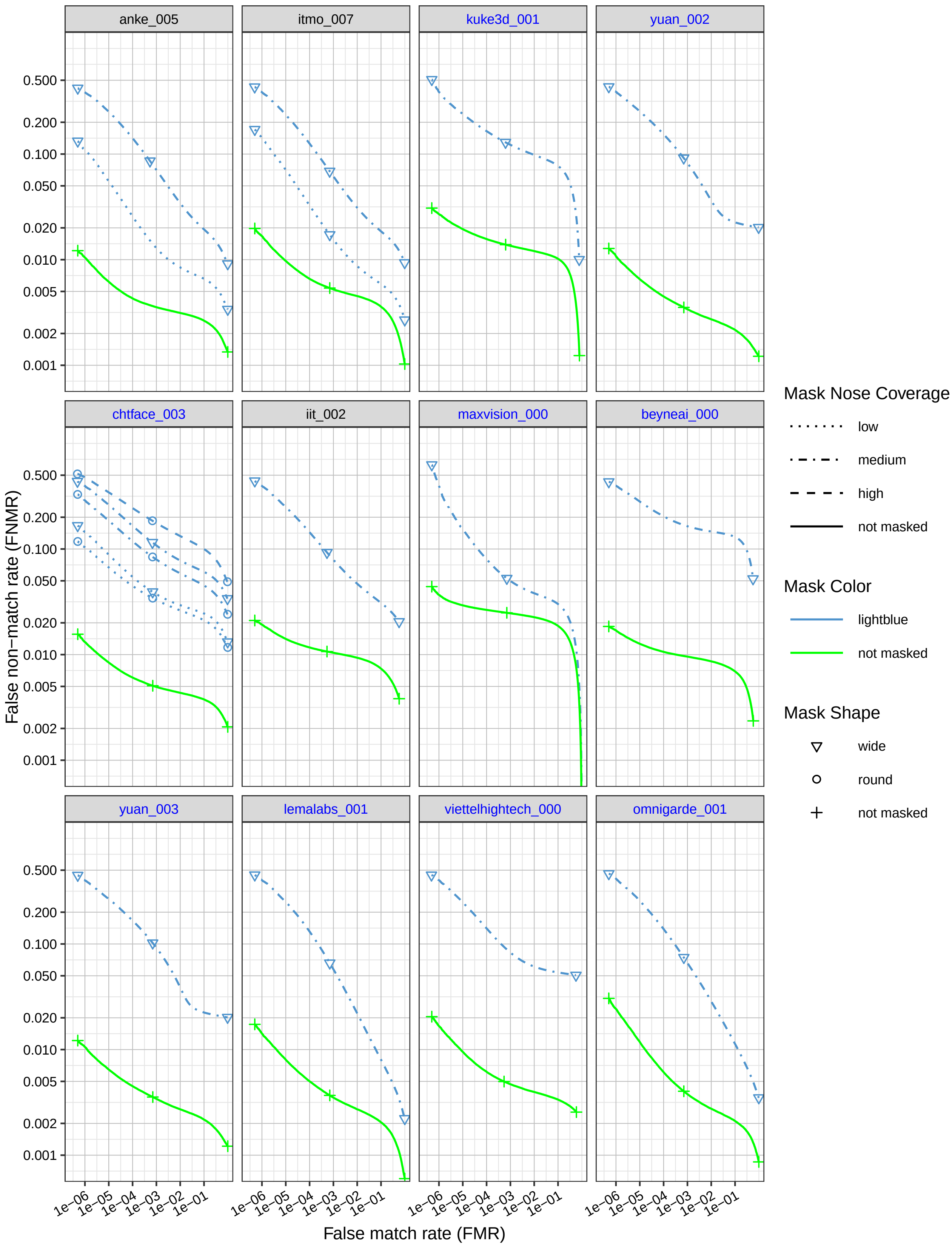

Figure 36: DET curves showing error rates on unmasked and masked probe images, broken out by mask shape and nose coverage. Algorithms in black were submitted prior to mid-March 2020, and algorithms in blue were submitted thereafter.

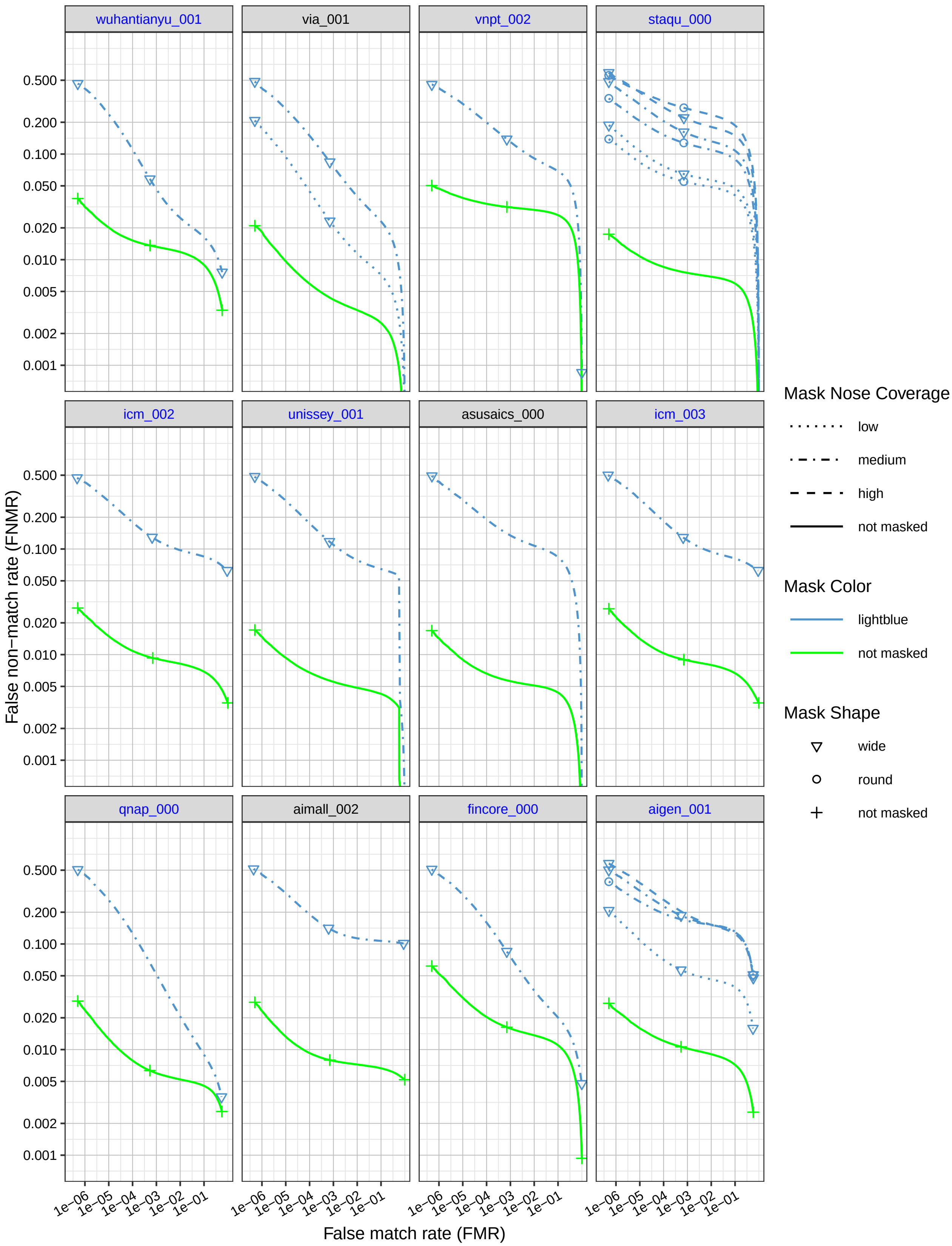

Figure 37: DET curves showing error rates on unmasked and masked probe images, broken out by mask shape and nose coverage. Algorithms in black were submitted prior to mid-March 2020, and algorithms in blue were submitted thereafter.

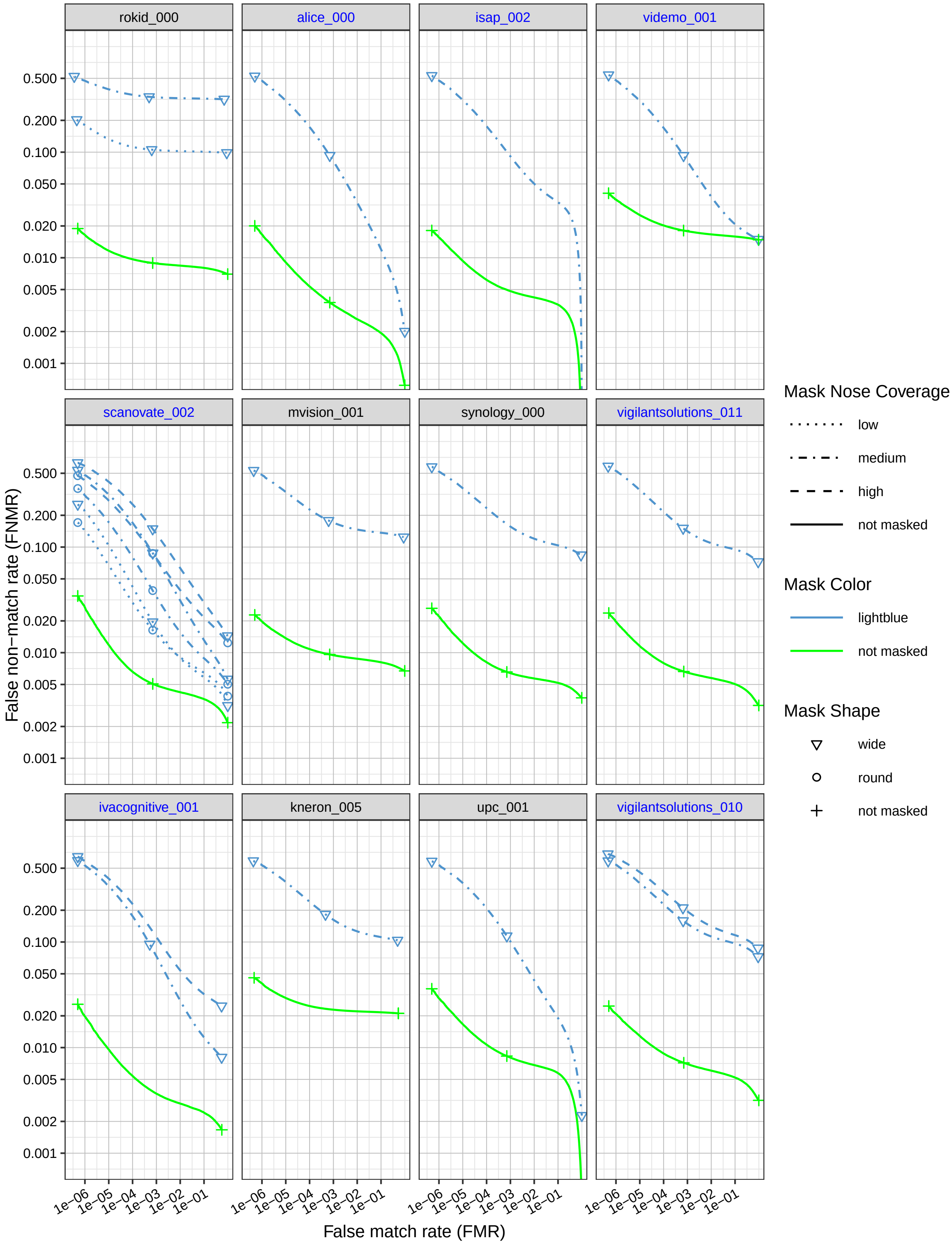

Figure 38: DET curves showing error rates on unmasked and masked probe images, broken out by mask shape and nose coverage. Algorithms in black were submitted prior to mid-March 2020, and algorithms in blue were submitted thereafter.

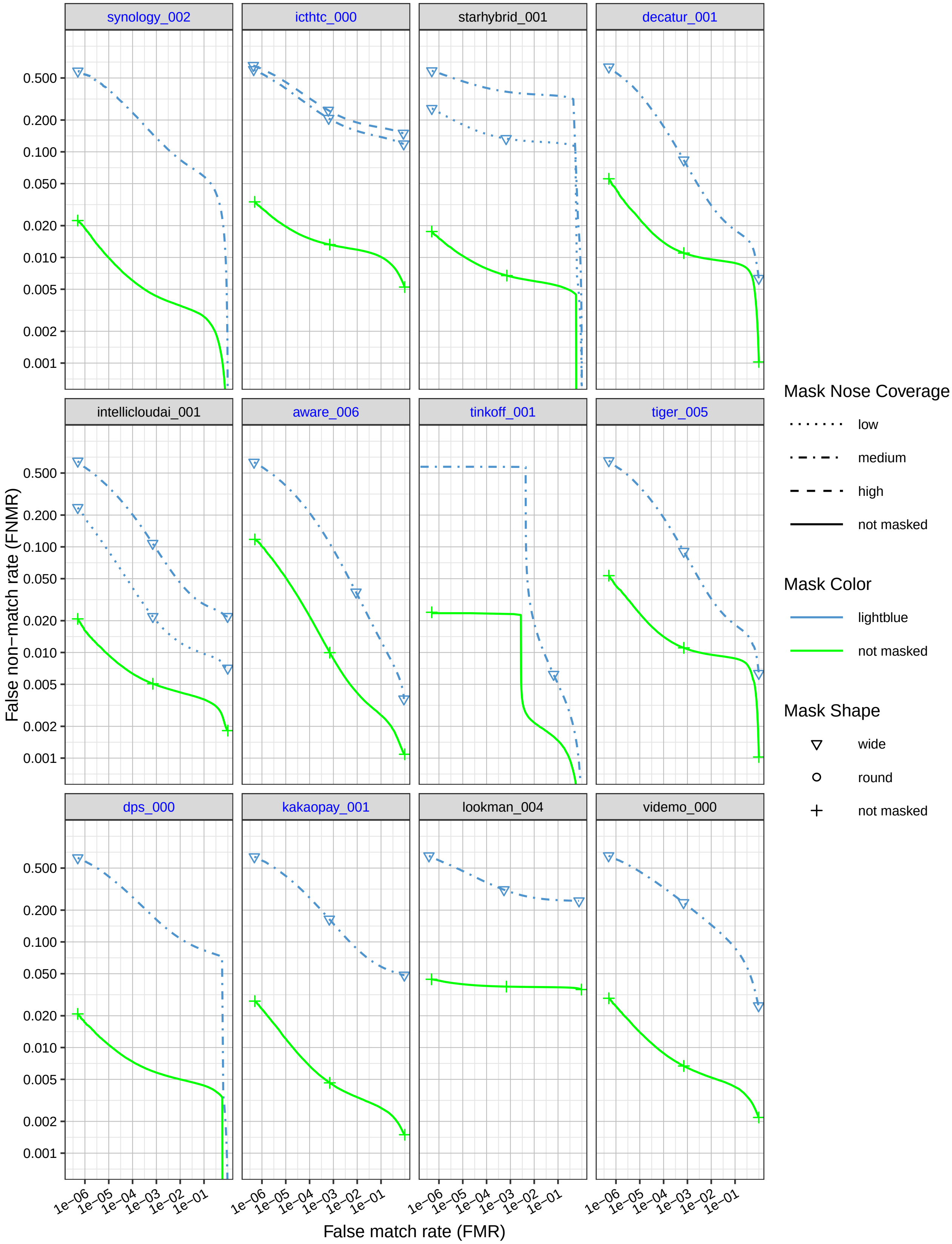

Figure 39: DET curves showing error rates on unmasked and masked probe images, broken out by mask shape and nose coverage. Algorithms in black were submitted prior to mid-March 2020, and algorithms in blue were submitted thereafter.

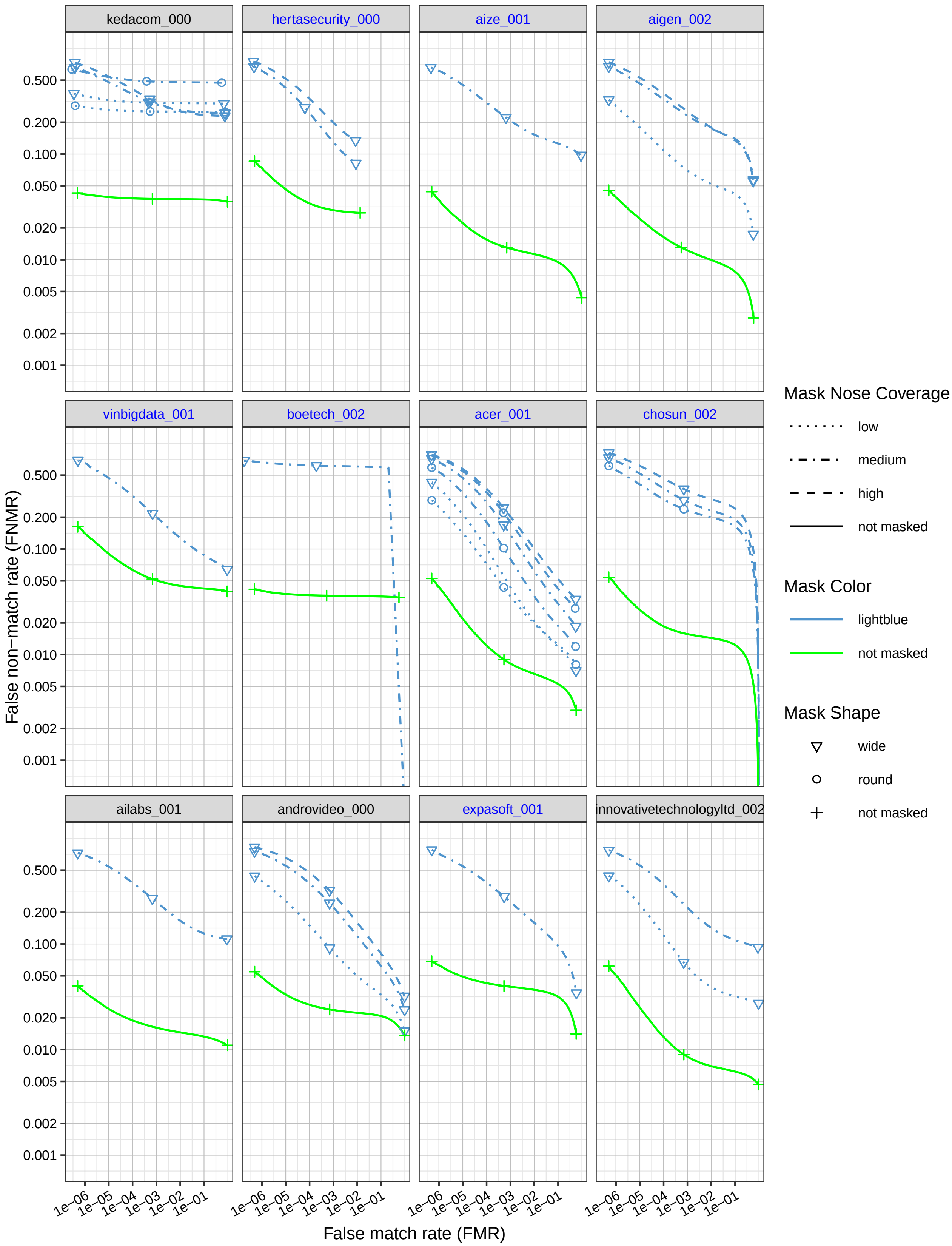

Figure 40: DET curves showing error rates on unmasked and masked probe images, broken out by mask shape and nose coverage. Algorithms in black were submitted prior to mid-March 2020, and algorithms in blue were submitted thereafter.

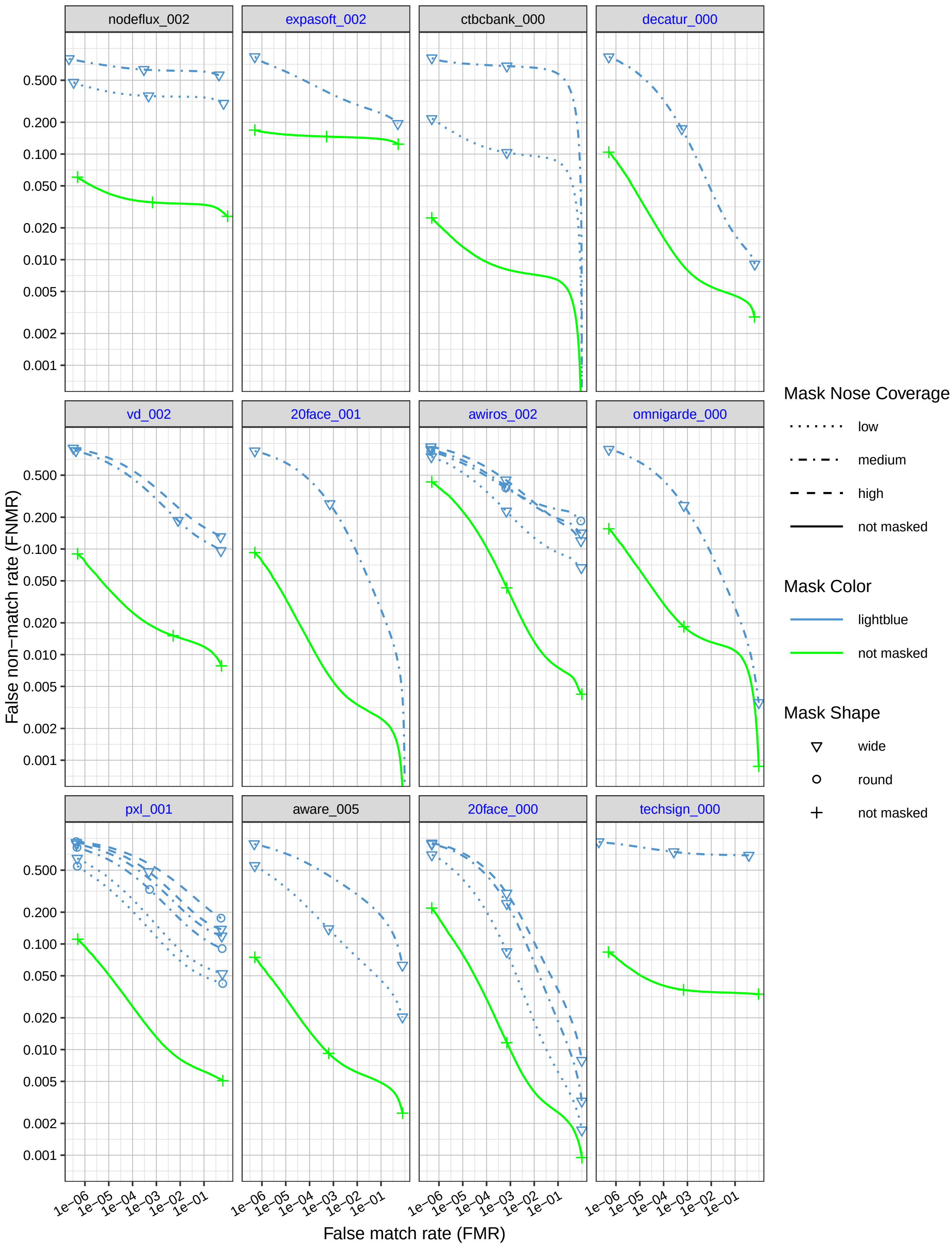

Figure 41: DET curves showing error rates on unmasked and masked probe images, broken out by mask shape and nose coverage. Algorithms in black were submitted prior to mid-March 2020, and algorithms in blue were submitted thereafter.

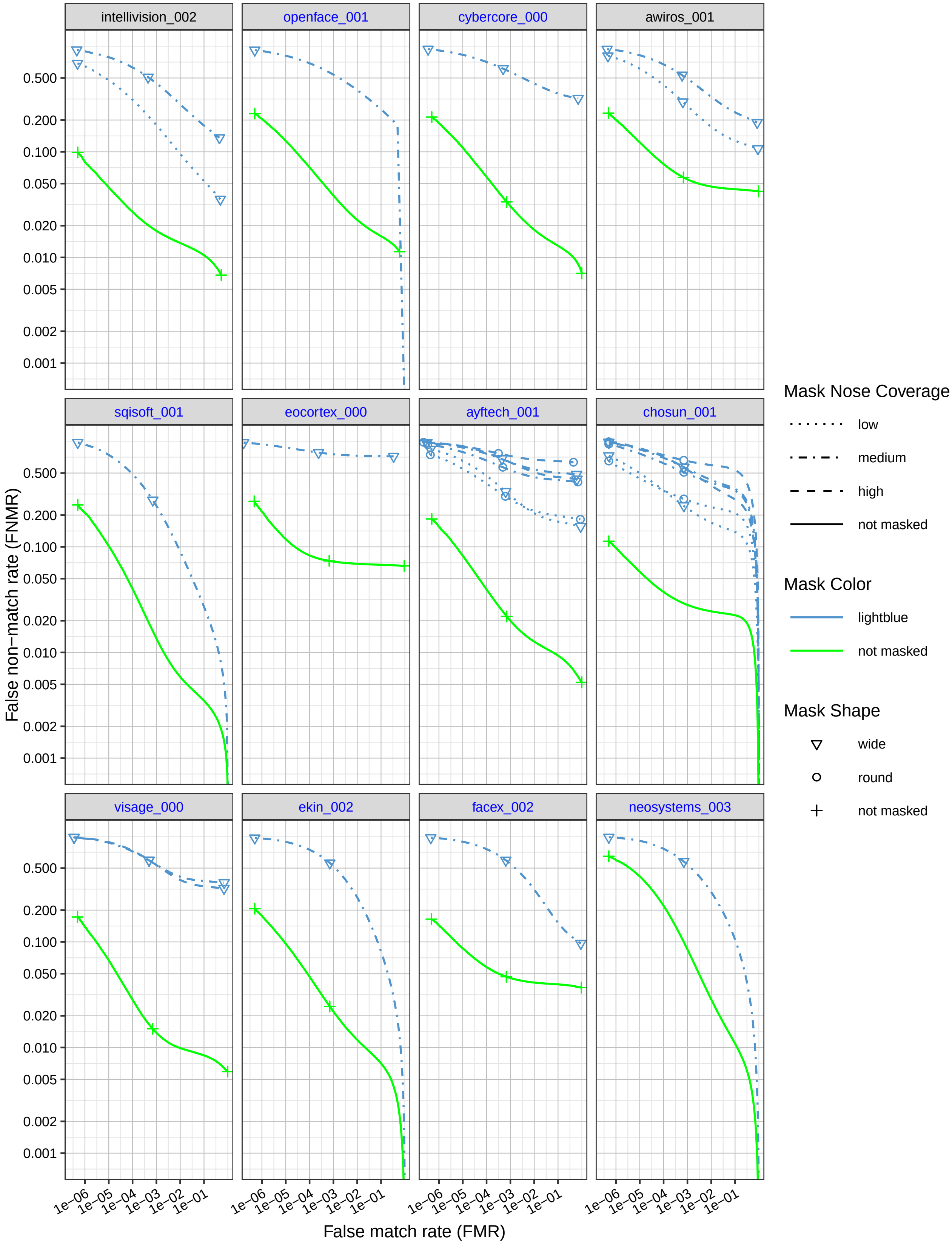

Figure 42: DET curves showing error rates on unmasked and masked probe images, broken out by mask shape and nose coverage. Algorithms in black were submitted prior to mid-March 2020, and algorithms in blue were submitted thereafter.

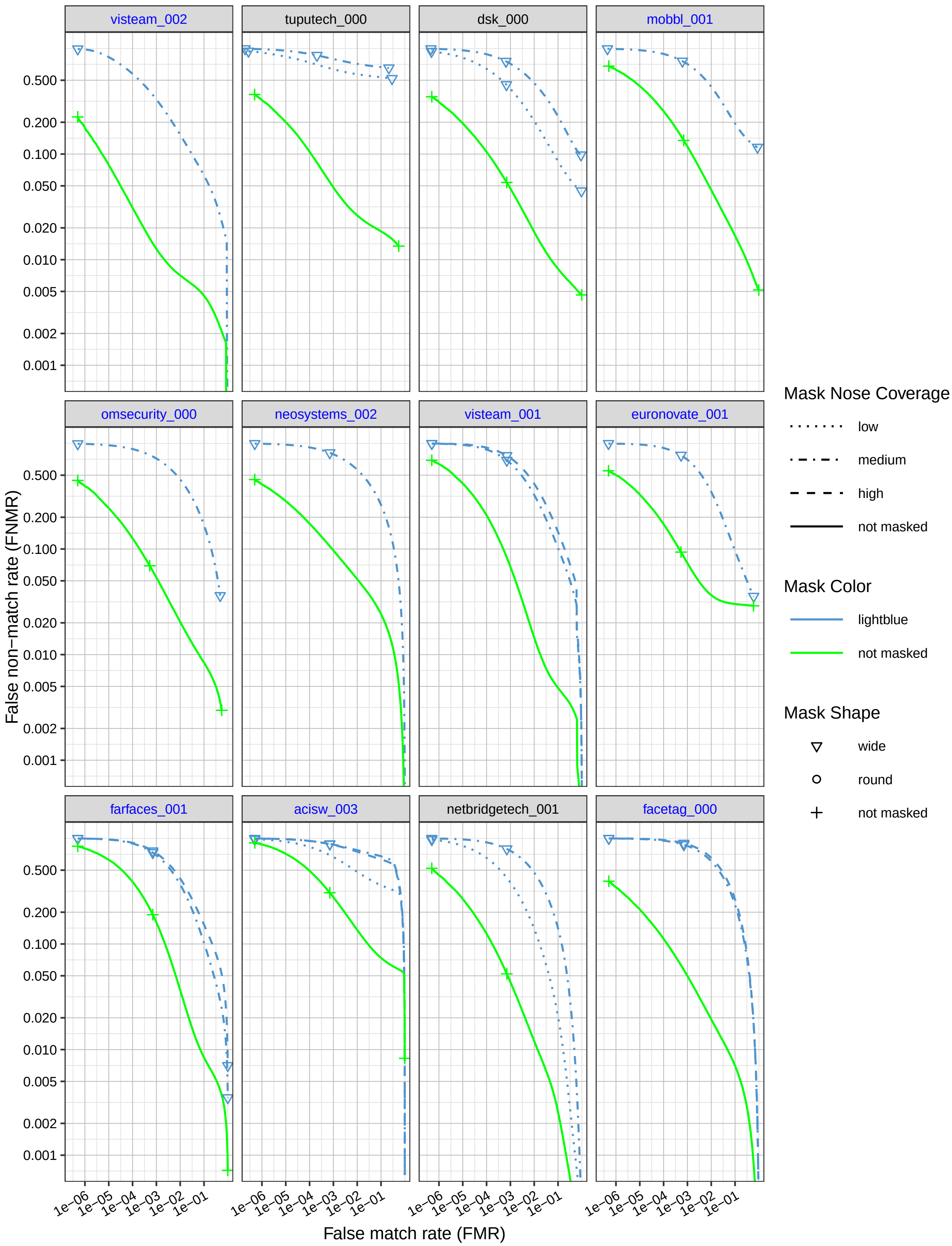

Figure 43: DET curves showing error rates on unmasked and masked probe images, broken out by mask shape and nose coverage. Algorithms in black were submitted prior to mid-March 2020, and algorithms in blue were submitted thereafter.

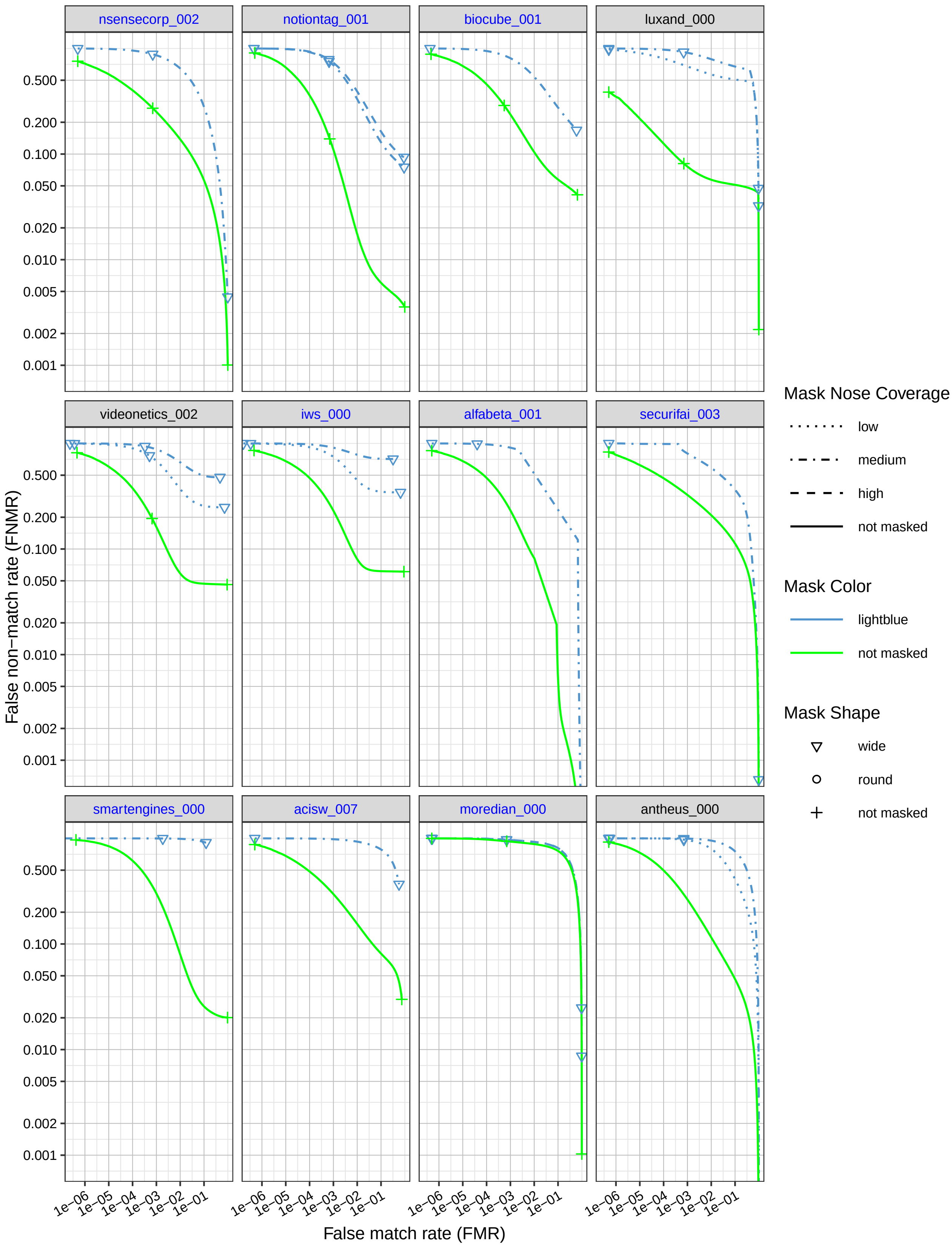

Figure 44: DET curves showing error rates on unmasked and masked probe images, broken out by mask shape and nose coverage. Algorithms in black were submitted prior to mid-March 2020, and algorithms in blue were submitted thereafter.

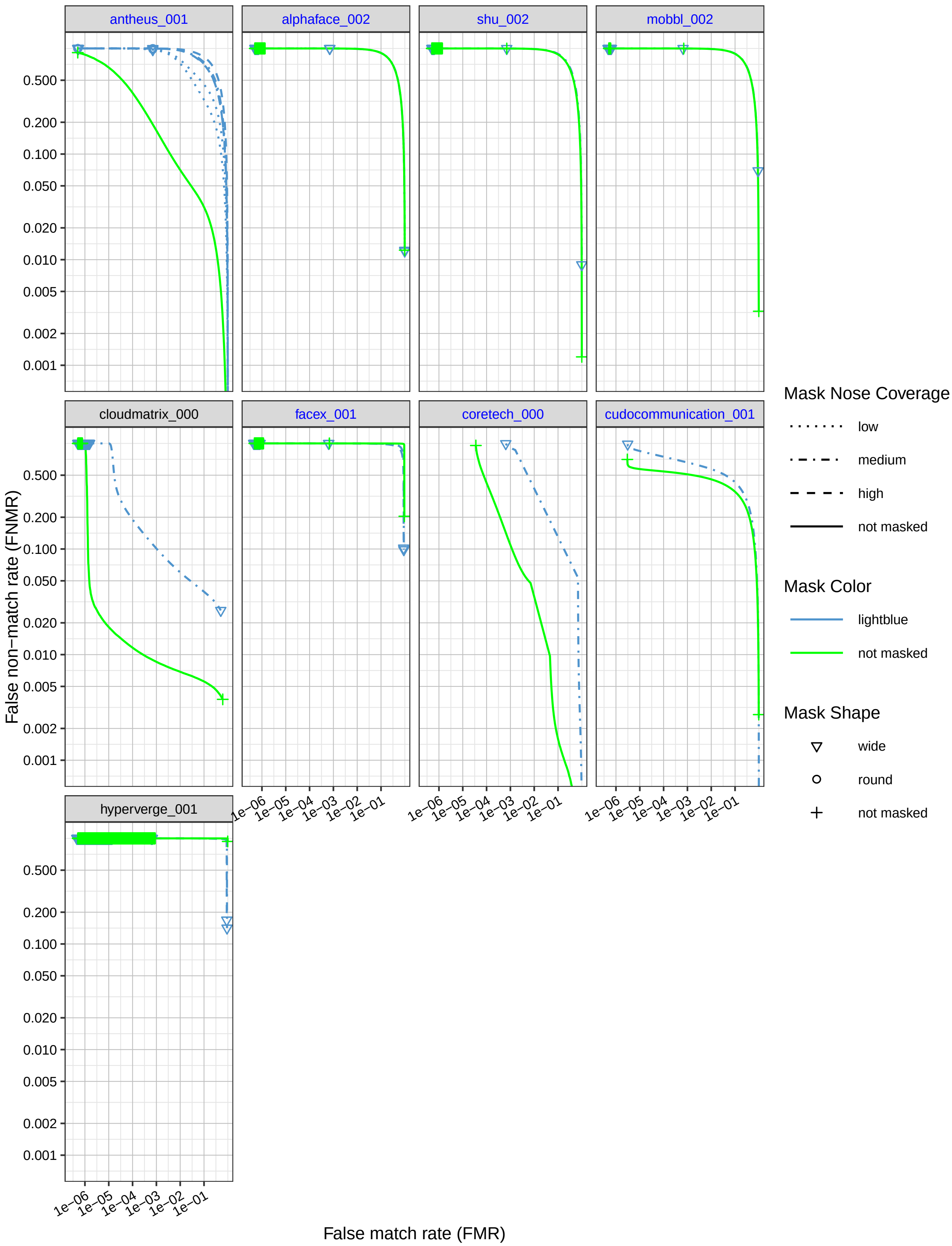

Figure 45: DET curves showing error rates on unmasked and masked probe images, broken out by mask shape and nose coverage. Algorithms in black were submitted prior to mid-March 2020, and algorithms in blue were submitted thereafter.

The following plots are detection error tradeoff (DET) characteristics for each algorithm, across different mask colors.

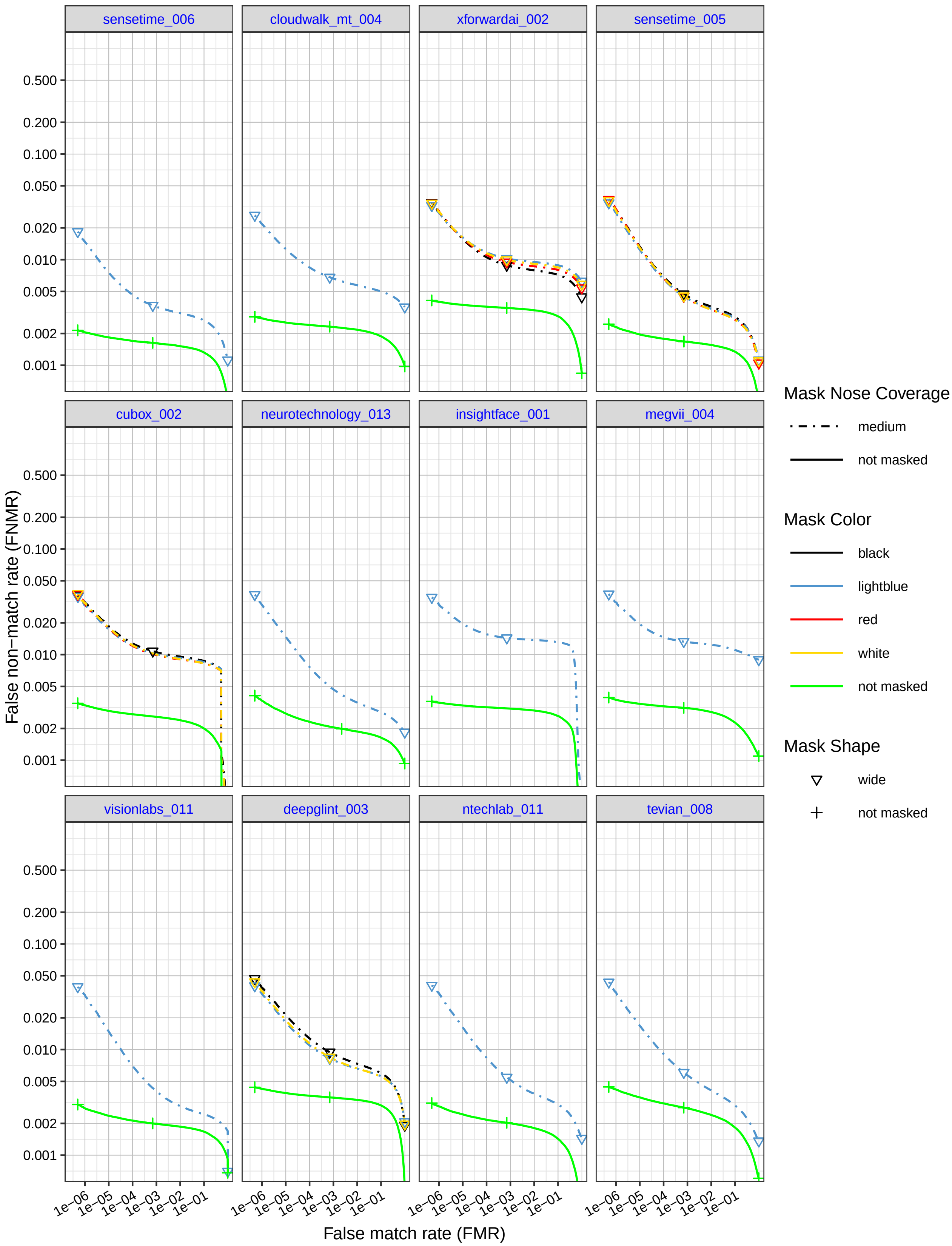

Figure 46: DET curves showing error rates on unmasked and masked probe images, broken out by mask color. Algorithms in black were submitted prior to mid-March 2020, and algorithms in blue were submitted thereafter.

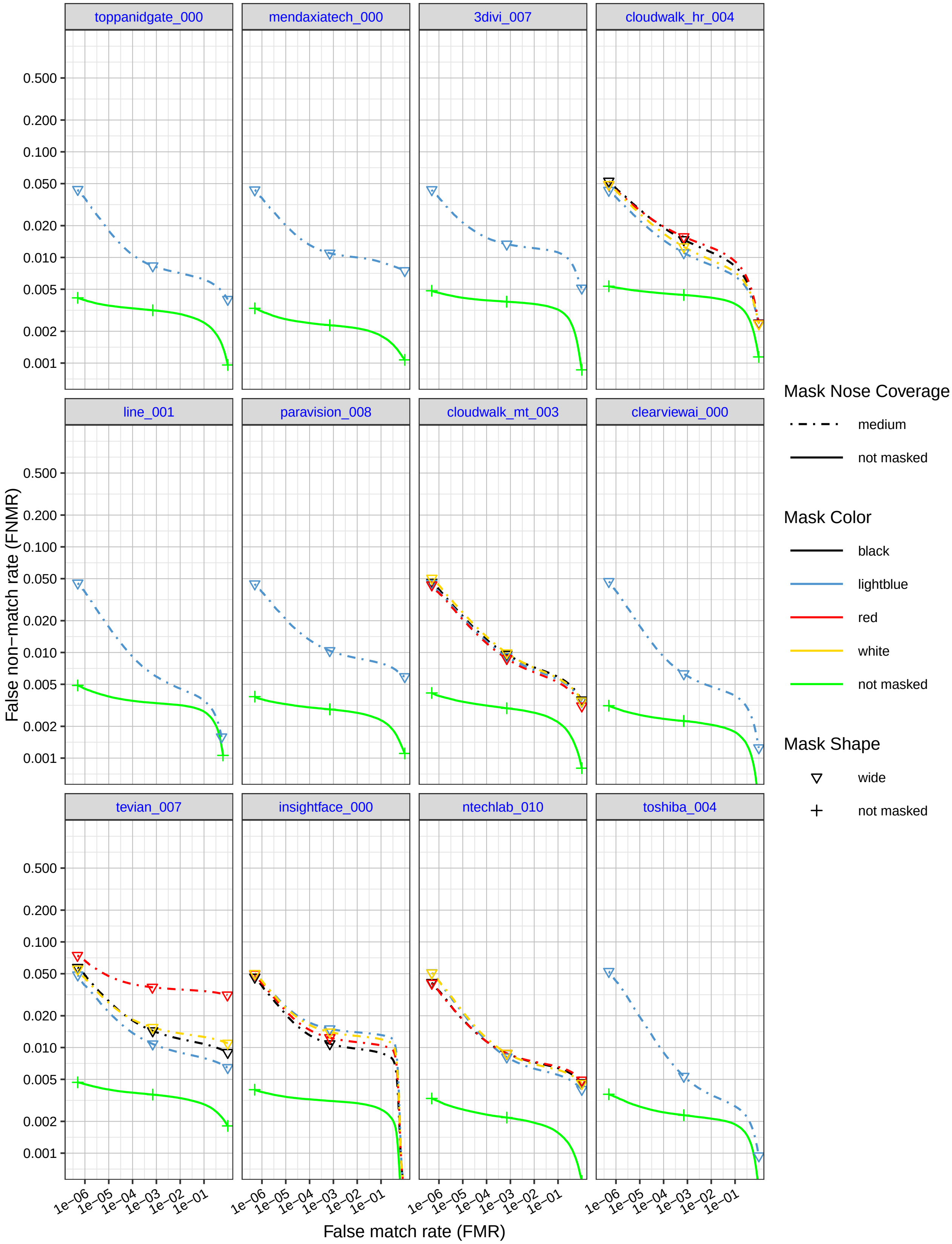

Figure 47: DET curves showing error rates on unmasked and masked probe images, broken out by mask color. Algorithms in black were submitted prior to mid-March 2020, and algorithms in blue were submitted thereafter.

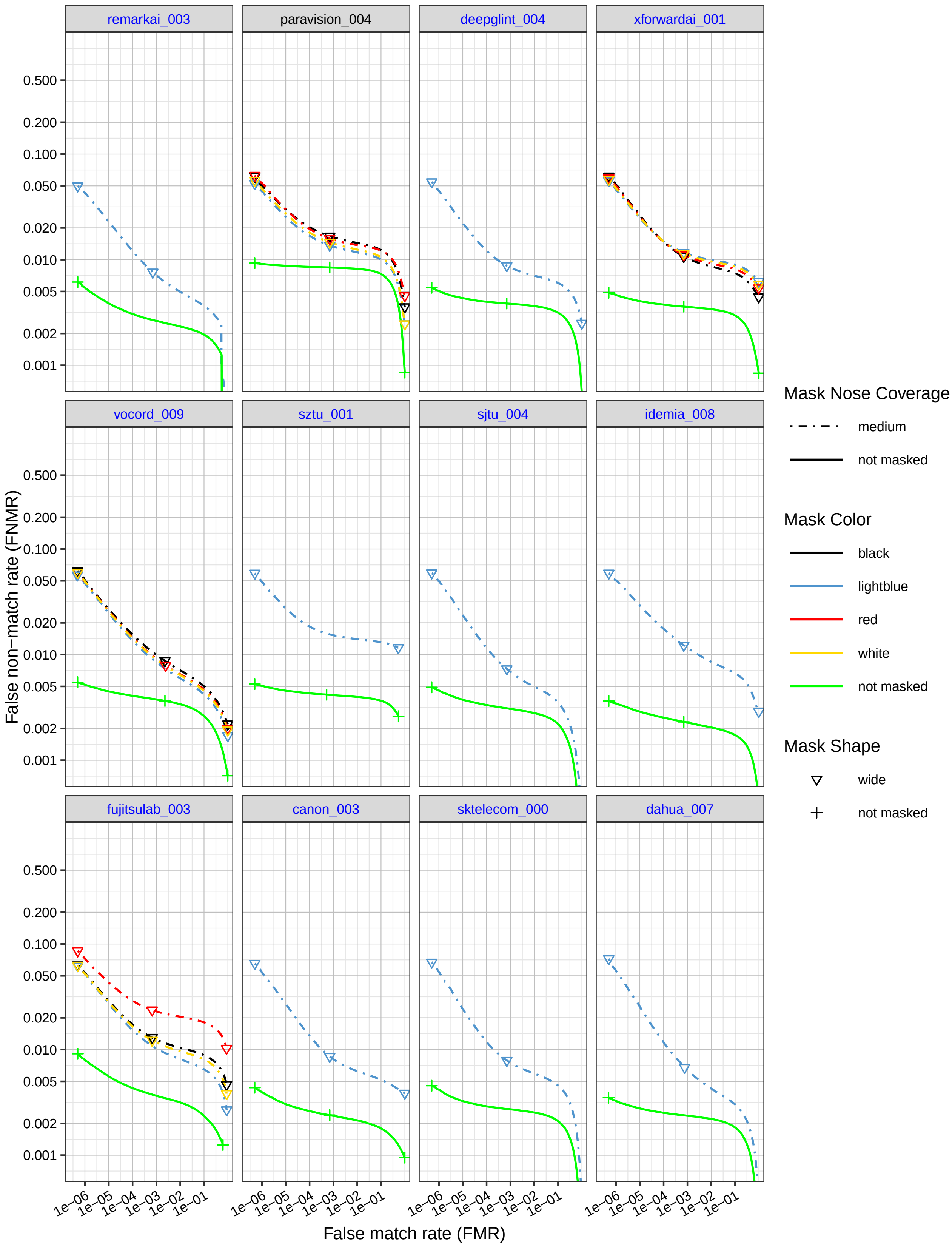

Figure 48: DET curves showing error rates on unmasked and masked probe images, broken out by mask color. Algorithms in black were submitted prior to mid-March 2020, and algorithms in blue were submitted thereafter.

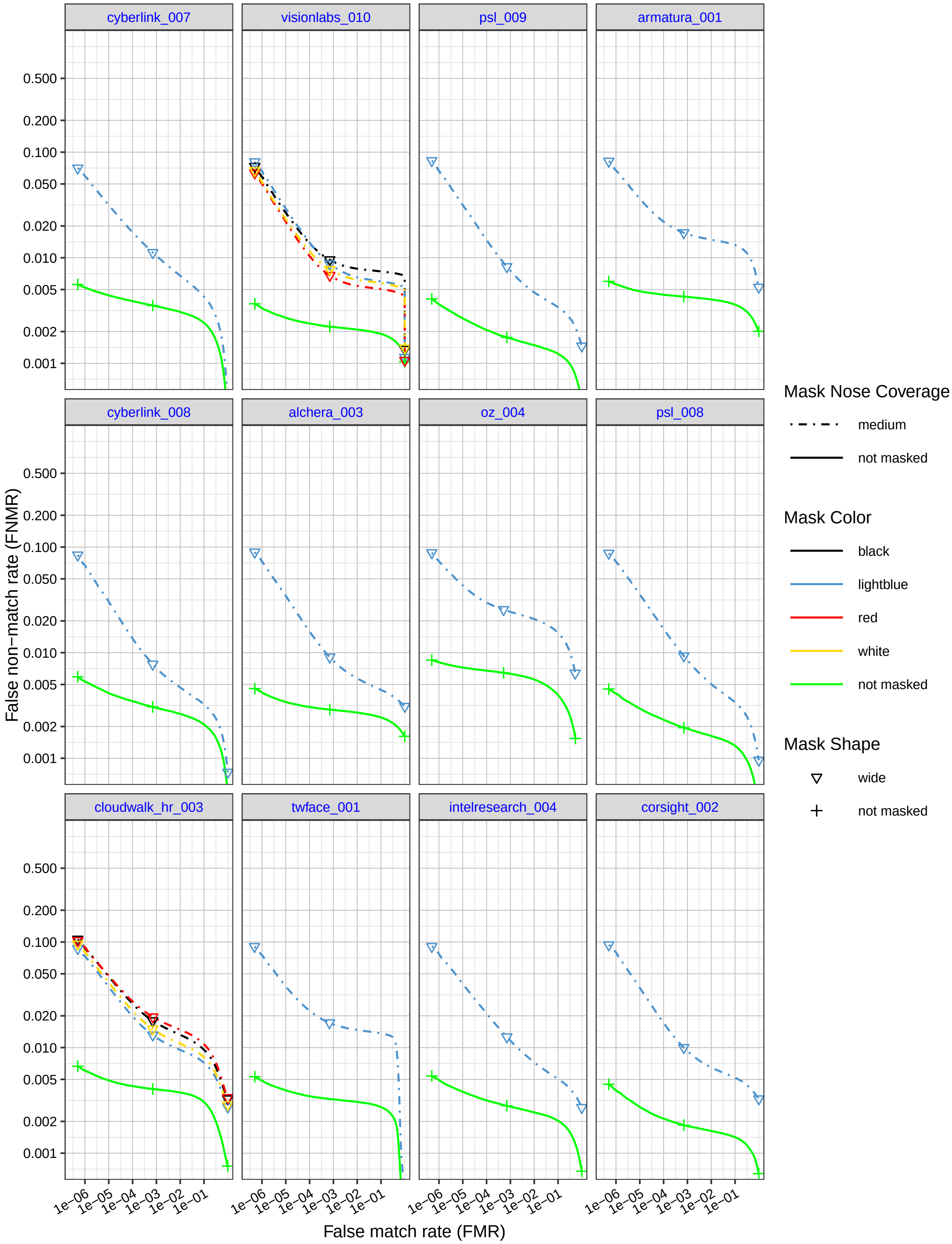

Figure 49: DET curves showing error rates on unmasked and masked probe images, broken out by mask color. Algorithms in black were submitted prior to mid-March 2020, and algorithms in blue were submitted thereafter.

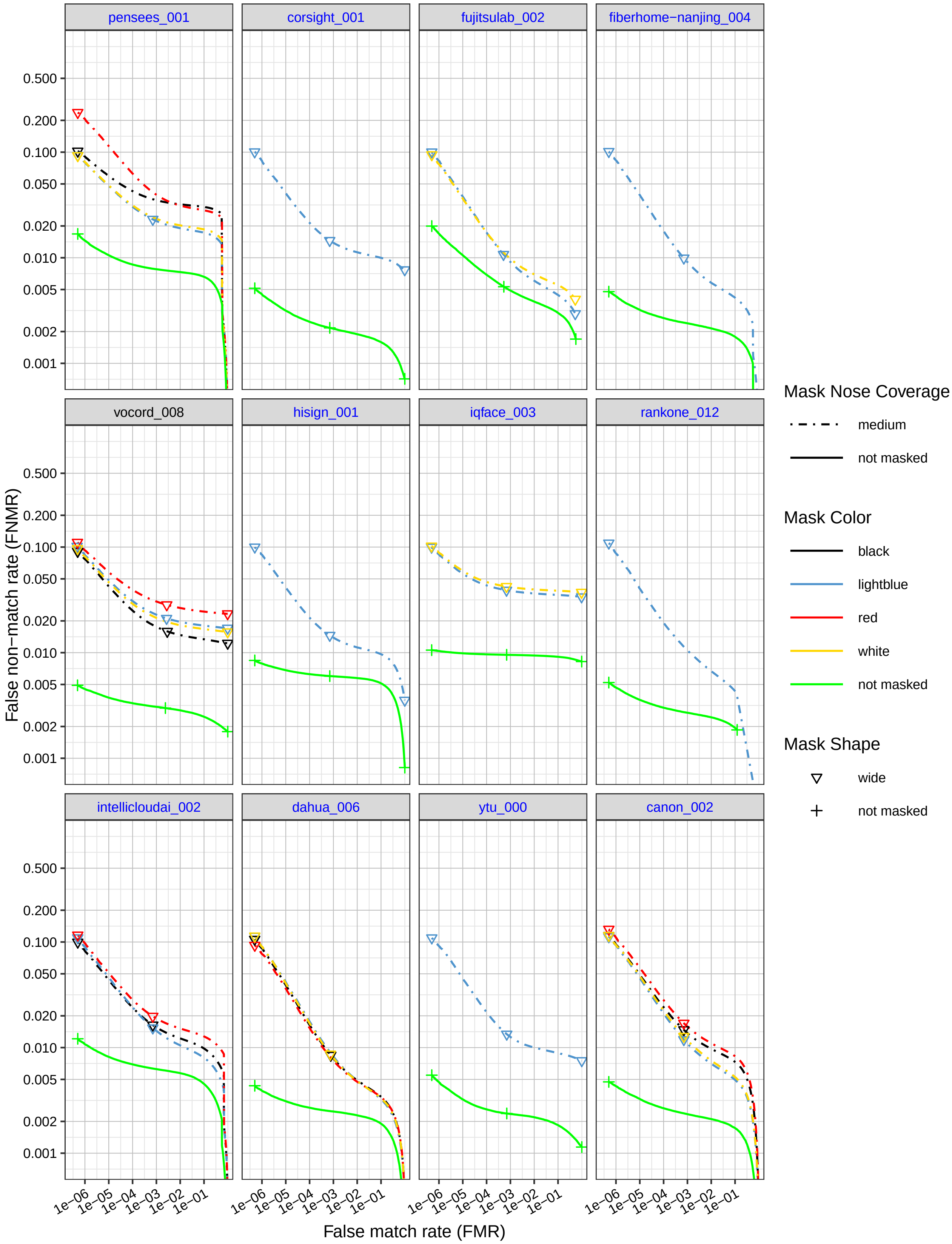

Figure 50: DET curves showing error rates on unmasked and masked probe images, broken out by mask color. Algorithms in black were submitted prior to mid-March 2020, and algorithms in blue were submitted thereafter.

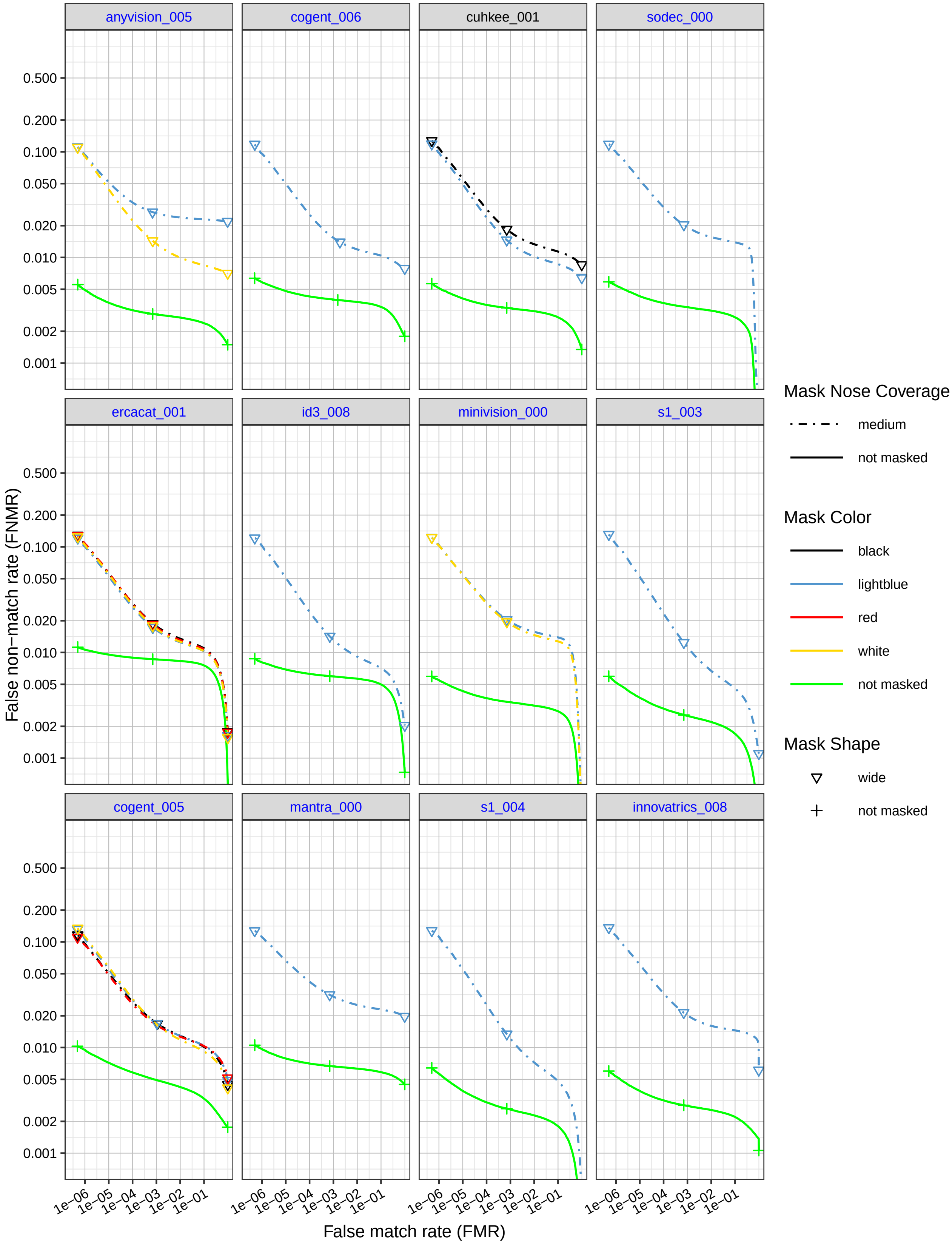

Figure 51: DET curves showing error rates on unmasked and masked probe images, broken out by mask color. Algorithms in black were submitted prior to mid-March 2020, and algorithms in blue were submitted thereafter.

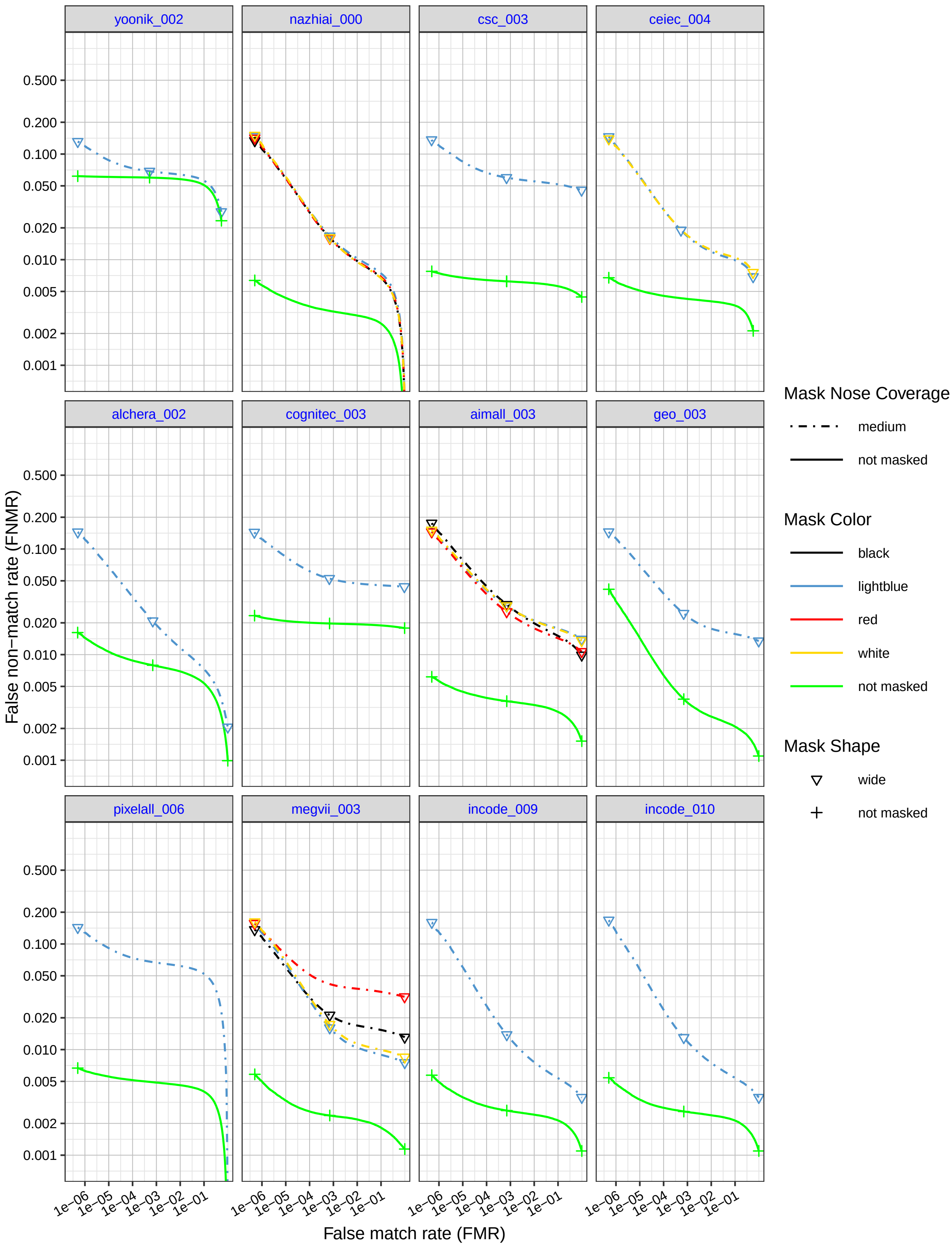

Figure 52: DET curves showing error rates on unmasked and masked probe images, broken out by mask color. Algorithms in black were submitted prior to mid-March 2020, and algorithms in blue were submitted thereafter.

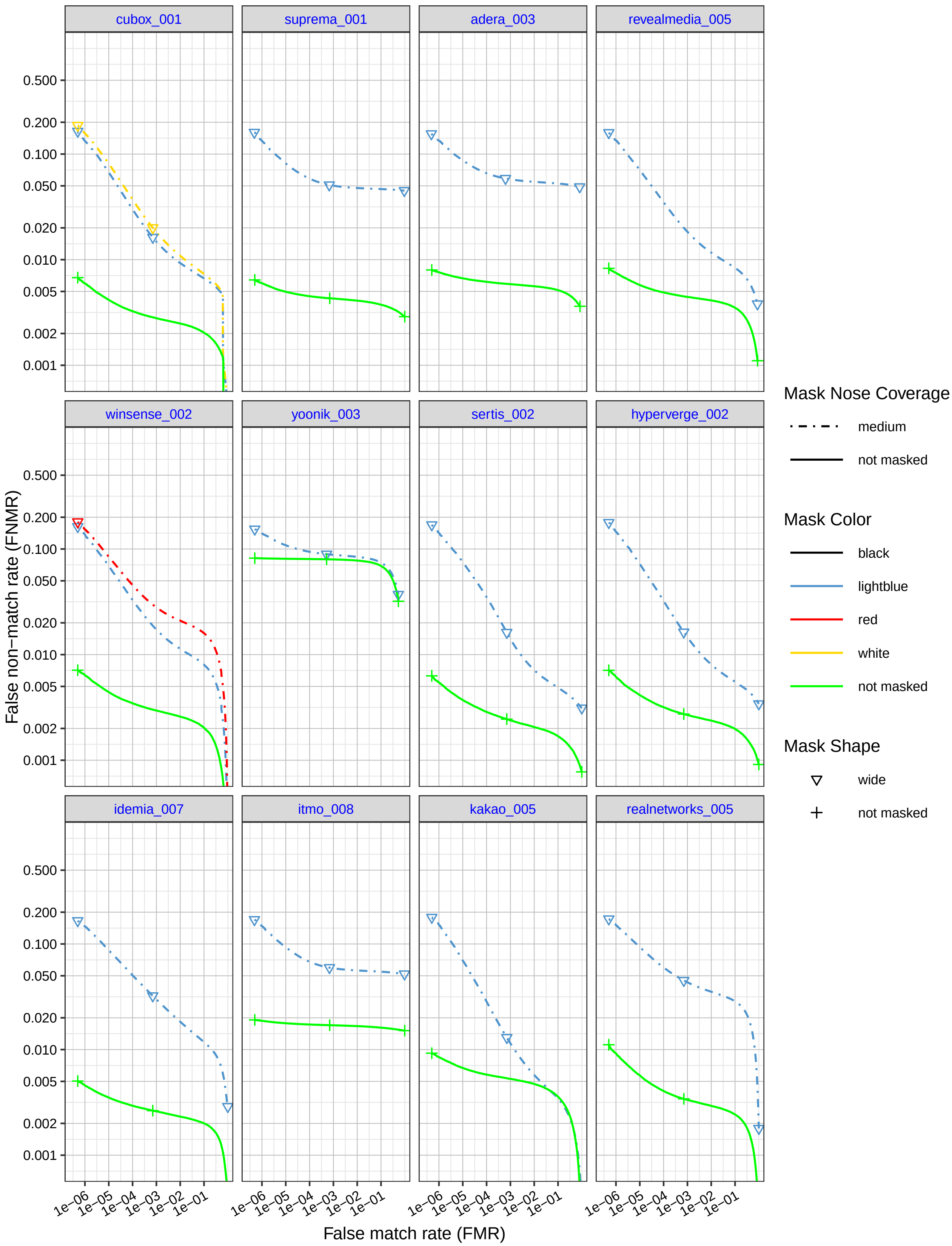

Figure 53: DET curves showing error rates on unmasked and masked probe images, broken out by mask color. Algorithms in black were submitted prior to mid-March 2020, and algorithms in blue were submitted thereafter.

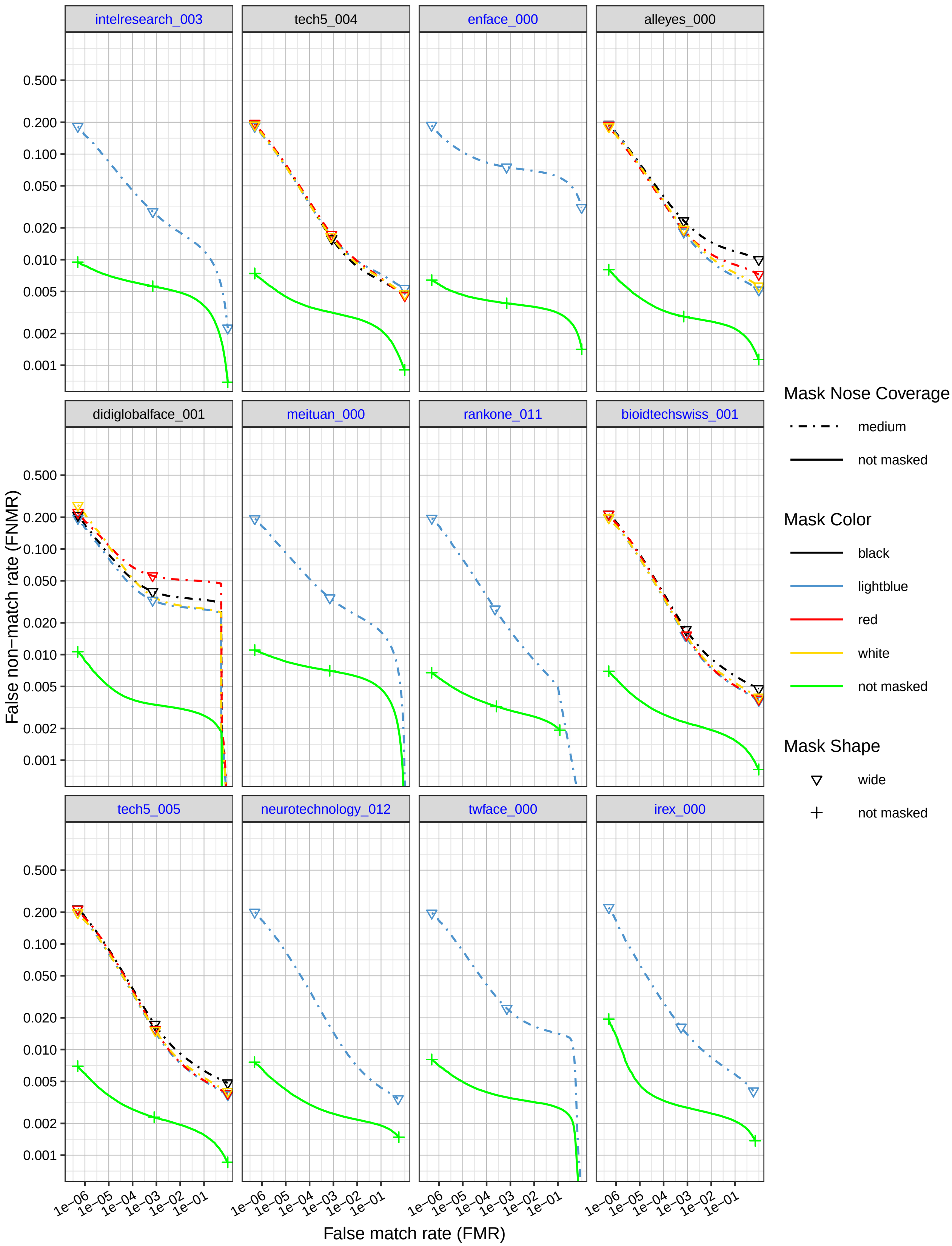

Figure 54: DET curves showing error rates on unmasked and masked probe images, broken out by mask color. Algorithms in black were submitted prior to mid-March 2020, and algorithms in blue were submitted thereafter.

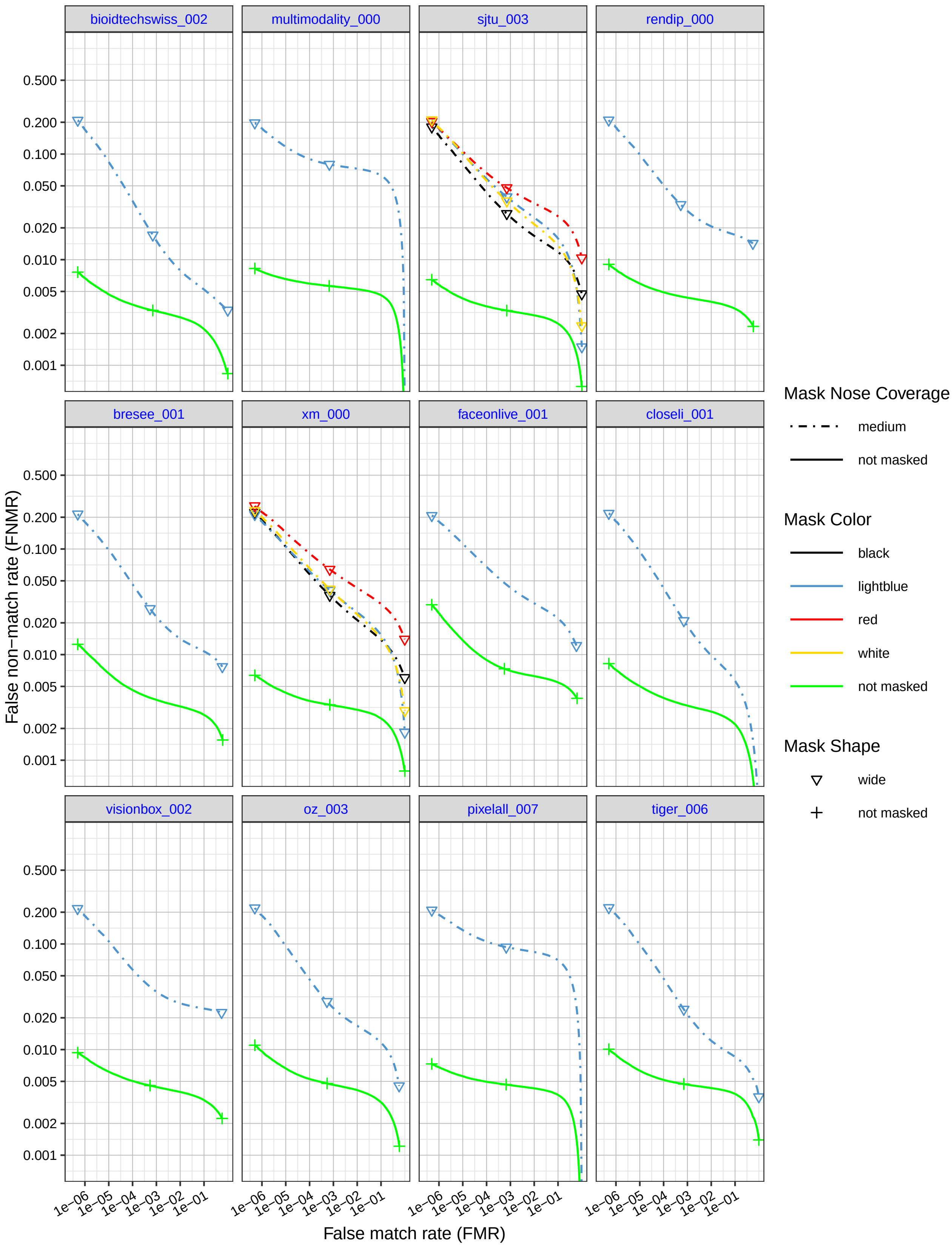

Figure 55: DET curves showing error rates on unmasked and masked probe images, broken out by mask color. Algorithms in black were submitted prior to mid-March 2020, and algorithms in blue were submitted thereafter.

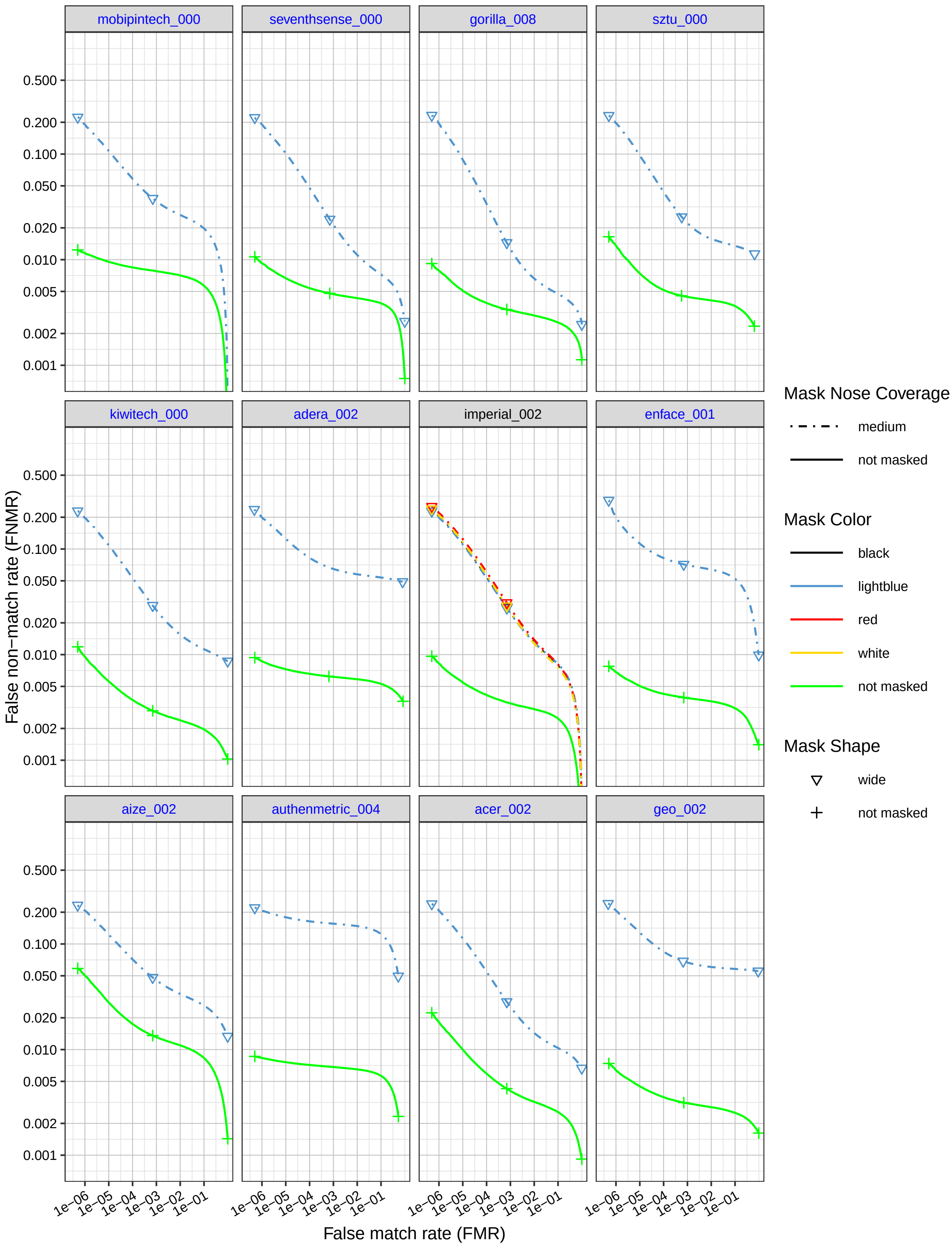

Figure 56: DET curves showing error rates on unmasked and masked probe images, broken out by mask color. Algorithms in black were submitted prior to mid-March 2020, and algorithms in blue were submitted thereafter.

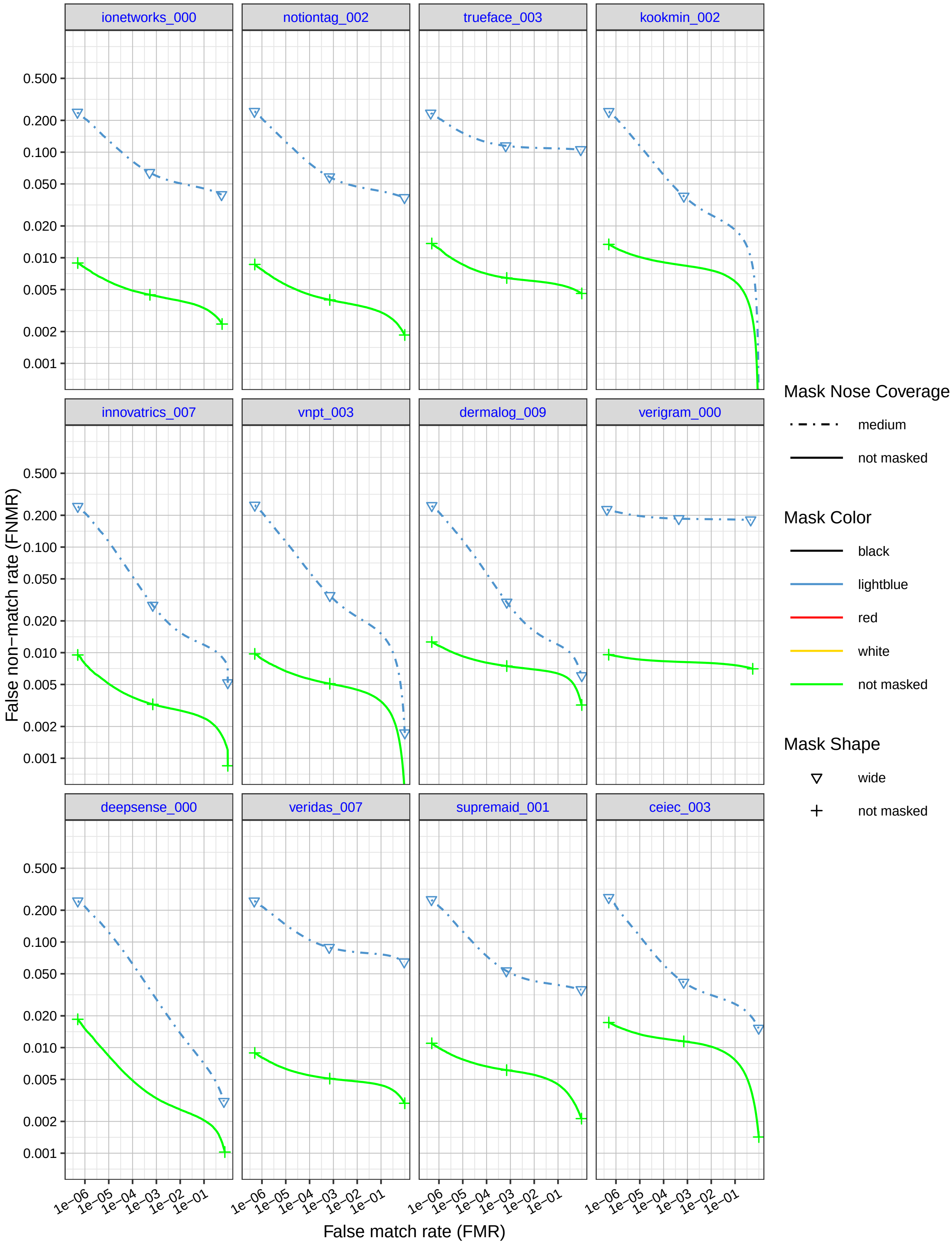

Figure 57: DET curves showing error rates on unmasked and masked probe images, broken out by mask color. Algorithms in black were submitted prior to mid-March 2020, and algorithms in blue were submitted thereafter.

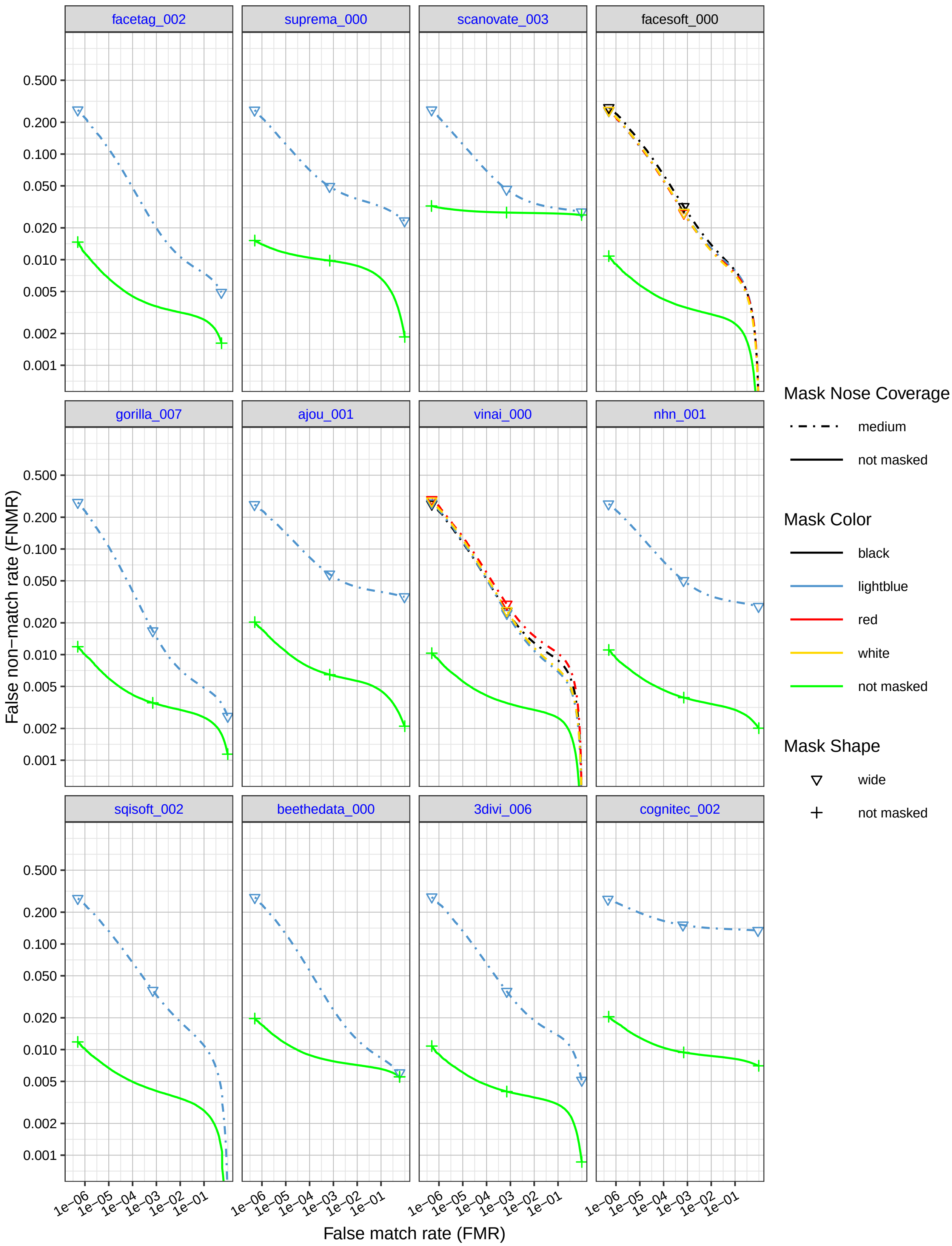

Figure 58: DET curves showing error rates on unmasked and masked probe images, broken out by mask color. Algorithms in black were submitted prior to mid-March 2020, and algorithms in blue were submitted thereafter.

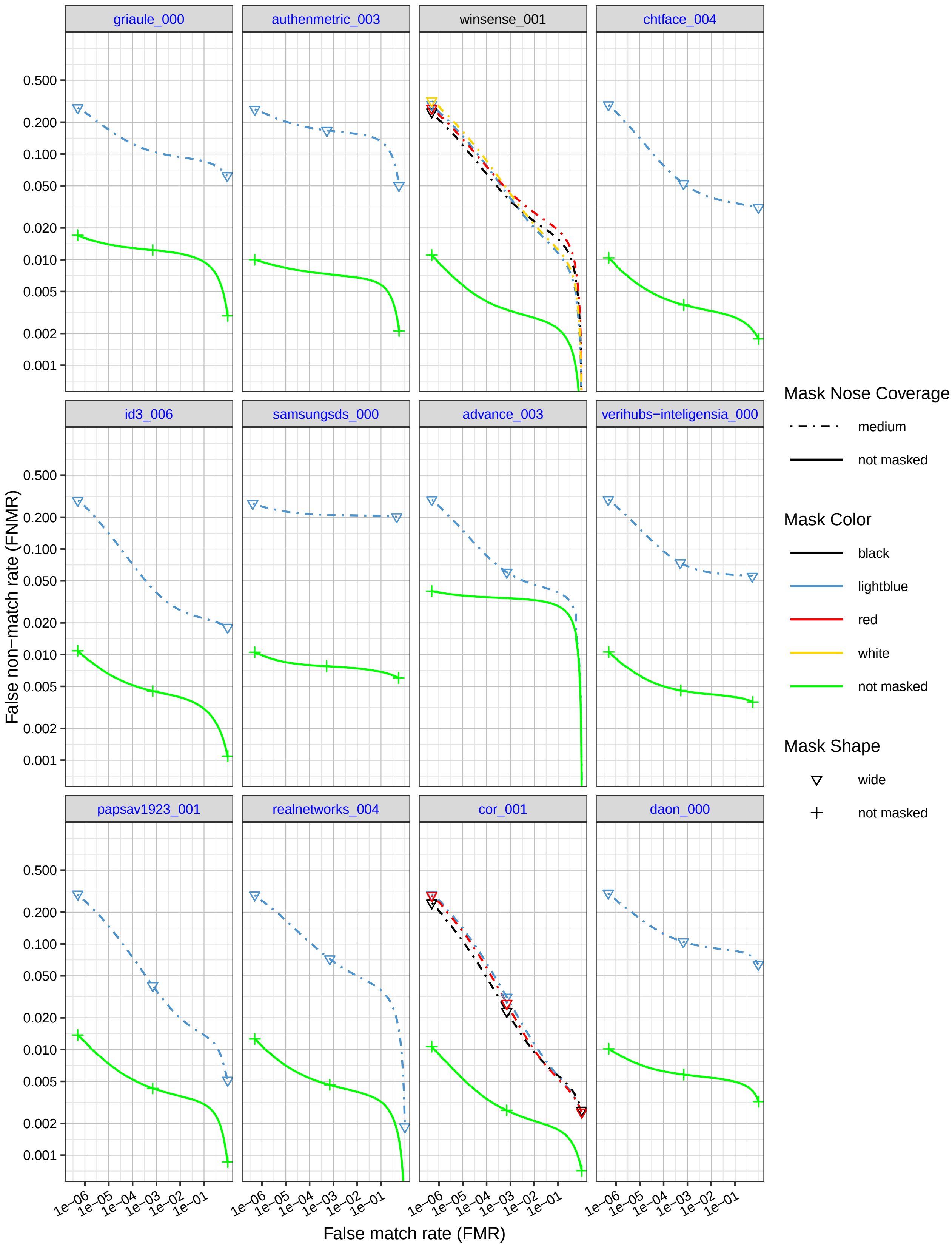

Figure 59: DET curves showing error rates on unmasked and masked probe images, broken out by mask color. Algorithms in black were submitted prior to mid-March 2020, and algorithms in blue were submitted thereafter.

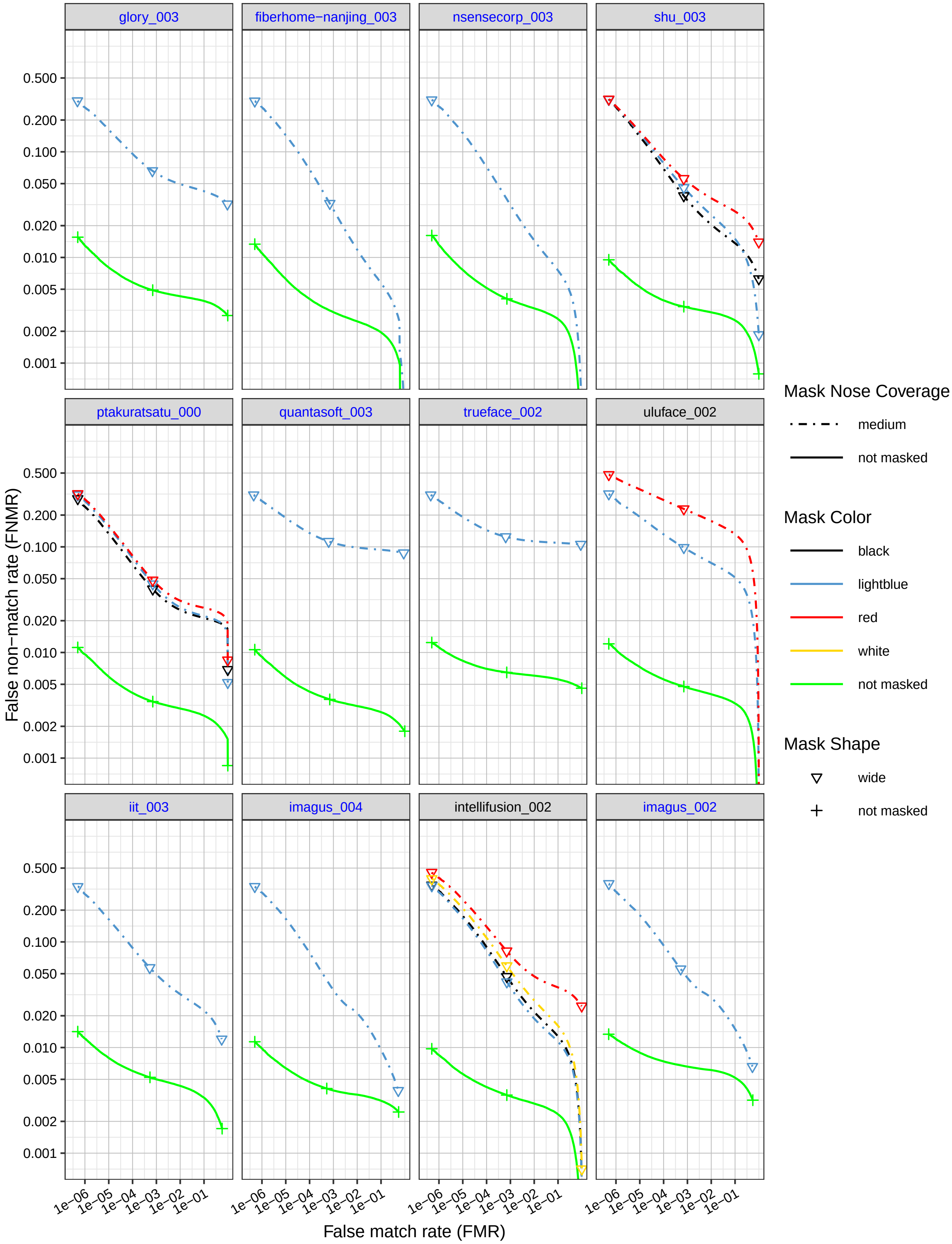

Figure 60: DET curves showing error rates on unmasked and masked probe images, broken out by mask color. Algorithms in black were submitted prior to mid-March 2020, and algorithms in blue were submitted thereafter.

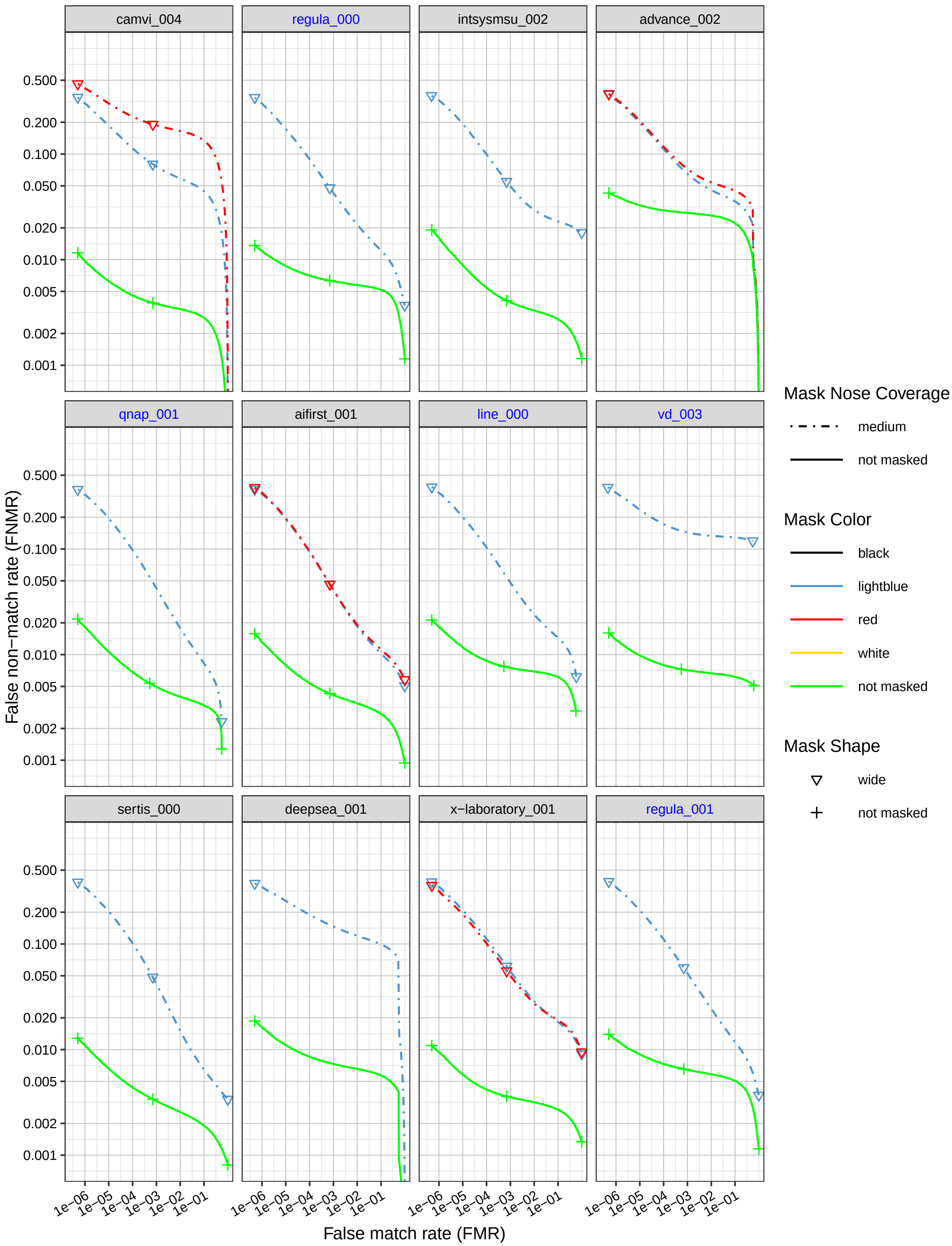

Figure 61: DET curves showing error rates on unmasked and masked probe images, broken out by mask color. Algorithms in black were submitted prior to mid-March 2020, and algorithms in blue were submitted thereafter.

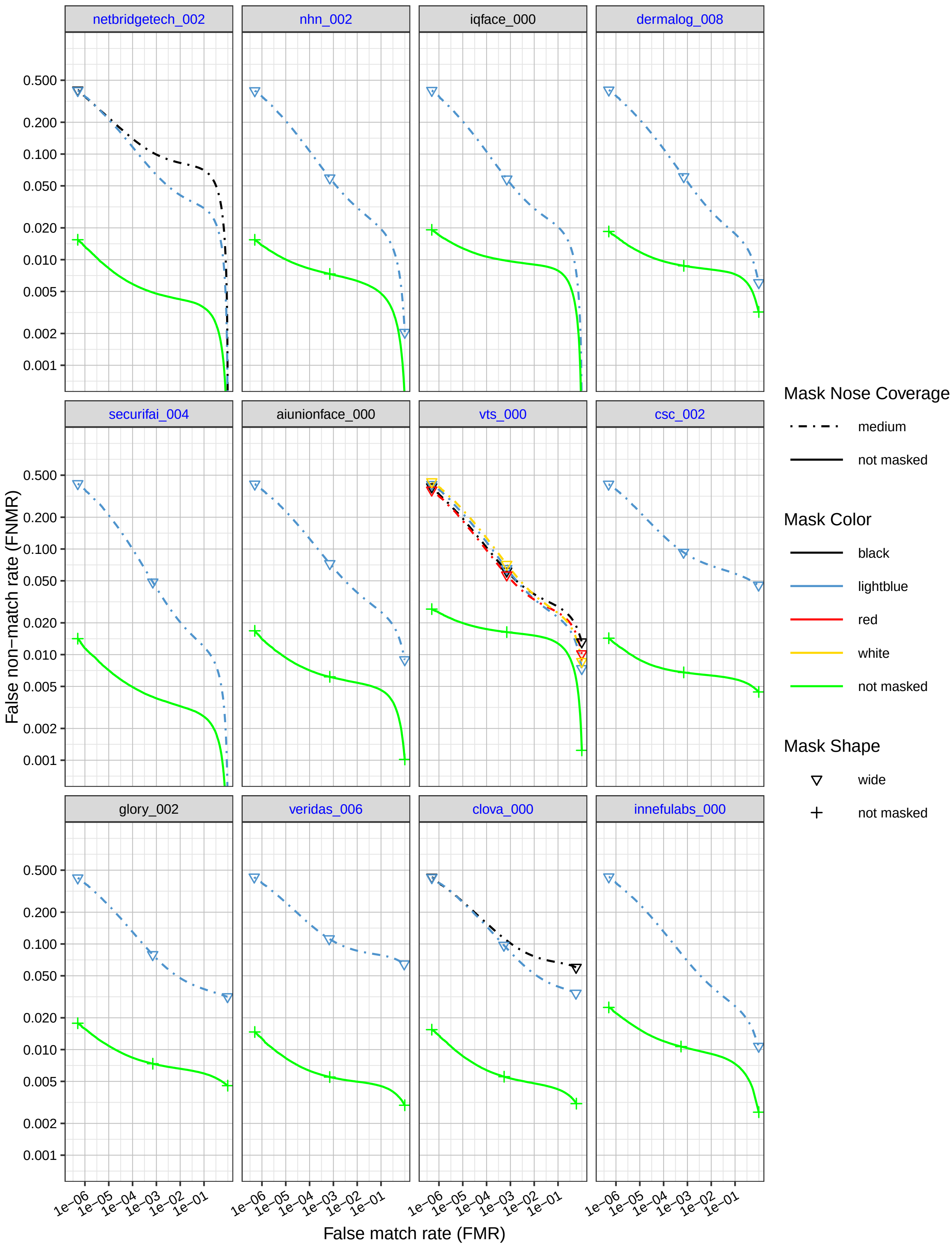

Figure 62: DET curves showing error rates on unmasked and masked probe images, broken out by mask color. Algorithms in black were submitted prior to mid-March 2020, and algorithms in blue were submitted thereafter.

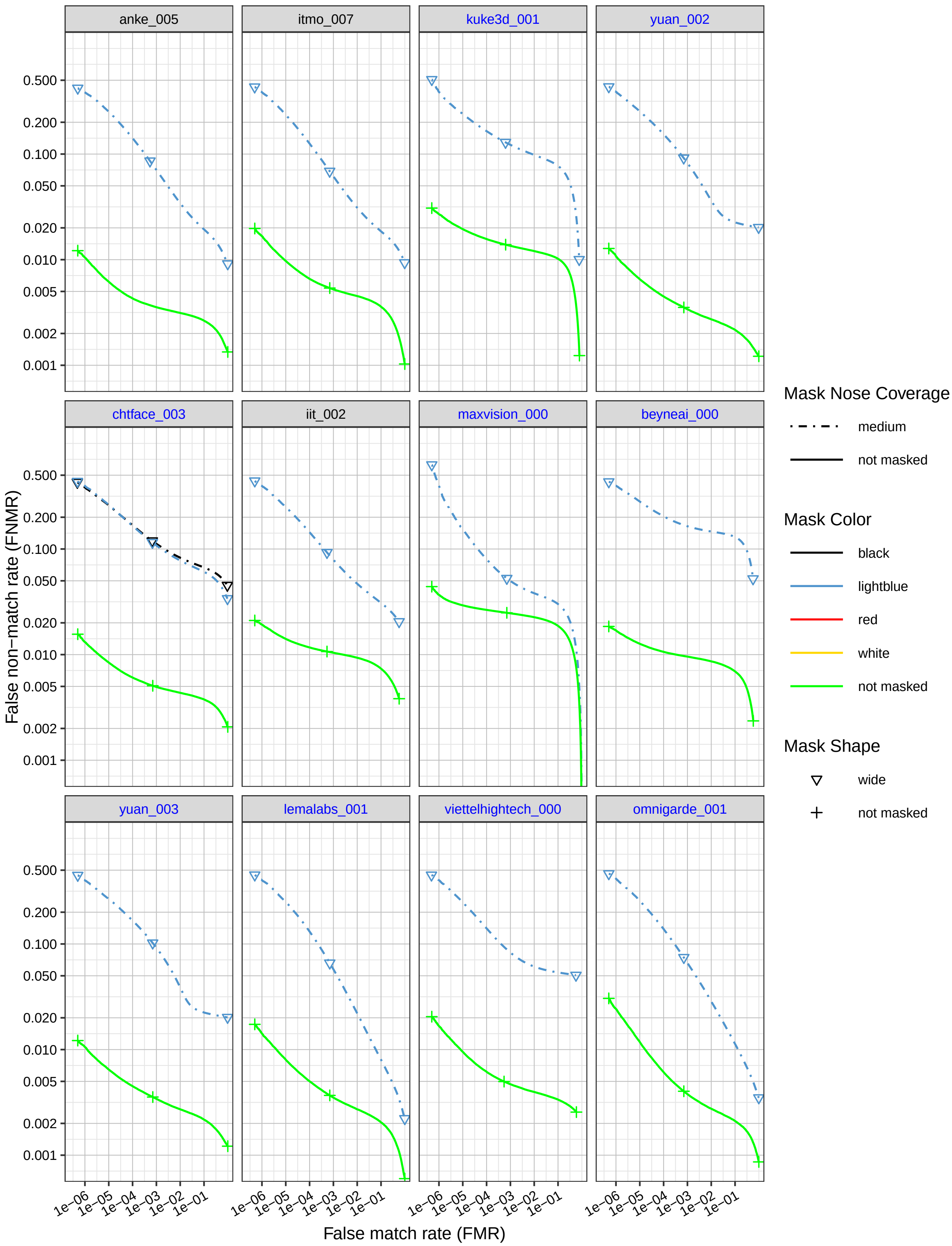

Figure 63: DET curves showing error rates on unmasked and masked probe images, broken out by mask color. Algorithms in black were submitted prior to mid-March 2020, and algorithms in blue were submitted thereafter.

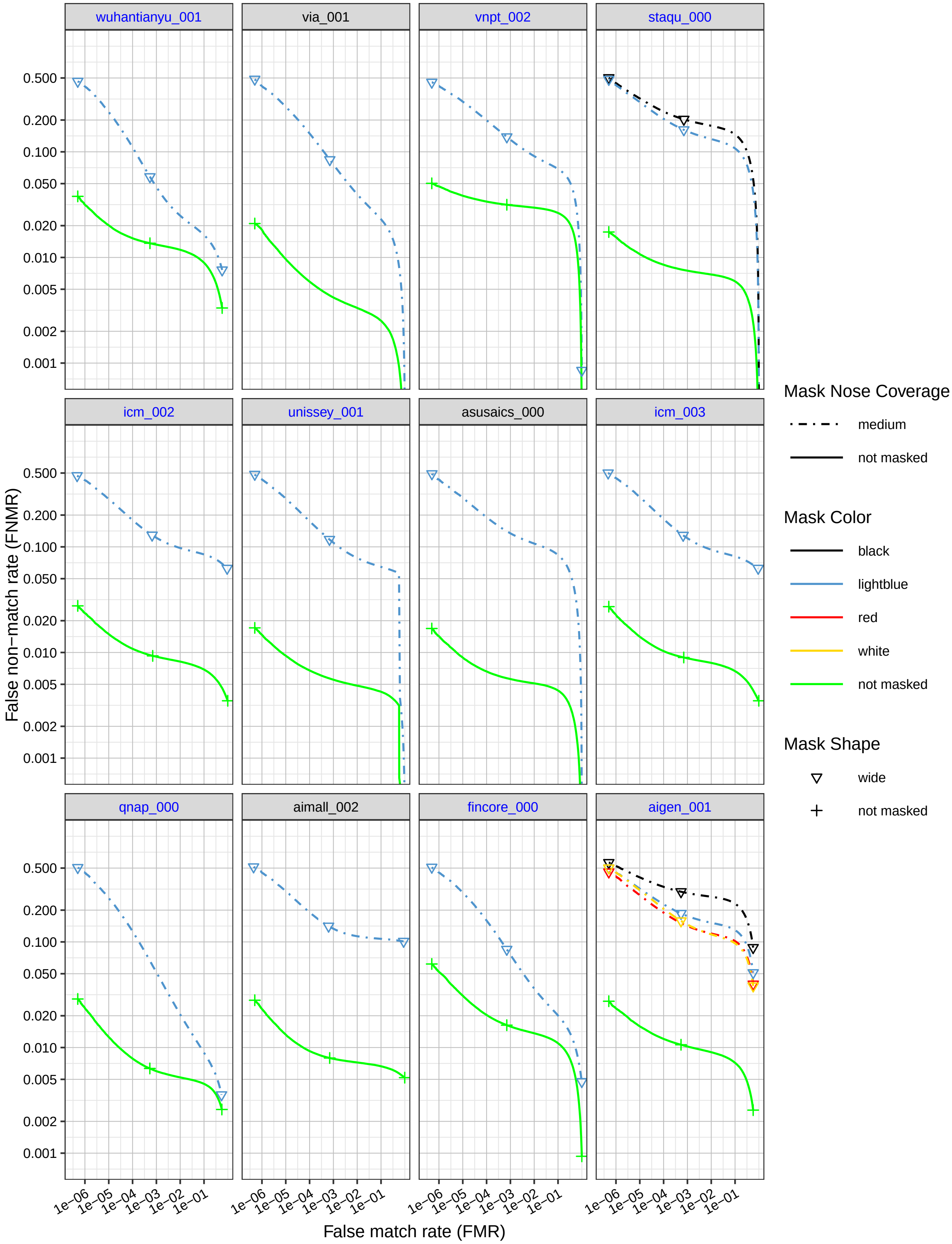

Figure 64: DET curves showing error rates on unmasked and masked probe images, broken out by mask color. Algorithms in black were submitted prior to mid-March 2020, and algorithms in blue were submitted thereafter.

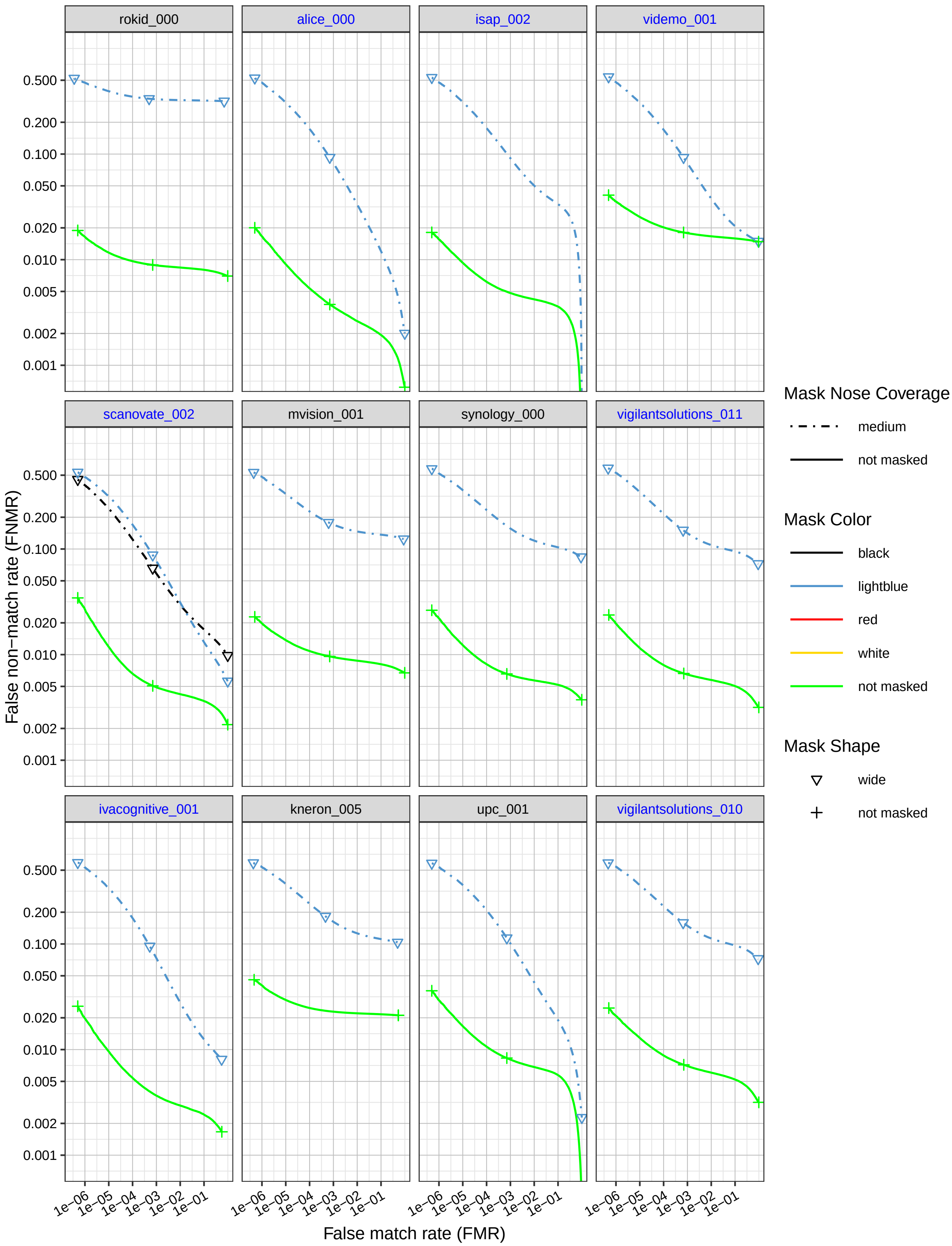

Figure 65: DET curves showing error rates on unmasked and masked probe images, broken out by mask color. Algorithms in black were submitted prior to mid-March 2020, and algorithms in blue were submitted thereafter.

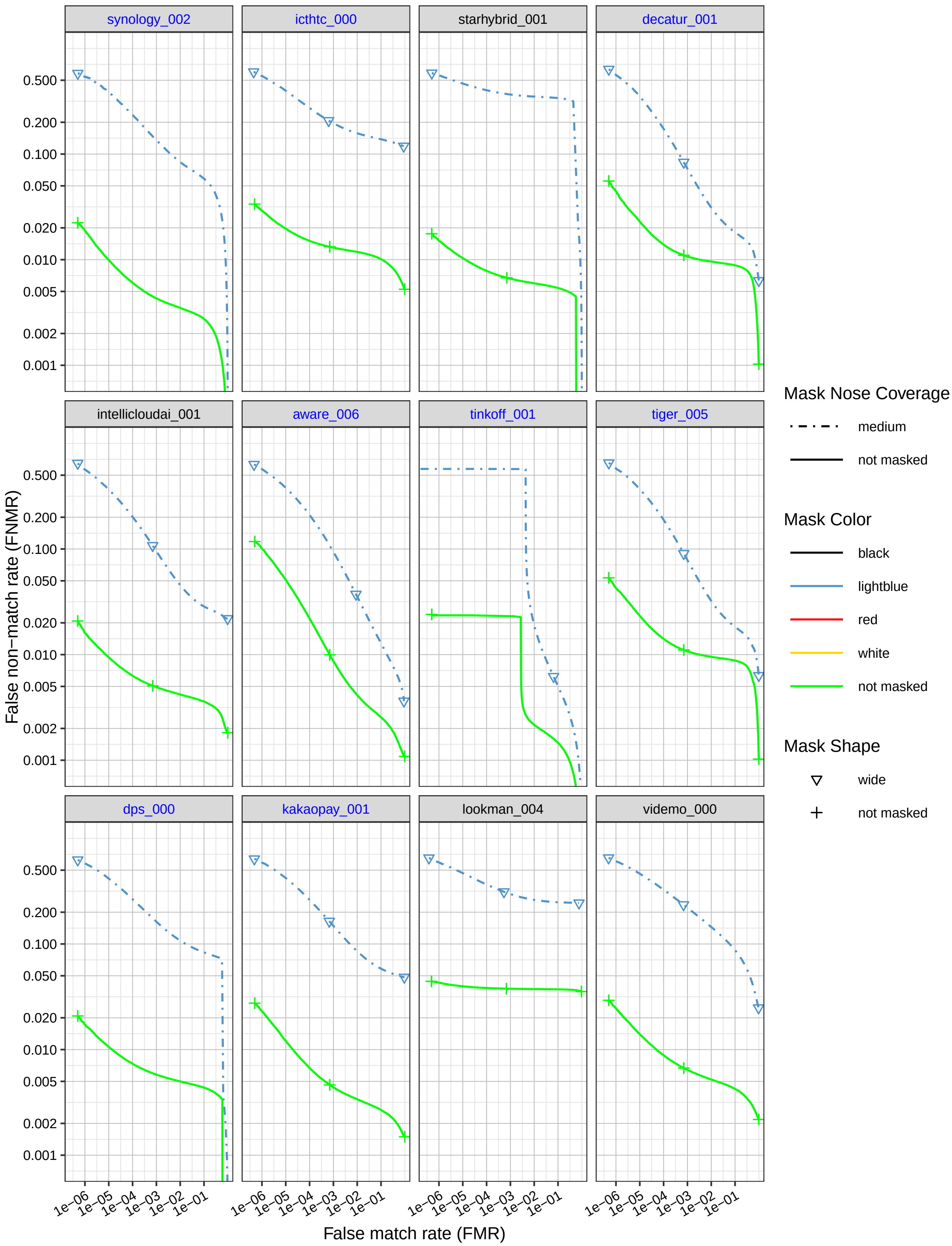

Figure 66: DET curves showing error rates on unmasked and masked probe images, broken out by mask color. Algorithms in black were submitted prior to mid-March 2020, and algorithms in blue were submitted thereafter.

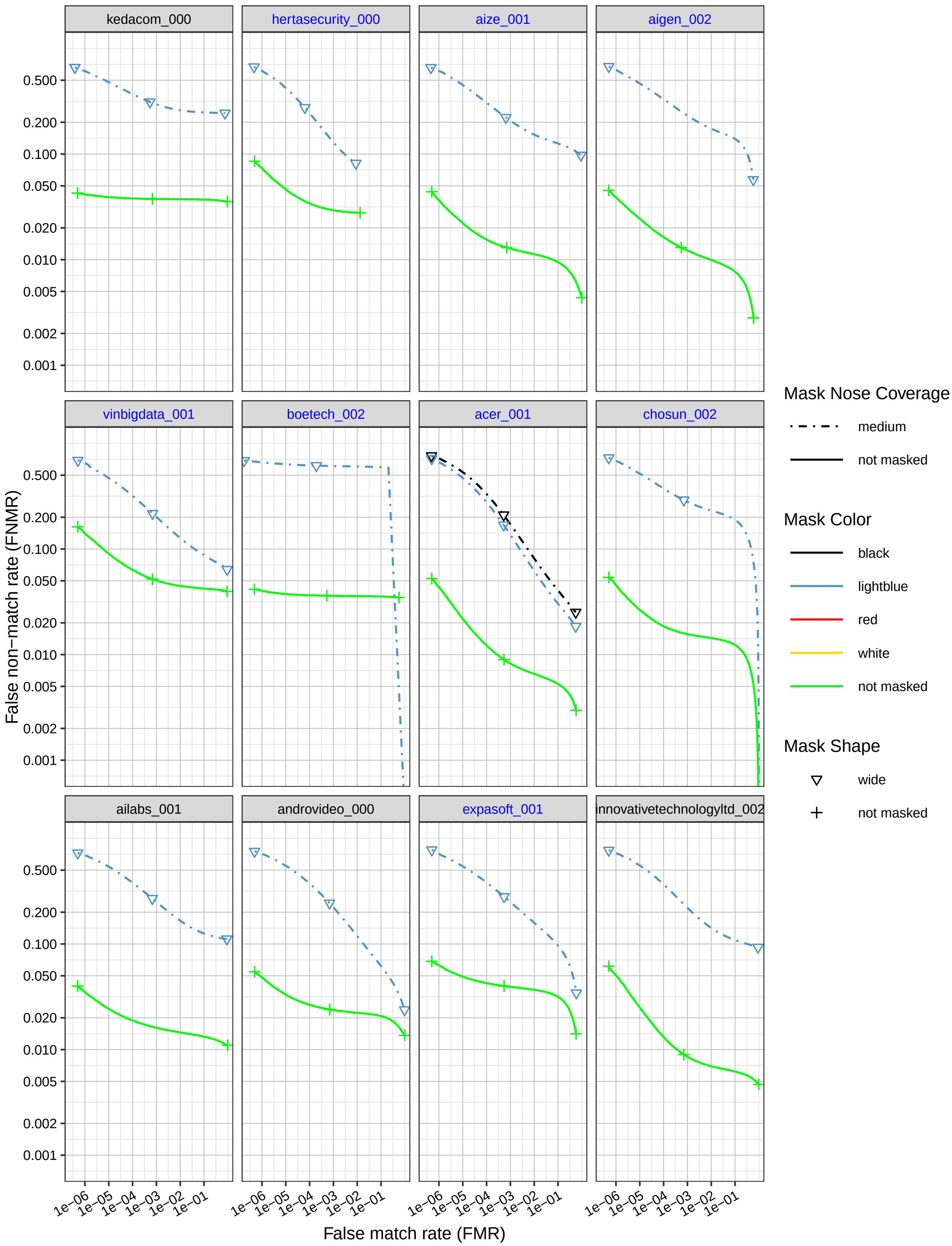

Figure 67: DET curves showing error rates on unmasked and masked probe images, broken out by mask color. Algorithms in black were submitted prior to mid-March 2020, and algorithms in blue were submitted thereafter.

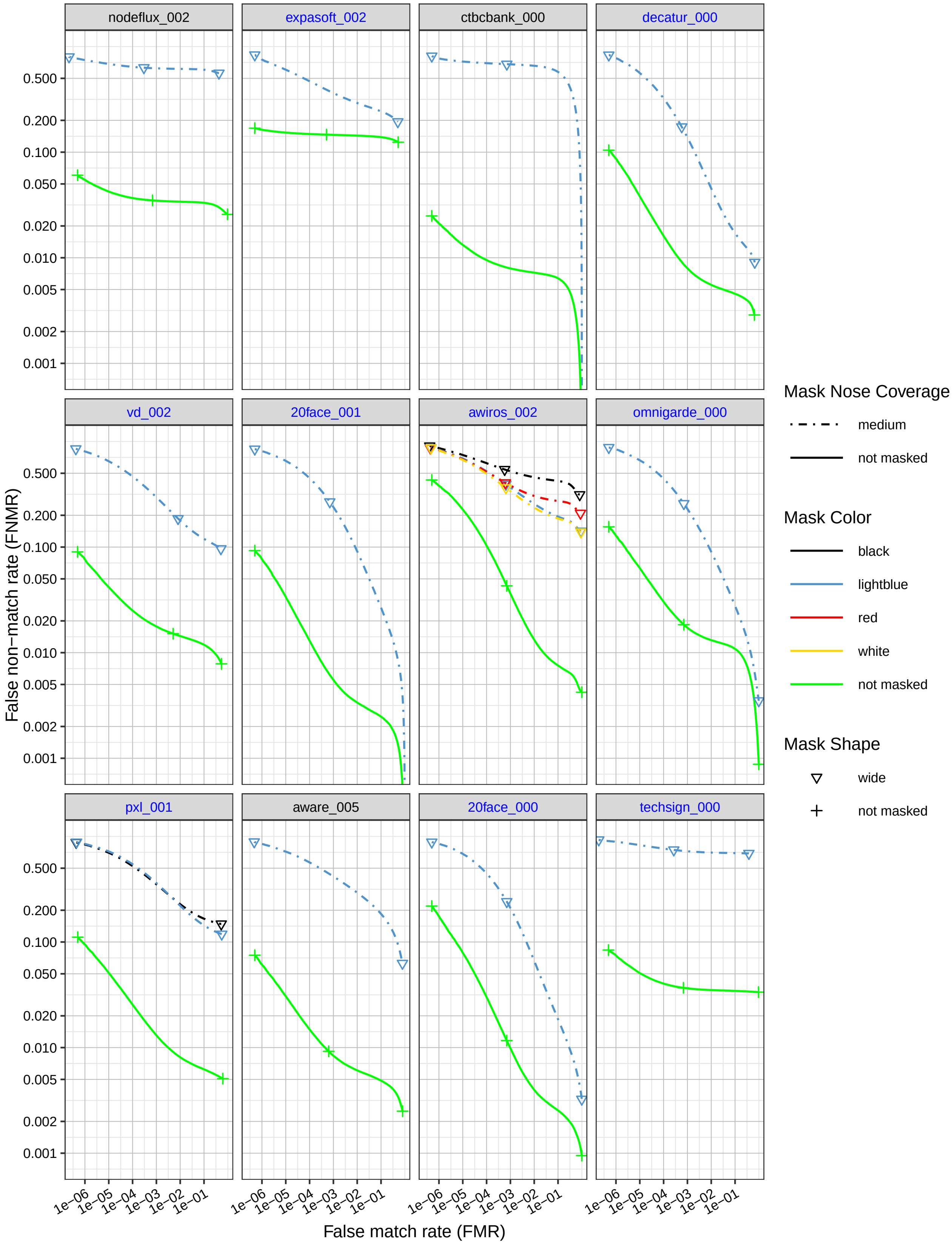

Figure 68: DET curves showing error rates on unmasked and masked probe images, broken out by mask color. Algorithms in black were submitted prior to mid-March 2020, and algorithms in blue were submitted thereafter.

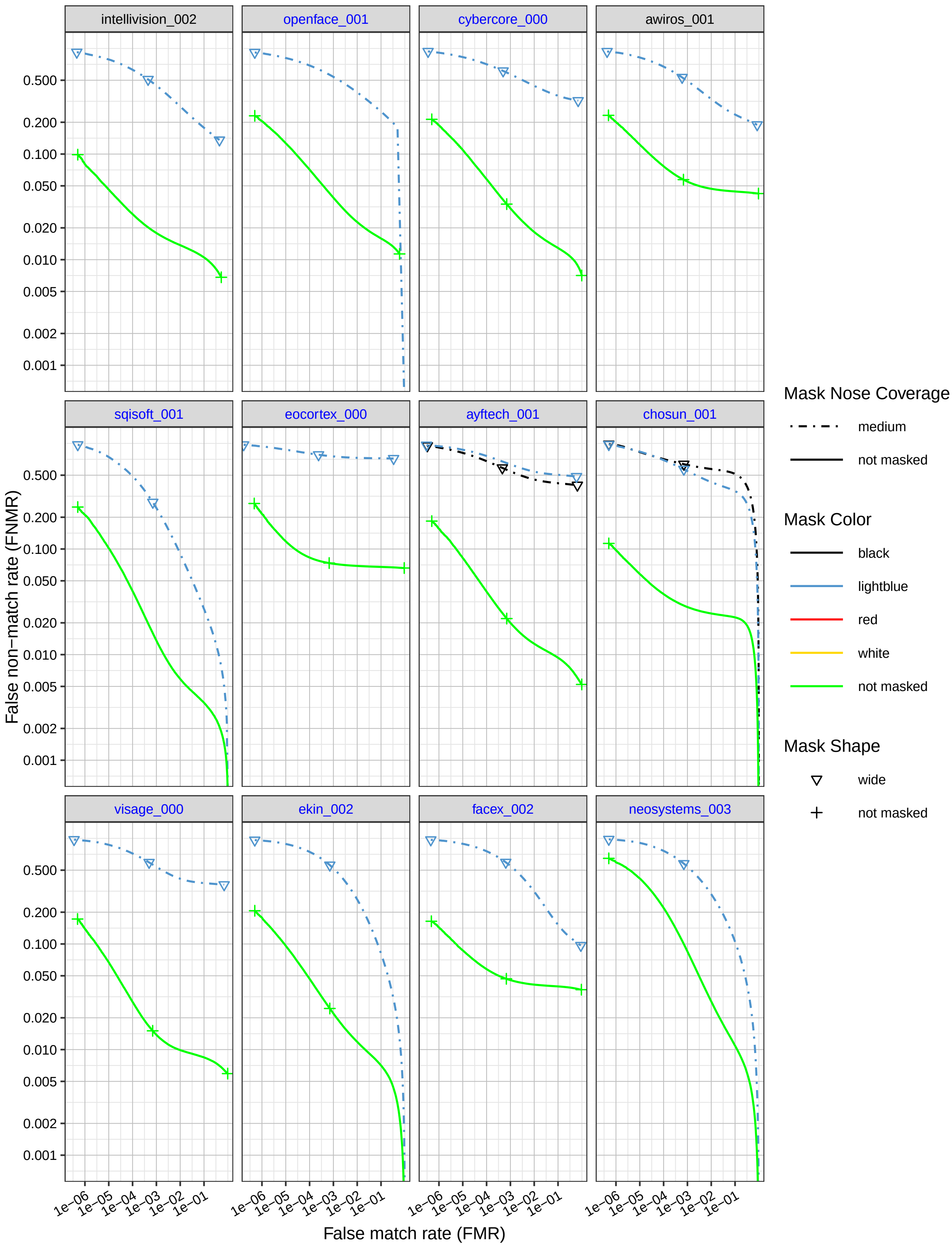

Figure 69: DET curves showing error rates on unmasked and masked probe images, broken out by mask color. Algorithms in black were submitted prior to mid-March 2020, and algorithms in blue were submitted thereafter.

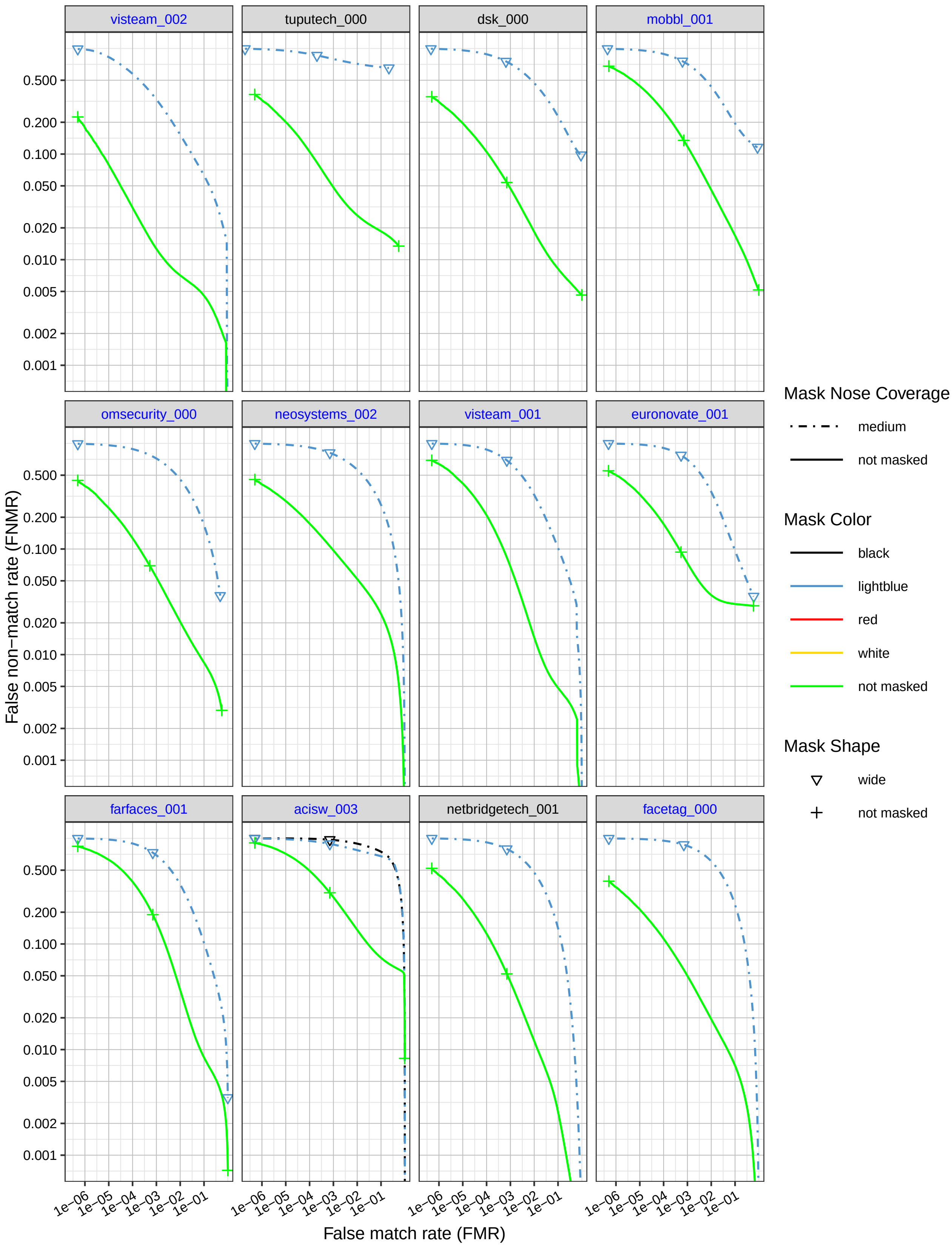

Figure 70: DET curves showing error rates on unmasked and masked probe images, broken out by mask color. Algorithms in black were submitted prior to mid-March 2020, and algorithms in blue were submitted thereafter.

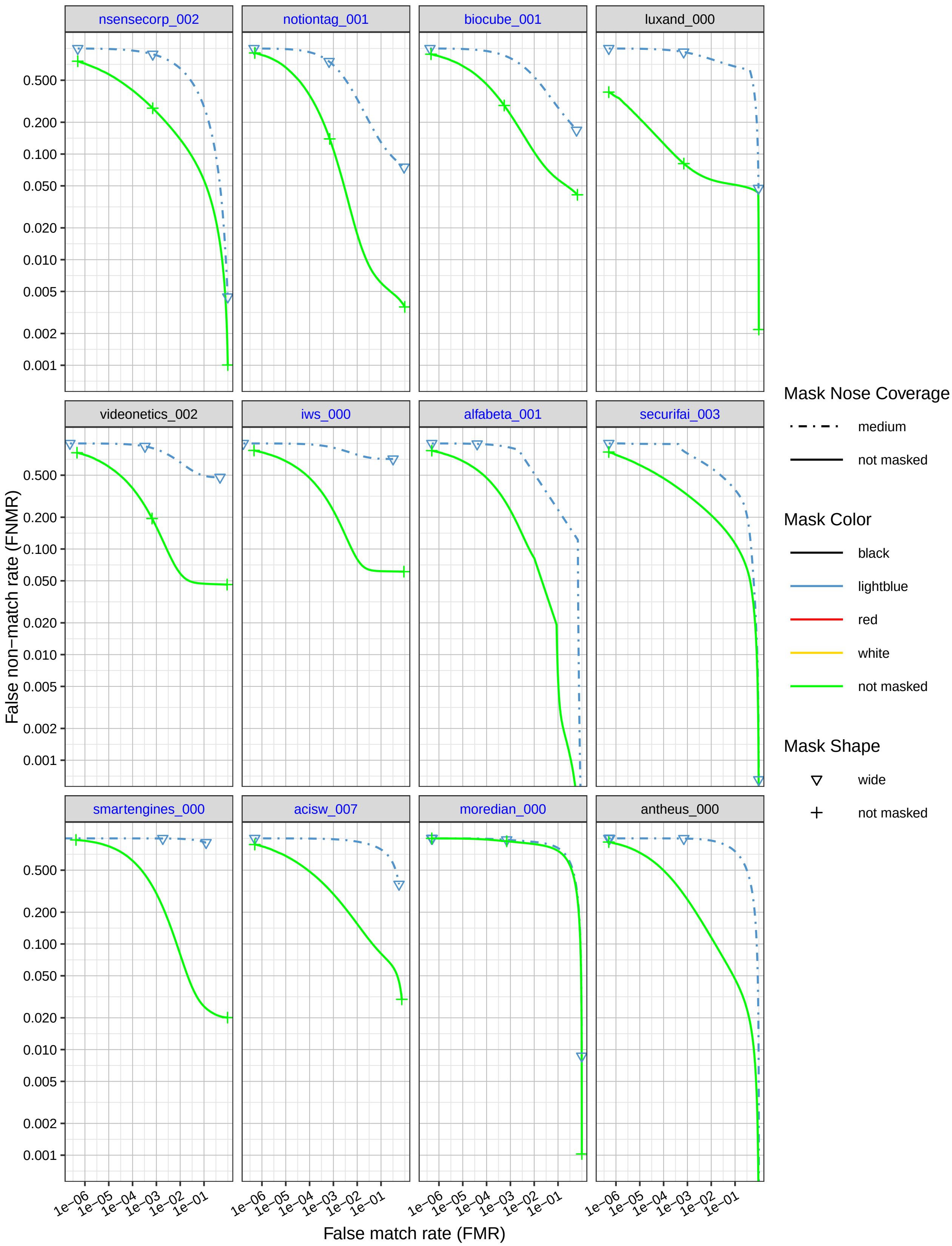

Figure 71: DET curves showing error rates on unmasked and masked probe images, broken out by mask color. Algorithms in black were submitted prior to mid-March 2020, and algorithms in blue were submitted thereafter.

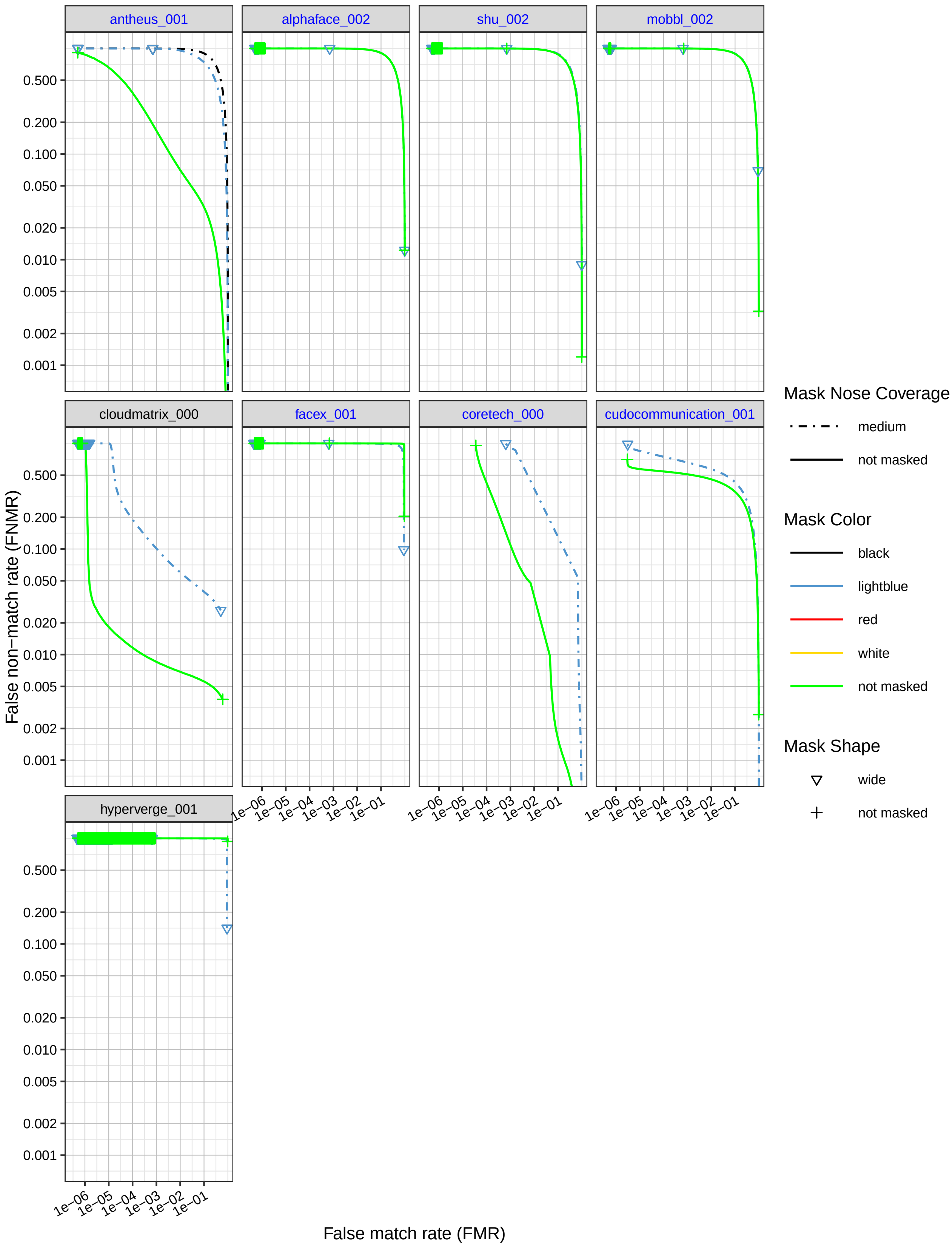

Figure 72: DET curves showing error rates on unmasked and masked probe images, broken out by mask color. Algorithms in black were submitted prior to mid-March 2020, and algorithms in blue were submitted thereafter.

The following plots show the explicit dependence of false non-match rate (FNMR) and false match rate (FMR) on score threshold for each algorithm, across different masked/unmasked combinations.

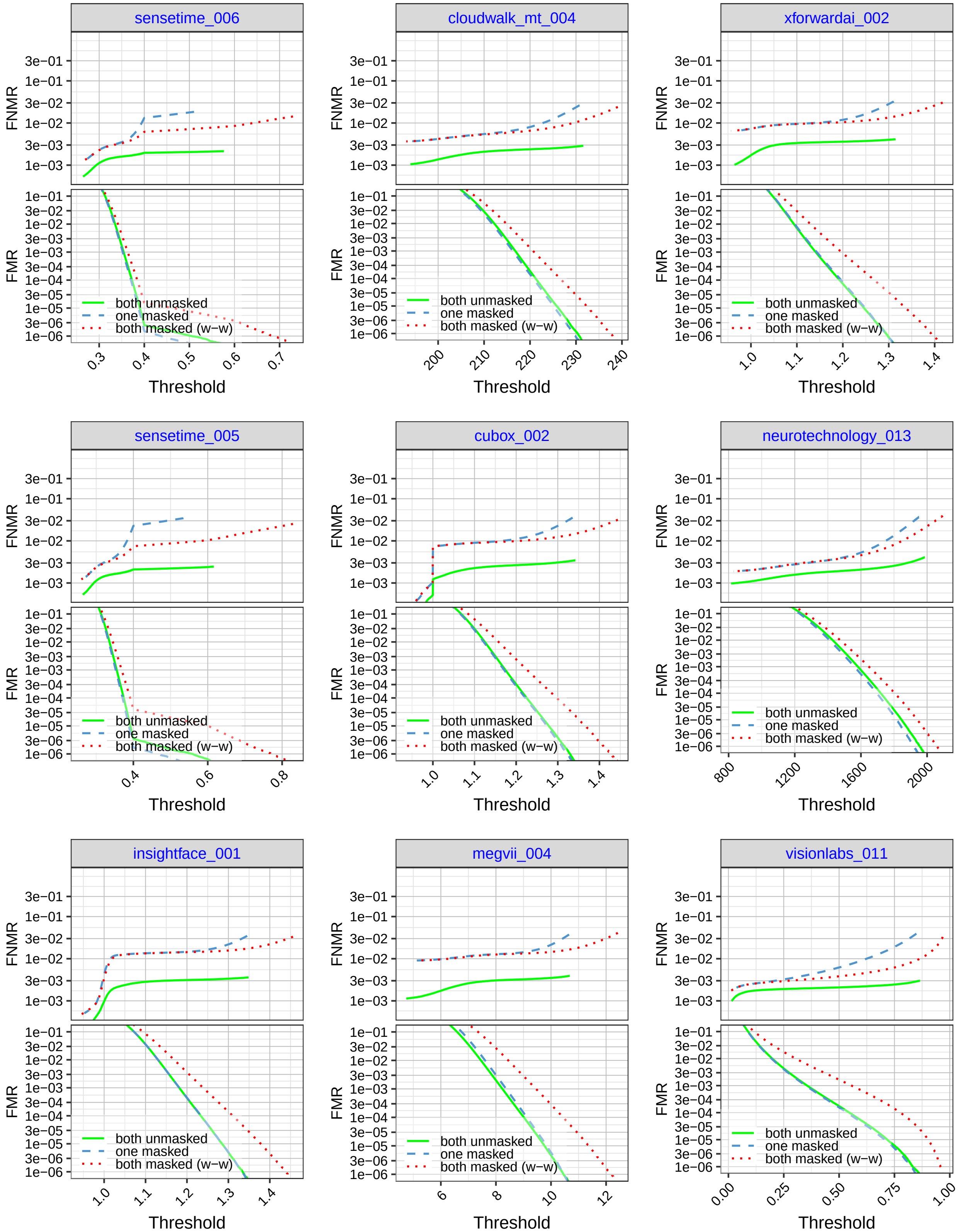

Figure 73: FNMR and FMR calibration curves on unmasked-to-unmasked (both unmasked), masked-to-unmasked with medium, wide, lightblue masks (one masked), masked-to-masked with medium, wide, lightblue masks (both masked (w-w)), and masked-to-masked with medium, round, white masks (enrollment image) and medium, wide, lightblue masks (verification image) (both masked (r-w)). Algorithms in black were submitted prior to mid-March 2020, and algorithms in blue were submitted thereafter.

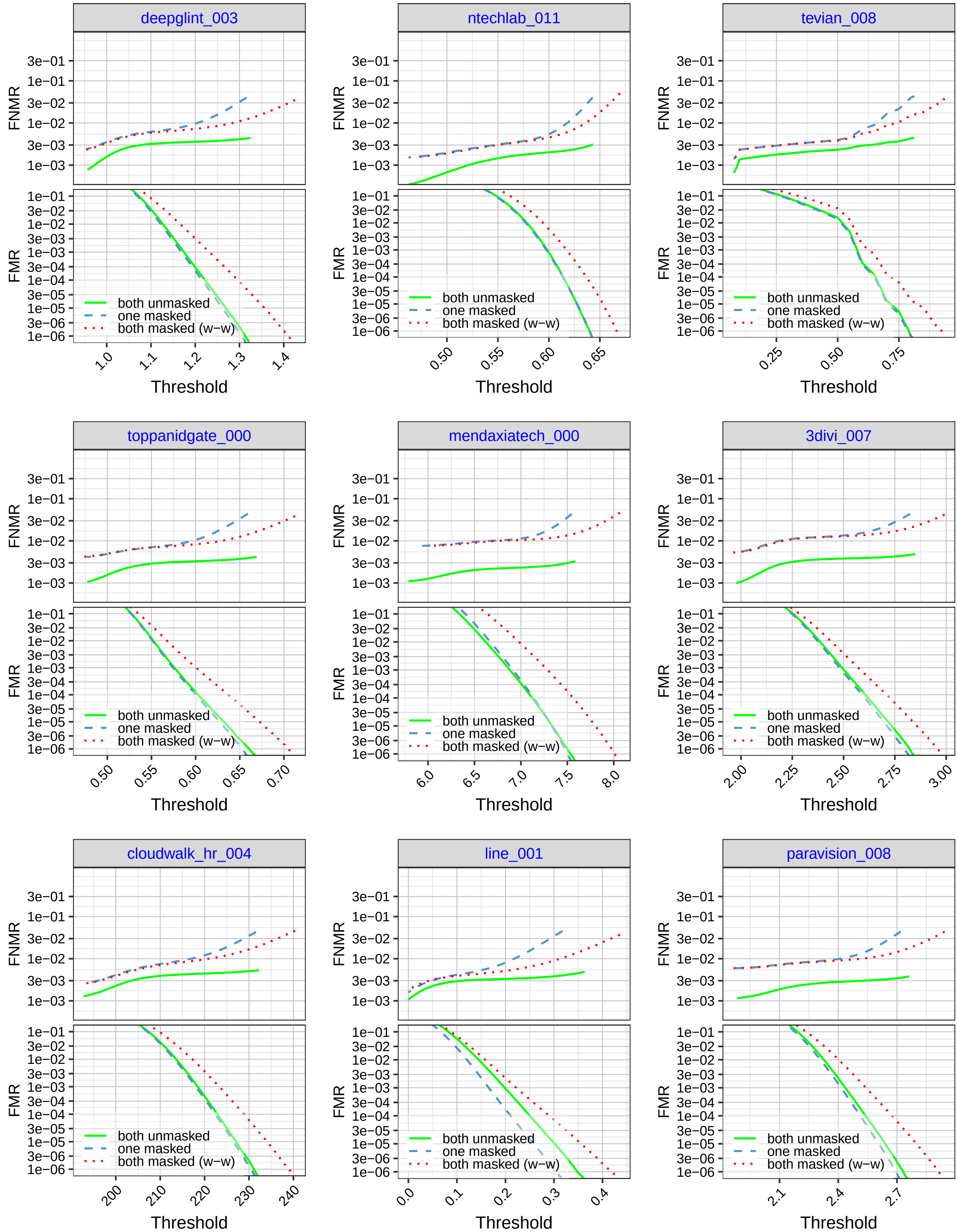

Figure 74: FNMR and FMR calibration curves on unmasked-to-unmasked (both unmasked), masked-to-unmasked with medium, wide, lightblue masks (one masked), masked-to-masked with medium, wide, lightblue masks (both masked (w-w)), and masked-to-masked with medium, round, white masks (enrollment image) and medium, wide, lightblue masks (verification image) (both masked (r-w)). Algorithms in black were submitted prior to mid-March 2020, and algorithms in blue were submitted thereafter.

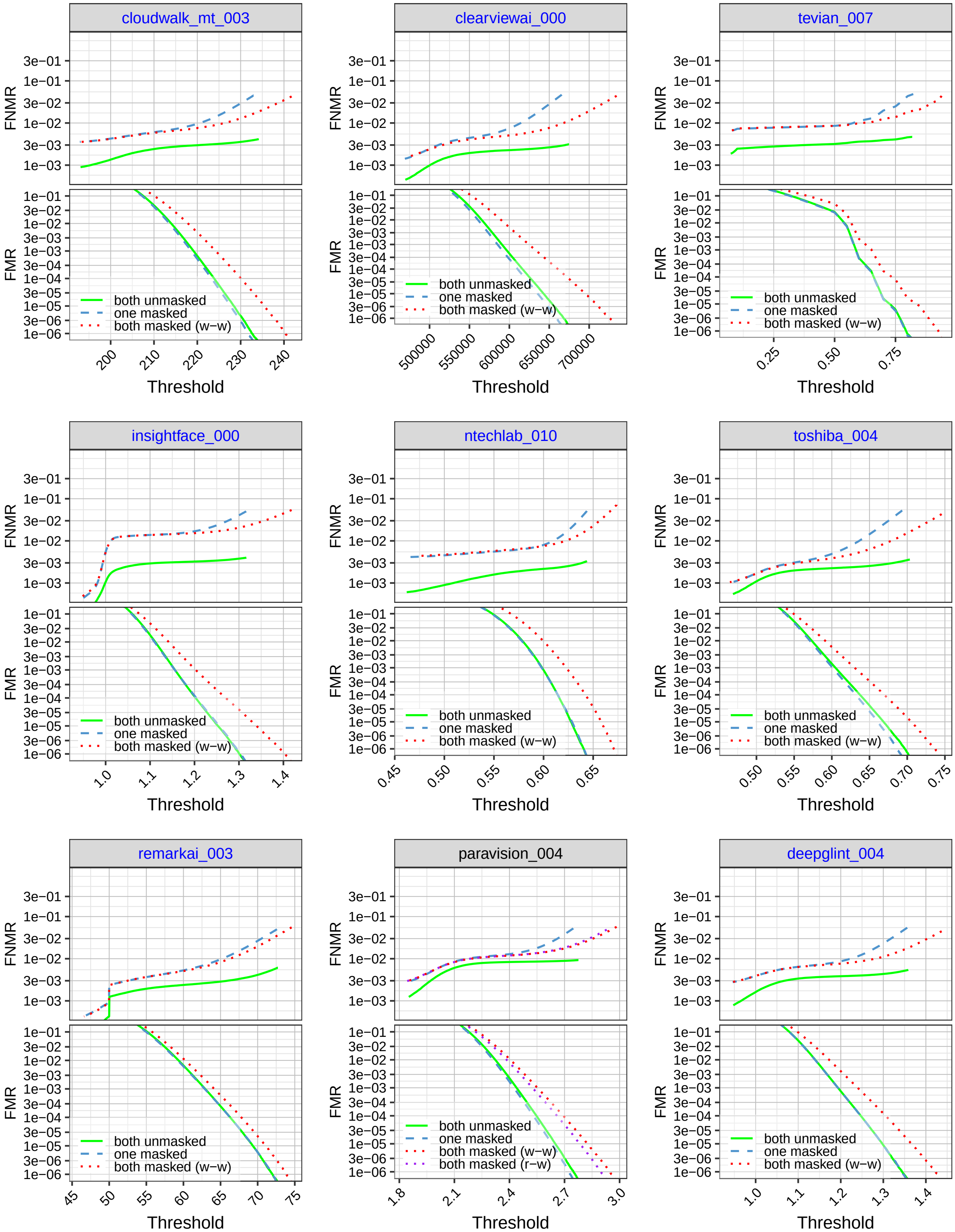

Figure 75: FNMR and FMR calibration curves on unmasked-to-unmasked (both unmasked), masked-to-unmasked with medium, wide, lightblue masks (one masked), masked-to-masked with medium, wide, lightblue masks (both masked (w-w)), and masked-to-masked with medium, round, white masks (enrollment image) and medium, wide, lightblue masks (verification image) (both masked (r-w)). Algorithms in black were submitted prior to mid-March 2020, and algorithms in blue were submitted thereafter.

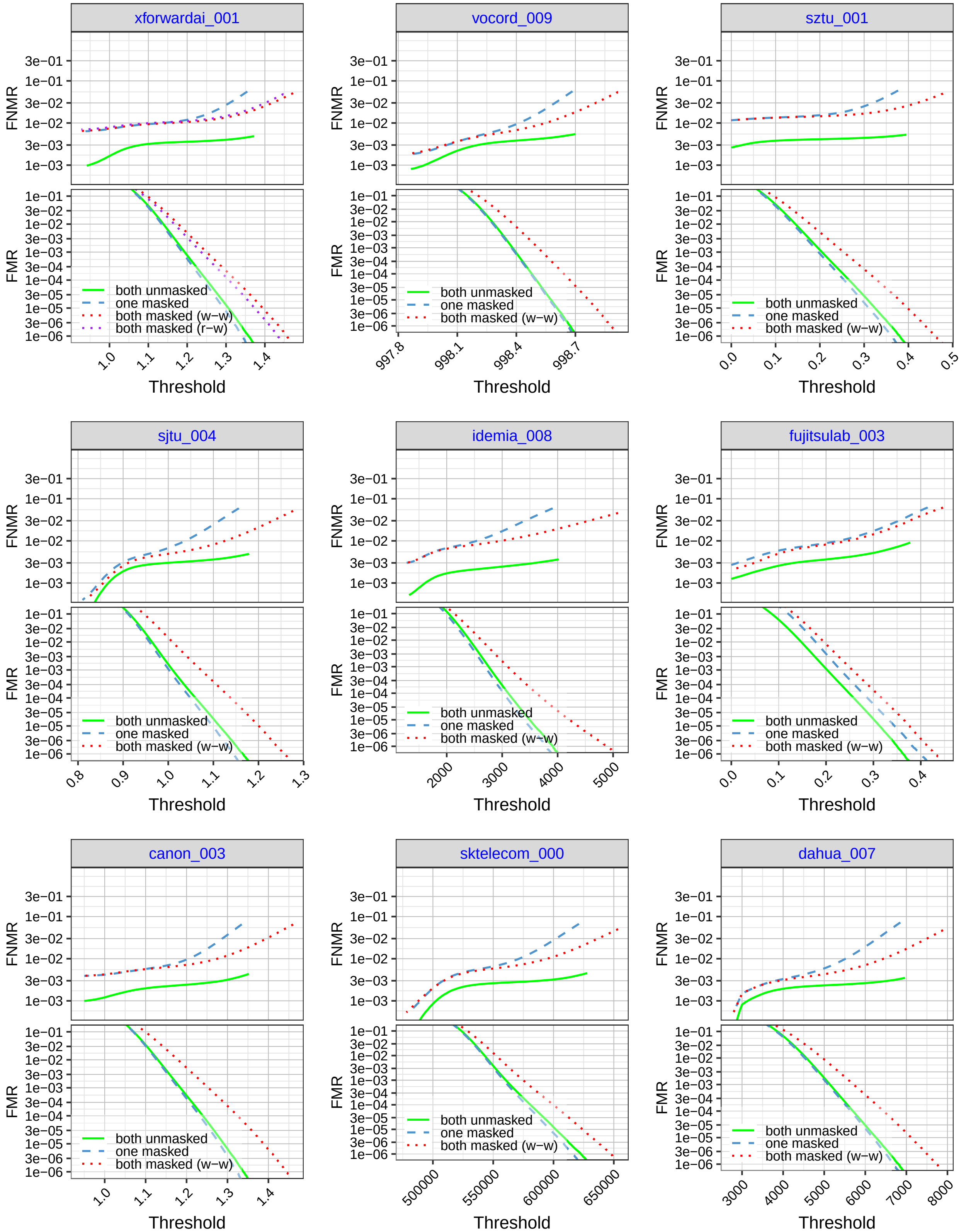

Figure 76: FNMR and FMR calibration curves on unmasked-to-unmasked (both unmasked), masked-to-unmasked with medium, wide, lightblue masks (one masked), masked-to-masked with medium, wide, lightblue masks (both masked (w-w)), and masked-to-masked with medium, round, white masks (enrollment image) and medium, wide, lightblue masks (verification image) (both masked (r-w)). Algorithms in black were submitted prior to mid-March 2020, and algorithms in blue were submitted thereafter.

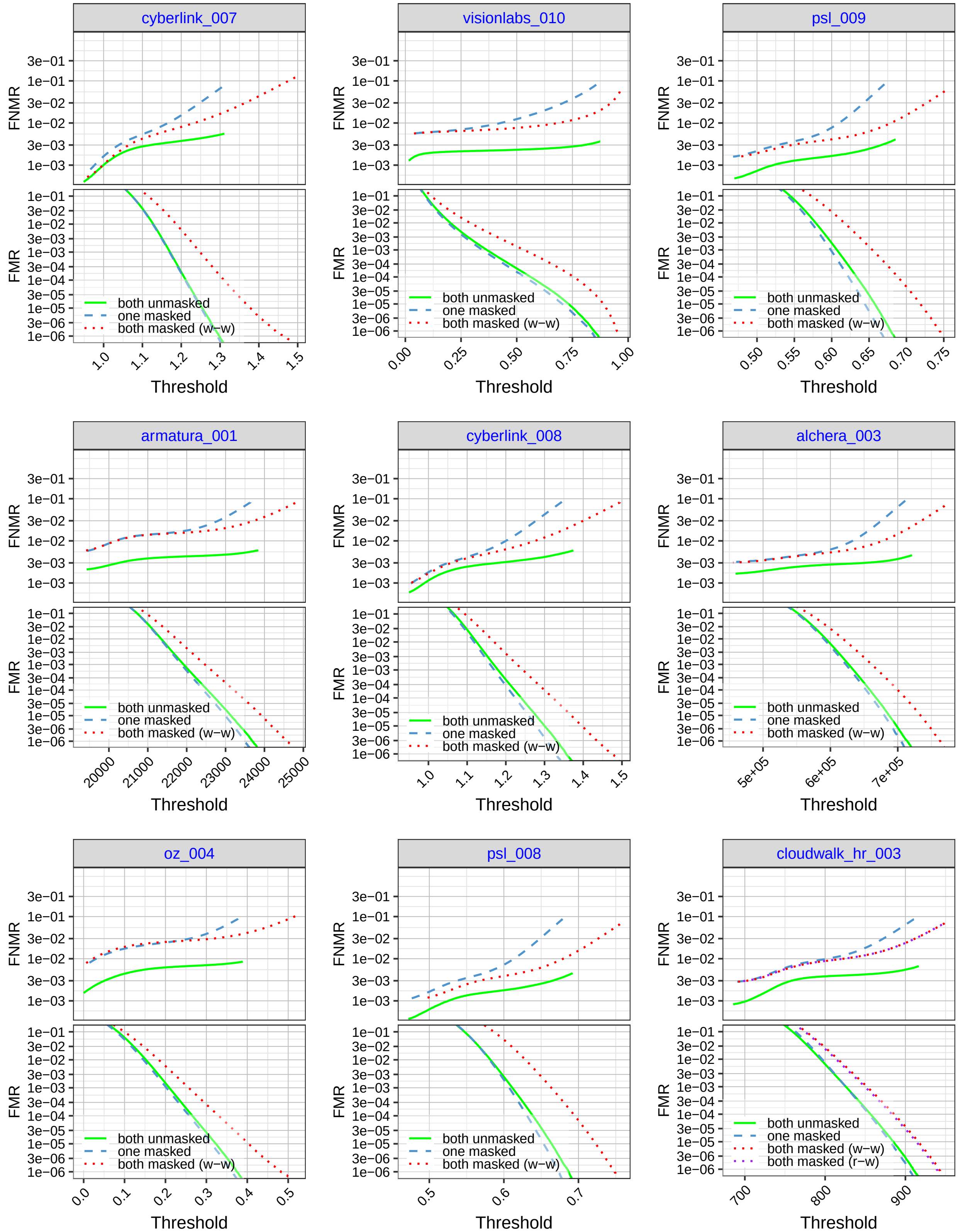

Figure 77: FNMR and FMR calibration curves on unmasked-to-unmasked (both unmasked), masked-to-unmasked with medium, wide, lightblue masks (one masked), masked-to-masked with medium, wide, lightblue masks (both masked (w-w)), and masked-to-masked with medium, round, white masks (enrollment image) and medium, wide, lightblue masks (verification image) (both masked (r-w)). Algorithms in black were submitted prior to mid-March 2020, and algorithms in blue were submitted thereafter.

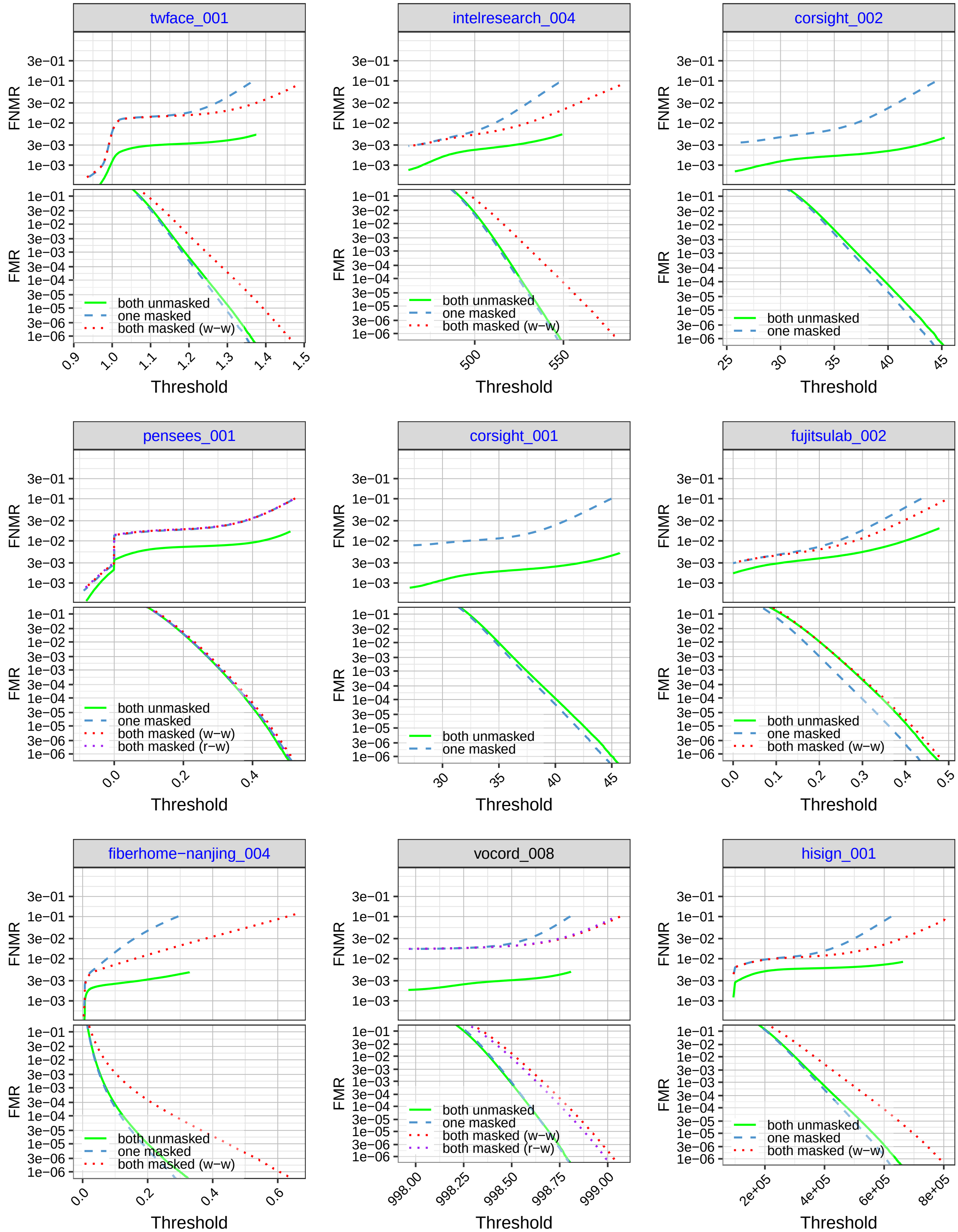

Figure 78: FNMR and FMR calibration curves on unmasked-to-unmasked (both unmasked), masked-to-unmasked with medium, wide, lightblue masks (one masked), masked-to-masked with medium, wide, lightblue masks (both masked (w-w)), and masked-to-masked with medium, round, white masks (enrollment image) and medium, wide, lightblue masks (verification image) (both masked (r-w)). Algorithms in black were submitted prior to mid-March 2020, and algorithms in blue were submitted thereafter.

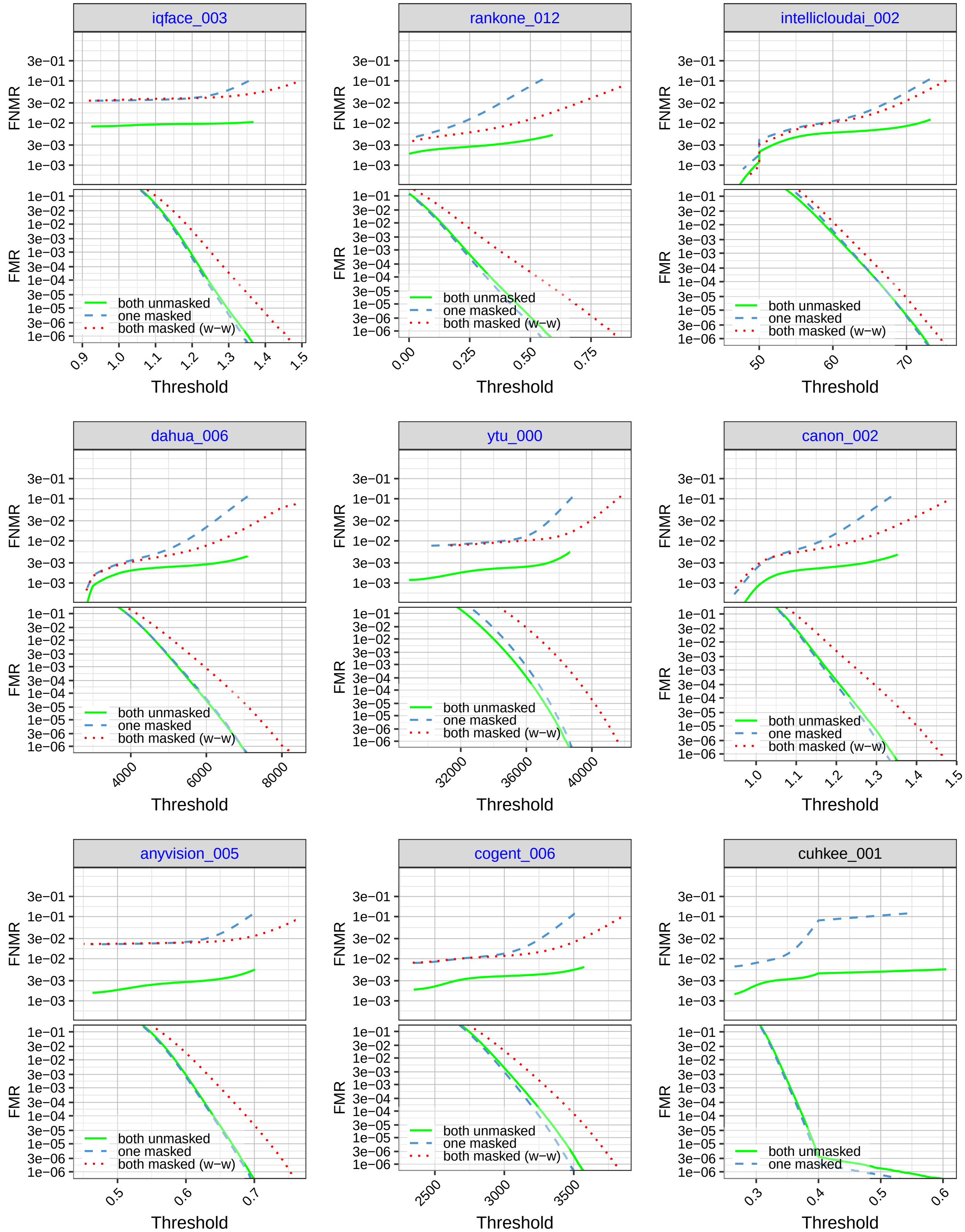

Figure 79: FNMR and FMR calibration curves on unmasked-to-unmasked (both unmasked), masked-to-unmasked with medium, wide, lightblue masks (one masked), masked-to-masked with medium, wide, lightblue masks (both masked (w-w)), and masked-to-masked with medium, round, white masks (enrollment image) and medium, wide, lightblue masks (verification image) (both masked (r-w)). Algorithms in black were submitted prior to mid-March 2020, and algorithms in blue *were submitted thereafter.*

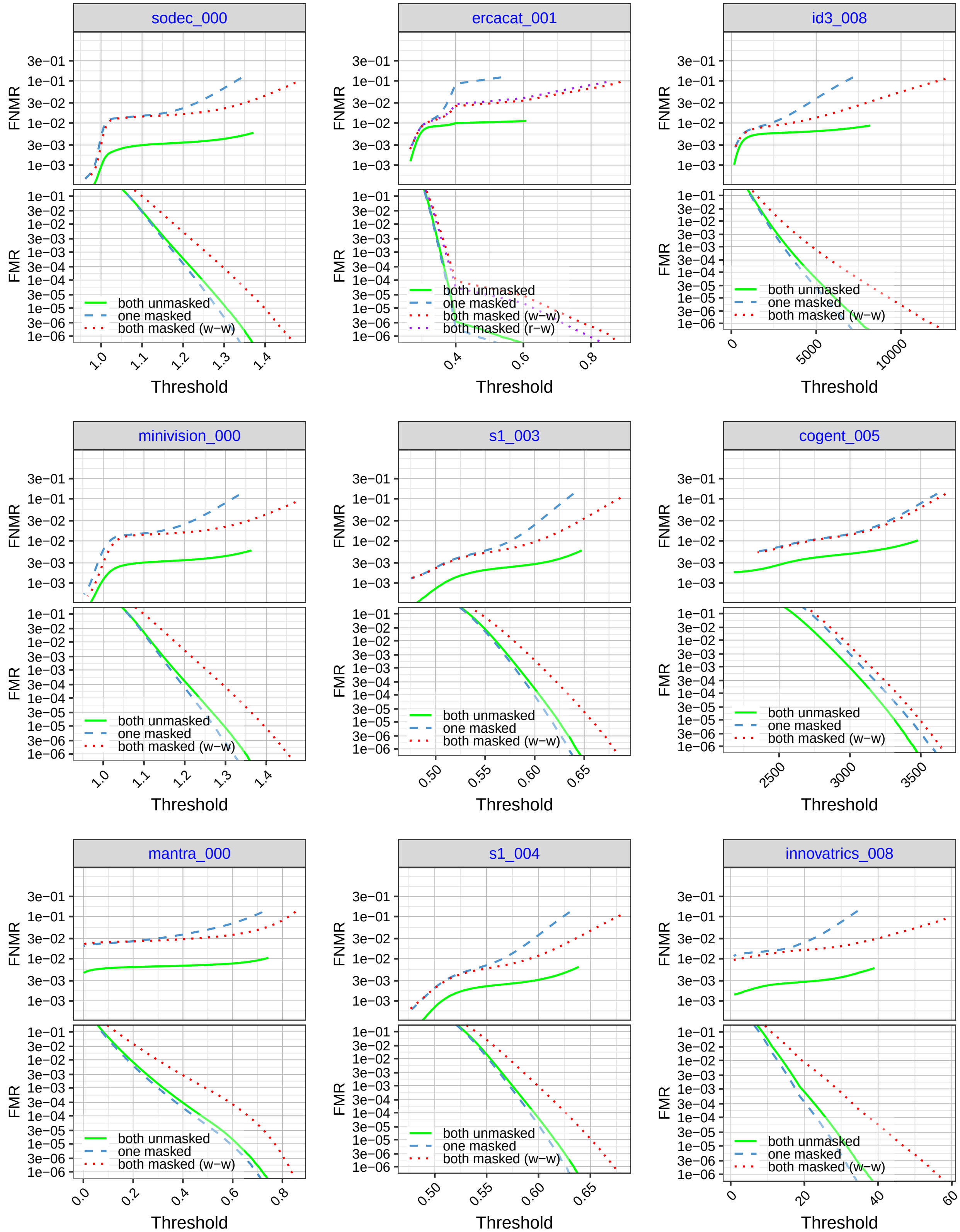

Figure 80: FNMR and FMR calibration curves on unmasked-to-unmasked (both unmasked), masked-to-unmasked with medium, wide, lightblue masks (one masked), masked-to-masked with medium, wide, lightblue masks (both masked (w-w)), and masked-to-masked with medium, round, white masks (enrollment image) and medium, wide, lightblue masks (verification image) (both masked (r-w)). Algorithms in black were submitted prior to mid-March 2020, and algorithms in blue were submitted thereafter.

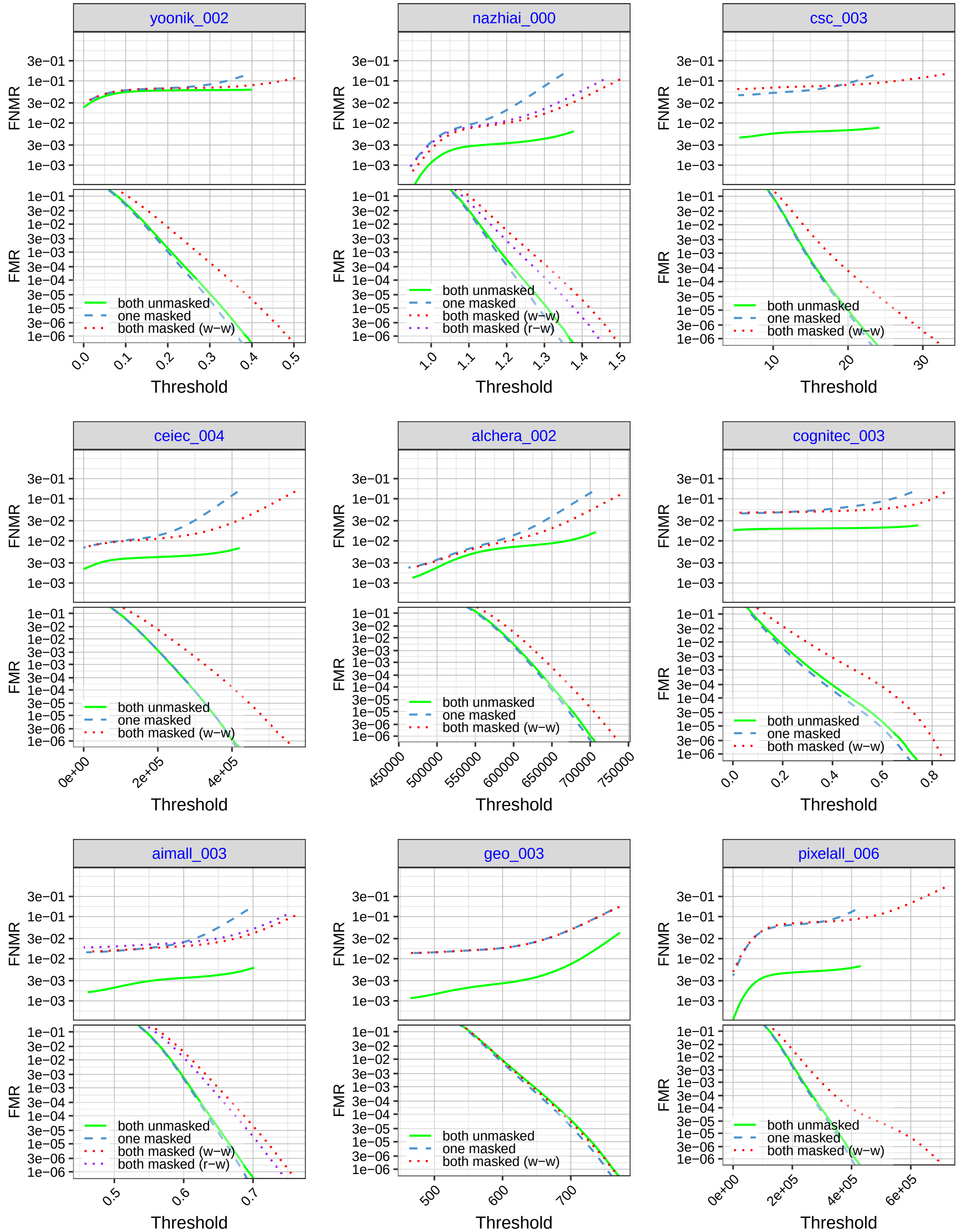

Figure 81: FNMR and FMR calibration curves on unmasked-to-unmasked (both unmasked), masked-to-unmasked with medium, wide, lightblue masks (one masked), masked-to-masked with medium, wide, lightblue masks (both masked (w-w)), and masked-to-masked with medium, round, white masks (enrollment image) and medium, wide, lightblue masks (verification image) (both masked (r-w)). Algorithms in black were submitted prior to mid-March 2020, and algorithms in blue were submitted thereafter.

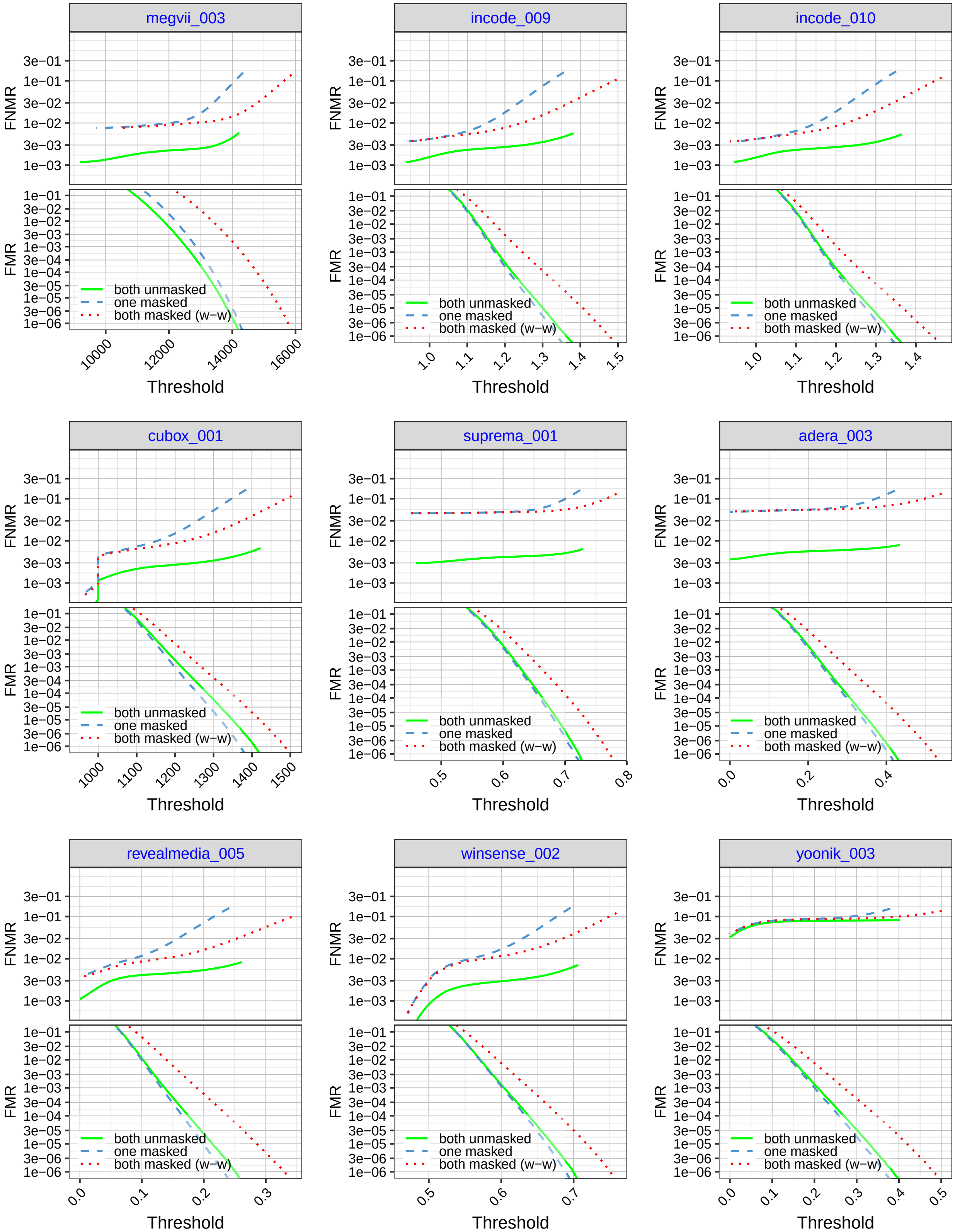

Figure 82: FNMR and FMR calibration curves on unmasked-to-unmasked (both unmasked), masked-to-unmasked with medium, wide, lightblue masks (one masked), masked-to-masked with medium, wide, lightblue masks (both masked (w-w)), and masked-to-masked with medium, round, white masks (enrollment image) and medium, wide, lightblue masks (verification image) (both masked (r-w)). Algorithms in black were submitted prior to mid-March 2020, and algorithms in blue were submitted thereafter.

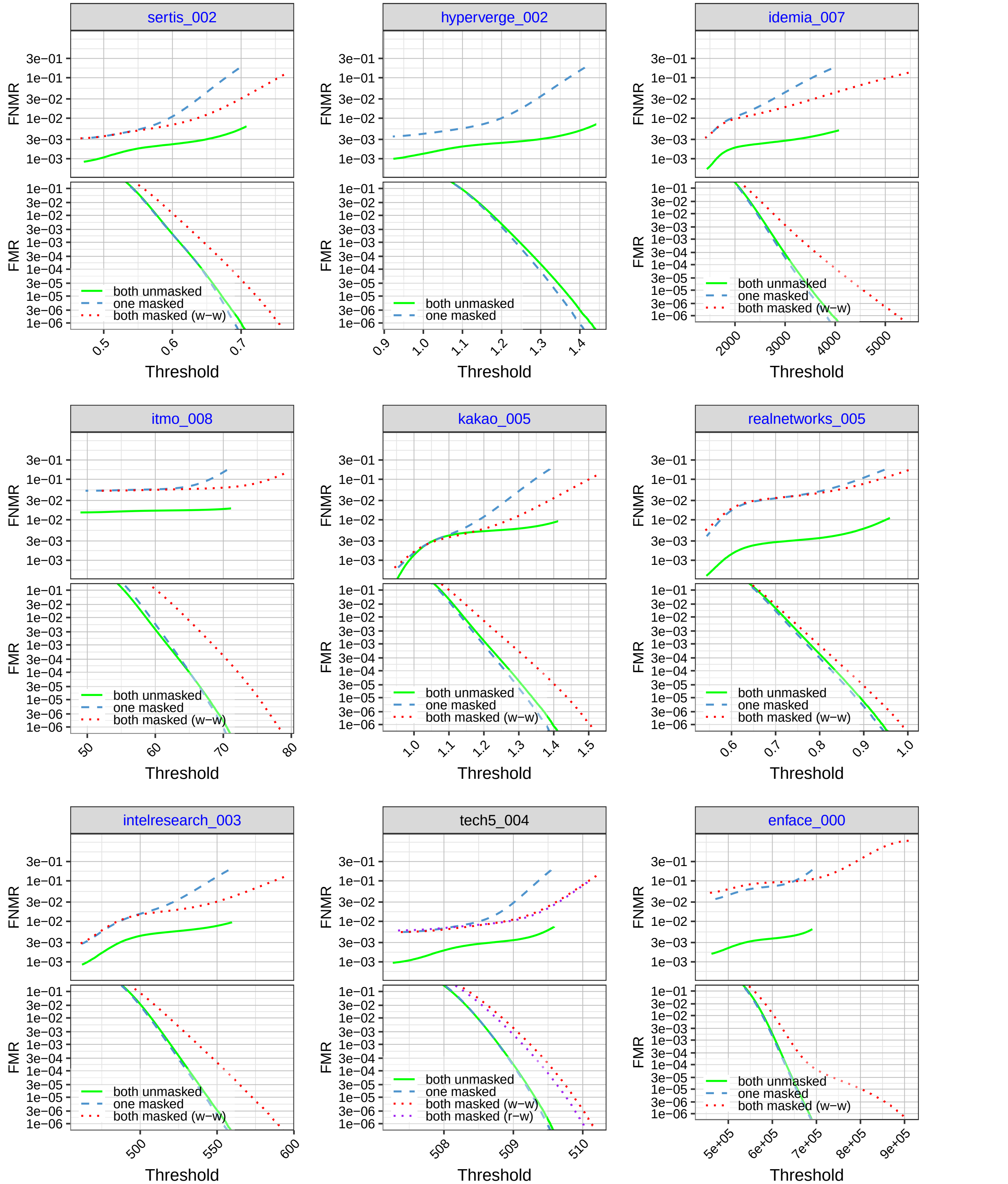

Figure 83: FNMR and FMR calibration curves on unmasked-to-unmasked (both unmasked), masked-to-unmasked with medium, wide, lightblue masks (one masked), masked-to-masked with medium, wide, lightblue masks (both masked (w-w)), and masked-to-masked with medium, round, white masks (enrollment image) and medium, wide, lightblue masks (verification image) (both masked (r-w)). Algorithms in black were submitted prior to mid-March 2020, and algorithms in blue were submitted thereafter.

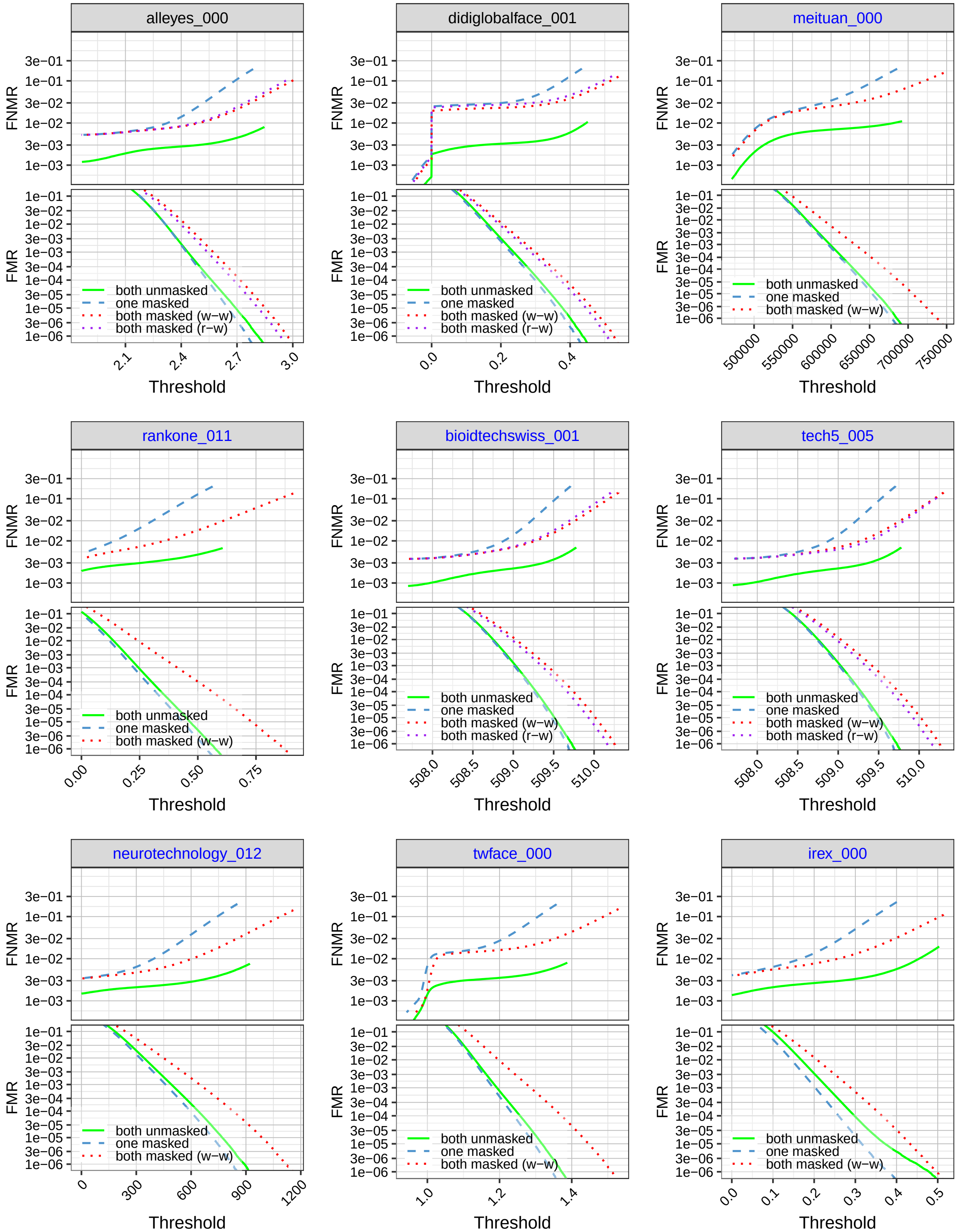

Figure 84: FNMR and FMR calibration curves on unmasked-to-unmasked (both unmasked), masked-to-unmasked with medium, wide, lightblue masks (one masked), masked-to-masked with medium, wide, lightblue masks (both masked (w-w)), and masked-to-masked with medium, round, white masks (enrollment image) and medium, wide, lightblue masks (verification image) (both masked (r-w)). Algorithms in black were submitted prior to mid-March 2020, and algorithms in blue were submitted thereafter.

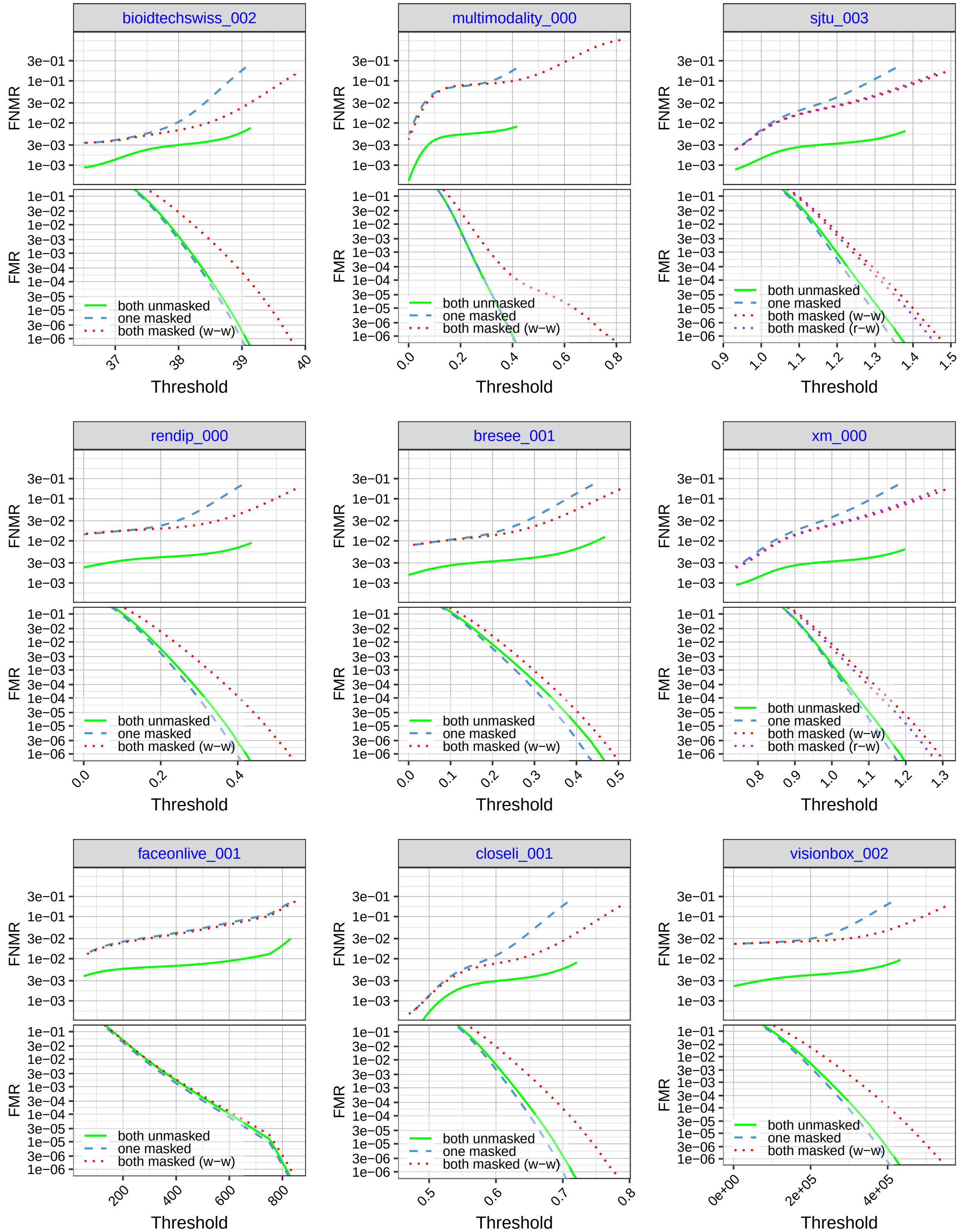

Figure 85: FNMR and FMR calibration curves on unmasked-to-unmasked (both unmasked), masked-to-unmasked with medium, wide, lightblue masks (one masked), masked-to-masked with medium, wide, lightblue masks (both masked (w-w)), and masked-to-masked with medium, round, white masks (enrollment image) and medium, wide, lightblue masks (verification image) (both masked (r-w)). Algorithms in black were submitted prior to mid-March 2020, and algorithms in blue were submitted thereafter.

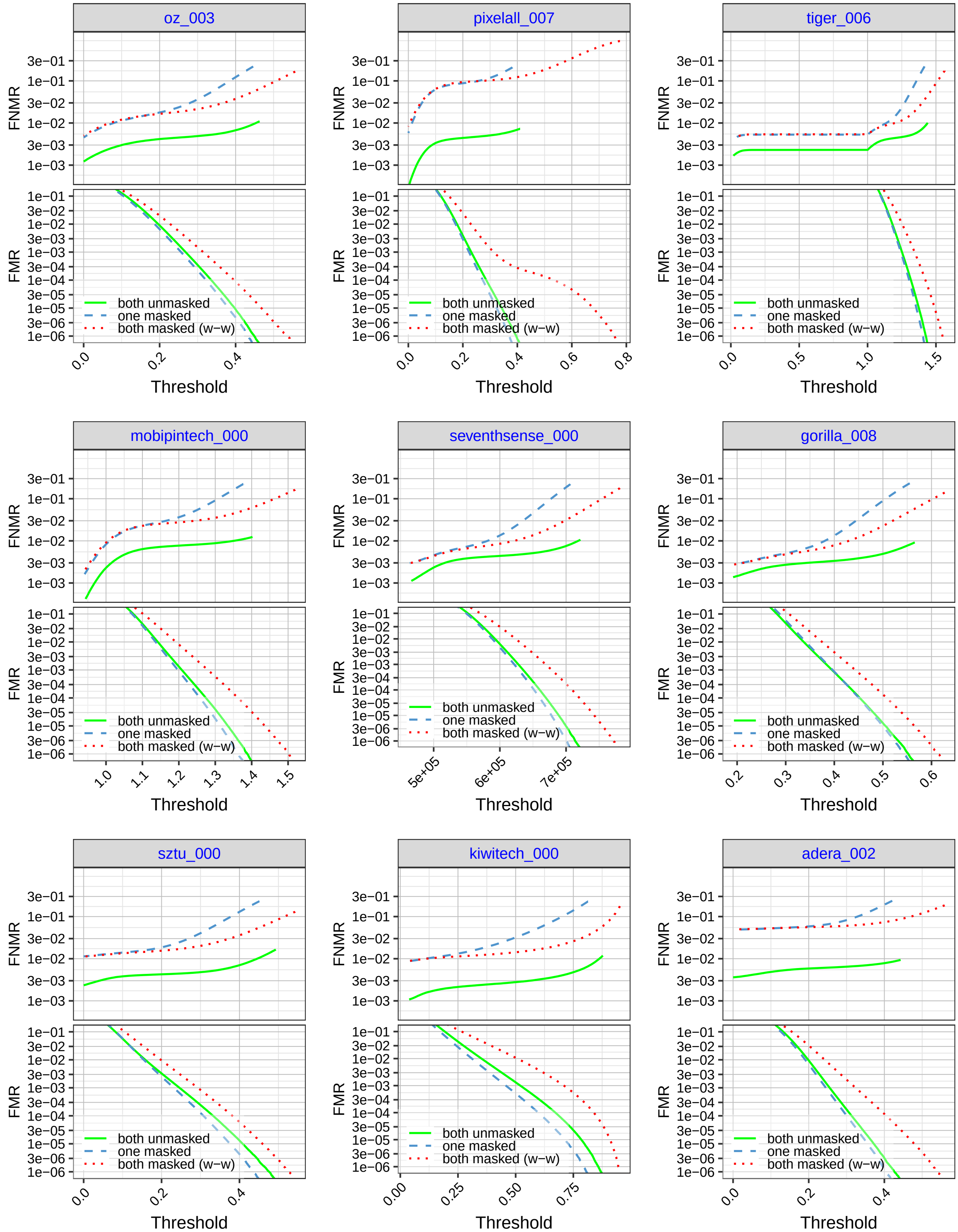

Figure 86: FNMR and FMR calibration curves on unmasked-to-unmasked (both unmasked), masked-to-unmasked with medium, wide, lightblue masks (one masked), masked-to-masked with medium, wide, lightblue masks (both masked (w-w)), and masked-to-masked with medium, round, white masks (enrollment image) and medium, wide, lightblue masks (verification image) (both masked (r-w)). Algorithms in black were submitted prior to mid-March 2020, and algorithms in blue were submitted thereafter.

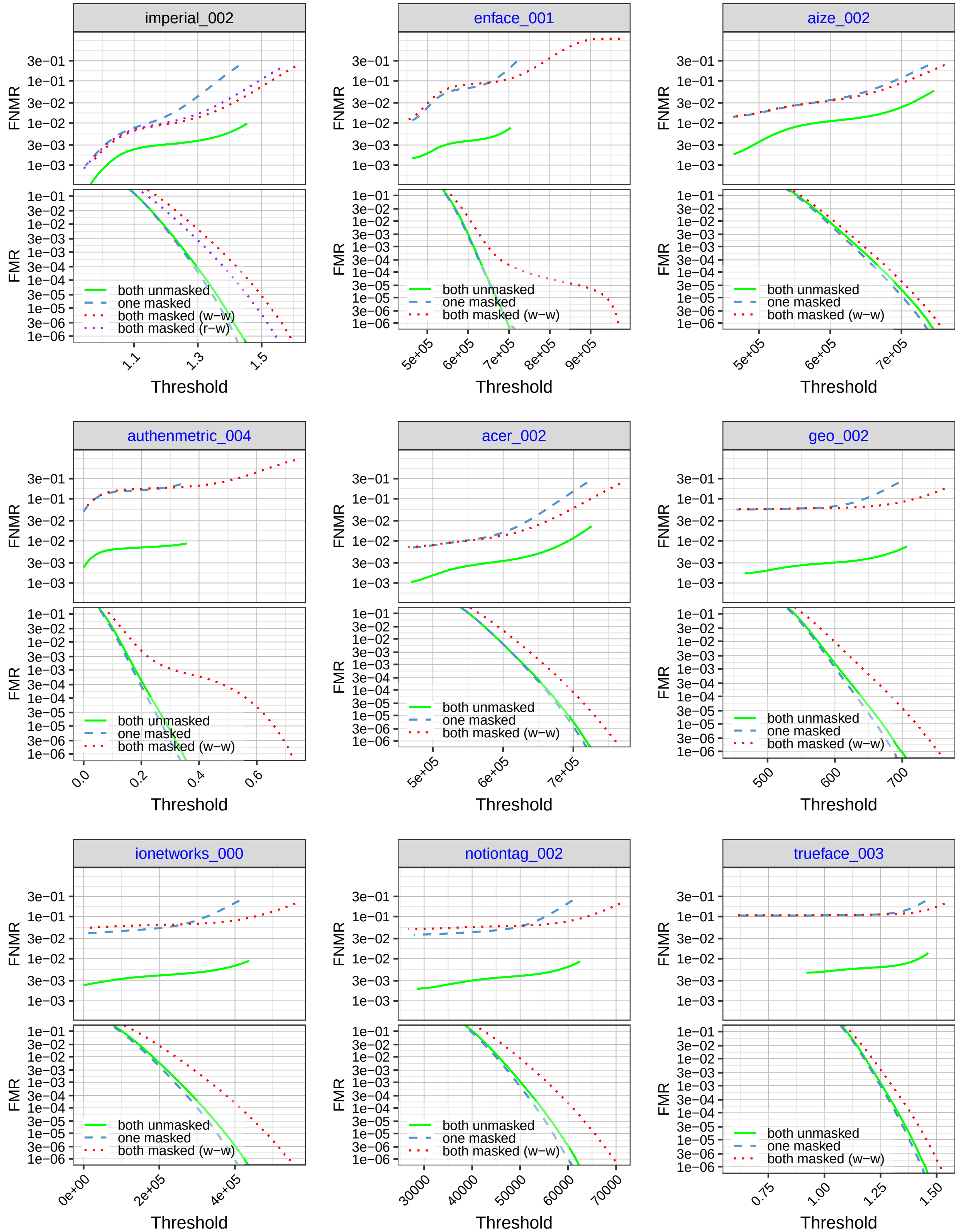

Figure 87: FNMR and FMR calibration curves on unmasked-to-unmasked (both unmasked), masked-to-unmasked with medium, wide, lightblue masks (one masked), masked-to-masked with medium, wide, lightblue masks (both masked (w-w)), and masked-to-masked with medium, round, white masks (enrollment image) and medium, wide, lightblue masks (verification image) (both masked (r-w)). Algorithms in black were submitted prior to mid-March 2020, and algorithms in blue were submitted thereafter.

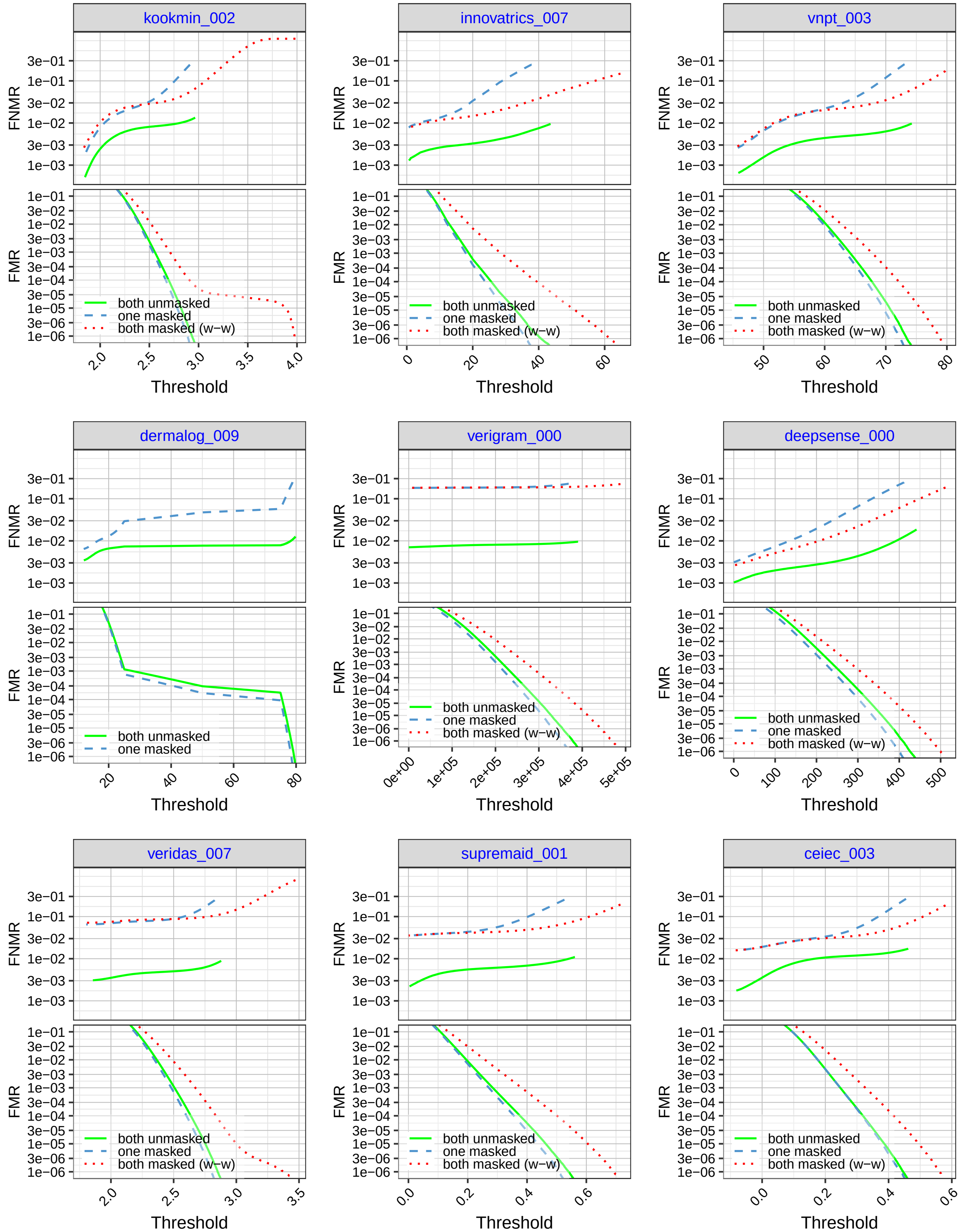

Figure 88: FNMR and FMR calibration curves on unmasked-to-unmasked (both unmasked), masked-to-unmasked with medium, wide, lightblue masks (one masked), masked-to-masked with medium, wide, lightblue masks (both masked (w-w)), and masked-to-masked with medium, round, white masks (enrollment image) and medium, wide, lightblue masks (verification image) (both masked (r-w)). Algorithms in black were submitted prior to mid-March 2020, and algorithms in blue were submitted thereafter.

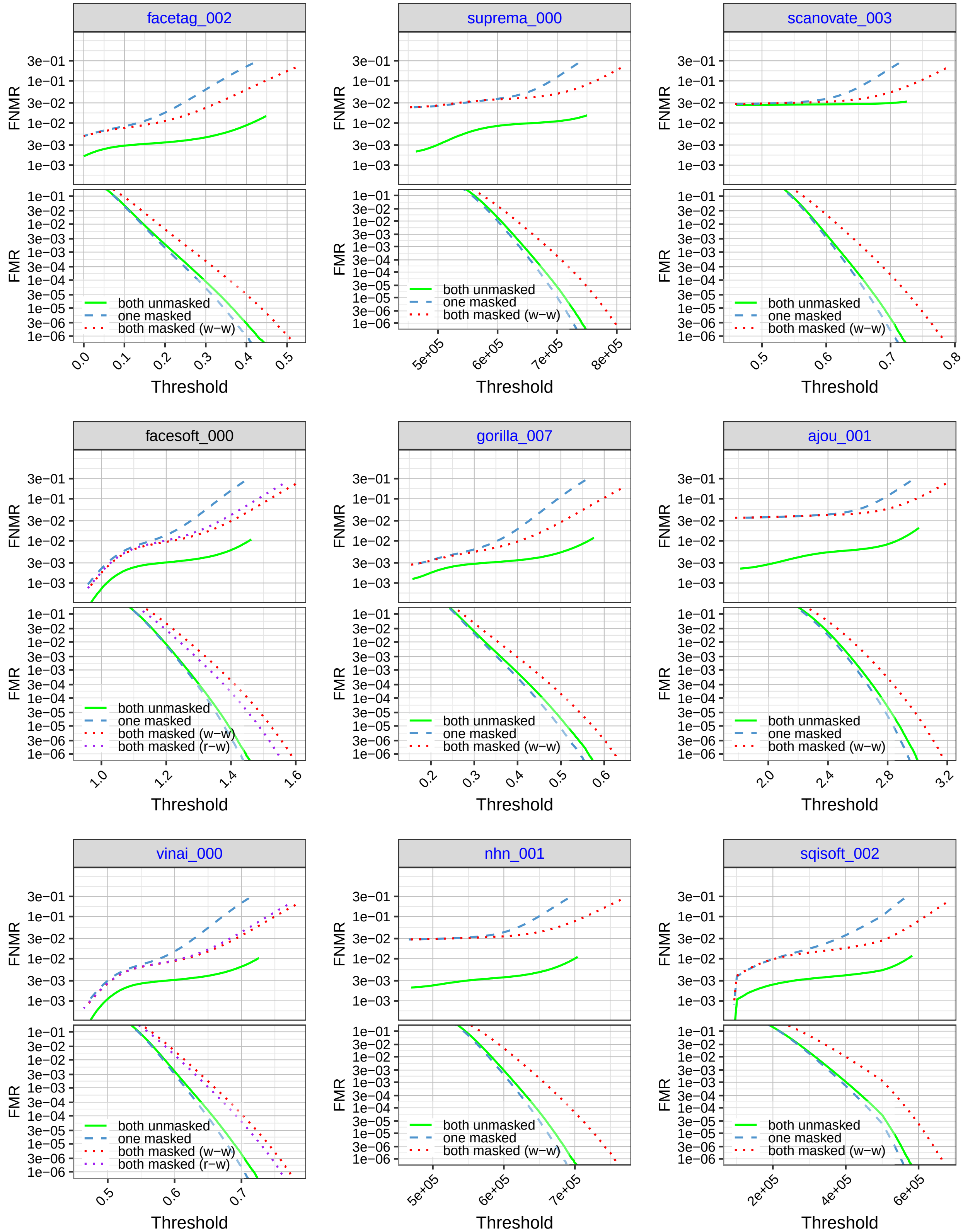

Figure 89: FNMR and FMR calibration curves on unmasked-to-unmasked (both unmasked), masked-to-unmasked with medium, wide, lightblue masks (one masked), masked-to-masked with medium, wide, lightblue masks (both masked (w-w)), and masked-to-masked with medium, round, white masks (enrollment image) and medium, wide, lightblue masks (verification image) (both masked (r-w)). Algorithms in black were submitted prior to mid-March 2020, and algorithms in blue were submitted thereafter.

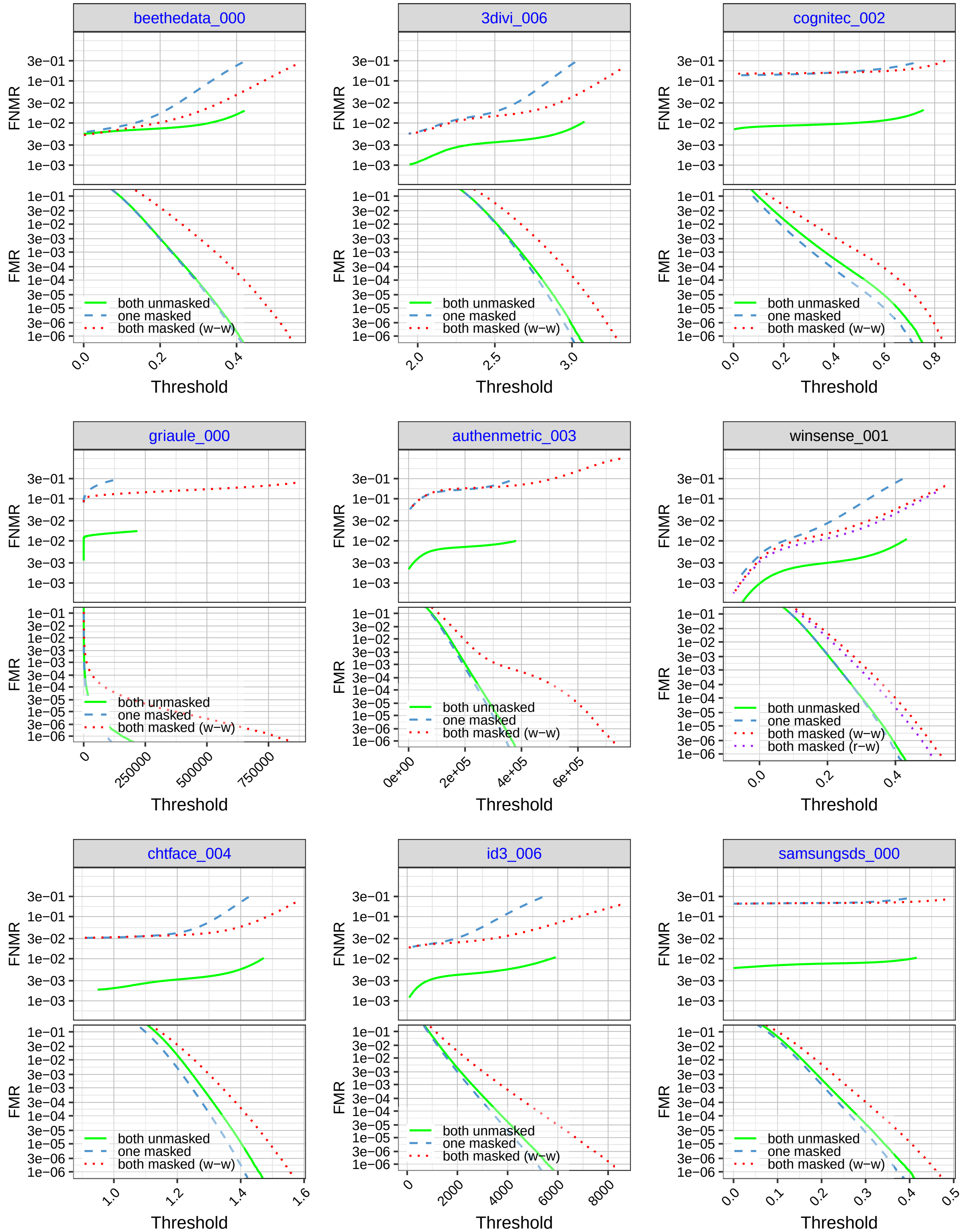

Figure 90: FNMR and FMR calibration curves on unmasked-to-unmasked (both unmasked), masked-to-unmasked with medium, wide, lightblue masks (one masked), masked-to-masked with medium, wide, lightblue masks (both masked (w-w)), and masked-to-masked with medium, round, white masks (enrollment image) and medium, wide, lightblue masks (verification image) (both masked (r-w)). Algorithms in black were submitted prior to mid-March 2020, and algorithms in blue were submitted thereafter.

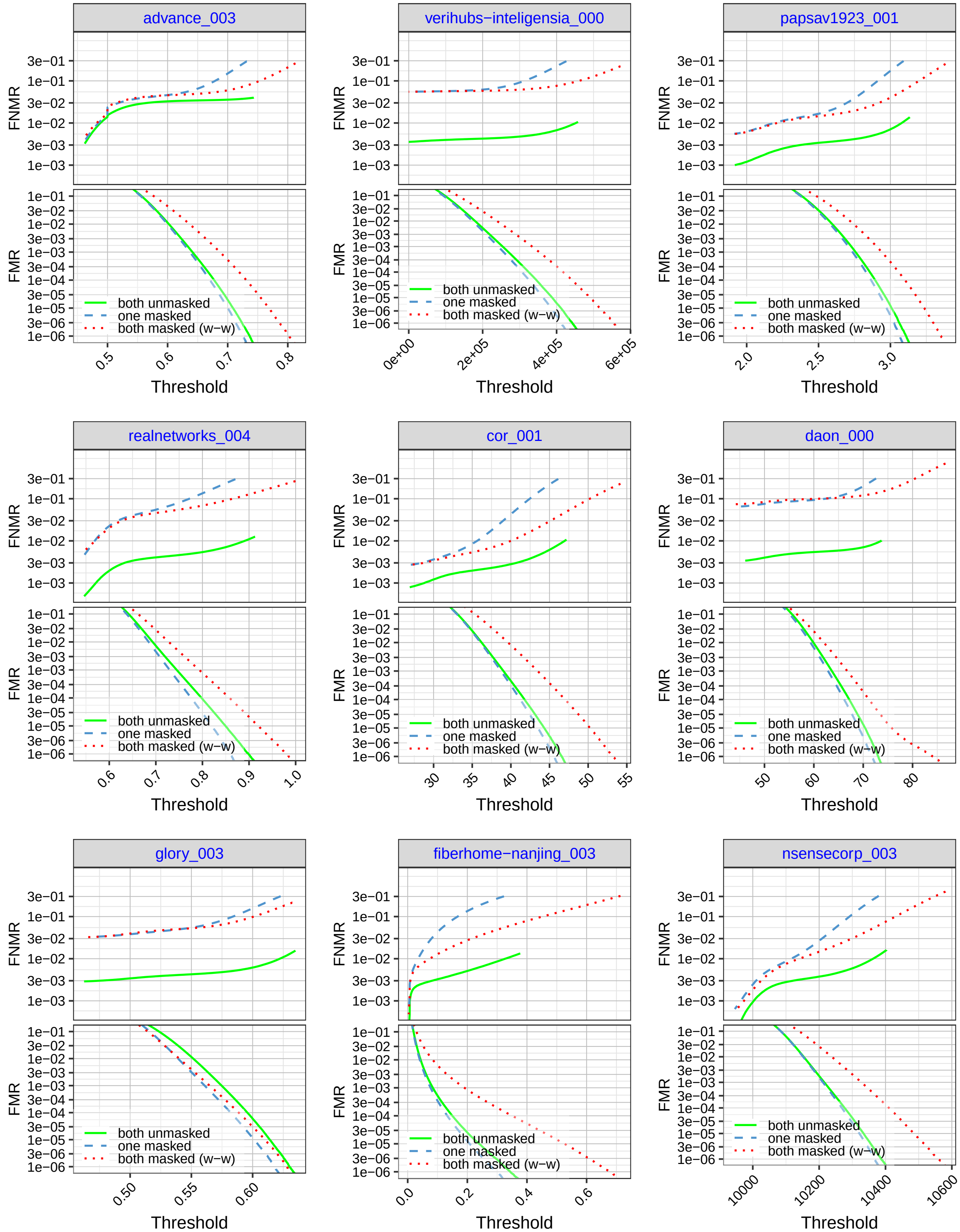

Figure 91: FNMR and FMR calibration curves on unmasked-to-unmasked (both unmasked), masked-to-unmasked with medium, wide, lightblue masks (one masked), masked-to-masked with medium, wide, lightblue masks (both masked (w-w)), and masked-to-masked with medium, round, white masks (enrollment image) and medium, wide, lightblue masks (verification image) (both masked (r-w)). Algorithms in black were submitted prior to mid-March 2020, and algorithms in blue were submitted thereafter.

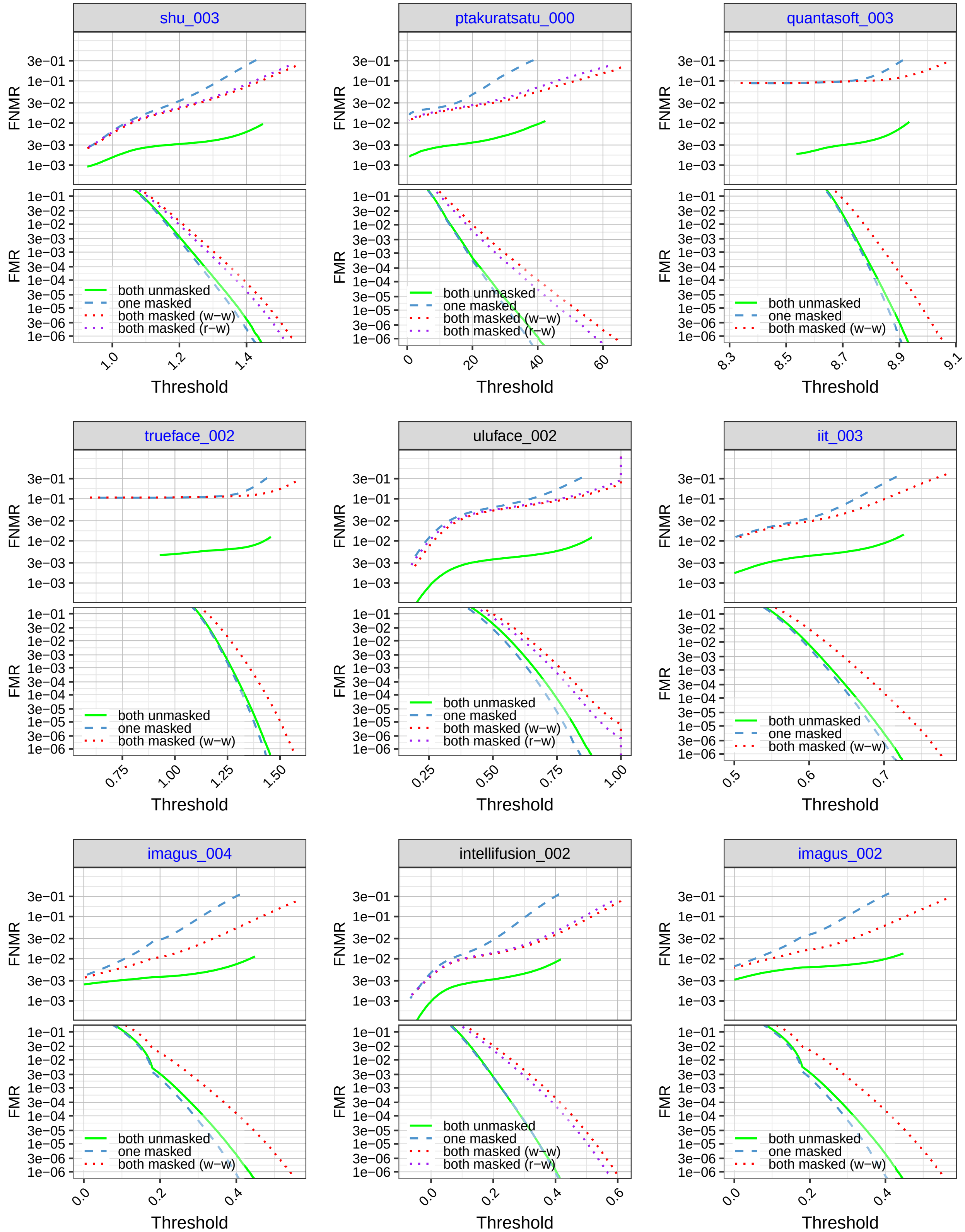

Figure 92: FNMR and FMR calibration curves on unmasked-to-unmasked (both unmasked), masked-to-unmasked with medium, wide, lightblue masks (one masked), masked-to-masked with medium, wide, lightblue masks (both masked (w-w)), and masked-to-masked with medium, round, white masks (enrollment image) and medium, wide, lightblue masks (verification image) (both masked (r-w)). Algorithms in black were submitted prior to mid-March 2020, and algorithms in blue were submitted thereafter.

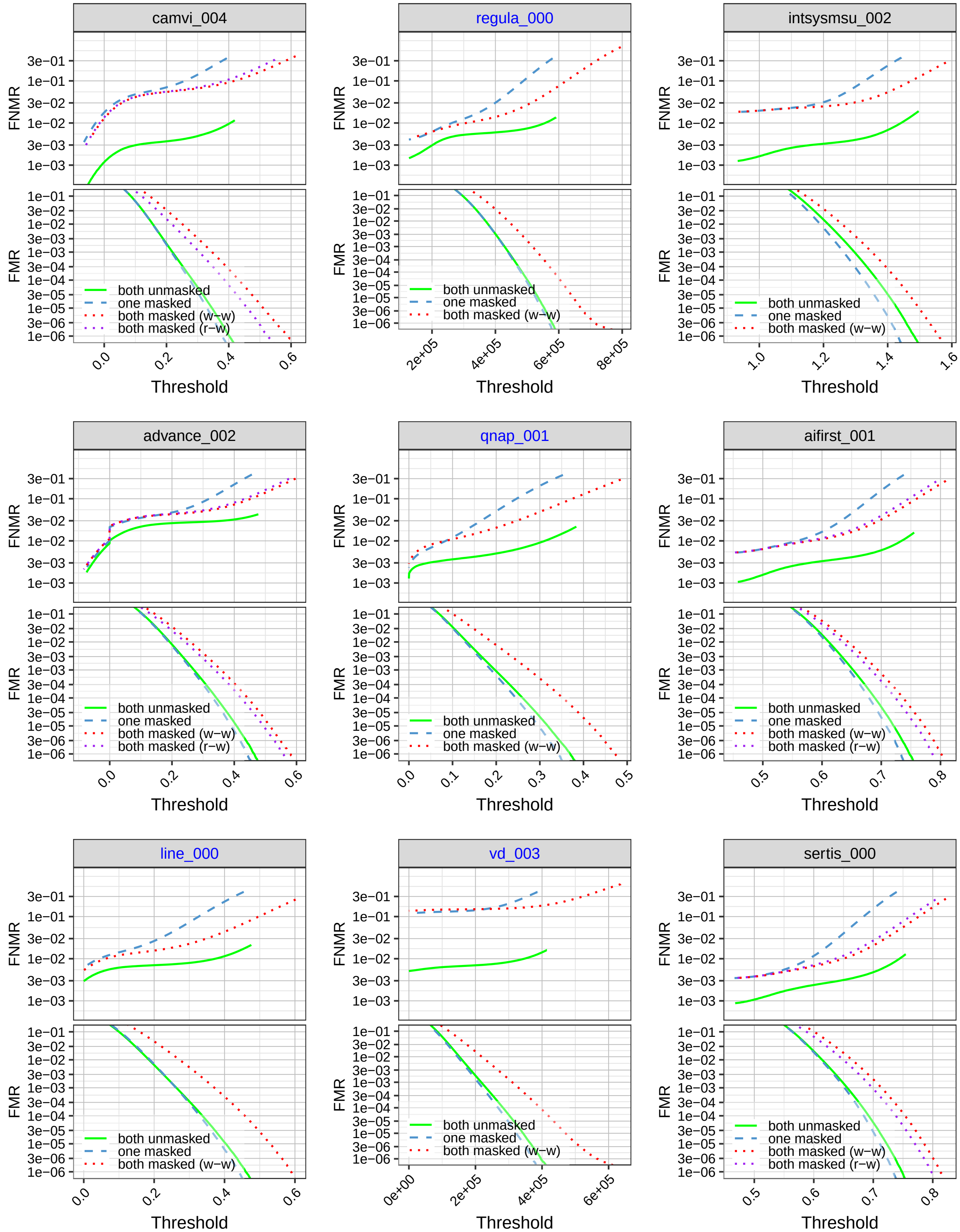

Figure 93: FNMR and FMR calibration curves on unmasked-to-unmasked (both unmasked), masked-to-unmasked with medium, wide, lightblue masks (one masked), masked-to-masked with medium, wide, lightblue masks (both masked (w-w)), and masked-to-masked with medium, round, white masks (enrollment image) and medium, wide, lightblue masks (verification image) (both masked (r-w)). Algorithms in black were submitted prior to mid-March 2020, and algorithms in blue were submitted thereafter.

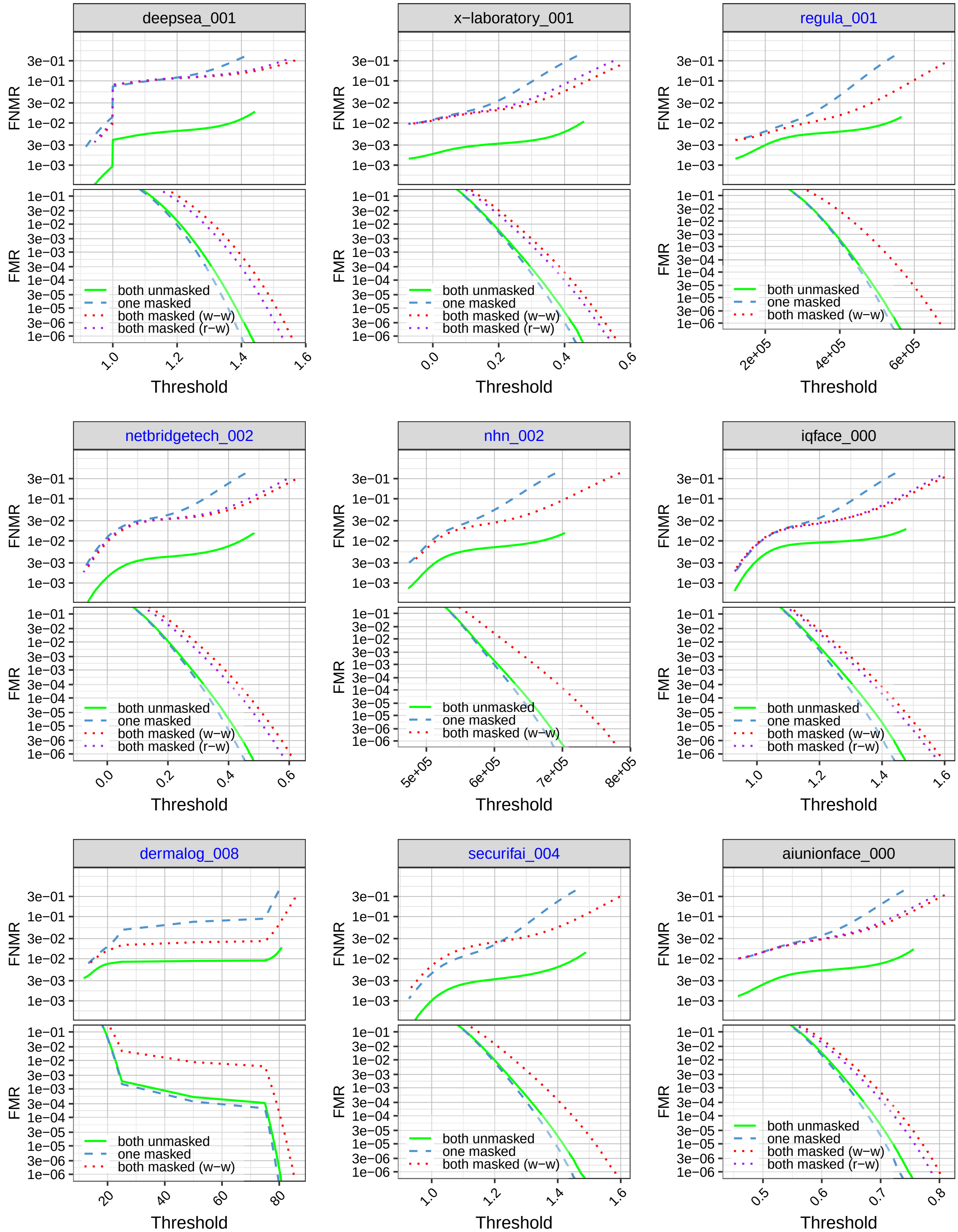

Figure 94: FNMR and FMR calibration curves on unmasked-to-unmasked (both unmasked), masked-to-unmasked with medium, wide, lightblue masks (one masked), masked-to-masked with medium, wide, lightblue masks (both masked (w-w)), and masked-to-masked with medium, round, white masks (enrollment image) and medium, wide, lightblue masks (verification image) (both masked (r-w)). Algorithms in black were submitted prior to mid-March 2020, and algorithms in blue were submitted thereafter.

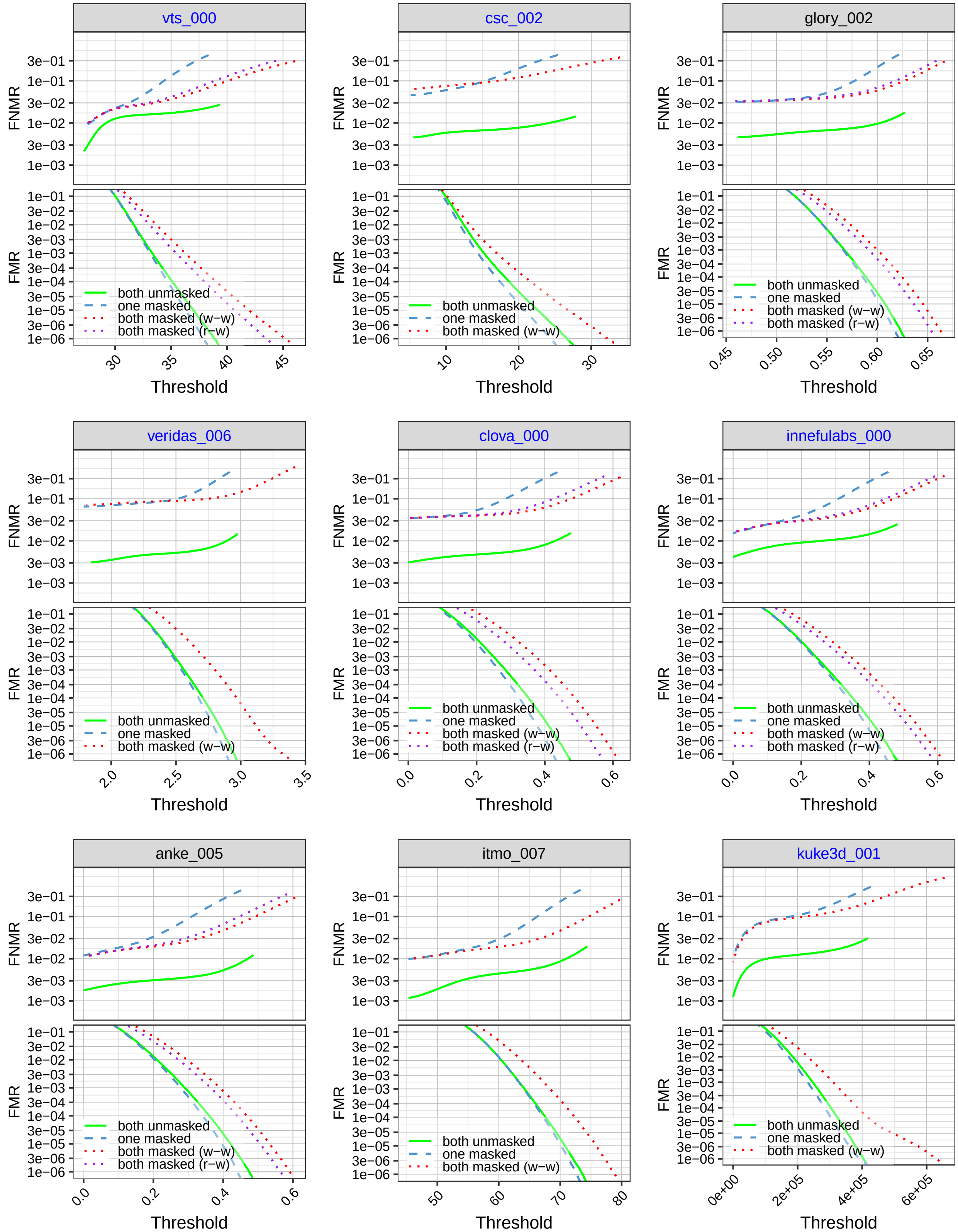

Figure 95: FNMR and FMR calibration curves on unmasked-to-unmasked (both unmasked), masked-to-unmasked with medium, wide, lightblue masks (one masked), masked-to-masked with medium, wide, lightblue masks (both masked (w-w)), and masked-to-masked with medium, round, white masks (enrollment image) and medium, wide, lightblue masks (verification image) (both masked (r-w)). Algorithms in black were submitted prior to mid-March 2020, and algorithms in blue were submitted thereafter.

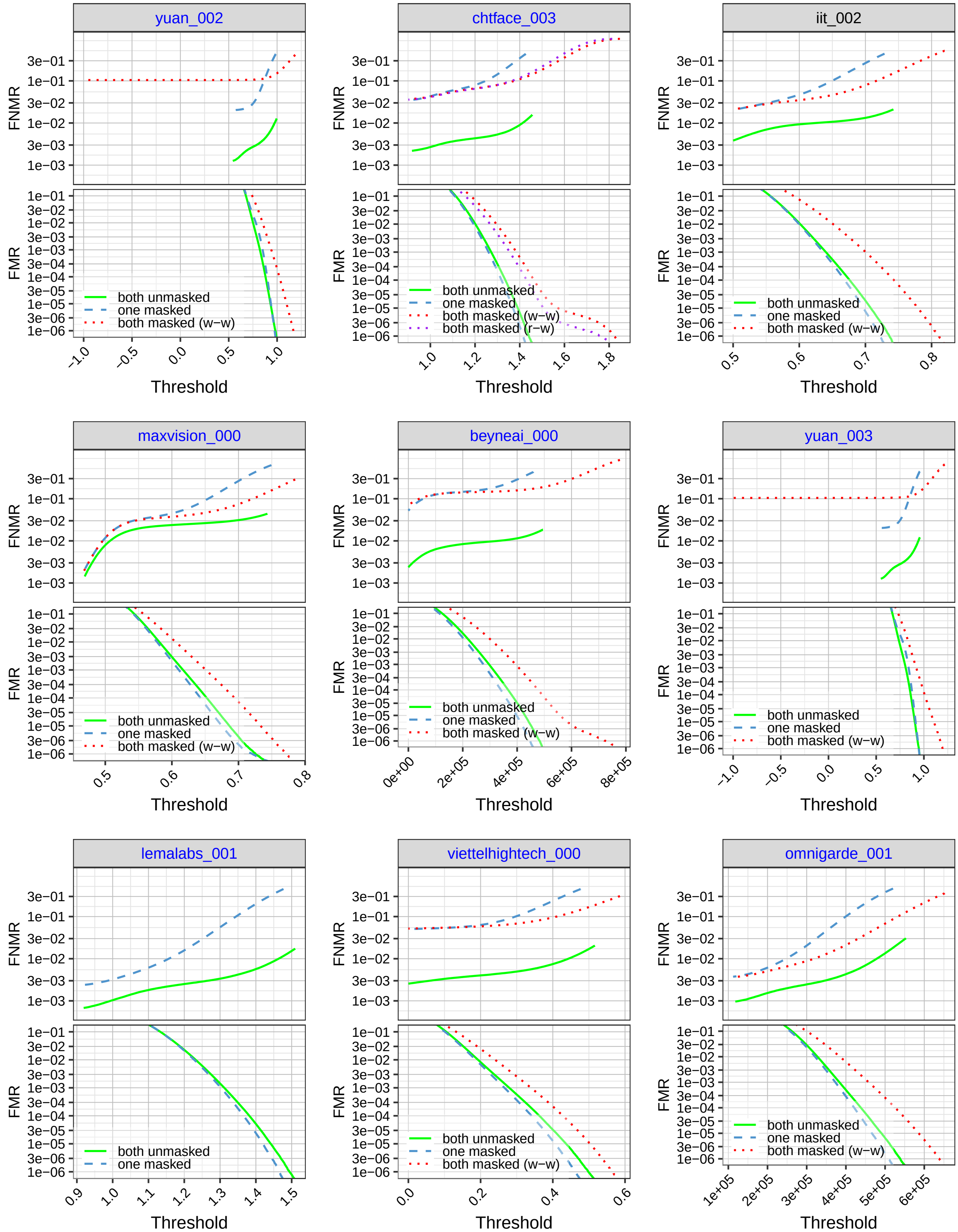

Figure 96: FNMR and FMR calibration curves on unmasked-to-unmasked (both unmasked), masked-to-unmasked with medium, wide, lightblue masks (one masked), masked-to-masked with medium, wide, lightblue masks (both masked (w-w)), and masked-to-masked with medium, round, white masks (enrollment image) and medium, wide, lightblue masks (verification image) (both masked (r-w)). Algorithms in black were submitted prior to mid-March 2020, and algorithms in blue were submitted thereafter.

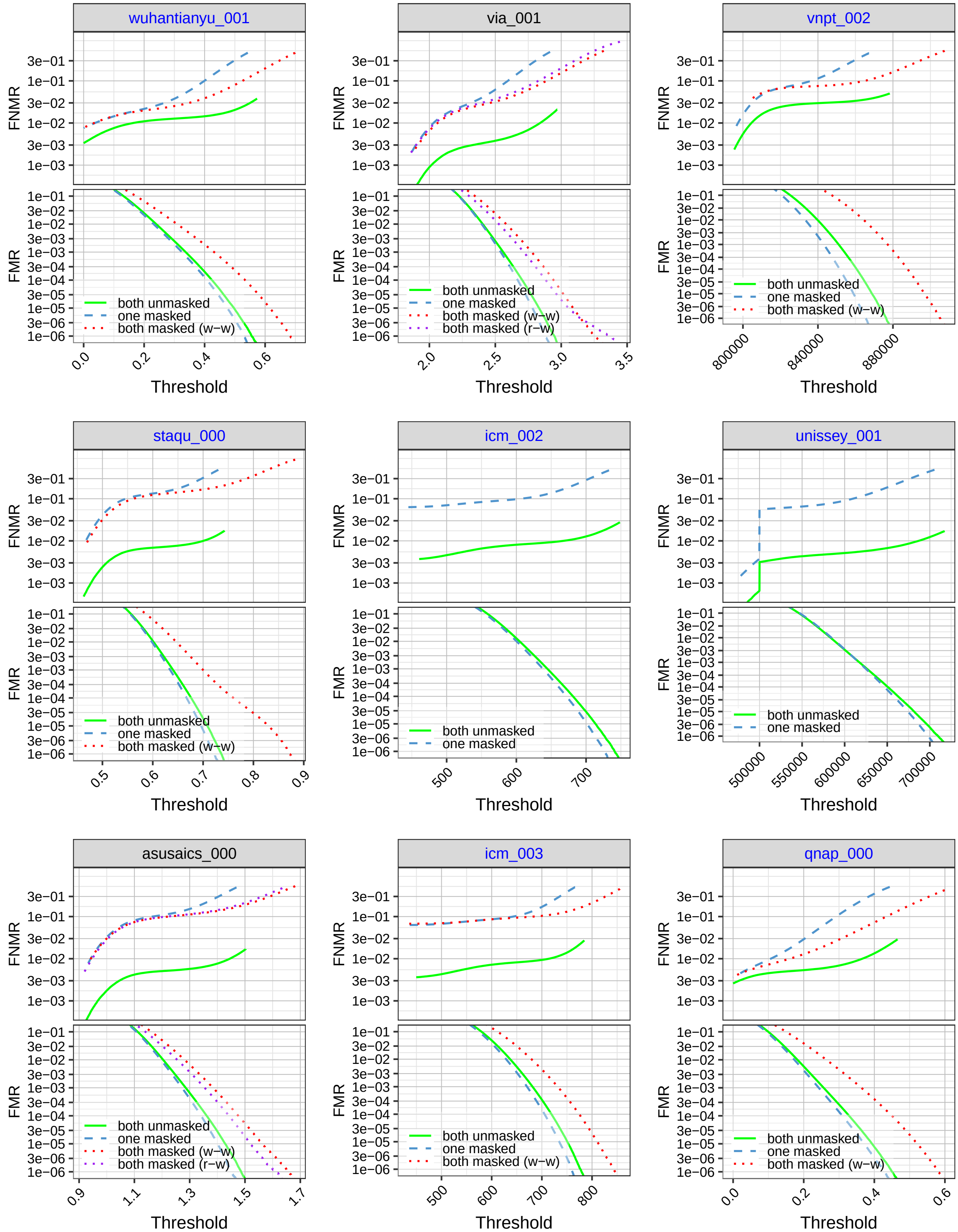

Figure 97: FNMR and FMR calibration curves on unmasked-to-unmasked (both unmasked), masked-to-unmasked with medium, wide, lightblue masks (one masked), masked-to-masked with medium, wide, lightblue masks (both masked (w-w)), and masked-to-masked with medium, round, white masks (enrollment image) and medium, wide, lightblue masks (verification image) (both masked (r-w)). Algorithms in black were submitted prior to mid-March 2020, and algorithms in blue were submitted thereafter.

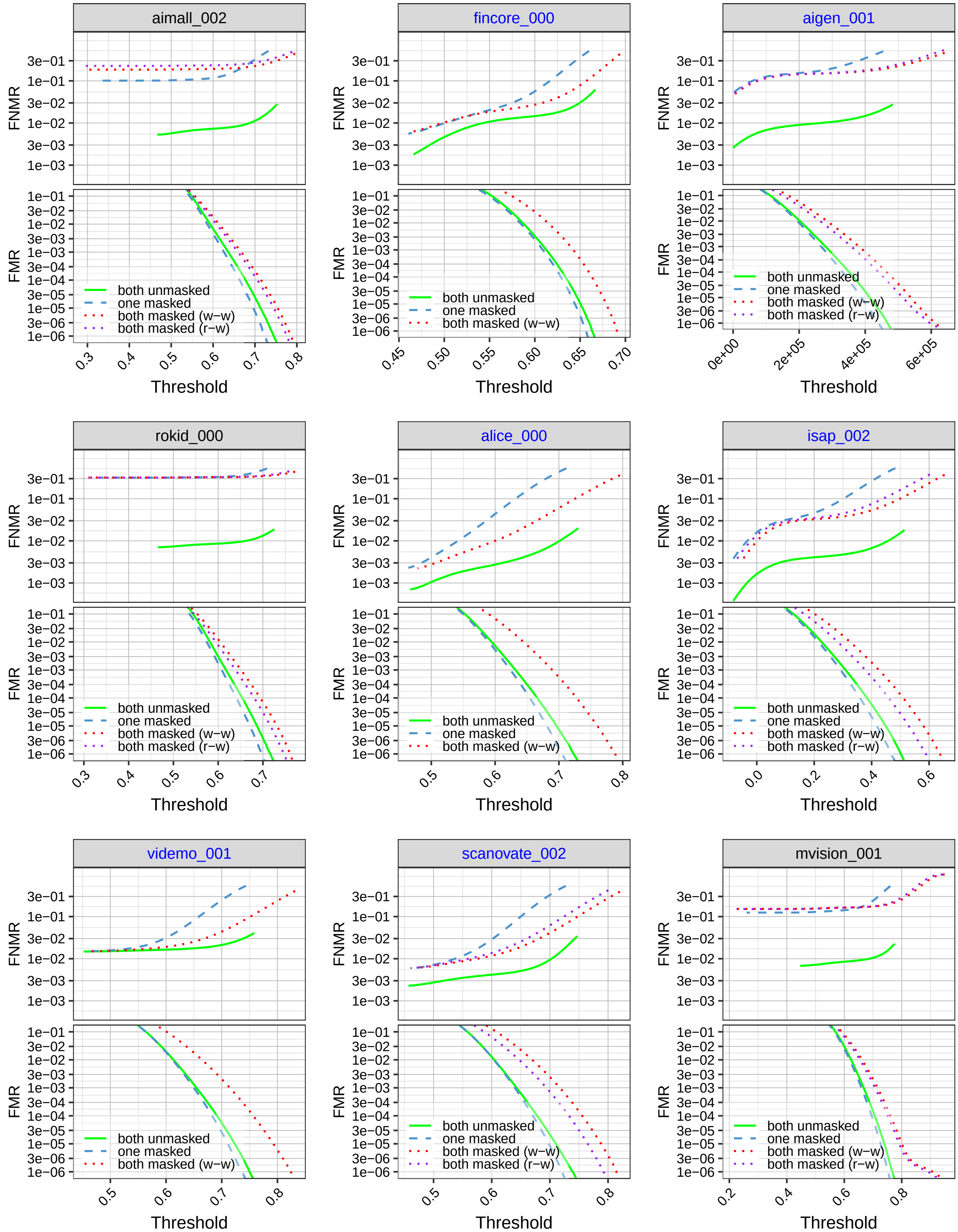

Figure 98: FNMR and FMR calibration curves on unmasked-to-unmasked (both unmasked), masked-to-unmasked with medium, wide, lightblue masks (one masked), masked-to-masked with medium, wide, lightblue masks (both masked (w-w)), and masked-to-masked with medium, round, white masks (enrollment image) and medium, wide, lightblue masks (verification image) (both masked (r-w)). Algorithms in black were submitted prior to mid-March 2020, and algorithms in blue were submitted thereafter.

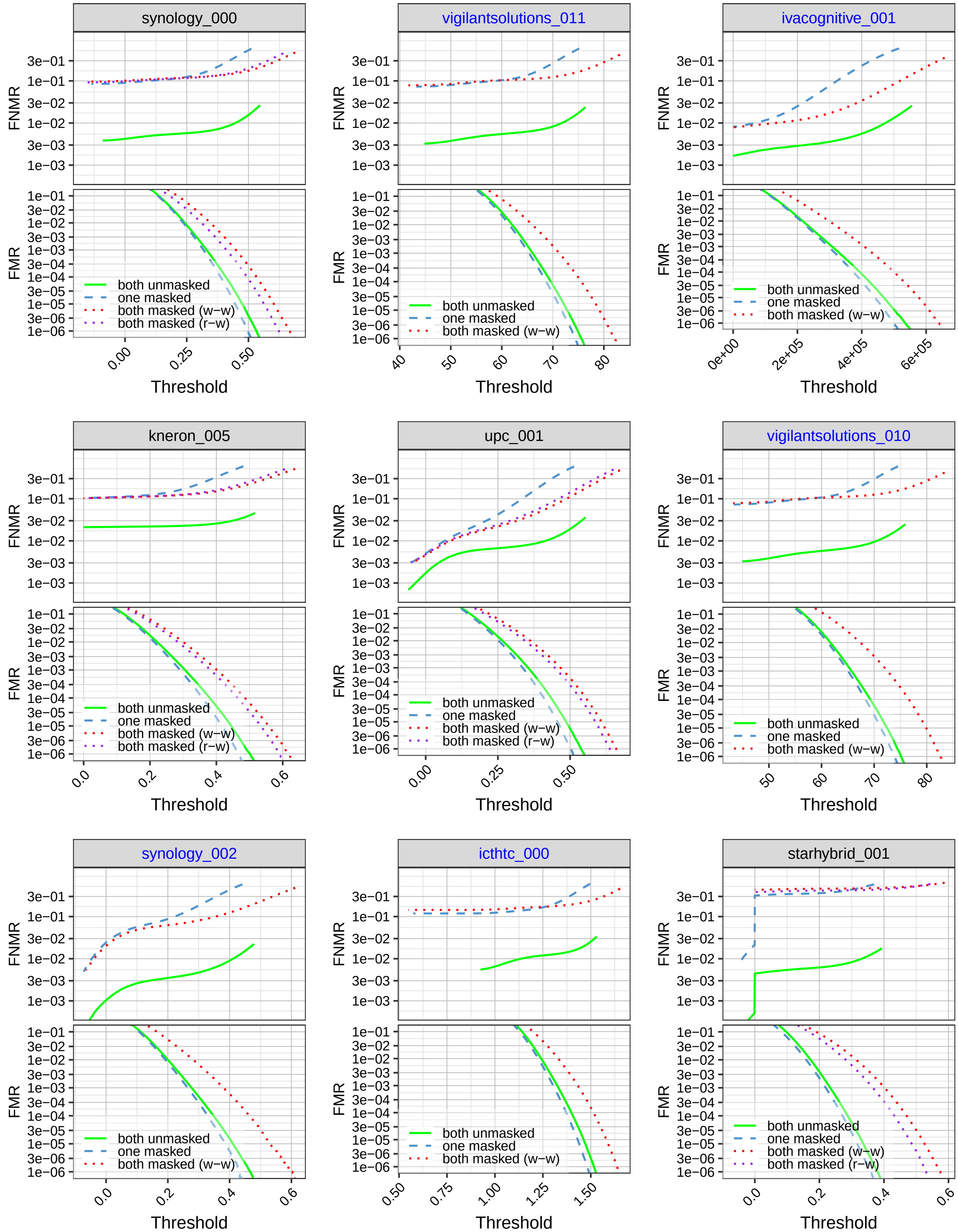

Figure 99: FNMR and FMR calibration curves on unmasked-to-unmasked (both unmasked), masked-to-unmasked with medium, wide, lightblue masks (one masked), masked-to-masked with medium, wide, lightblue masks (both masked (w-w)), and masked-to-masked with medium, round, white masks (enrollment image) and medium, wide, lightblue masks (verification image) (both masked (r-w)). Algorithms in black were submitted prior to mid-March 2020, and algorithms in blue were submitted thereafter.

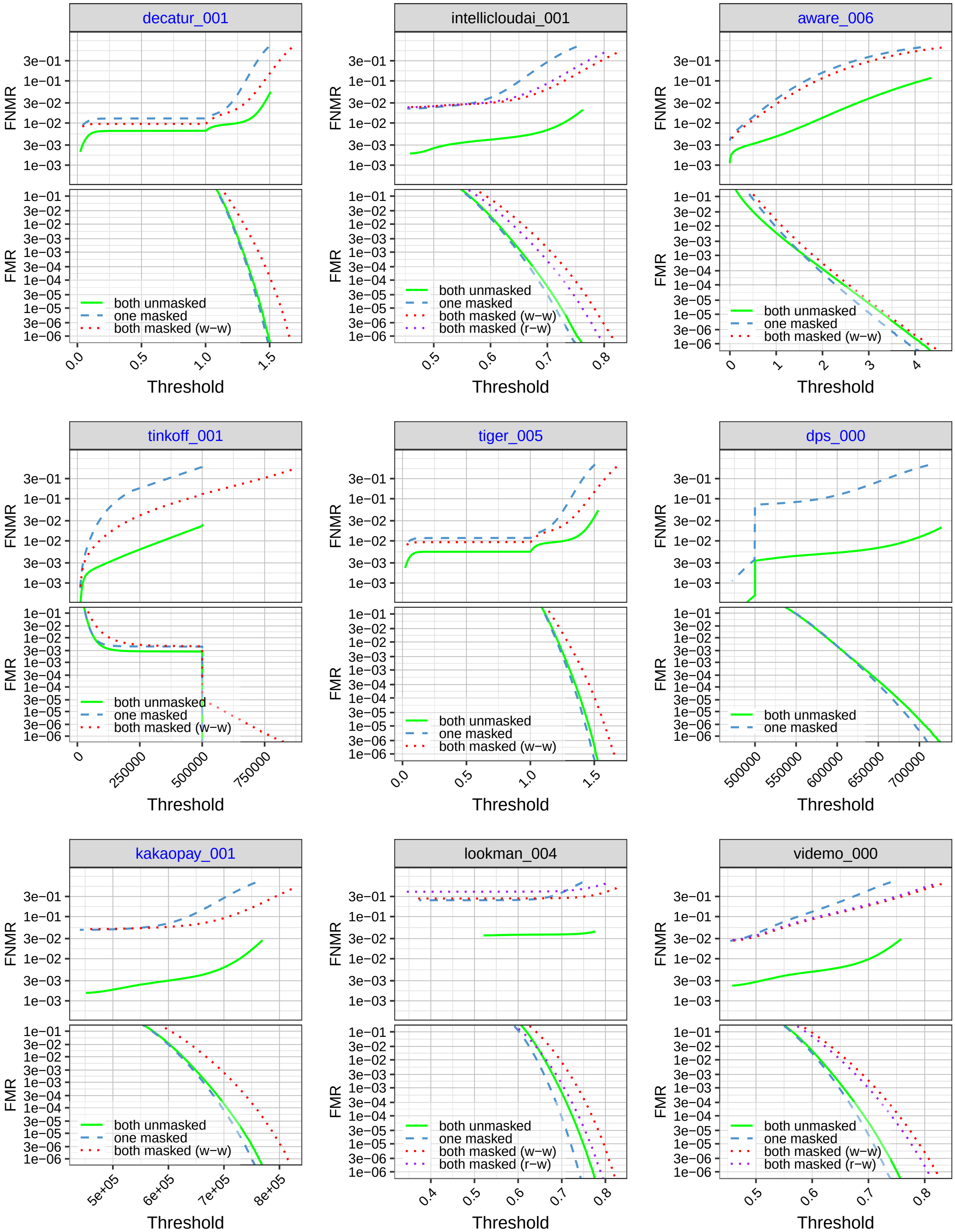

Figure 100: FNMR and FMR calibration curves on unmasked-to-unmasked (both unmasked), masked-to-unmasked with medium, wide, lightblue masks (one masked), masked-to-masked with medium, wide, lightblue masks (both masked (w-w)), and masked-to-masked with medium, round, white masks (enrollment image) and medium, wide, lightblue masks (verification image) (both masked (r-w)). Algorithms in black were submitted prior to mid-March 2020, and algorithms in blue were submitted thereafter.

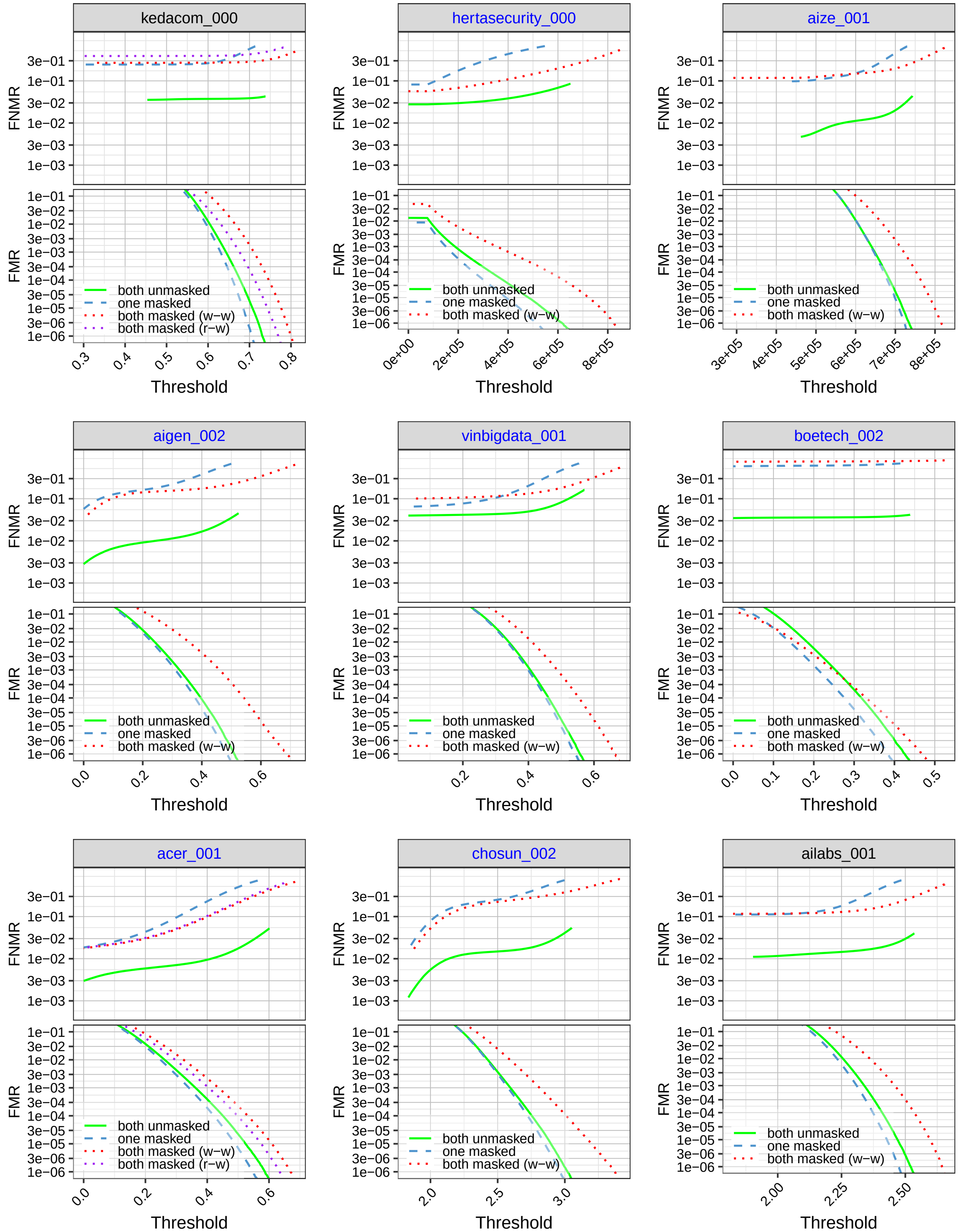

Figure 101: FNMR and FMR calibration curves on unmasked-to-unmasked (both unmasked), masked-to-unmasked with medium, wide, lightblue masks (one masked), masked-to-masked with medium, wide, lightblue masks (both masked (w-w)), and masked-to-masked with medium, round, white masks (enrollment image) and medium, wide, lightblue masks (verification image) (both masked (r-w)). Algorithms in black were submitted prior to mid-March 2020, and algorithms in blue were submitted thereafter.

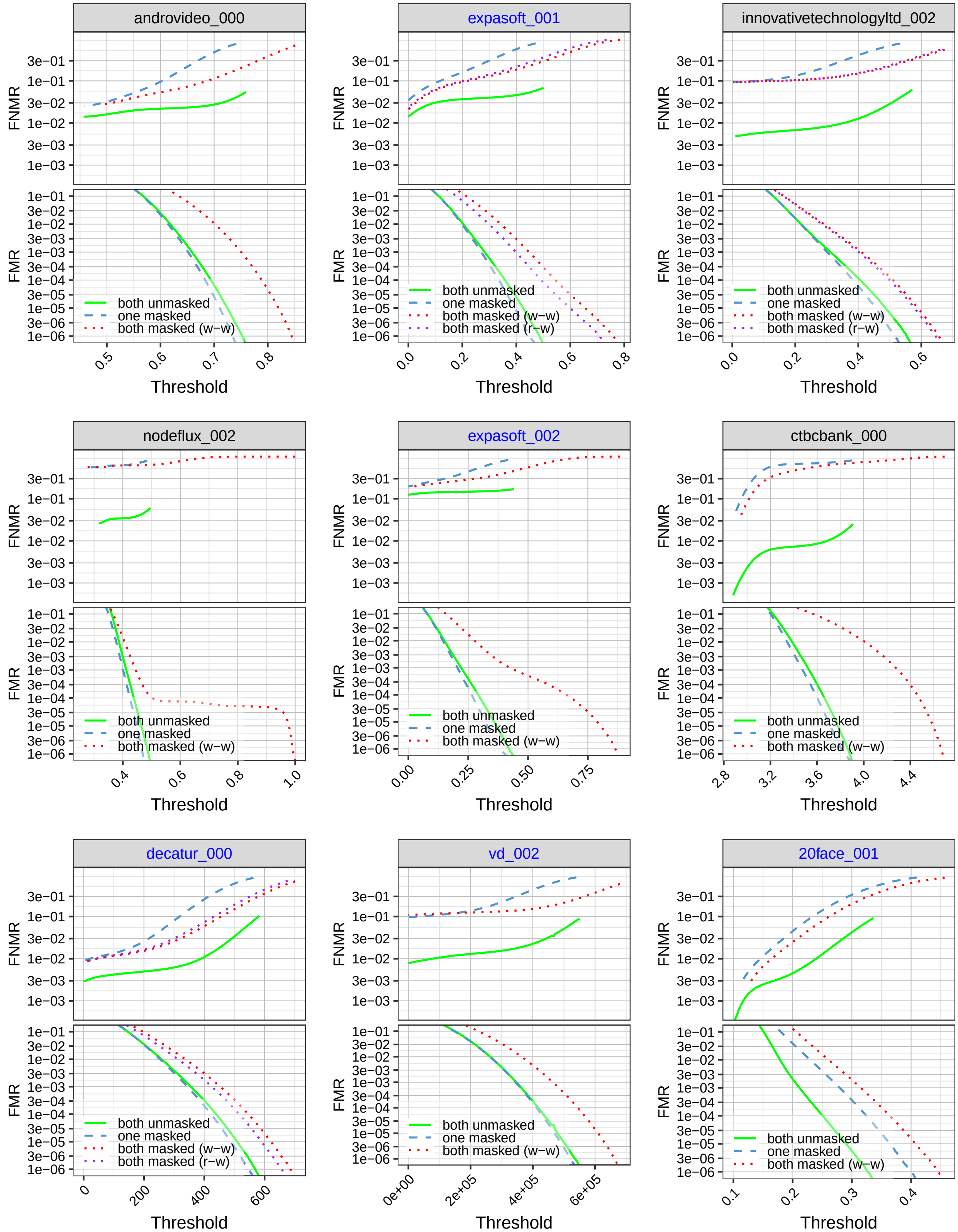

Figure 102: FNMR and FMR calibration curves on unmasked-to-unmasked (both unmasked), masked-to-unmasked with medium, wide, lightblue masks (one masked), masked-to-masked with medium, wide, lightblue masks (both masked (w-w)), and masked-to-masked with medium, round, white masks (enrollment image) and medium, wide, lightblue masks (verification image) (both masked (r-w)). Algorithms in black were submitted prior to mid-March 2020, and algorithms in blue were submitted thereafter.

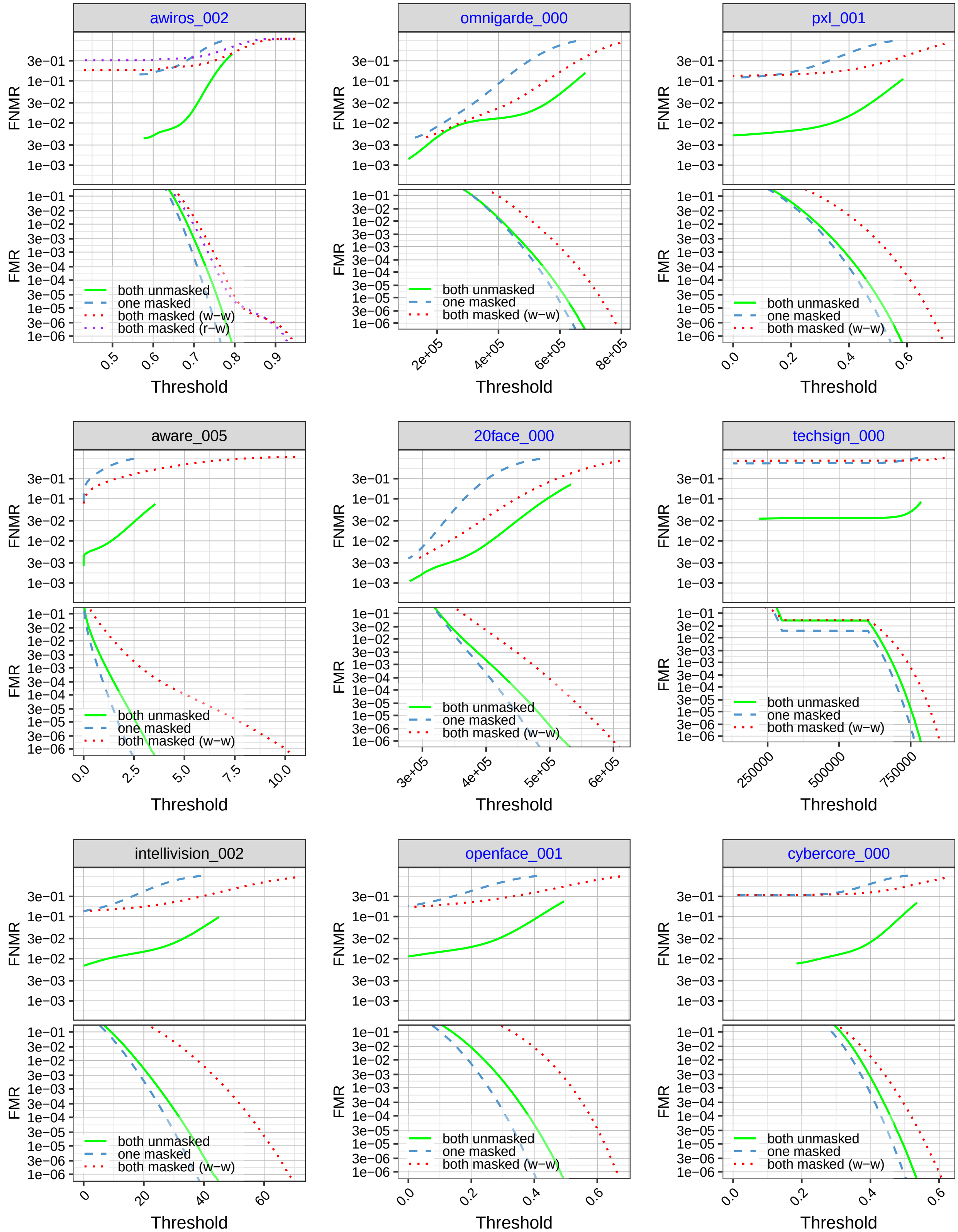

Figure 103: FNMR and FMR calibration curves on unmasked-to-unmasked (both unmasked), masked-to-unmasked with medium, wide, lightblue masks (one masked), masked-to-masked with medium, wide, lightblue masks (both masked (w-w)), and masked-to-masked with medium, round, white masks (enrollment image) and medium, wide, lightblue masks (verification image) (both masked (r-w)). Algorithms in black were submitted prior to mid-March 2020, and algorithms in blue were submitted thereafter.

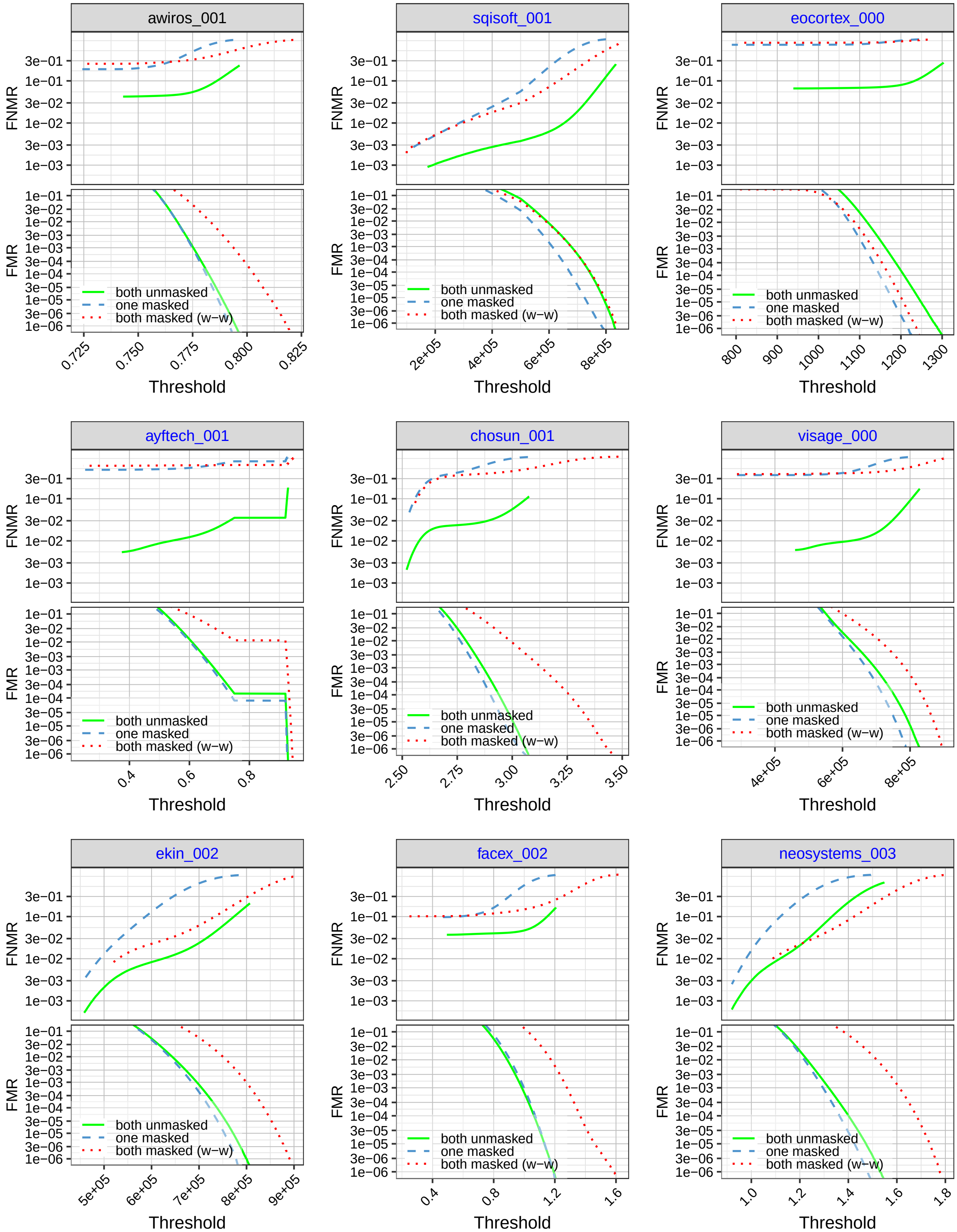

Figure 104: FNMR and FMR calibration curves on unmasked-to-unmasked (both unmasked), masked-to-unmasked with medium, wide, lightblue masks (one masked), masked-to-masked with medium, wide, lightblue masks (both masked (w-w)), and masked-to-masked with medium, round, white masks (enrollment image) and medium, wide, lightblue masks (verification image) (both masked (r-w)). Algorithms in black were submitted prior to mid-March 2020, and algorithms in blue were submitted thereafter.

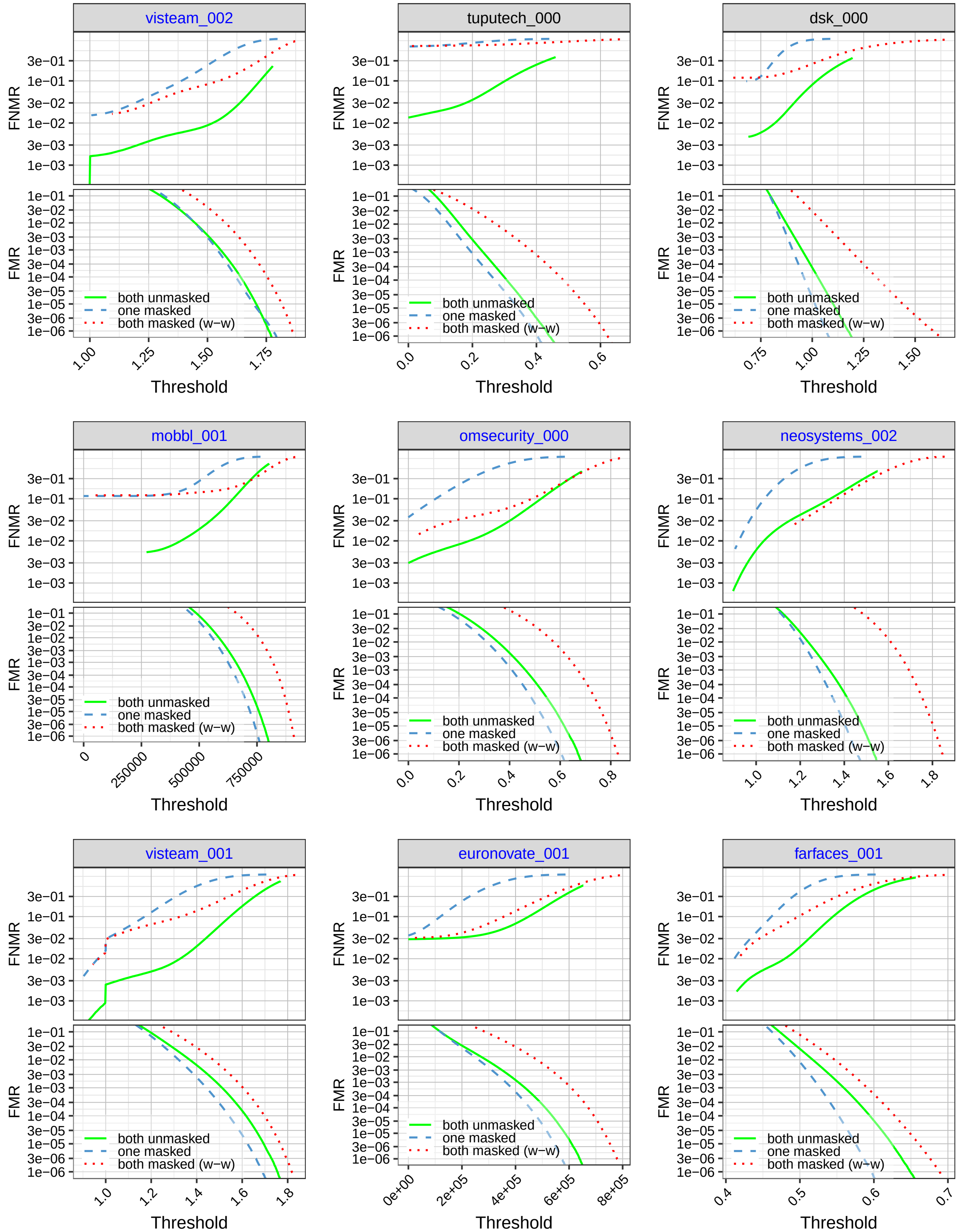

Figure 105: FNMR and FMR calibration curves on unmasked-to-unmasked (both unmasked), masked-to-unmasked with medium, wide, lightblue masks (one masked), masked-to-masked with medium, wide, lightblue masks (both masked (w-w)), and masked-to-masked with medium, round, white masks (enrollment image) and medium, wide, lightblue masks (verification image) (both masked (r-w)). Algorithms in black were submitted prior to mid-March 2020, and algorithms in blue were submitted thereafter.

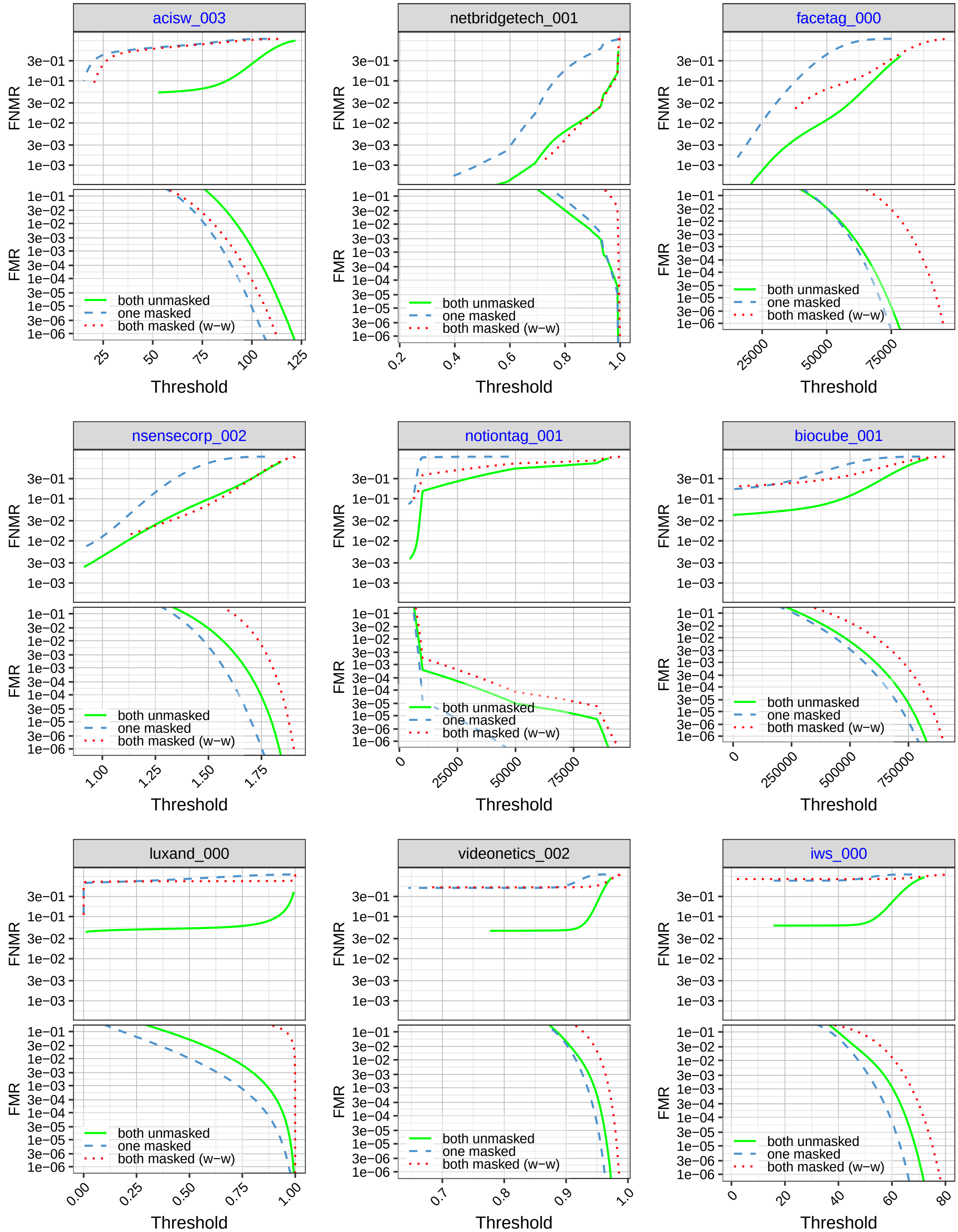

Figure 106: FNMR and FMR calibration curves on unmasked-to-unmasked (both unmasked), masked-to-unmasked with medium, wide, lightblue masks (one masked), masked-to-masked with medium, wide, lightblue masks (both masked (w-w)), and masked-to-masked with medium, round, white masks (enrollment image) and medium, wide, lightblue masks (verification image) (both masked (r-w)). Algorithms in black were submitted prior to mid-March 2020, and algorithms in blue were submitted thereafter.

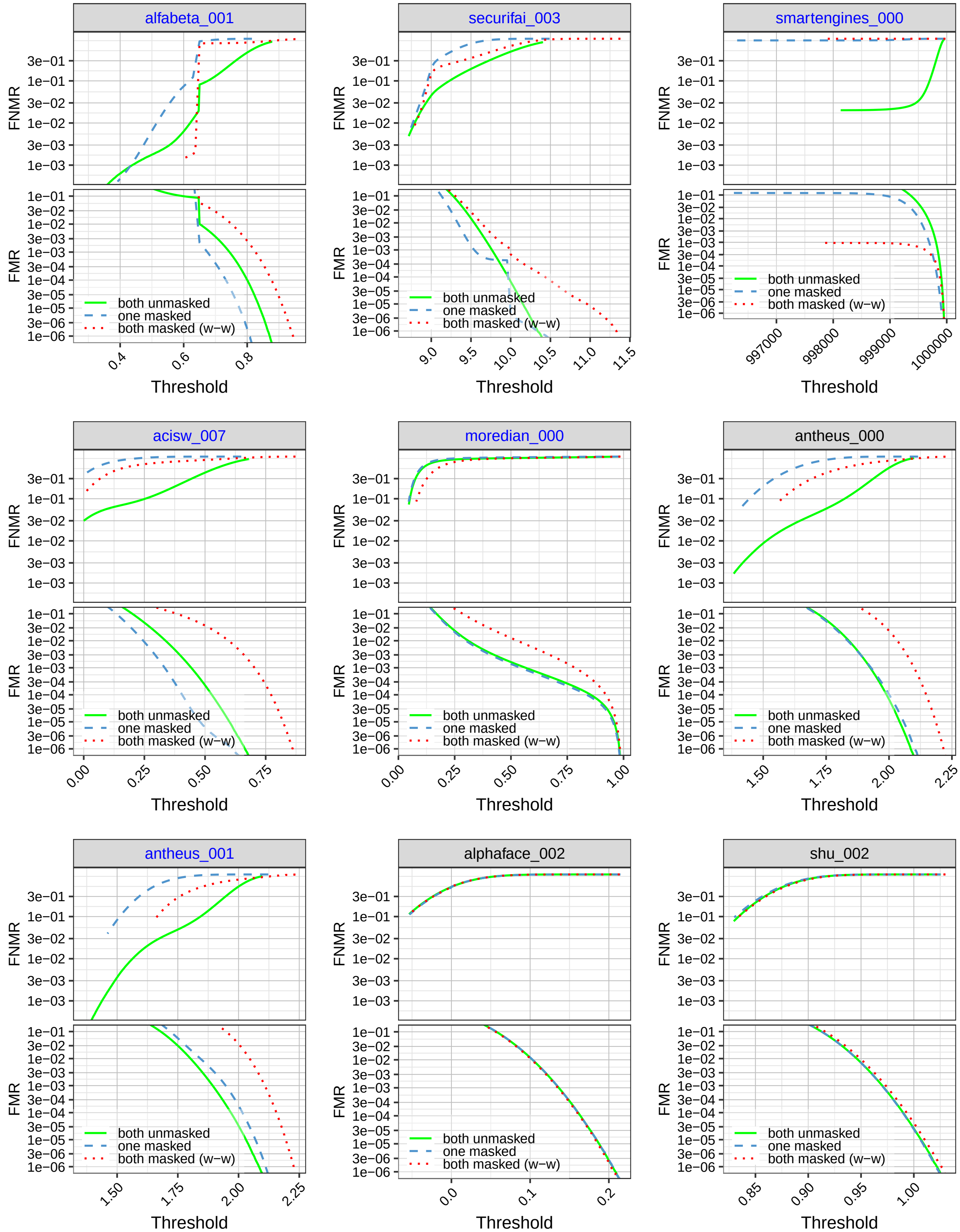

Figure 107: FNMR and FMR calibration curves on unmasked-to-unmasked (both unmasked), masked-to-unmasked with medium, wide, lightblue masks (one masked), masked-to-masked with medium, wide, lightblue masks (both masked (w-w)), and masked-to-masked with medium, round, white masks (enrollment image) and medium, wide, lightblue masks (verification image) (both masked (r-w)). Algorithms in black were submitted prior to mid-March 2020, and algorithms in blue were submitted thereafter.

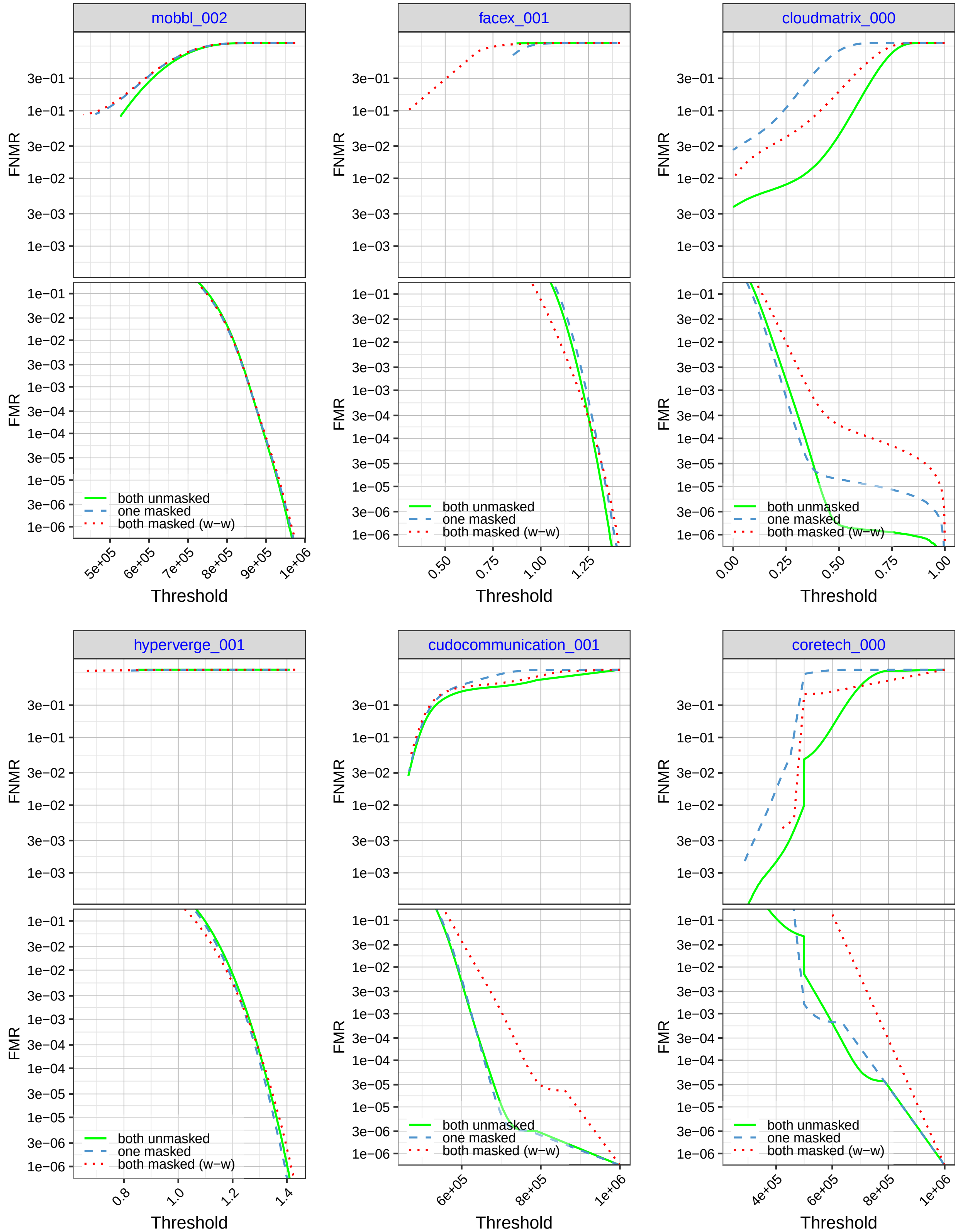

Figure 108: FNMR and FMR calibration curves on unmasked-to-unmasked (both unmasked), masked-to-unmasked with medium, wide, lightblue masks (one masked), masked-to-masked with medium, wide, lightblue masks (both masked (w-w)), and masked-to-masked with medium, round, white masks (enrollment image) and medium, wide, lightblue masks (verification image) (both masked (r-w)). Algorithms in black were submitted prior to mid-March 2020, and algorithms in blue were submitted thereafter.

References

[1] ISO/IEC 19794-5:2011 - Information technology - Biometric data interchange formats - Part 5: Face image data.

[2] N95 Respirators, Surgical Masks, and Face Masks. https://www.fda.gov/medical-devices/personal-protective-equipment-infection-control/n95-respirators-surgical-masks-and-face-masks.

[3] NIST Special Database 32 - Multiple Encounter Dataset (MEDS-II). https://www.nist.gov/itl/iad/image-group/special-database-32-multiple-encounter-dataset-meds.

[4] Patrick Grother, George Quinn, and Mei Ngan. Face in video evaluation (five) face recognition of non-cooperative subjects. Interagency Report 8173, National Institute of Standards and Technology, March 2017. https://doi.org/10.6028/NIST.IR.8173.

[5] J. Hanley and A. Lippman-Hand. If nothing goes wrong, is everything all right? interpreting zero numerators. *JAMA*, 249 13:1743–5, 1983.

[6] Davis E. King. Dlib-ml: A machine learning toolkit. *Journal of Machine Learning Research*, 10:1755–1758, 2009. http://dlib.net.

[7] Mei Ngan, Patrick Grother, and Kayee Hanaoka. NISTIR 8311 - Ongoing FRVT Part 6A: Face recognition accuracy with face masks using pre-COVID-19 algorithms. Interagency Report 8311, National Institute of Standards and Technology, July 2020. https://doi.org/10.6028/NIST.IR.8311.

[8] Patrick Grother and Mei Ngan and Kayee Hanaoka. NIST Ongoing Face Recognition Vendor Test (FRVT) 1:1 Verification Application Programming Interface (API), April 2019. https://pages.nist.gov/frvt/api/FRVT_ongoing_11_api_4.0.pdf.

[9] Zhongyuan Wang, Guangcheng Wang, Baojin Huang, Zhangyang Xiong, Qi Hong, Hao Wu, Peng Yi, Kui Jiang, Nanxi Wang, Yingjiao Pei, Heling Chen, Yu Miao, Zhibing Huang, and Jinbi Liang. Masked face recognition dataset and application, 2020.

Appendix A Dlib Masking Methodology

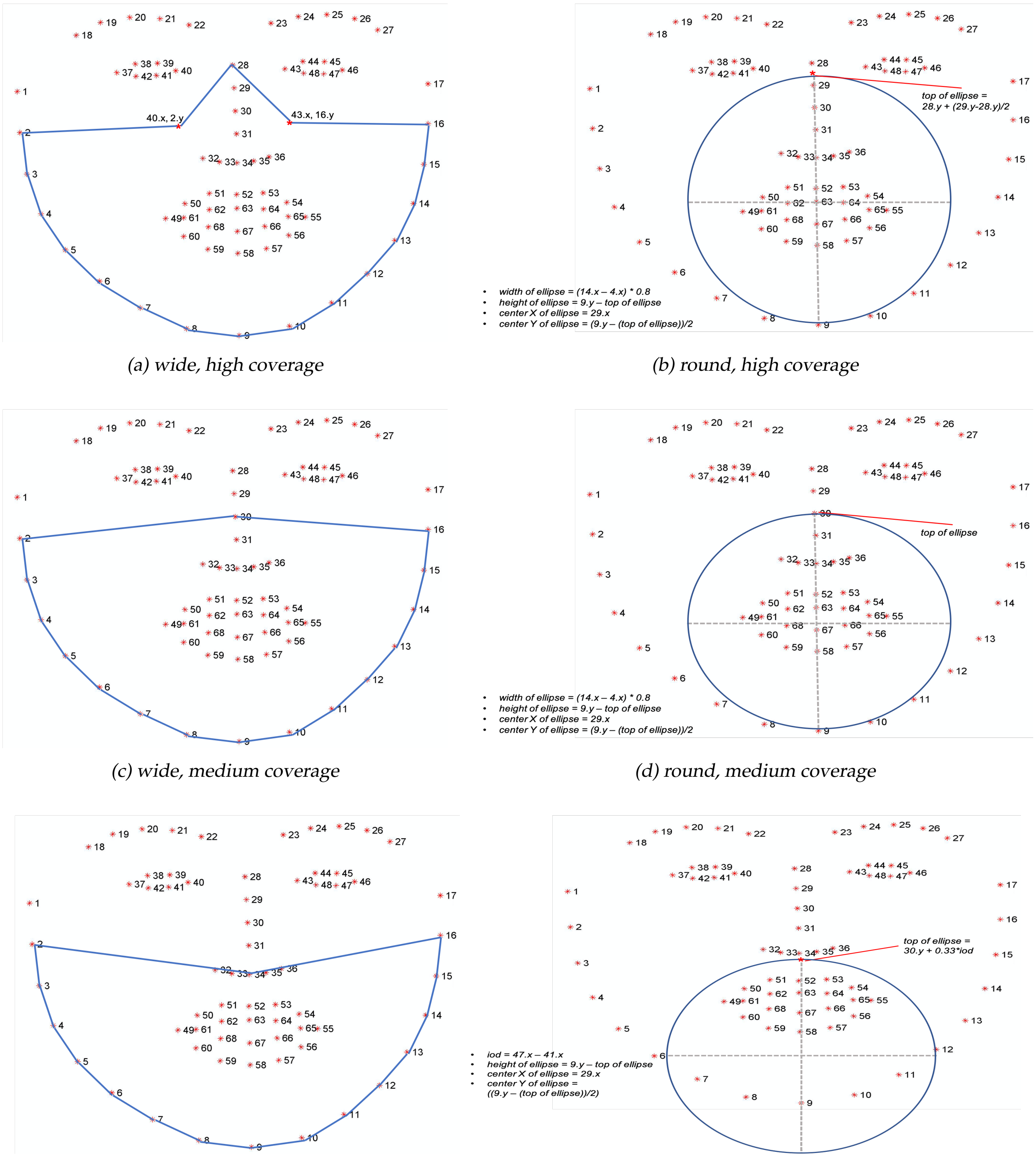

(a) wide, high coverage *(b) round, high coverage*

(c) wide, medium coverage *(d) round, medium coverage*

(e) wide, low coverage *(f) round, low coverage*

Figure 109: This figure shows the Dlib facial points used to create the various synthetic masks used in this report. For wide masks, the specified Dlib facial points were used to generate a closed polygon and two additional points were interpolated between each dlib facial point used for smoothing purposes. For round masks, the specified Dlib facial points were used to generate an ellipse. The Dlib C++ toolkit version 19.19, configured with the common histogram of gradients (HoG)-based face detector and 68 face landmark shape predictor was used to generate the 68 facial landmarks.